Third Workshop on Density Functional Theory:
Fundamentals, Developments, and Applications (DFT2025)

DFT-Based Quantum Embedding Approach for X-ray Spectroscopy Calculations

Atsushi Hariki

Osaka Metropolitan University

Atomic radial function
(from atomic Hartree-Fock calc.)

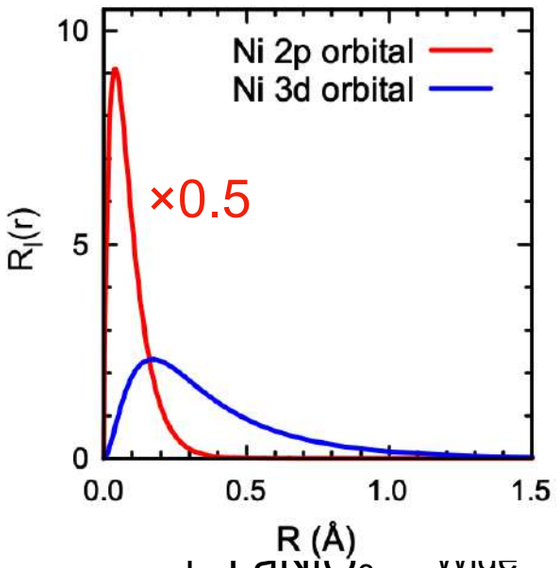

3d, 4d, 5d transition metal, 4f, 5f lanthanide actinide

ray spectroscopy and correlated electron physics

energy spectroscopy

l excitations (1-10eV)

Elementary excitations, magnetism,
metal-insulator transition (near E_F < 1eV)

I also discus the core-level "spectral function"

Half part of my talk

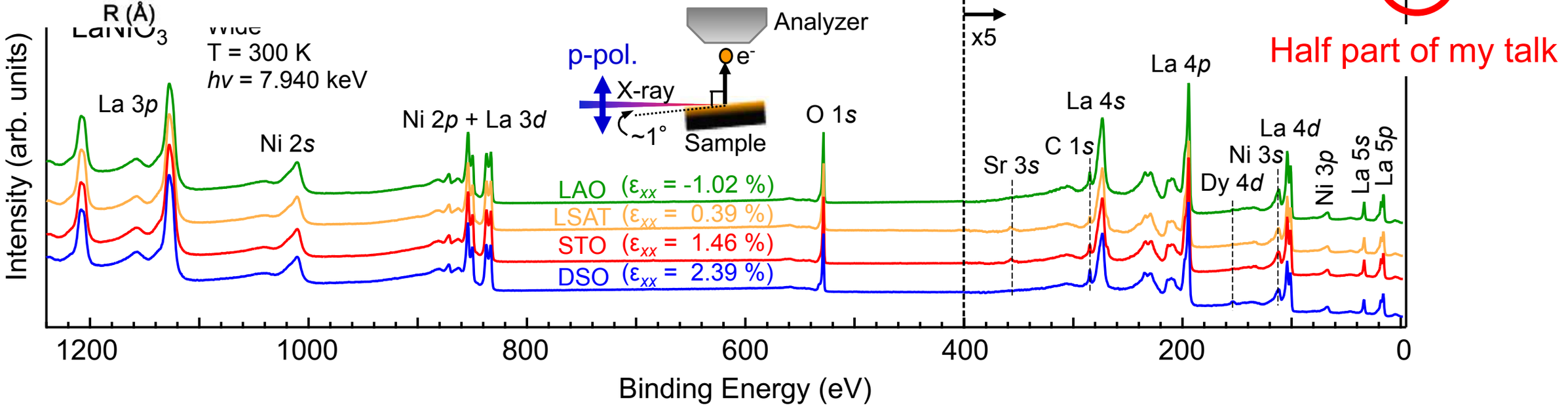

XPS spectrum in $LaNiO_3$ K. Yamagami et al., Appl. Phys. Lett. 118, 161601 (2021)

1. Why core-level excitation to study material properties (low-energy excitations)?
2. Why DFT (+many-body theory) is needed for simulating core-level excitations?

   Note. Our Interest is NOT element dependence of the core binding energies

Calc. LDA+DMFT Anderson model

A. Hariki et al., PRB **96**, 045111 (2017)

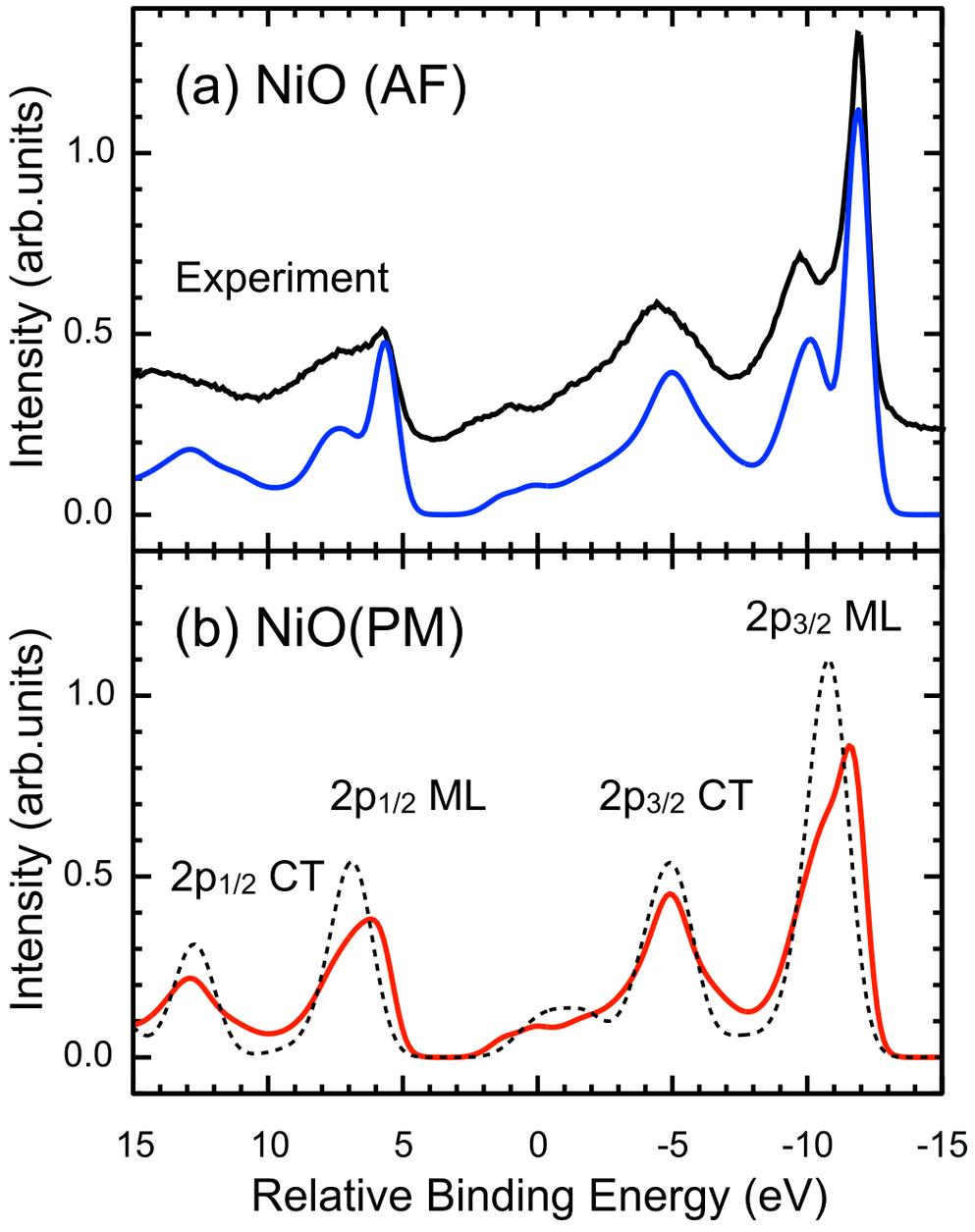

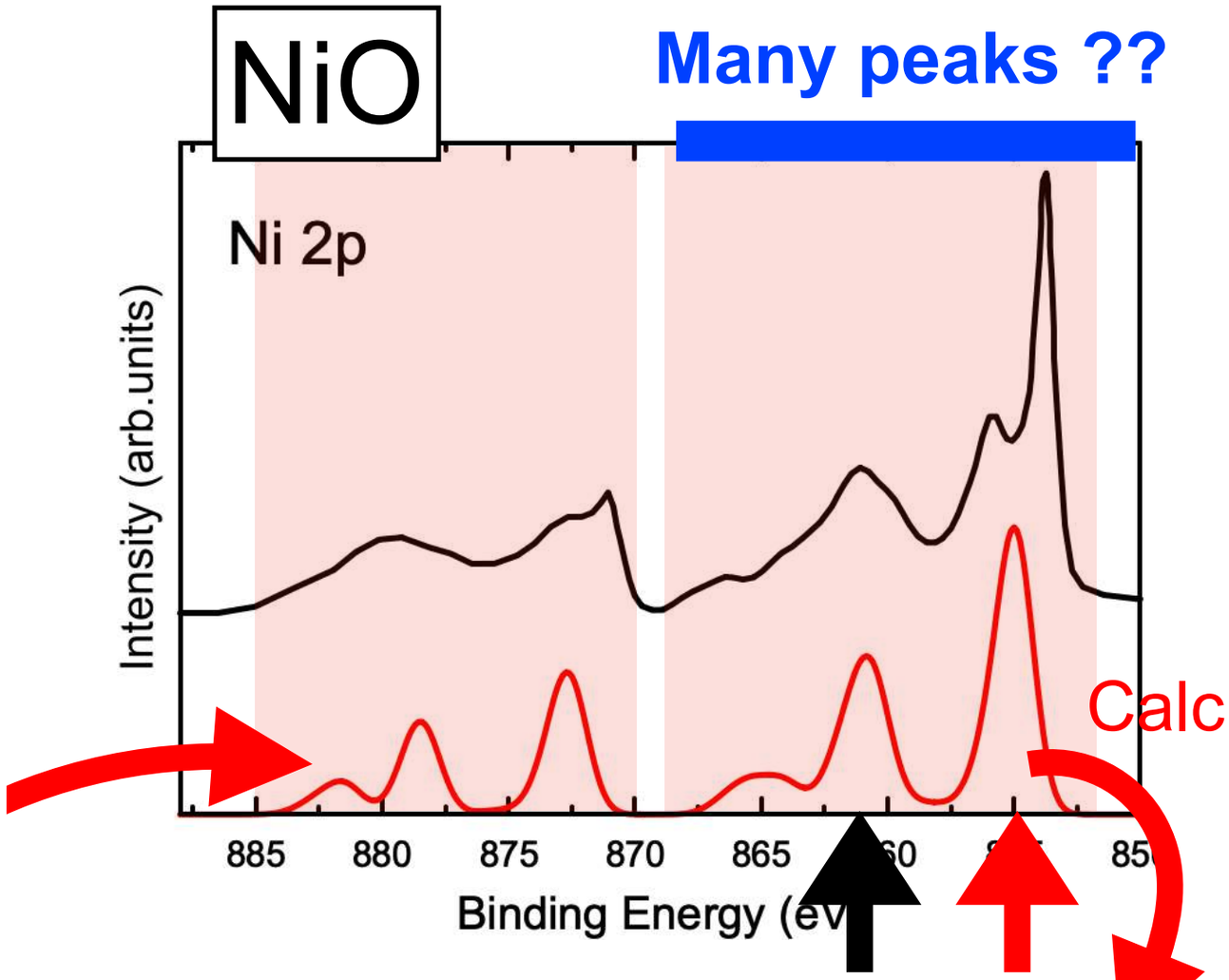

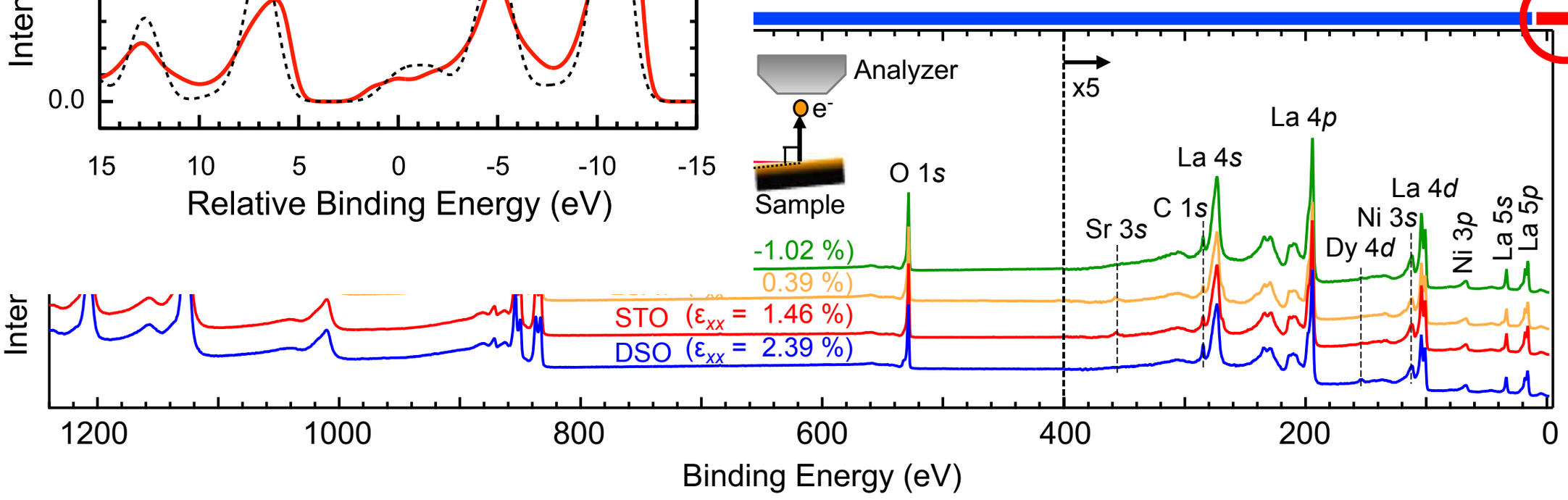

Table of contents

1. Core-level X-ray spectroscopy and DFT-based embedding approach

★ **Method**. DFT+ dynamical mean-field theory (DMFT)

A. Hariki, T. Uozumi, and J. Kuneš, Phys. Rev. B **96**. 045111 (2017)

A. Hariki, M. Winder, and J. Kuneš, Phys. Rev. Lett. **121**, 126403 (2018)

A. Hariki, M. Winder, T. Uozumi, and J. Kuneš, Phys. Rev. B **101**, 115130 (2020)

2. Application to various optical processes and compounds

★ **Excitations**. XPS, XAS, RIXS ★ **Materials**. *d*, *f* electron systems

★ **Physics**. Magnetism, valence structure, elementary excitations

K. Higashi, M. Winder, J. Kuneš, and A. Hariki, Phys. Rev. X **11**, 041009 (2021)

D. Takegami, A. Hariki et al., Phys. Rev. X **12**, 011017 (2022)

M. C. Rahn, K. Kummer, A. Hariki, et al., Nat. Commun. **13**, 6129 (2022)

J. Li, A. Hariki et al., Phys. Rev. X **13**, 011012 (2023)

A. Hariki et al., Phys. Rev. Let. **132**, 176701 (2024)

X-ray photoemission spectroscopies and DFT theory

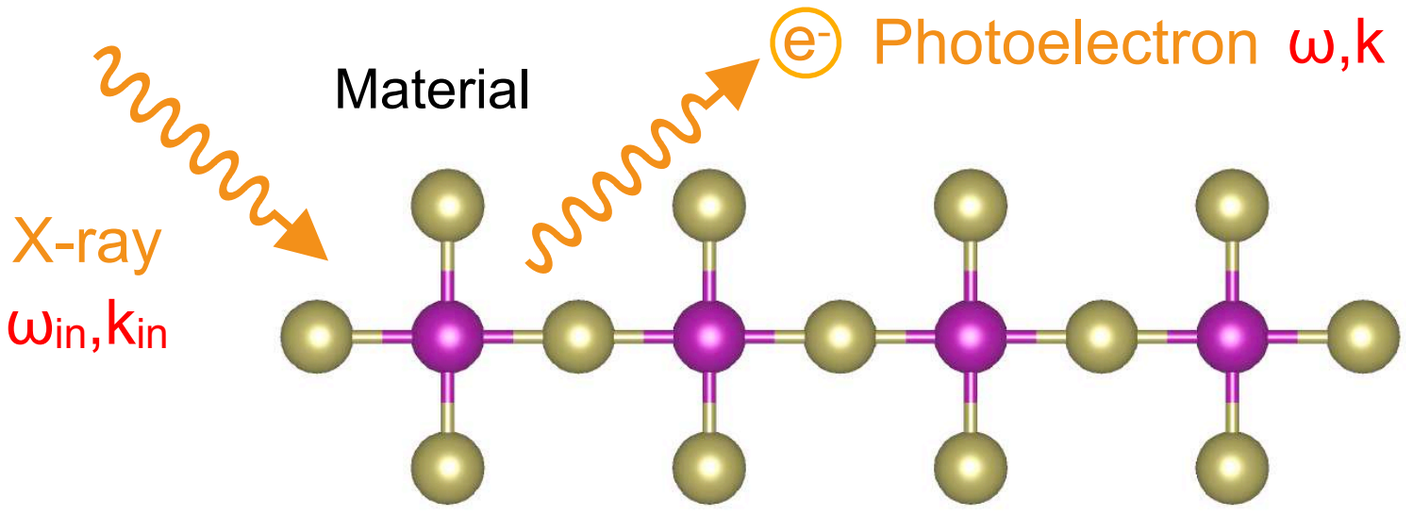

X-ray photoemission spectroscopy:

- Valence-band XPS (ARPES)
  directly measure the low-energy states
- Core-level XPS
  Site/element specific excitation

XPS spectrum in $LaNiO_3$ K. Yamagami et al., Appl. Phys. Lett. 118, 161601 (2021)

Core levels Valence bands Near Fermi (QP)

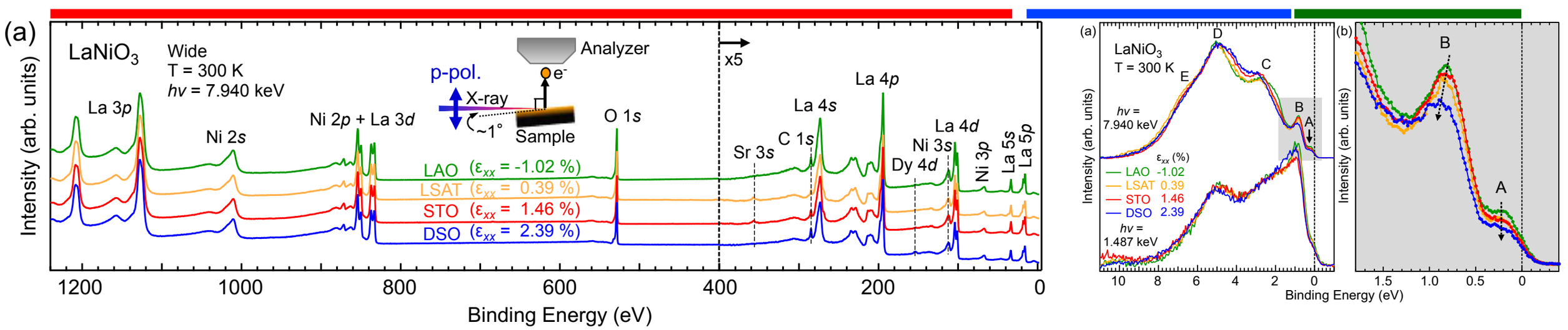

1-particle Green's function

$$G_r(\varepsilon) = \langle \Phi_0^{(N)} | c_r^\dagger \frac{1}{\varepsilon - (E_0^{(N)} - \mathscr{H}) + i\delta} c_r | \Phi_0^{(N)} \rangle + \langle \Phi_0^{(N)} | c_r \frac{1}{\varepsilon - (\mathscr{H} - E_0^{(N)}) + i\delta} c_r^\dagger | \Phi_0^{(N)} \rangle$$

photoemission

$$= \sum_n \left[\frac{|\langle \Phi_n^{(N-1)} | c_r | \Phi_0^{(N)} \rangle|^2}{\varepsilon - (E_0^{(N)} - E_n^{(N-1)}) + i\delta} + \frac{|\langle \Phi_n^{(N+1)} | c_r^\dagger | \Phi_0^{(N)} \rangle|^2}{\varepsilon - (E_n^{(N+1)} - E_0^{(N)}) + i\delta} \right]$$

Inverse photoemission

X-ray photoemission spectroscopies and DFT theory

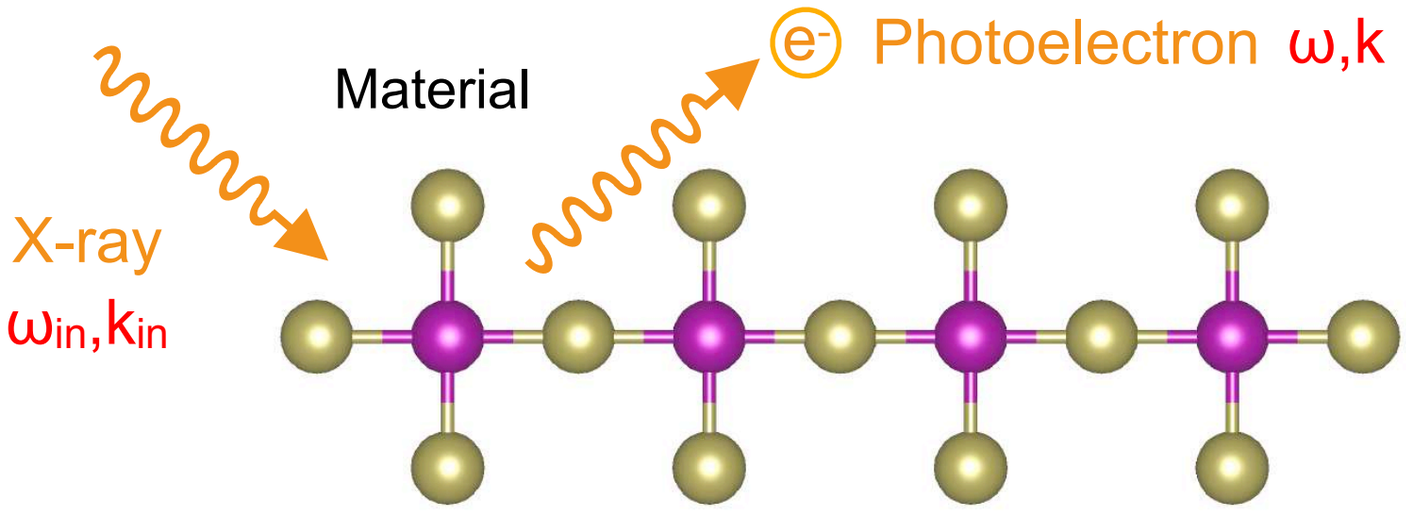

X-ray photoemission spectroscopy:

- Valence-band XPS (ARPES)
  directly measure the low-energy states
- Core-level XPS
  Site/element specific excitation

XPS spectrum in $LaNiO_3$ K. Yamagami et al., Appl. Phys. Lett. 118, 161601 (2021)

Core levels Valence bands Near Fermi (QP)

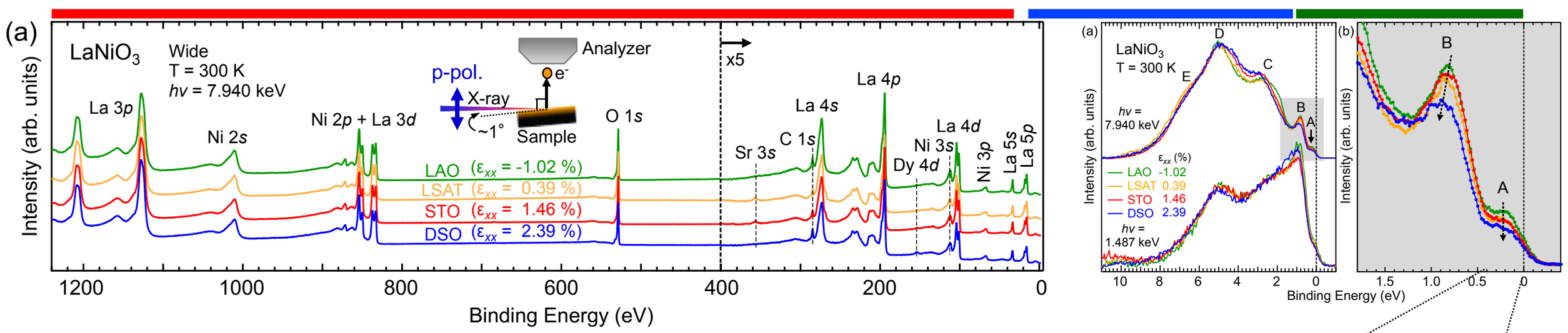

Core levels (no momentum dependence)

Core electrons (holes) completely localized at each ion

- Element specific information (valency)
- Local electronic structure
  (Hund's multiplet, crystal field, and more …)

ARPES:
resolve the momentum

E. A. Nowadnick et al.,
Phys. Rev. B **92**, 245109 (2015)

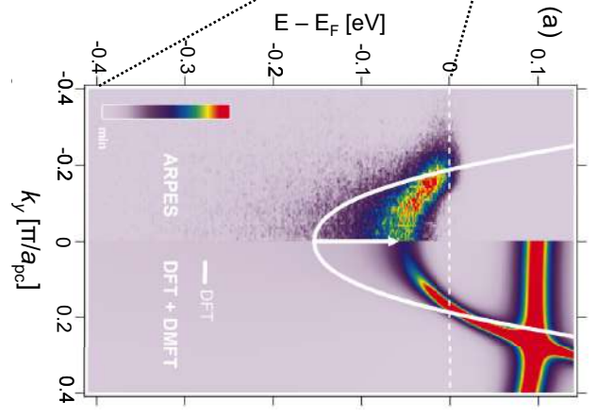

X-ray photoemission spectroscopies and DFT theory

DFT calculation; indispensable for understanding the material dependence of the valence electronic structure (valence spectra, i.e. valence band PES)

NiO (LDA, Wien2K)

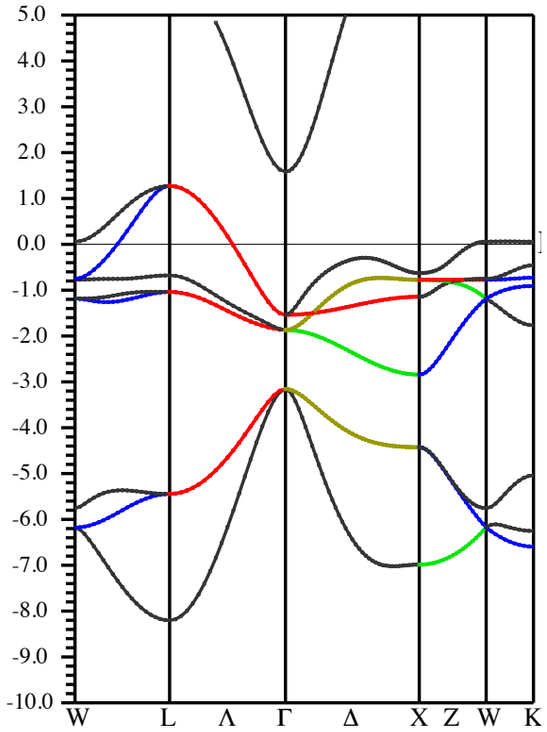

Density of states

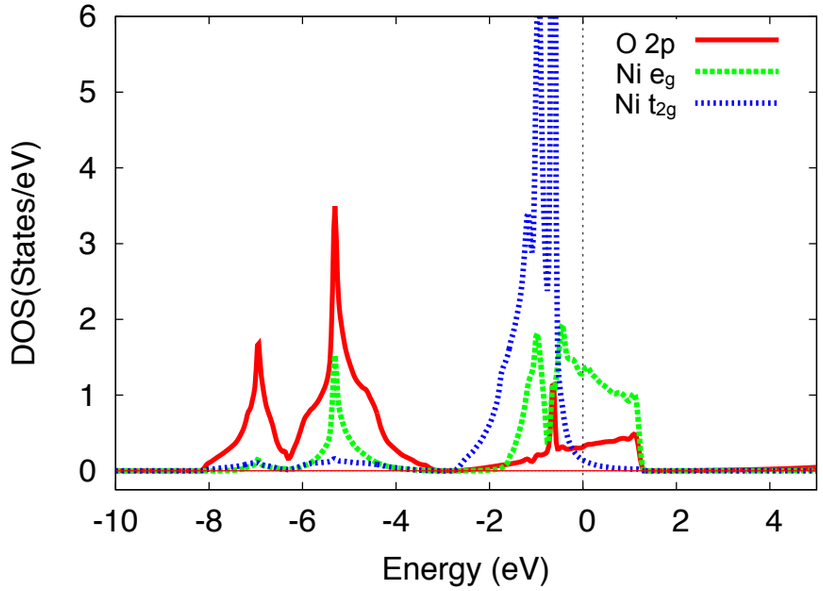

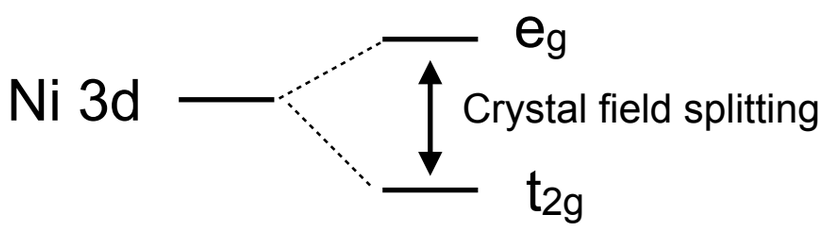

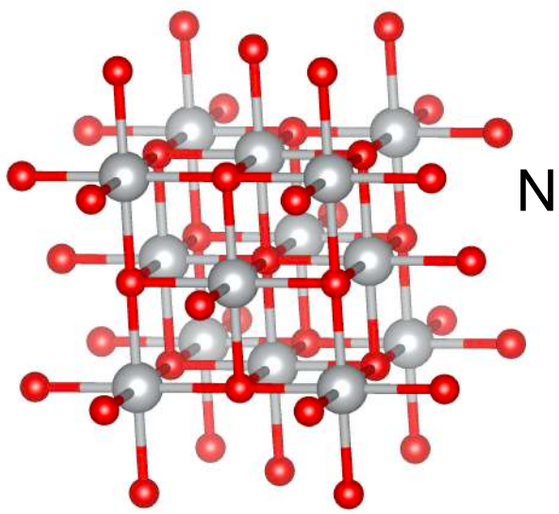

Ni^{2+} (d^8)

Partially filled

VOLUME 53, NUMBER 24 PHYSICAL REVIEW LETTERS 10 DECEMBER 1984

Magnitude and Origin of the Band Gap in NiO

G. A. Sawatzky[(a)] and J. W. Allen
Xerox Palo Alto Research Center, Palo Alto, California 94304

(Received 5 July 1984)

Photoemission and bremsstrahlung-isochromat-spectroscopy data on a cleaved NiO single crystal are presented and compared to band- and cluster-theory predictions. In contrast to band-theory predictions the band gap is found to be large but not determined solely by the even larger *d-d* Coulomb interactions so that NiO is not a Mott-Hubbard insulator in the simplest sense. A large *d-d* interaction need not prevent NiS from being a metal.

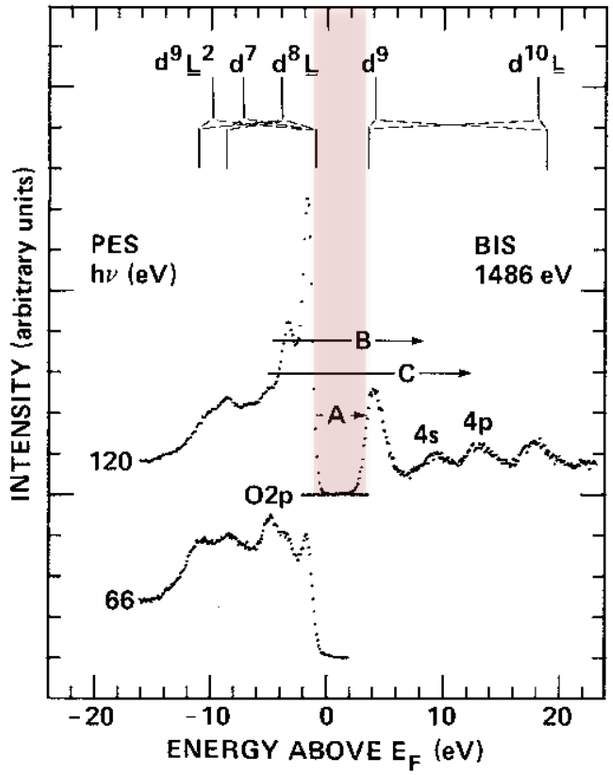

Simple DFT often fails to simulate the valence structure in d (and f) electron systems due to inaccurate treatment of electronic correlation

X-ray photoemission spectroscopies and DFT theory

Hubbard model (Kinetic energy + On-site Coulomb repulsion)

Hubbard term $H_{\mathrm{Hubbard}} = \sum_i U n_{i\uparrow} n_{i\downarrow}$

Hopping t Repulsion U

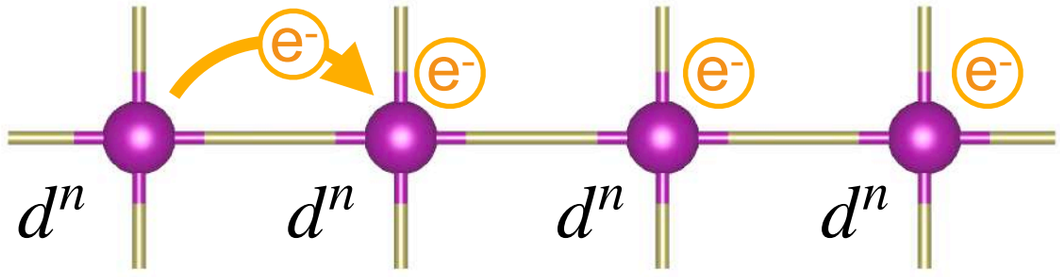

Before: d^n d^n $\quad {}_nC_2 \times U + {}_nC_2 \times U$

After : d^{n-1} d^{n+1} $\quad {}_{n-1}C_2 \times U + {}_{n+1}C_2 \times U$

Energy cost U

When U is larger than the band width W,
the system can be an insulator with localized electrons

: Mott insulator

G. Kotliar and D. Vollhardt, Physics Today 57 (2004)
: solved by dynamical mean-field theory (DMFT)

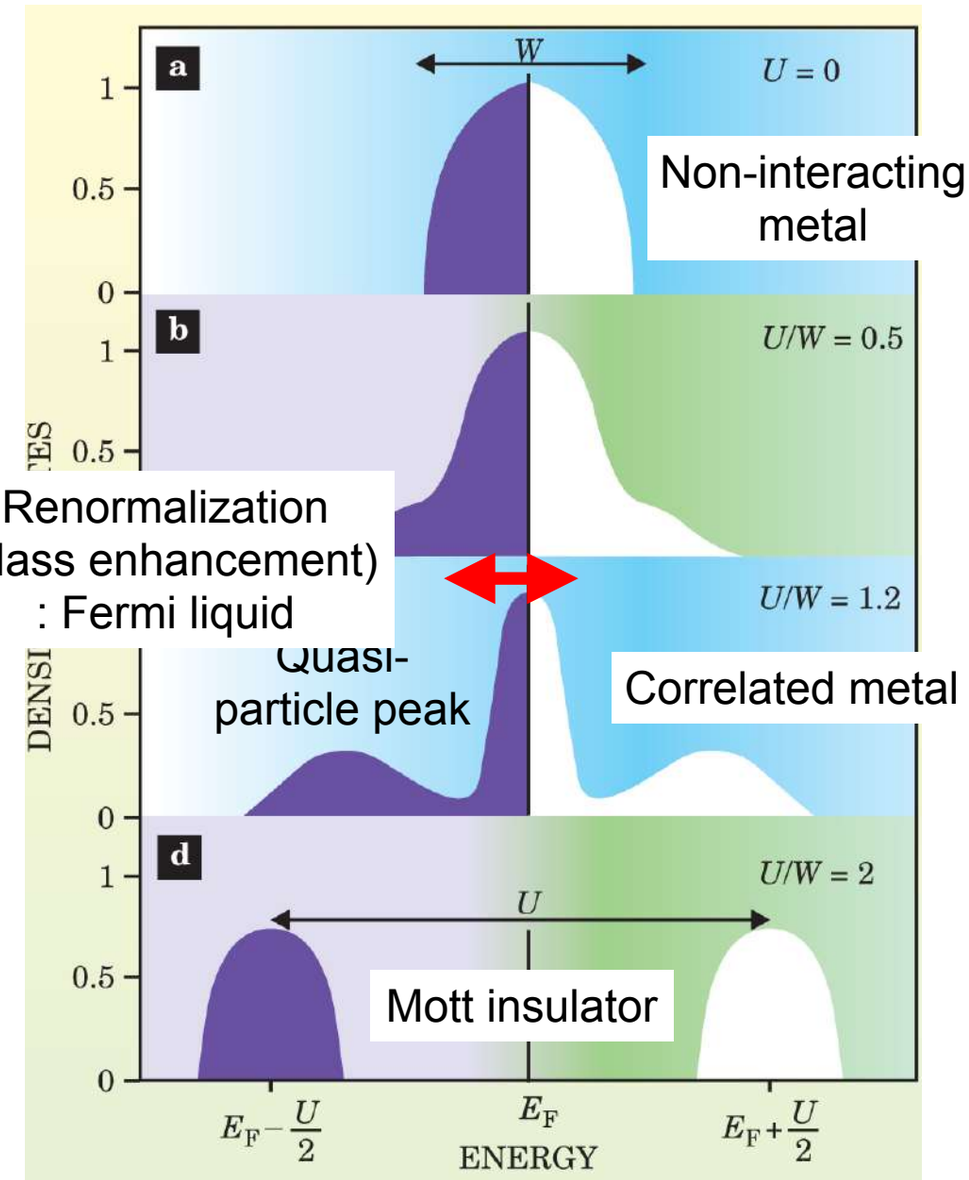

X-ray photoemission spectroscopies and DFT theory

Hubbard model (Kinetic energy + On-site Coulomb repulsion)

Valence-band photoemission spectroscopy in d^1 compounds

A. Sekiyama et al., Phys. Rev. Lett. **93**, 156402 (2004)

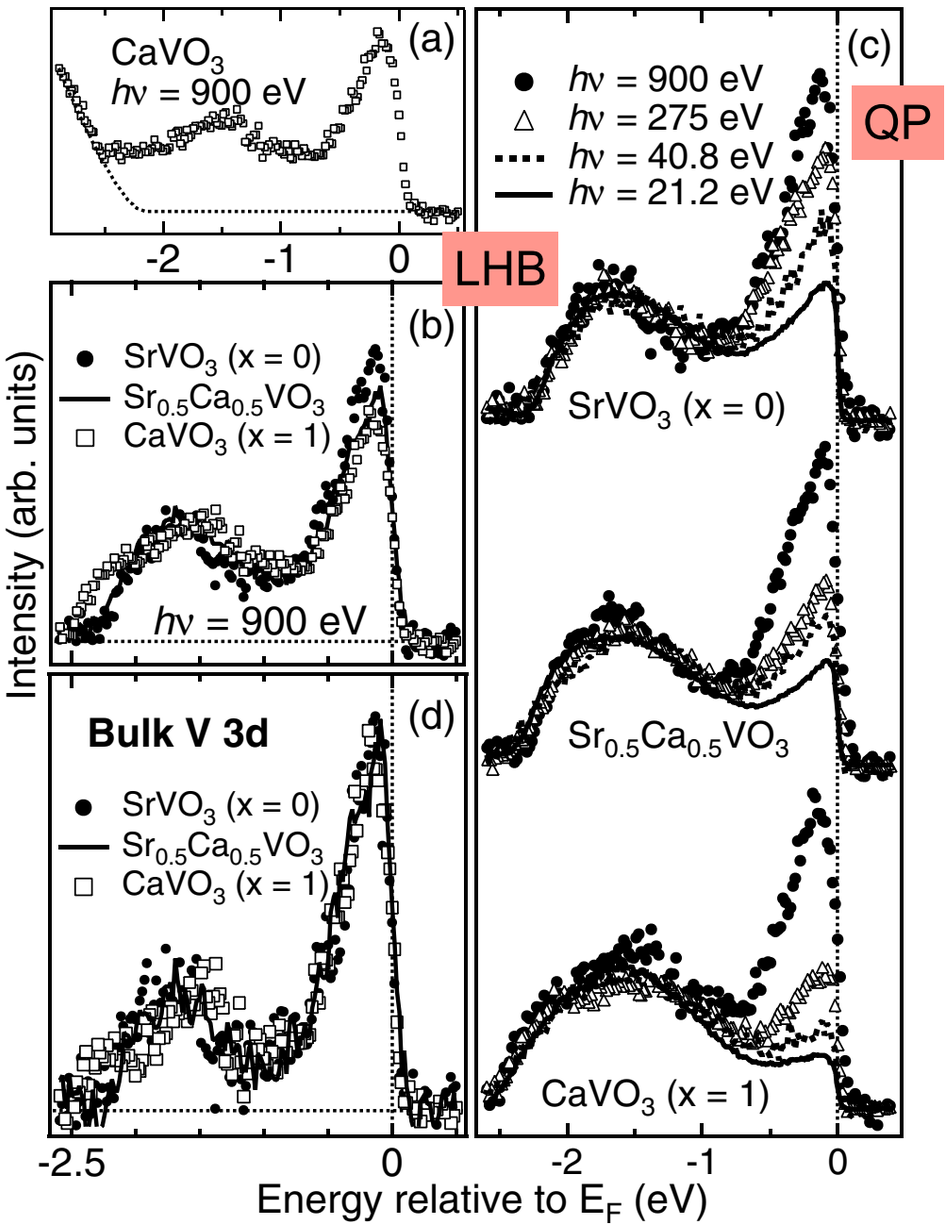

G. Kotliar and D. Vollhardt, Physics Today 57 (2004)

: solved by dynamical mean-field theory (DMFT)

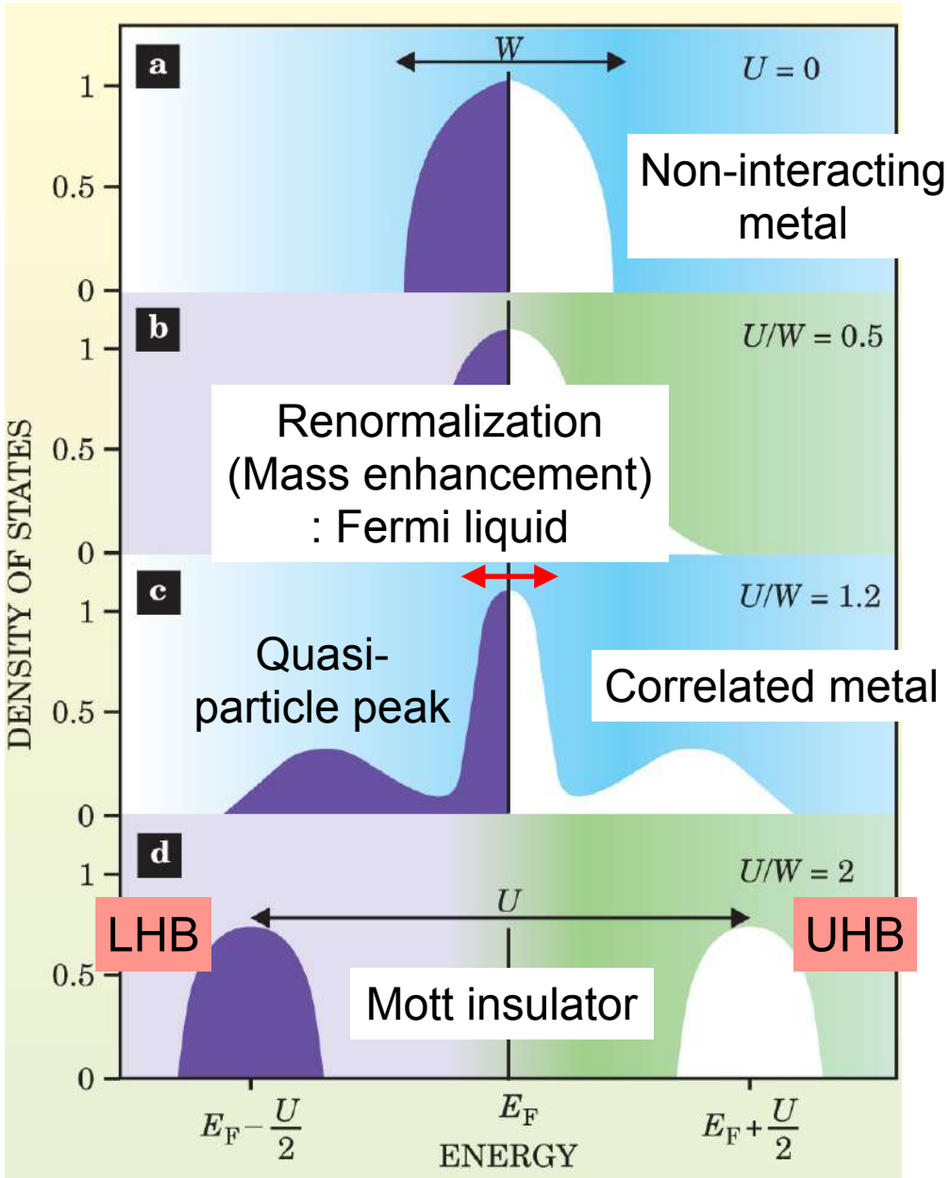

X-ray photoemission spectroscopies and DFT theory

Hubbard model with ligand orbitals included (*dp* model)

Hubbard term $H_{\mathrm{Hubbard}} = \sum_i U n_{i\uparrow} n_{i\downarrow}$

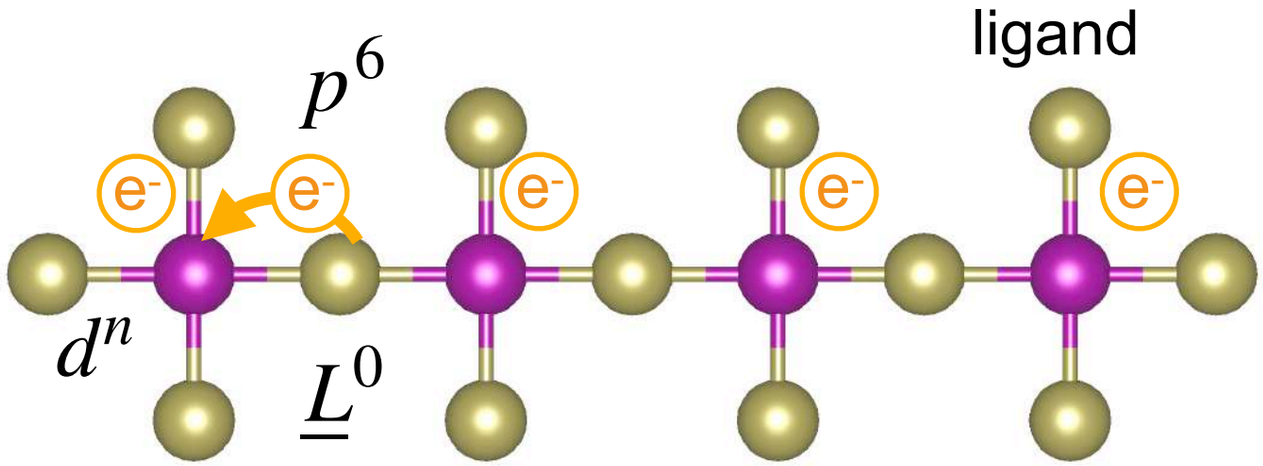

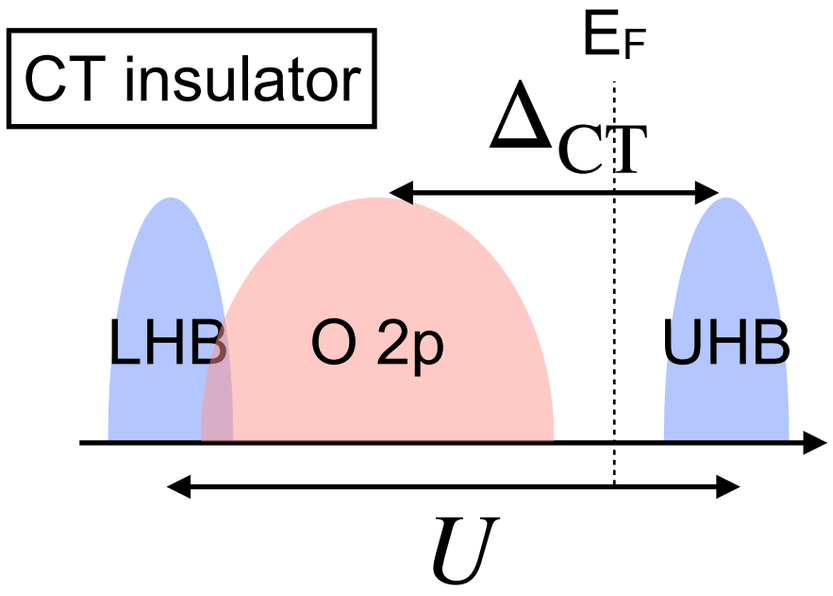

Before: $d^n \quad p^6\ (\underline{L}^0) \quad n\varepsilon_d +_n C_2 \times U + 6\varepsilon_p$

After : $d^{n+1} \quad p^5\ (\underline{L}^1) \quad (n+1)\varepsilon_d +_{n+1} C_2 \times U + 5\varepsilon_p$

Energy cost Δ_{CT} (Charge-transfer energy)

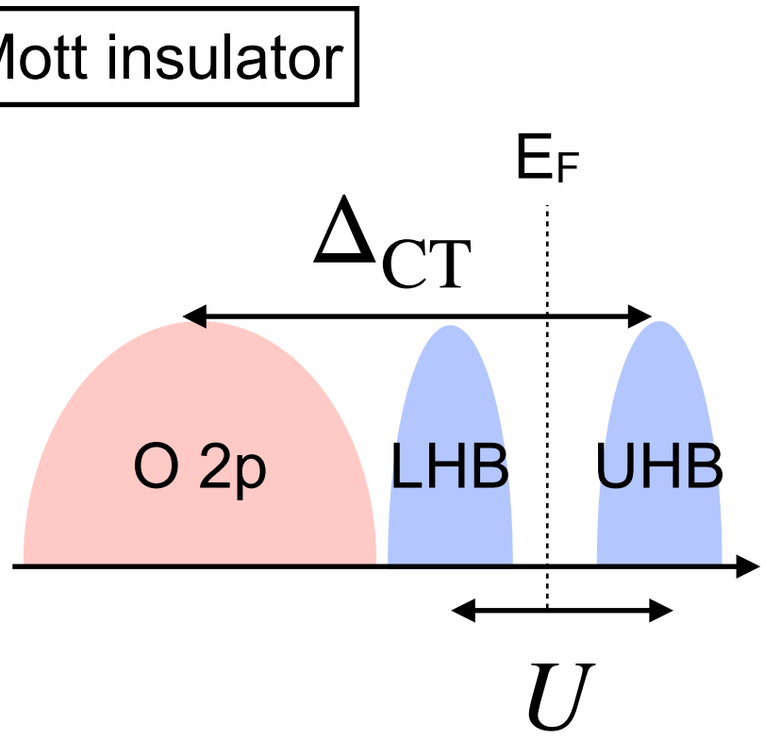

When U > Δ_{CT}, the band gap is characterized by upper Hubbard band (above E_F) and O 2*p* bands (below E_F)

: Charge-transfer insulator

X-ray photoemission spectroscopies and DFT theory

Zaanen-Sawatzky-Allen diagram

J. Zaanen, G. A. Sawatzky, J. W. Allen, PRL **55**, 418 (1985)

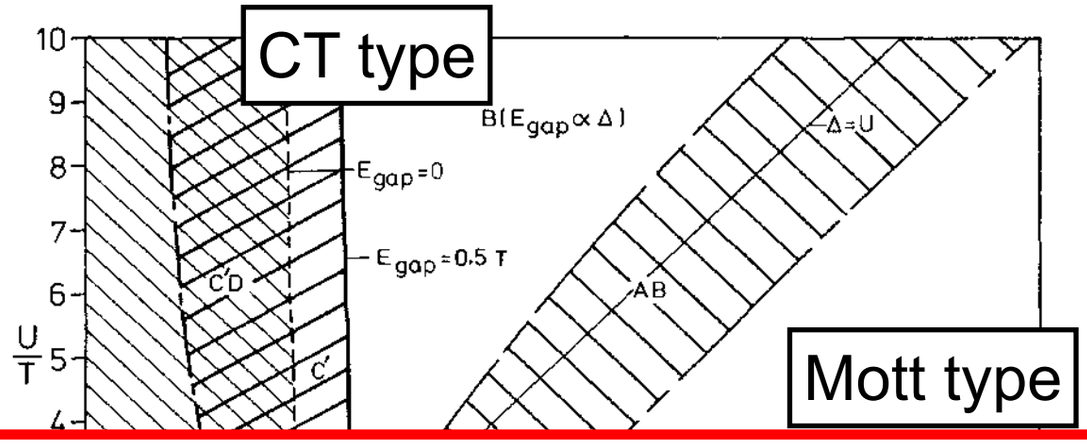

A. E. Bocquet et al., PRB **53**, 1161 (1996)

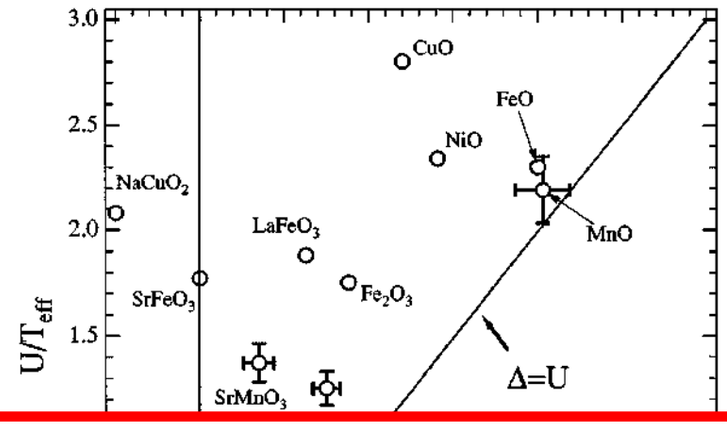

Both correlated *d* states and noninteracting (or weakly interacting) ligands are important in characterizing the low-energy excitations

CT insulator

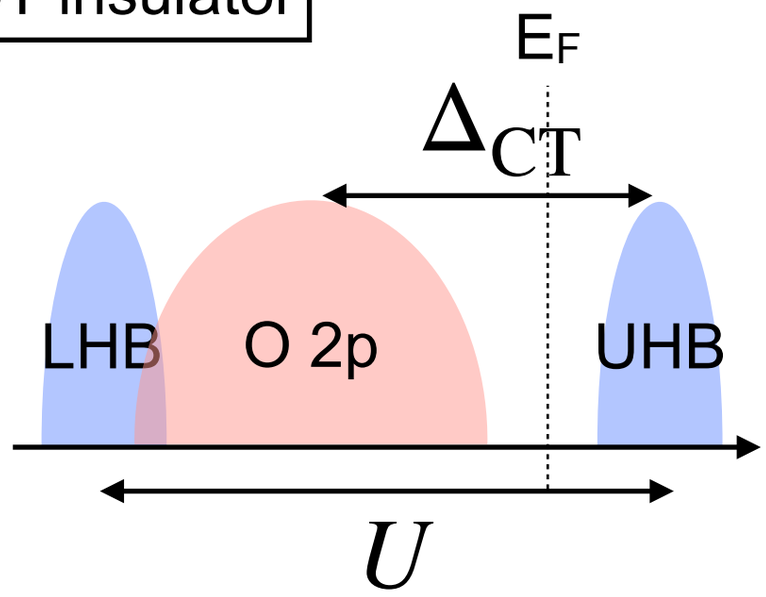

Mott insulator

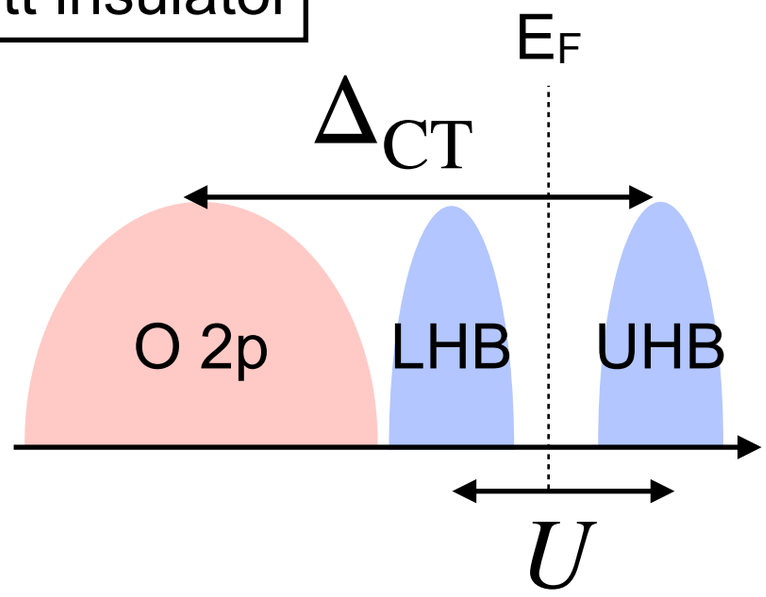

Dynamical mean-field theory (DMFT)

Ref. A. Georges et al., RMP **68**, 13 (1996), G. Kotliar et al., RMP. **78**, 865 (2006)

Lattice model

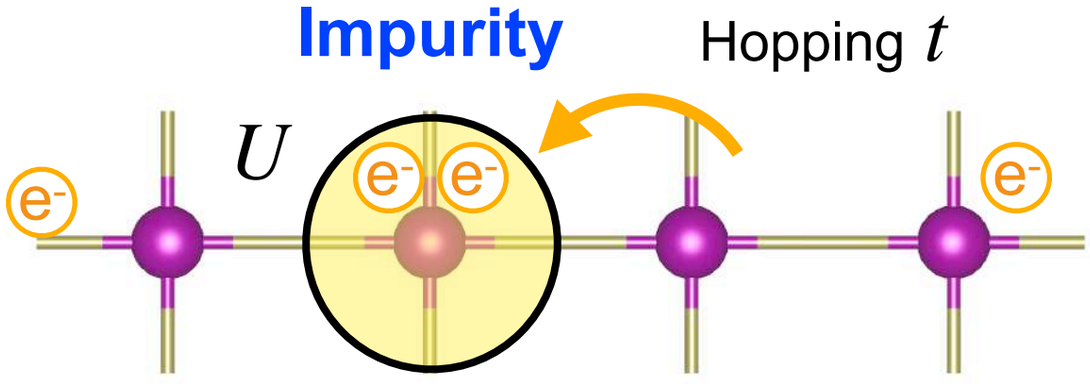

$$H_{\text{lattice}} = \sum_{i\sigma} \varepsilon_d n_{i,\sigma} + \sum_i U n_{i\uparrow} n_{i\downarrow} + t \sum_{i,\sigma} \left(d^{\dagger}_{i+1,\sigma} d_{i,\sigma} + d^{+}_{i,\sigma} d_{i+1,\sigma} \right)$$

Embedding

$$G_{\text{loc}}(\omega) = \frac{1}{\omega - \varepsilon_d - \Delta(\omega)} = \frac{1}{N_k} \sum_k \frac{1}{\omega - \varepsilon_k}$$

Hybridization density
(between impurity and the rest of the lattice)

Anderson impurity model

$$\sum_i U n_{i\uparrow} n_{i\downarrow}$$

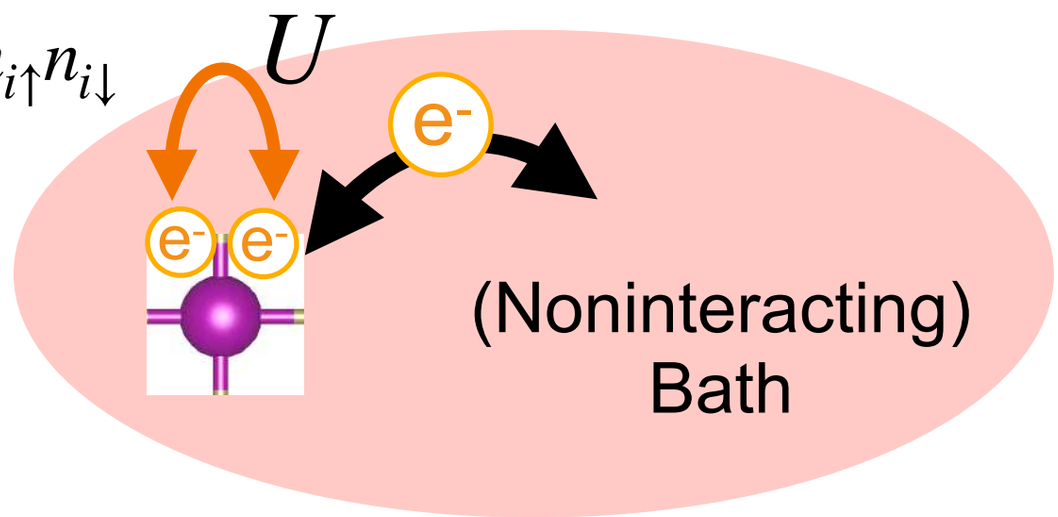

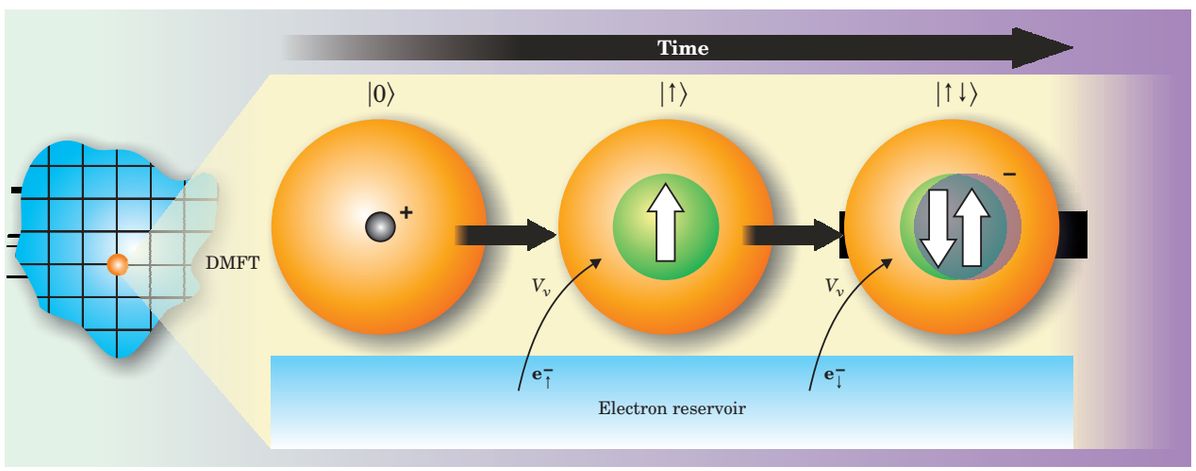

Dynamical mean-field theory (DMFT)

Ref. A. Georges et al., RMP **68**, 13 (1996), G. Kotliar et al., RMP. **78**, 865 (2006)

Lattice model

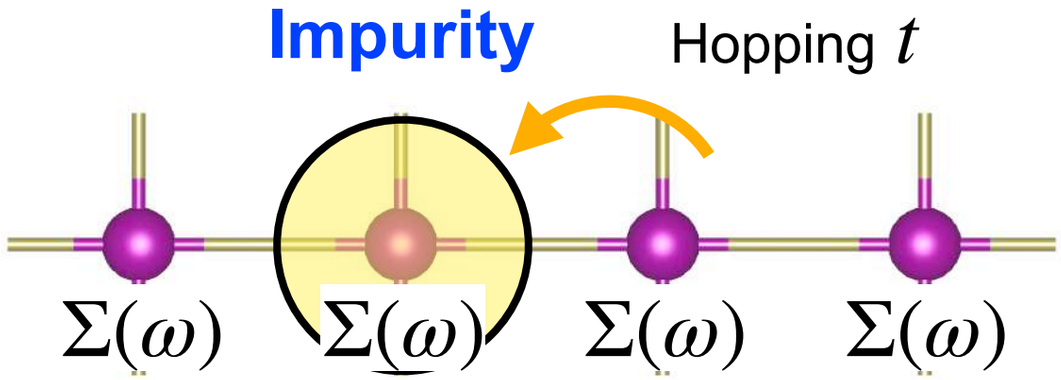

$$H_{\text{lattice}} = \sum_{i\sigma} \varepsilon_d n_{i,\sigma} + \sum_i U n_{i\uparrow} n_{i\downarrow} + t \sum_{i,\sigma} \left(d^{\dagger}_{i+1,\sigma} d_{i,\sigma} + d^{+}_{i,\sigma} d_{i+1,\sigma} \right)$$

$$G_{\text{AIM}}(\omega) = \frac{1}{\omega - \varepsilon_d - \Delta(\omega) - \Sigma(\omega)}$$

$$\Sigma(\omega, \cancel{\mathbf{k}})$$

No $\mathbf{k}$ dep.

Local electron self-energy

(correlated dynamics at transition-metal site)

Anderson impurity model

$$\sum_i U n_{i\uparrow} n_{i\downarrow}$$

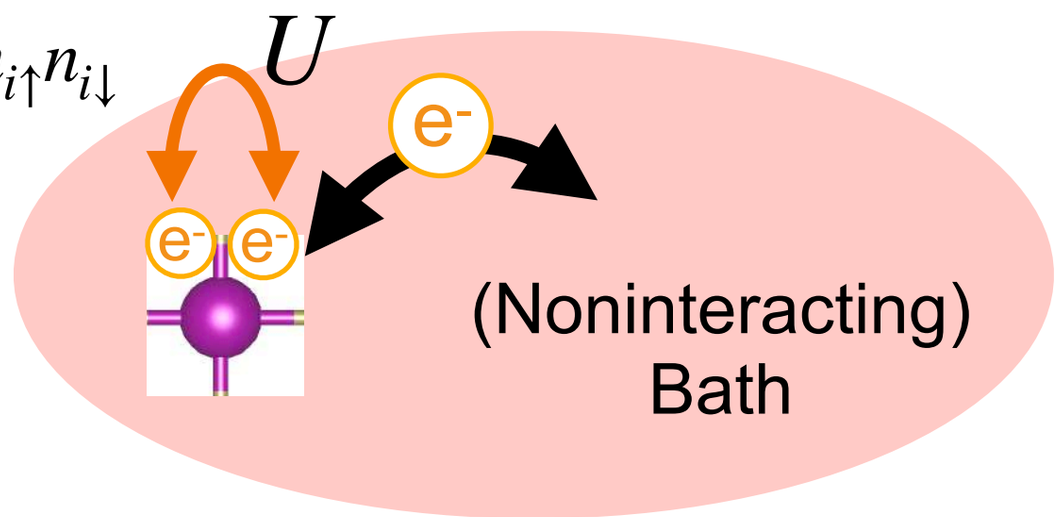

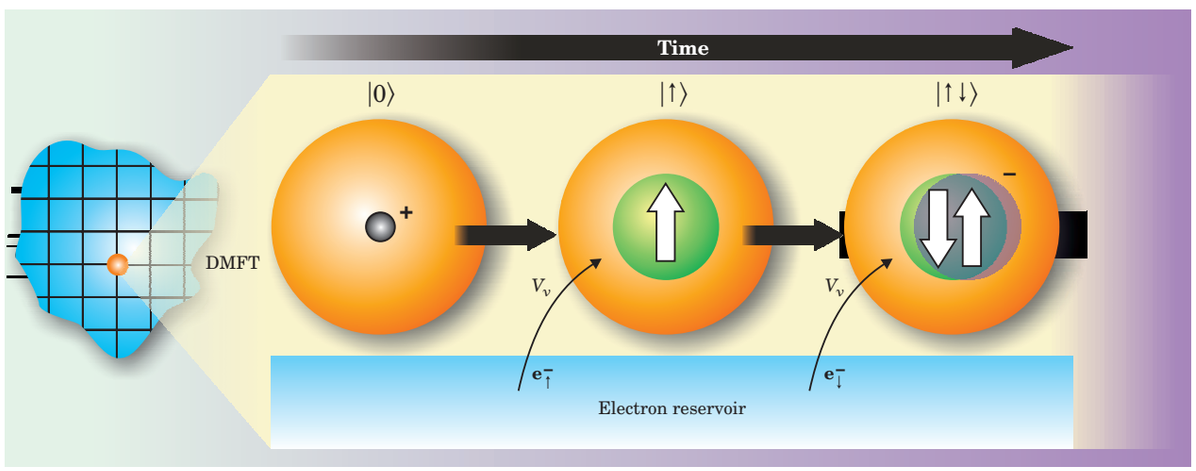

Dynamical mean-field theory (DMFT)

Ref. A. Georges et al., RMP **68**, 13 (1996), G. Kotliar et al., RMP. **78**, 865 (2006)

Lattice model

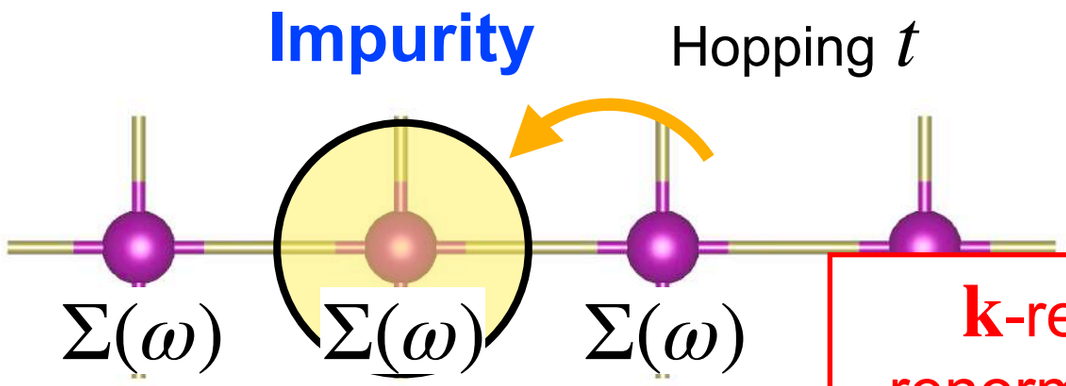

$$H_{\text{lattice}} = \sum_{i\sigma} \varepsilon_d n_{i,\sigma} + \sum_i U n_{i\uparrow} n_{i\downarrow} + \sum \left(d^{\dagger}_{i,\sigma} d_{i,\sigma} + d^{+}_{i,\sigma} d_{i+1,\sigma} \right)$$

k-resolved spectral density renormalized by local interaction

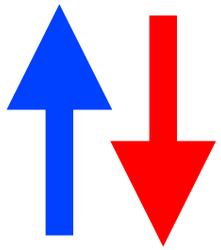

$$G_{\text{loc}}(\omega) = \frac{1}{N_k} \sum_k \frac{1}{\omega - \varepsilon_k - \Sigma(\omega)} = G_{\text{imp}}(\omega)$$

: self-consistent condition

Anderson impurity model

$$\sum_i U n_{i\uparrow} n_{i\downarrow}$$

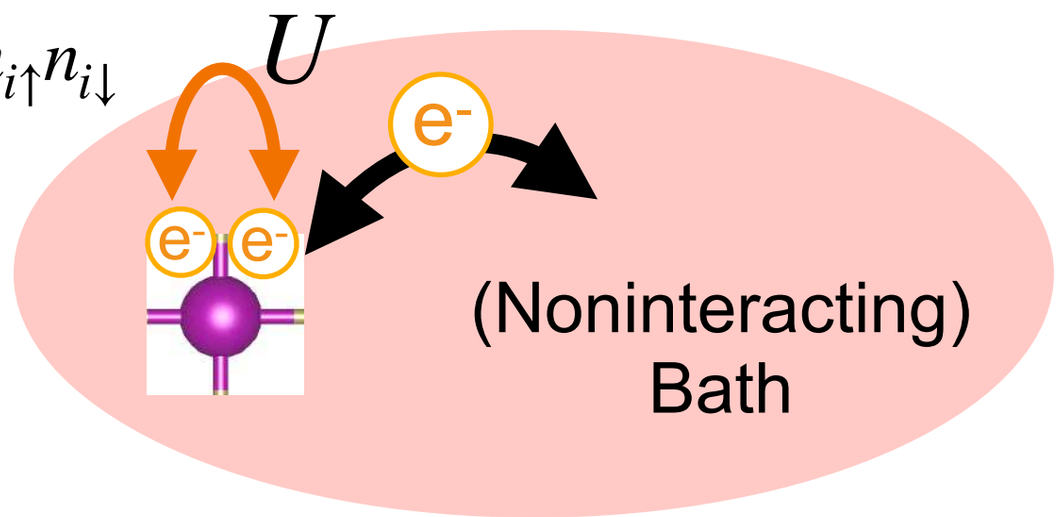

$\Sigma(\omega, \mathbf{k})$: exact in infinite lattice dimension

(incl. all local skeleton diagram contributions)

No **k** dep.

Extension of DMFT to recover **k**-dependence

- Cluster embedding
- Diagrammatic extension …

Ref. G. Rohrenger et al., Rev. Mod. Phys. **90**, 025003 (2018)
T. Maier et al., Rev. Mod. Phys. **77**, 1027 (2005)

DFT + Dynamical mean-field theory (DMFT)

There are different implementations, see e.g.
K. Haule et al., Phys. Rev. Lett. **115**, 256402 (2015)

dp space (Ni 3*d* + O 2*p*)

✔ Both low- and high-energy physics can be captured, incl. cases where ligands (non-interacting bands) are directly involved

✖ The double-counting correction must be properly determined

NiO (LDA, Wien2K)

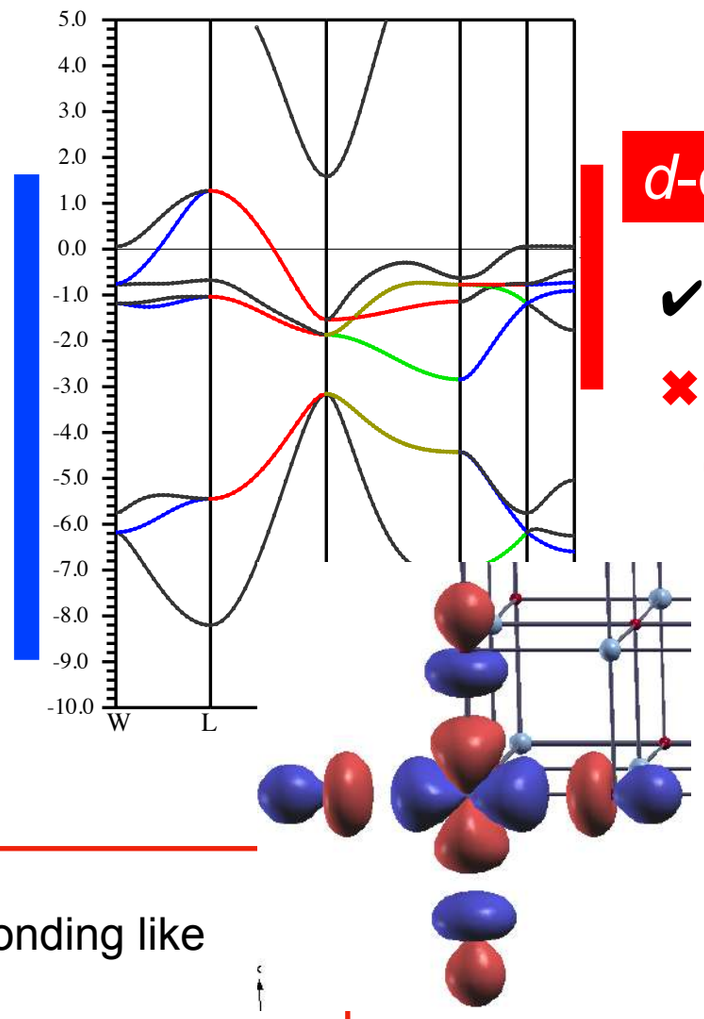

d-only space (Ni 3*d* dominant)

✔ Computationally cheap, simple

✖ Ligand *p* not included (explicitly)
(Covent bonding information encoded in the low-energy band)

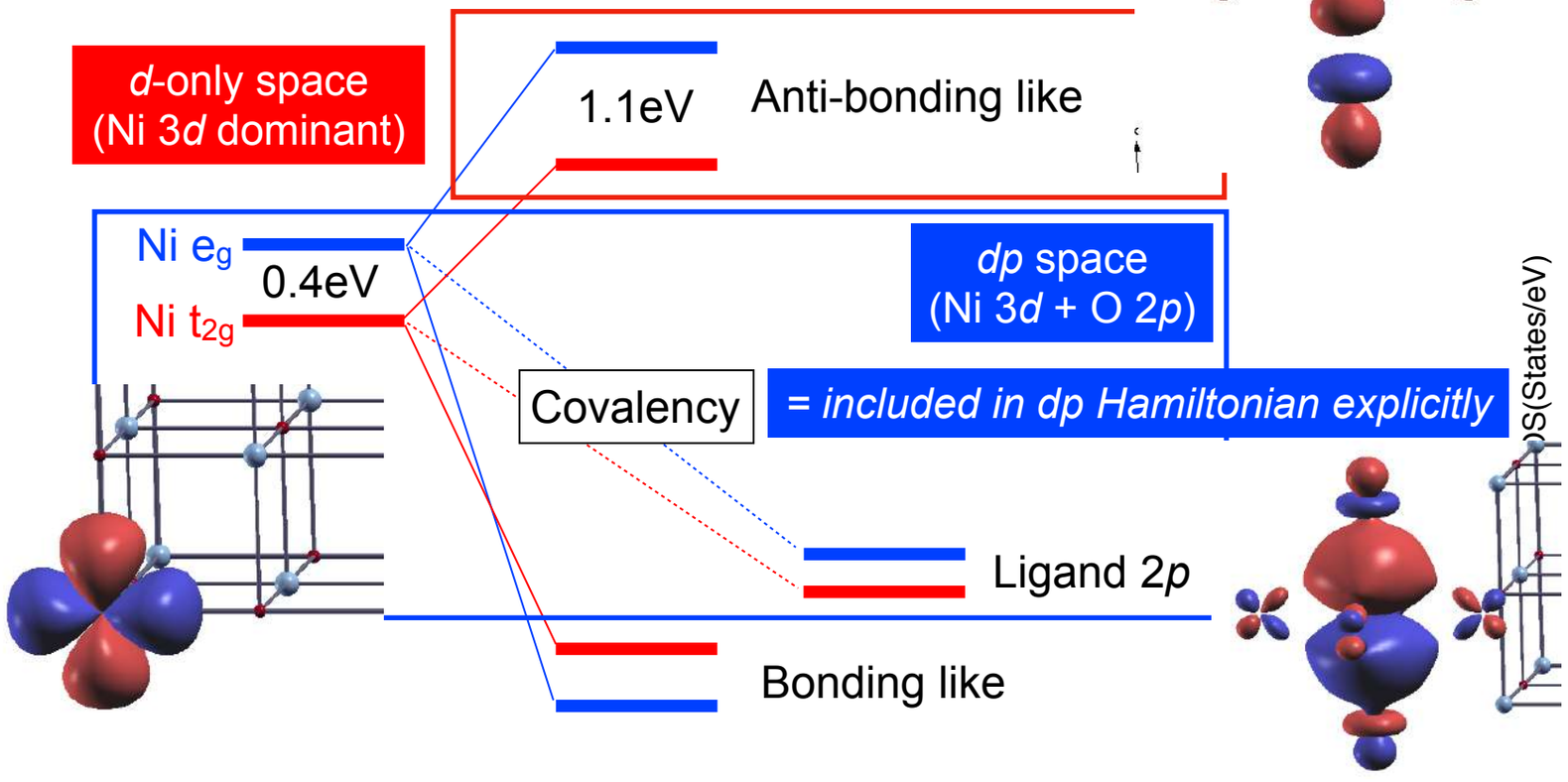

Density of states

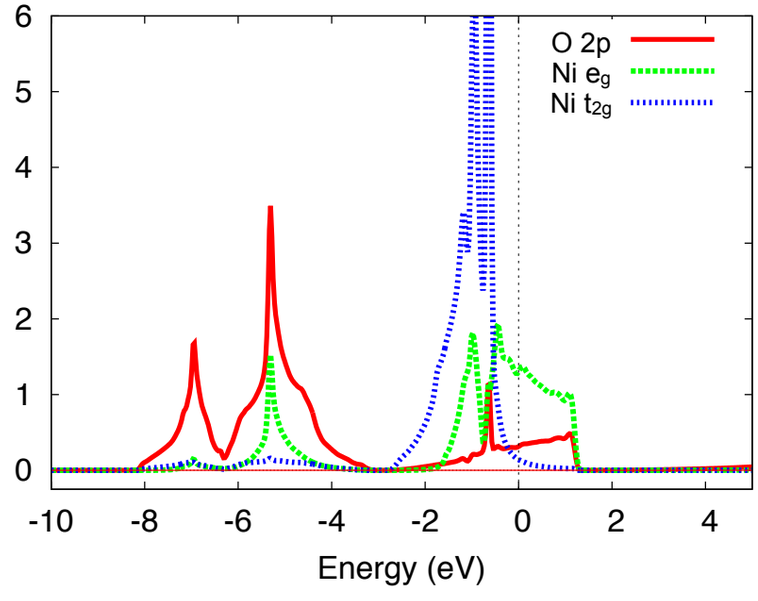

DFT + Dynamical mean-field theory (DMFT)

dp space (Ni 3*d* + O 2*p*)

✔ Both low- and high-energy physics can be captured, incl. cases where ligands (non-interacting bands) are directly involved

✖ The double-counting correction must be properly determined

NiO (LDA, Wien2K)

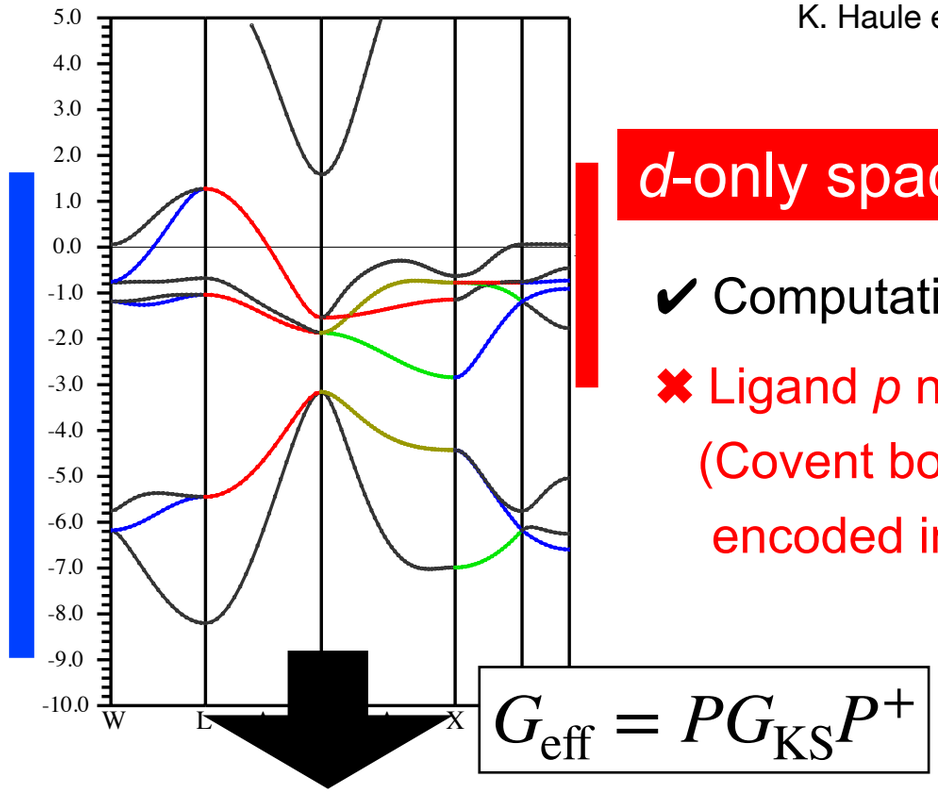

There are different implementations, see e.g.

K. Haule et al., Phys. Rev. Lett. **115**, 256402 (2015)

d-only space (Ni 3*d* dominant)

✔ Computationally cheap, simple

✖ Ligand *p* not included (explicitly) (Covent bonding information encoded in the low-energy band)

Tight-binding model from the target bands (*d*-only, *dp*) via wannier function

WANNIER90

wannier90: A tool for obtaining maximally-localised Wannier functions

A. A. Mostofi, et al., Comput. Phys. Commun. 178, 685 (2008)

with 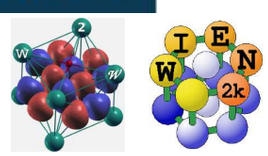

$$|\mathbf{R}, n\rangle = \frac{V}{(2\pi)^3}\int_{\mathrm{BZ}}\sum_{m} U_{nm}^{(\mathbf{k})}\,|\psi_m(\mathbf{k})\rangle e^{-i\mathbf{k}\cdot\mathbf{R}} d^3\mathbf{k}$$

(Localized) Wannier functions = basis for tight-binding model

Bloch bands

The k-dependent phase (unitary matrix) is often chosen to minimize the spread of Wannier functions.

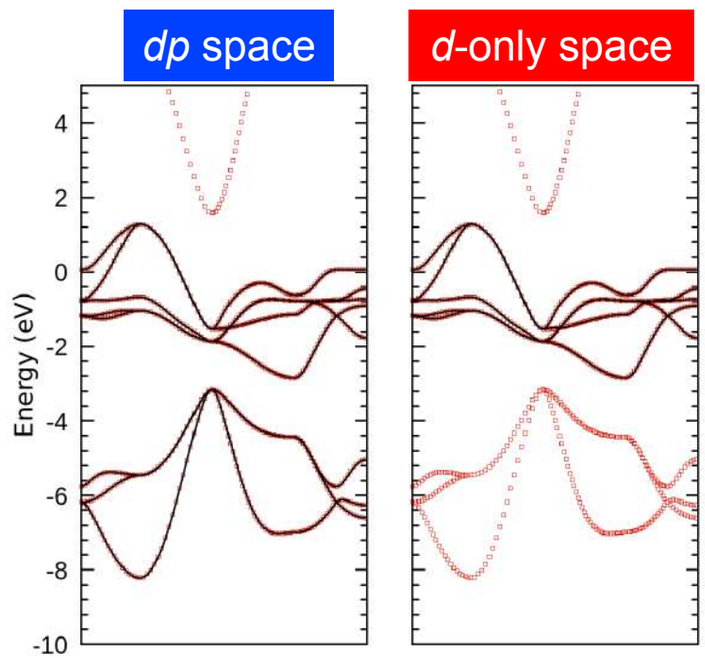

DFT + Dynamical mean-field theory (DMFT)

There are different implementations, see e.g.
K. Haule et al., Phys. Rev. Lett. **115**, 256402 (2015)

dp space (Ni 3*d* + O 2*p*)

✔ Both low- and high-energy physics can be captured, incl. cases where ligands (non-interacting bands) are directly involved

✖ The double-counting correction must be properly determined

NiO (LDA, Wien2K)

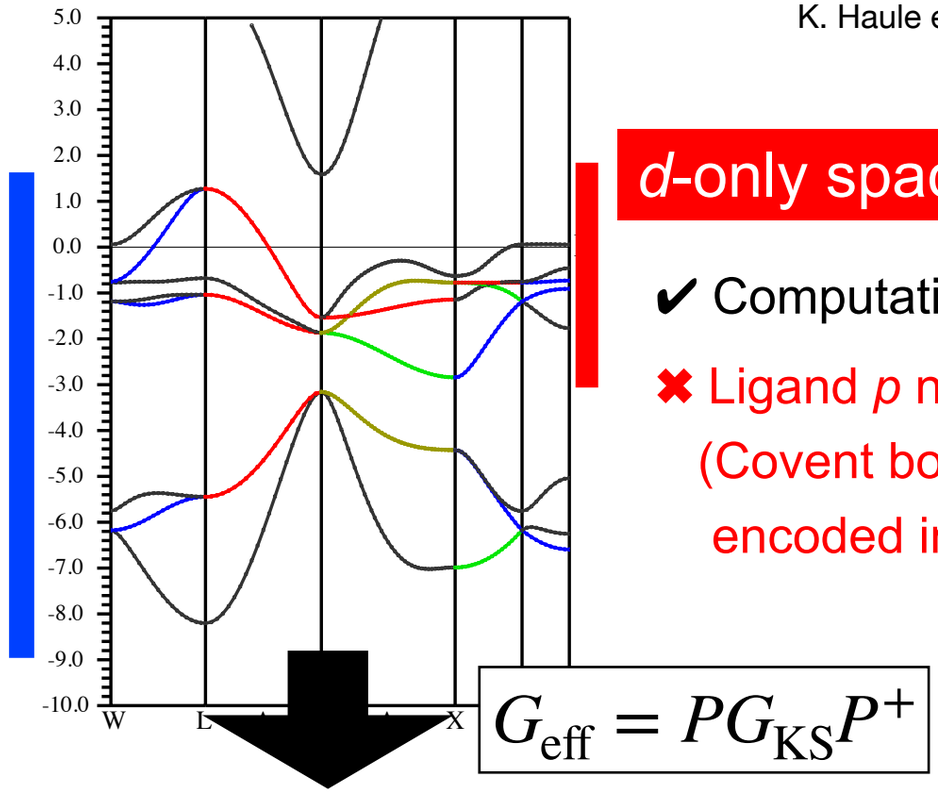

d-only space (Ni 3*d* dominant)

✔ Computationally cheap, simple

✖ Ligand *p* not included (explicitly)
(Covent bonding information encoded in the low-energy band)

Tight-binding model from the target bands (*d*-only, *dp*) via wannier function

Non-interacting → Interacting

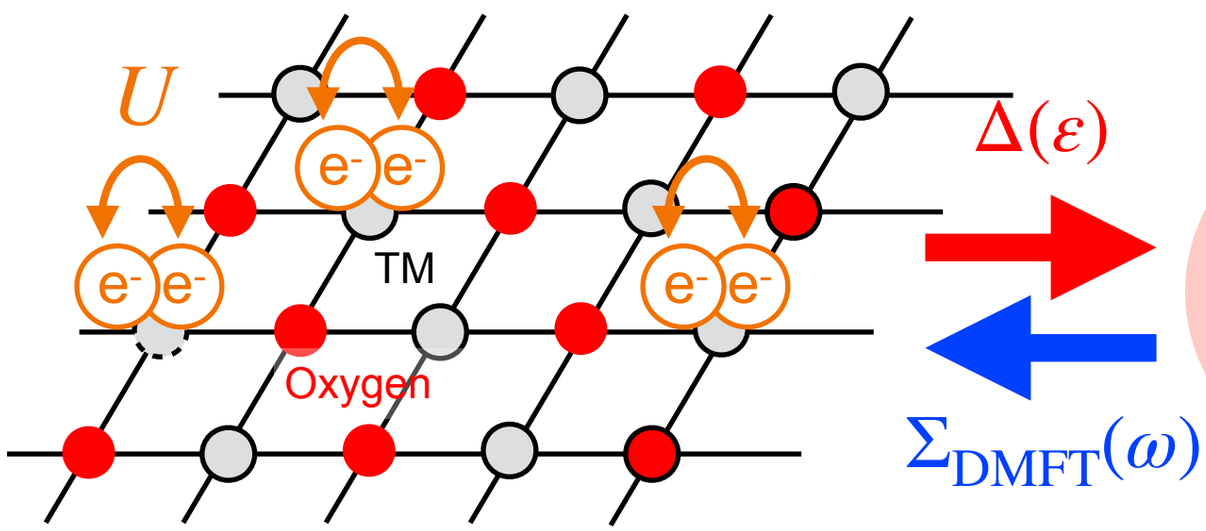

Embedding: lattice → Impurity coupled with noninteracting bath

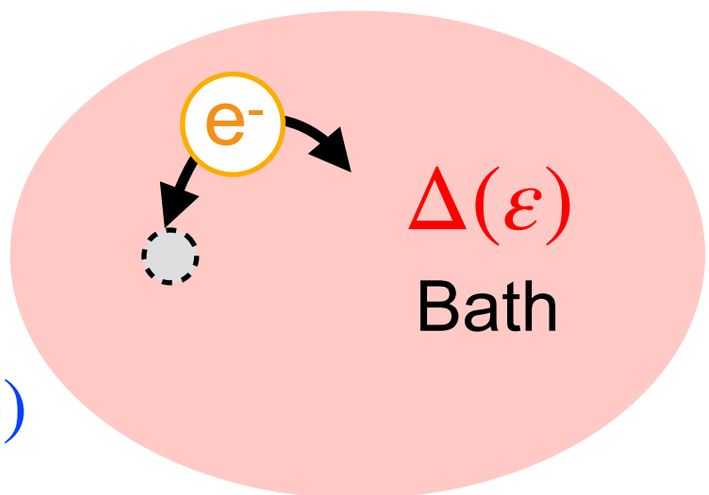

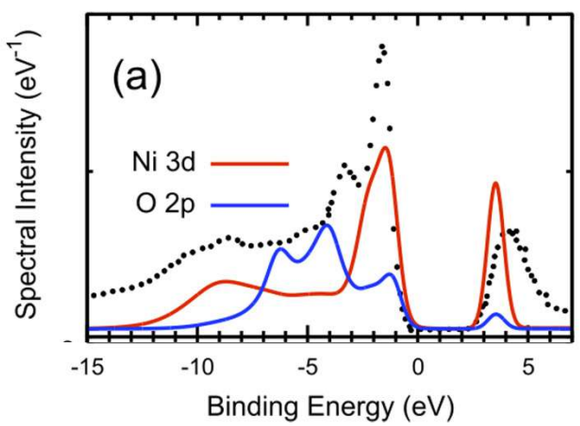

DFT + Dynamical mean-field theory (DMFT)

VOLUME 53, NUMBER 24 PHYSICAL REVIEW LETTERS 10 DECEMBER 1984

Magnitude and Origin of the Band Gap in NiO

G. A. Sawatzky[(a)] and J. W. Allen
Xerox Palo Alto Research Center, Palo Alto, California 94304
(Received 5 July 1984)

Photoemission and bremsstrahlung-isochromat-spectroscopy data on a cleaved NiO single crystal are presented and compared to band- and cluster-theory predictions. In contrast to band-theory predictions the band gap is found to be large but not determined solely by the even larger d-d Coulomb interactions so that NiO is not a Mott-Hubbard insulator in the simplest sense. A large d-d interaction need not prevent NiS from being a metal.

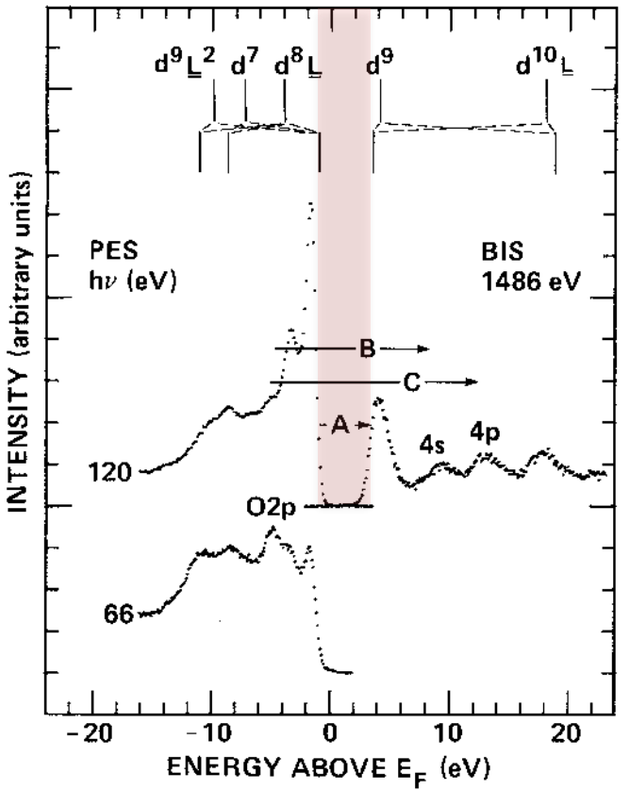

LDA density of states

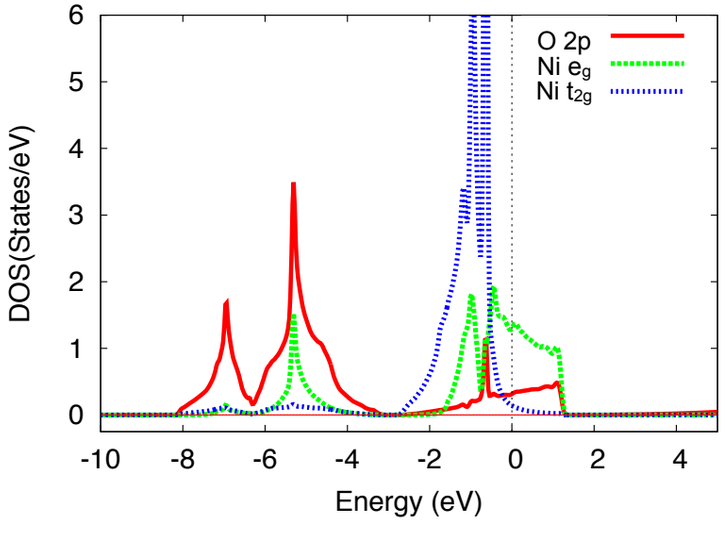

NiO (LDA, Wien2K)

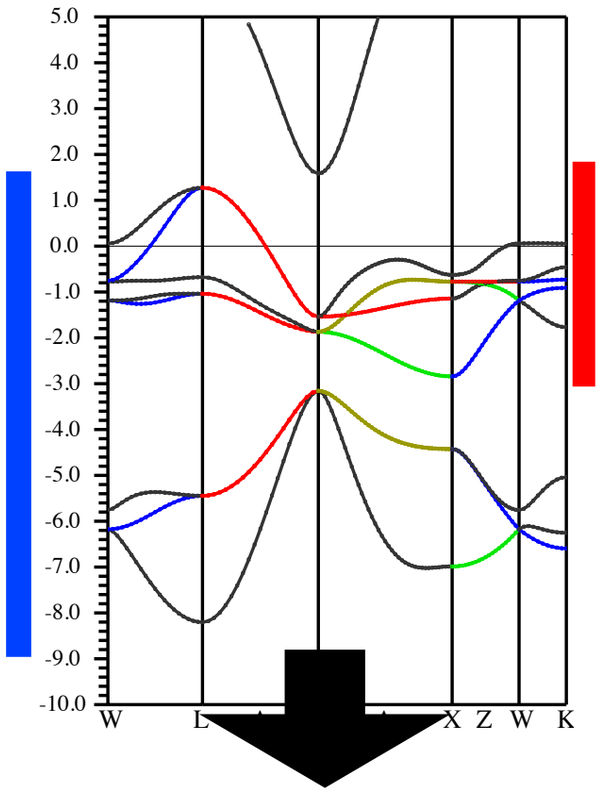

There are different implementations, see e.g.
K. Haule et al., Phys. Rev. Lett. **115**, 256402 (2015)

d-only space (Ni 3*d* dominant)

✔ Computationally cheap, simple

✖ Ligand *p* not included (explicitly)
(Covent bonding information
encoded in the low-energy band)

DFT + DMFT

A. Hariki et al., Phys. Rev. B **101**, 115130 (2020)

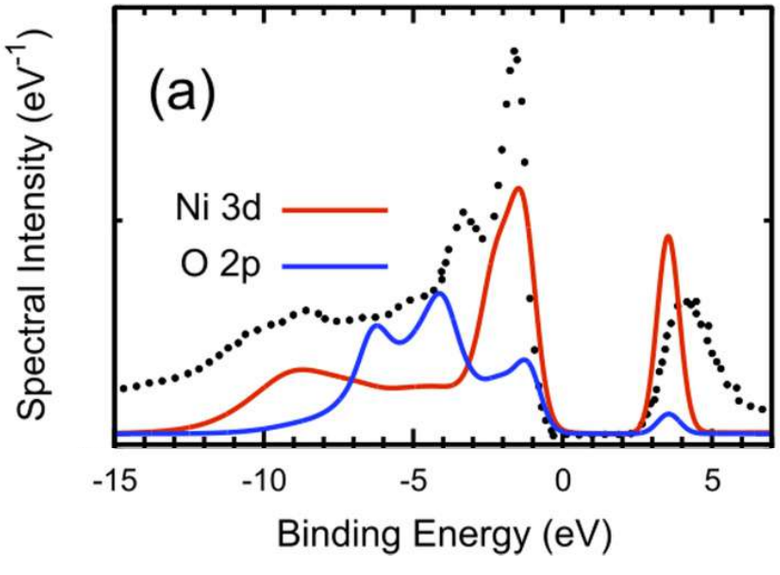

✔ Large insulating gap
in paramagnetic solution

✔ Complex spectral distribution
due to many-body effect

DFT + Dynamical mean-field theory (DMFT)

Q1. How to determine the interacting part of the Hamiltonian

DFT based routes

✔ Constrained LDA, Constrained RPA

F. Aryasetiawan et al., Phys. Rev. B **70**, 195104 (2004)

Experimental routes

✔ Fitting various spectroscopic experiment

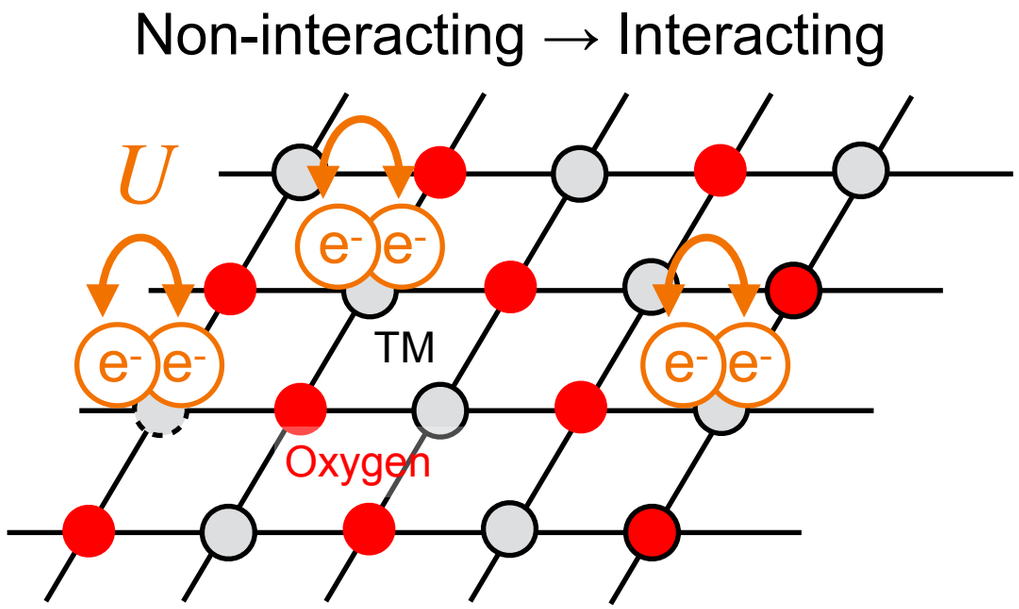

Screened interaction W

F. Aryasetiawan et al., Phys. Rev. B **70**, 195104 (2004)

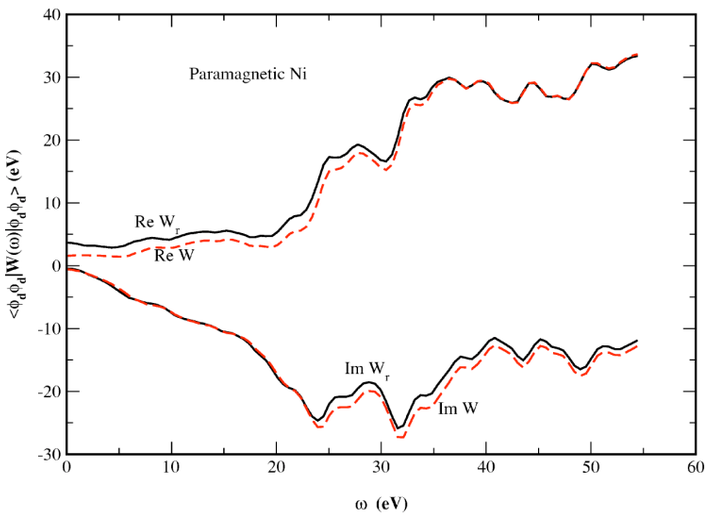

Polarisation: $P = Pd + Pr$

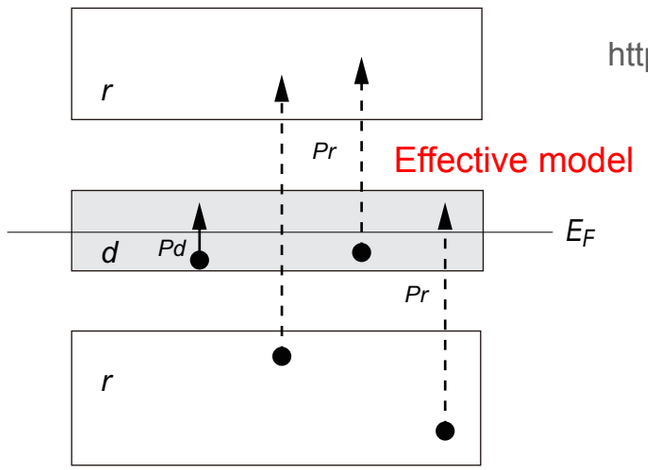

Julich Autumn School on Correlated Electrons (2011)

https://www.cond-mat.de/events/correl11/manuscripts/aryasetiawan.pdf

7 The Constrained RPA Method for Calculating the Hubbard *U* from First-Principles

F. Aryasetiawan,[1] T. Miyake,[2,3] and R. Sakuma[1]

[1] Graduate School of Advanced Integration Science Chiba University, Japan

[2] Nanosystem Research Institute, AIST, Japan

[3] Japan Science and Technology Agency, CREST

Fully screened Coulomb interaction $W = [1 - W_d P_d]^{-1} W_d$

Screened Coulomb interaction in effective model

PHYSICAL REVIEW RESEARCH 6, 033068 (2024)

Editors' Suggestion

Quantifying the U 5*f* covalence and degree of localization in U intermetallics

Andrea Marino,[1,2,*] Denise S. Christovam,[1] Daisuke Takegami,[1,3] Johannes Falke,[1] Miguel M. F. Carvalho,[1,4] Takaki Okauchi,[5] Chun-Fu Chang,[1] Simone G. Altendorf,[1] Andrea Amorese,[1,4,†] Martin Sundermann,[1,6] Andrei Gloskovskii,[6] Hlynur Gretarsson,[6,7] Bernhard Keimer,[7] Alexandr V. Andreev,[8] Ladislav Havela,[9] Andreas Leithe-Jasper,[1] Andrea Severing,[4,1] Jan Kuneš,[10] Liu Hao Tjeng,[1,‡] and Atsushi Hariki[5,§]

[1]*Max Planck Institute for Chemical Physics of Solids, Nöthnitzer Straße 40, 01187 Dresden, Germany*

[2]*Institute of Solid State and Materials Physics, TU Dresden, 01069 Dresden, Germany*

[3]*Department of Applied Physics, Waseda University, 3-4-1 Okubo, Shinjuku-ku, Tokyo 169-8555, Japan*

[4]*Institute of Physics II, University of Cologne, Zülpicher Straße 77, 50937 Cologne, Germany*

[5]*Department of Physics and Electronics, Osaka Metropolitan University 1-1 Gakuen-cho, Nakaku, Sakai, Osaka 599-8531, Japan*

[6]*PETRA III, Deutsches Elektronen-Synchrotron DESY, Notkestraße 85, 22607 Hamburg, Germany*

[7]*Max Planck Institute for Solid State Research, Heisenbergstraße 1, 70569 Stuttgart, Germany*

[8]*Institute of Physics, Academy of Sciences of the Czech Republic, Na Slovance 1999/2, 182 21 Prague 8, Czech Republic*

[9]*Department of Condensed Matter Physics, Faculty of Mathematics and Physics, Charles University, Ke Karlovu 5, 121 16 Prague 2, Czech Republic*

[10]*Department of Condensed Matter Physics, Faculty of Science, Masaryk University, Kotlářská 2, 611 37 Brno, Czechia*

- ✔ UGa_2 (5*f* localized), UB_2 (5*f* delocalized) with mixed (or fluctuating) valence
- ✔ Different elements (orbital) have different photoionization cross-sections

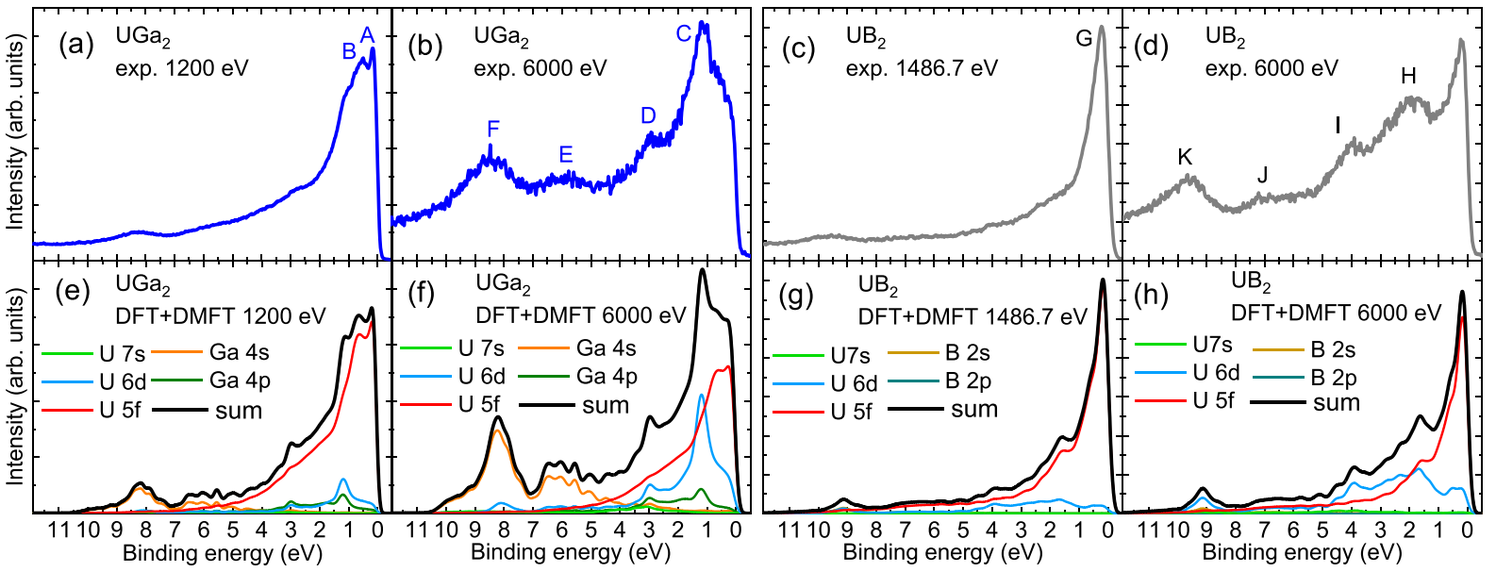

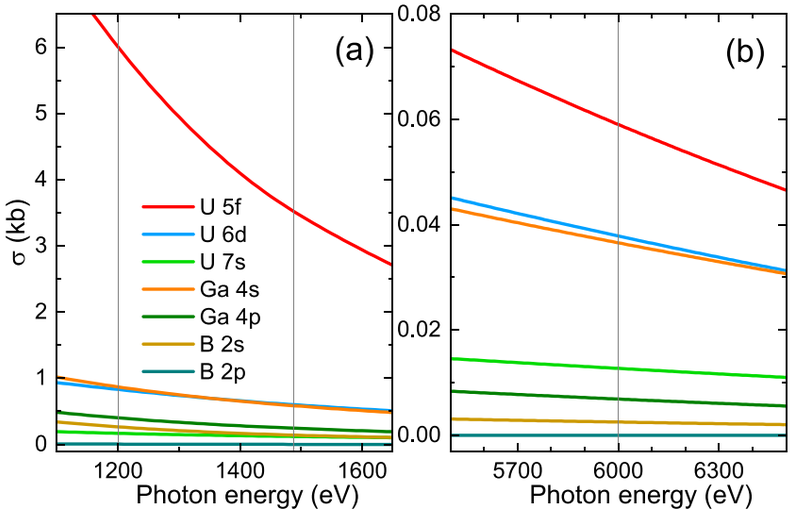

FIG. 3. Photoionization cross sections of U 5*f*, U 6*d*, U 7*s*, Ga 4*s*, Ga 4*p*, B 2*s*, B 2*p* as interpolated from Refs. [25–27]. The vertical lines indicate the photon energies where the experiments

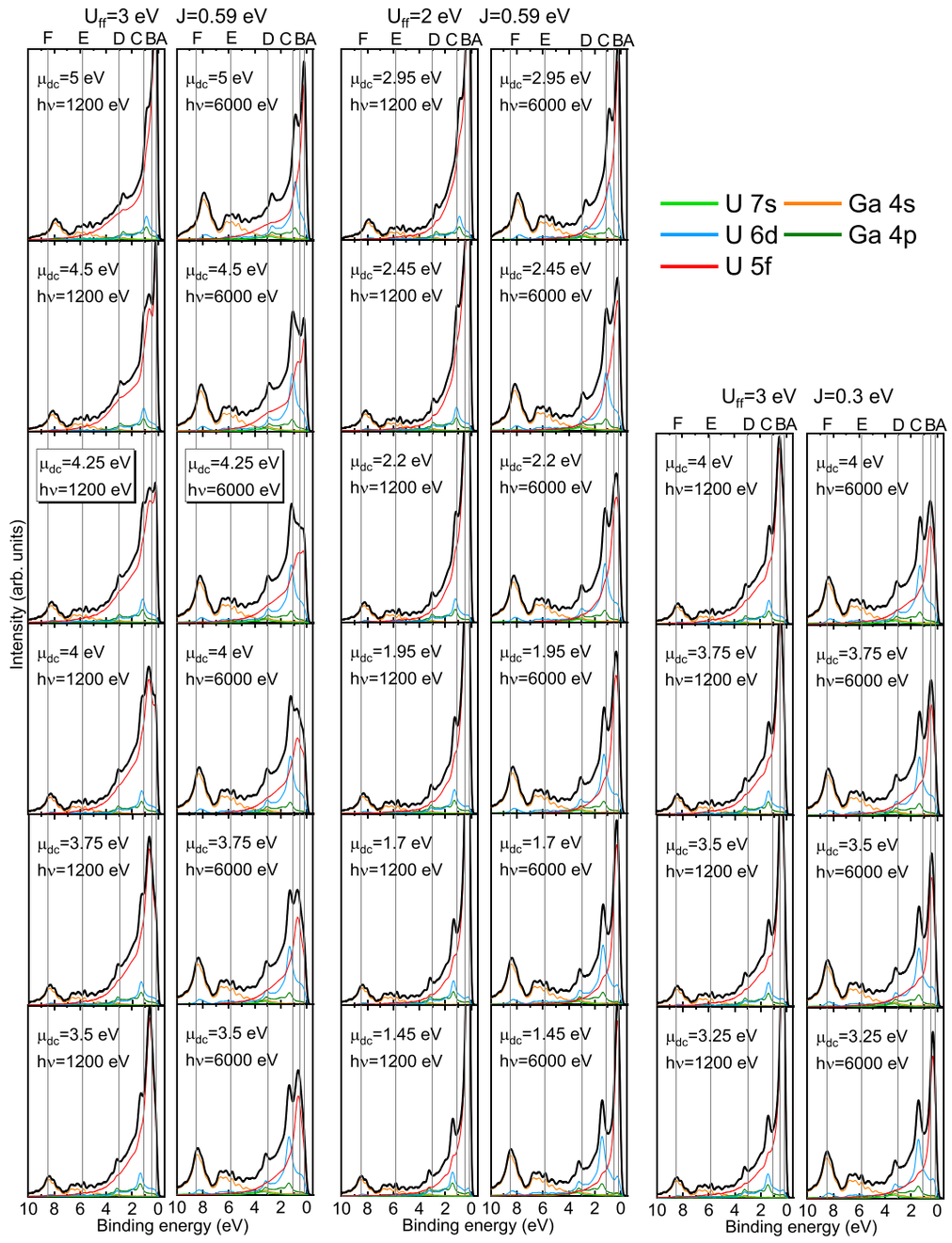

$CaCu_3Ru_4O_{12}$: A High-Kondo-Temperature Transition-Metal Oxide

D. Takegami,[1] C.-Y. Kuo,[1,2] K. Kasebayashi,[3] J.-G. Kim,[4] C. F. Chang,[1] C. E. Liu,[1,5] C. N. Wu,[1,6] D. Kasinathan,[1] S. G. Altendorf,[1] K. Hoefer,[1] F. Meneghin,[1] A. Marino,[1] Y. F. Liao,[2] K. D. Tsuei,[2] C. T. Chen,[2] K.-T. Ko,[4] A. Günther,[7] S. G. Ebbinghaus,[8] J. W. Seo,[1] D. H. Lee,[1] G. Ryu,[1] A. C. Komarek,[1] S. Sugano,[9] Y. Shimakawa,[9] A. Tanaka,[10] T. Mizokawa,[11] J. Kuneš,[12] L. H. Tjeng,[1,*] and A. Hariki[3,12,†]

[1]*Max Planck Institute for Chemical Physics of Solids, Nöthnitzer Straße 40, 01187 Dresden, Germany*
[2]*National Synchrotron Radiation Research Center, 101 Hsin-Ann Road, 30076 Hsinchu, Taiwan*
[3]*Department of Physics and Electronics, Osaka Prefecture University, 1-1 Gakuen-cho, Nakaku, Sakai, Osaka 599-8531, Japan*
[4]*Department of Physics, POSTECH, Pohang 37673, Korea*
[5]*Department of Electrophysics, National Yang Ming Chiao Tung University (NYCU), Hsinchu 30010, Taiwan*
[6]*Department of Physics, National Tsing Hua University, Hsinchu 30013, Taiwan*
[7]*Experimental Physics V, University of Augsburg, 86135 Augsburg, Germany*
[8]*Institute of Chemistry, Martin Luther University Halle-Wittenberg, 06120 Halle, Germany*
[9]*Institute for Chemical Research, Kyoto University, Uji, Kyoto 611-0011, Japan*
[10]*Quantum Matter Program, Hiroshima University, Higashi-Hiroshima 739-8530, Japan*
[11]*Department of Applied Physics, Waseda University, Shinjuku, Tokyo 169-8555, Japan*
[12]*Institute of Solid State Physics, TU Wien, 1040 Vienna, Austria*

Experimental magnetic susceptibility

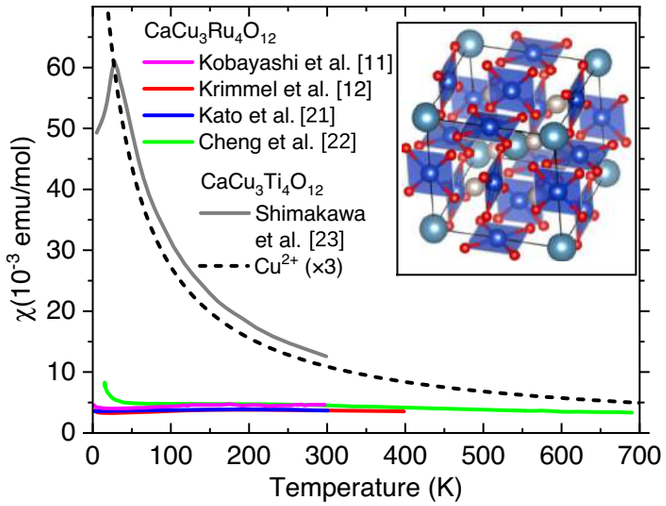

Cu^{2+}: S=1/2

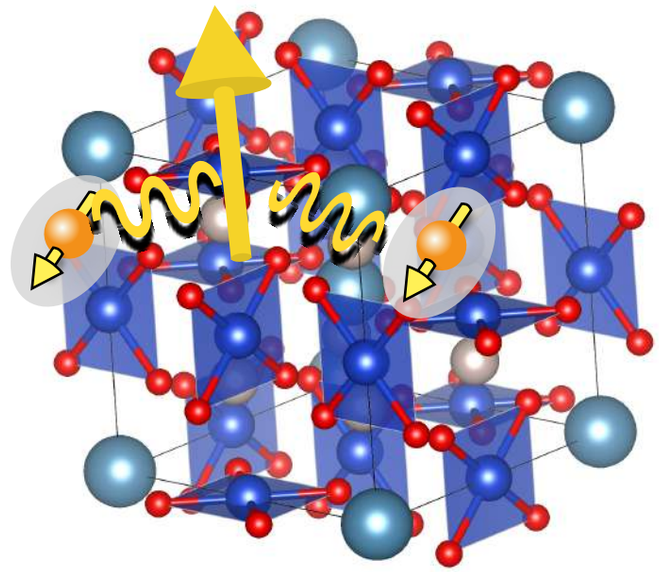

Photon-energy dependent PES

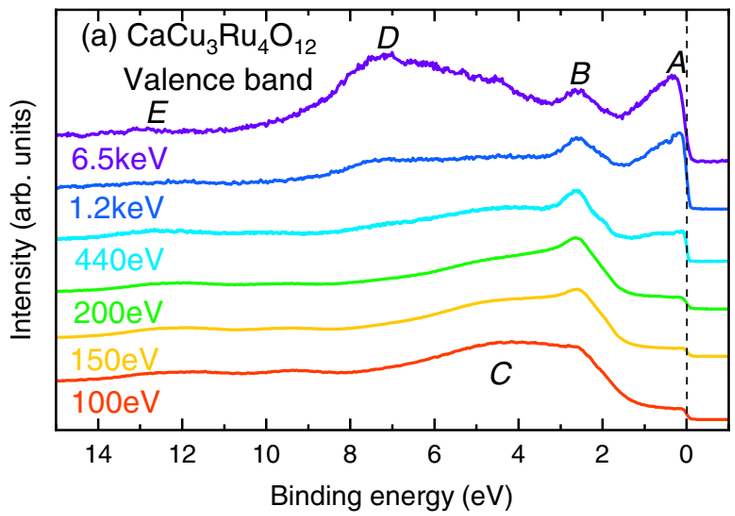

Photoionization cross-section

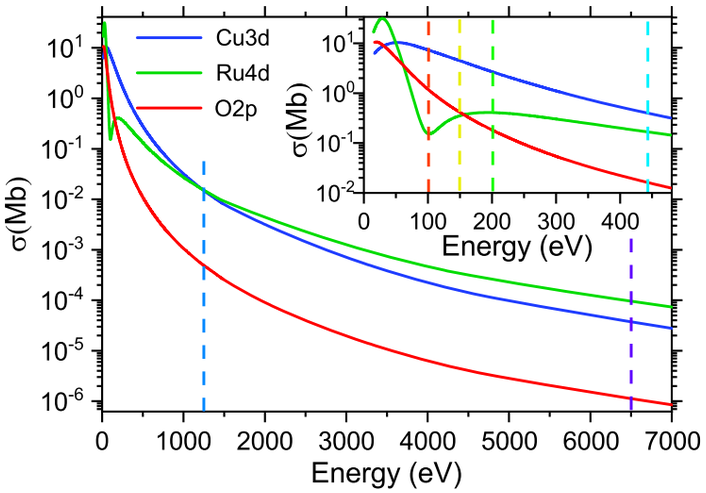

$$\chi_{\mathrm{loc}}(T) = \int_0^{1/T} d\tau \langle m_z(\tau) m_z(0) \rangle .$$

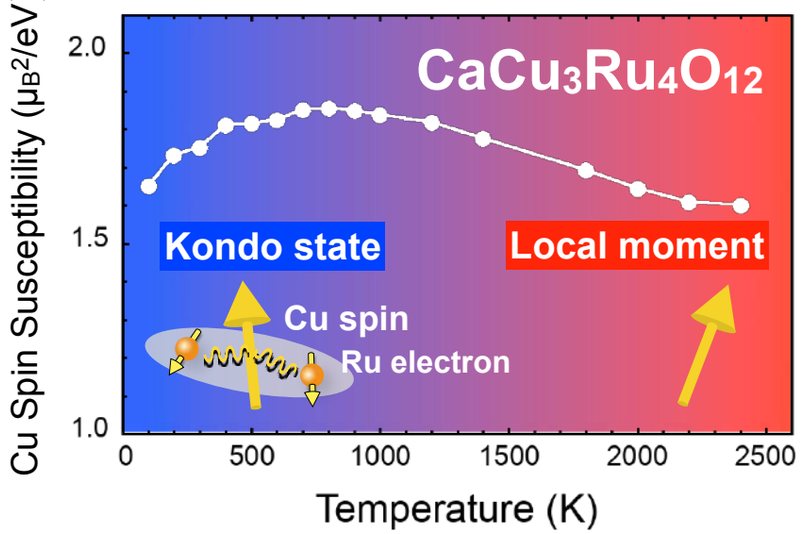

- ✔ Different elements (orbital) have different photoionization cross-sections
- ✔ DMFT is capable of many-body physics (Kondo effect) in complex correlated materials

DFT + Dynamical mean-field theory (DMFT)

Q1. How to determine the interacting part of the Hamiltonian

DFT based routes

✔ Constrained LDA, Constrained RPA

F. Aryasetiawan et al., Phys. Rev. B **70**, 195104 (2004)

Experimental routes

✔ Fitting various spectroscopic experiment

Non-interacting → Interacting

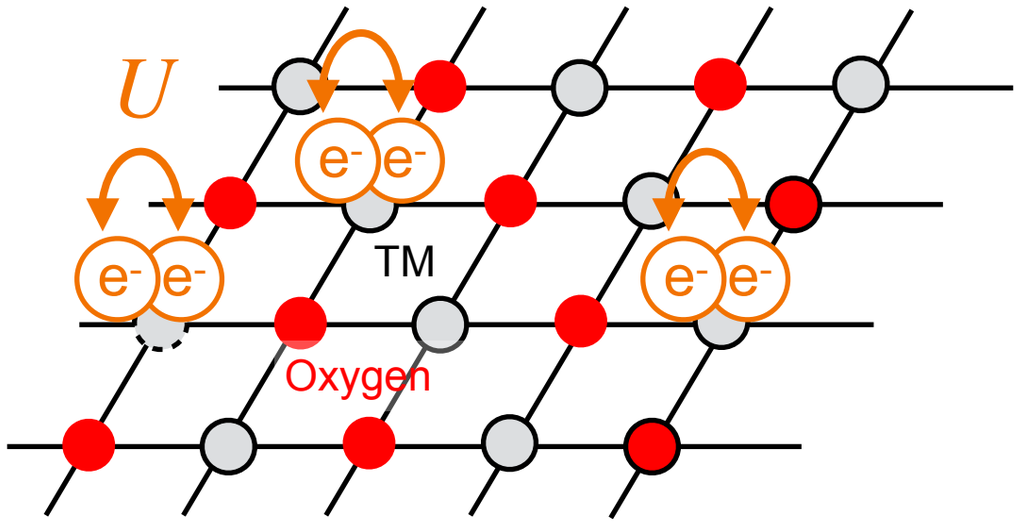

Q2. How to determine double-counting correction?

$$\varepsilon_d - \mu_{\mathrm{dc}} + \Sigma_{\mathrm{DMFT}}(\omega)$$

DFT routes

✔ Ansatz for energy functional incl. U

Ref. Double counting in LDA + DMFT — The example of NiO
M. Karolak et al., J. Electron Spectrosc. Relat. Phenom. 181 (2010) 11–15

Exact double-counting

K. Haule, Phys. Rev. Lett. **115**, 196403 (2015)

Experimental routes

✔ Fitting valence-band photoemission spectra measured with different photon energies (cross-section)

Refs.
A. Marino, A. Hariki et al., Phys. Rev. Research **6**, 033068 (2024)
K. Higashi, M. Winder, J. Kuneš, and A. Hariki, Phys. Rev. X **11**, 041009 (2021)
D. Takegami, A. Hariki et al., Phys. Rev. X **12**, 011017 (2022)

Q3. How to solve the impurity Anderson model?

✔ Development of various numerically-reliable impurity solver (e.g. continuous time quantum Monte-Carlo solver)

DCore
DCore
integrated DMFT software for Correlated electrons

Kondo Dynamics by RIXS: $CePd_3$

M. C. Rahn, AH et al.,
Nat. Commun.**13**, 6129 (2022)

- Archetypal Kondo lattice
- T_{coh}~130K, T_K~600K
- N_f~0.75 (from XAS)

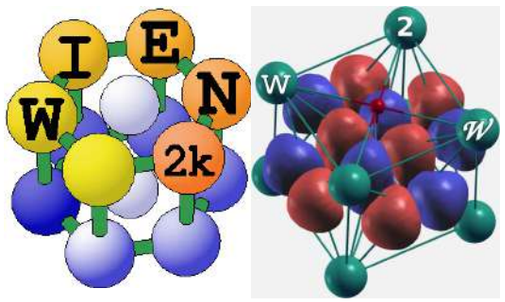

4f wannier basis (from LDA with SOC)
with Wien2K and wannier90

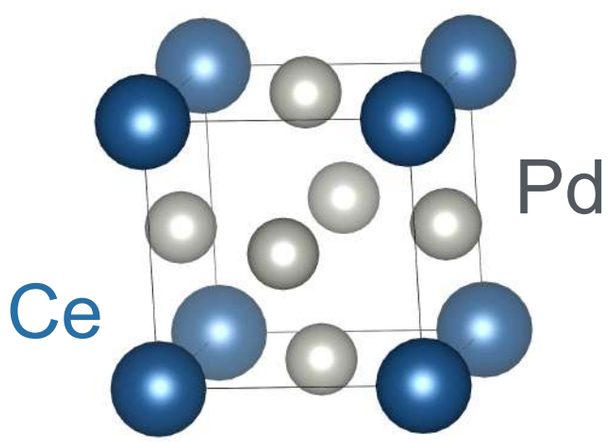

$J = \frac{7}{2}$

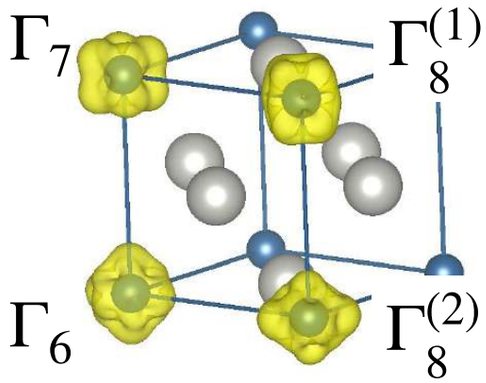

$J = \frac{5}{2}$

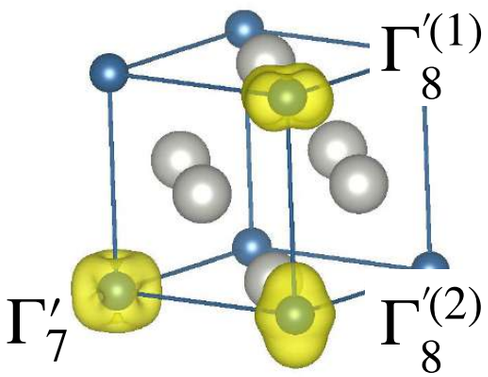

$\Gamma_6(2)$	$\Gamma_7(2)$	$\Gamma_8(4)$	$\Gamma_7'(2)$	$\Gamma_8'(4)$
0.4881 0 / 0 0.4881	0	0	0	0
0.5218 0 / 0 0.5218	0	0	0.0994 0 / 0 -0.0994	0
$J = \frac{7}{2}$		0.5846 0 0 0 / 0 0.5846 0 0 / 0 0 0.5846 0 / 0 0 0 0.5846	0	-0.0714 0 0 0 / 0 0.0714 0 0 / 0 0 -0.0714 0 / 0 0 0 0.0714
			0.2102 0 / 0 0.2102	0
			$J = \frac{5}{2}$	0.2033 0 0 0 / 0 0.2033 0 0 / 0 0 0.2033 0 / 0 0 0 0.2033

$\Delta\xi_{soc} \sim 300$ meV

$H_{\text{loc@Ce site}} =$

Kondo Dynamics by RIXS: $CePd_3$

M. C. Rahn, AH et al.,
Nat. Commun.**13**, 6129 (2022)

DFT+DMFT calc.

Below T_{coh}

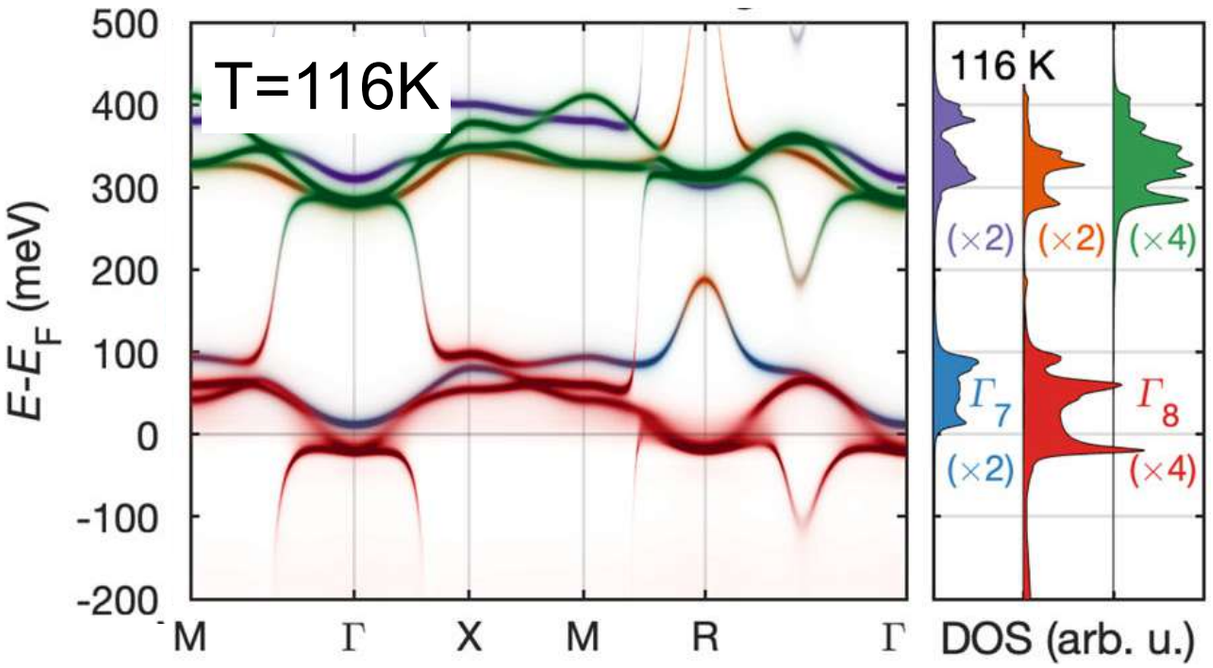

Exp. ARPES @ Γ point

$T_{coh} \approx 130$ K

$T_K \approx 600$ K

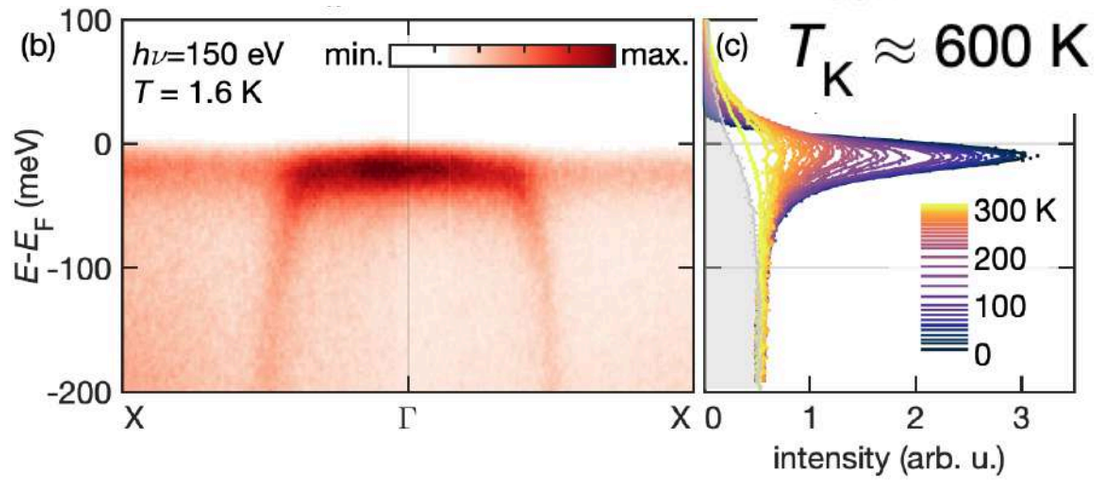

- Sharp Kondo resonance near E_F
- Blind to spectral change above E_F with Kondo crossover

Above T_K ← → *Above T_{coh}*

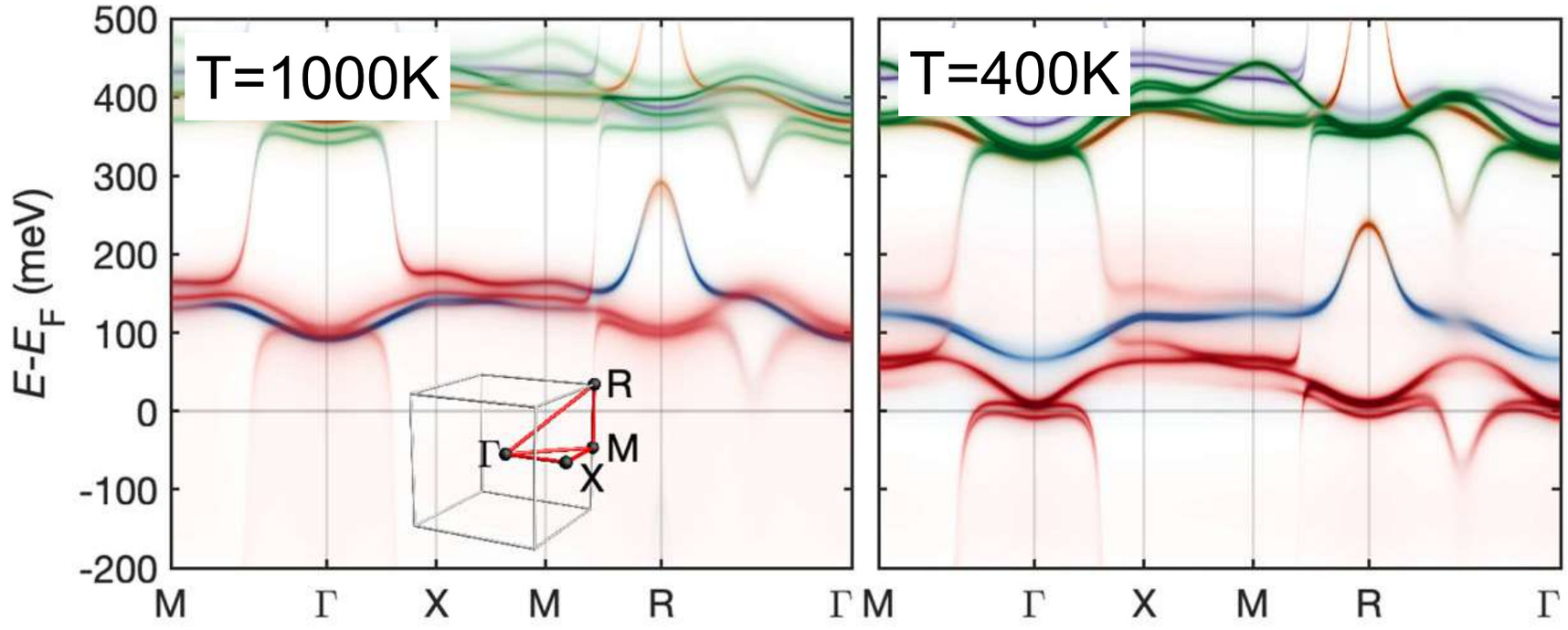

Core-level x-ray spectroscopies

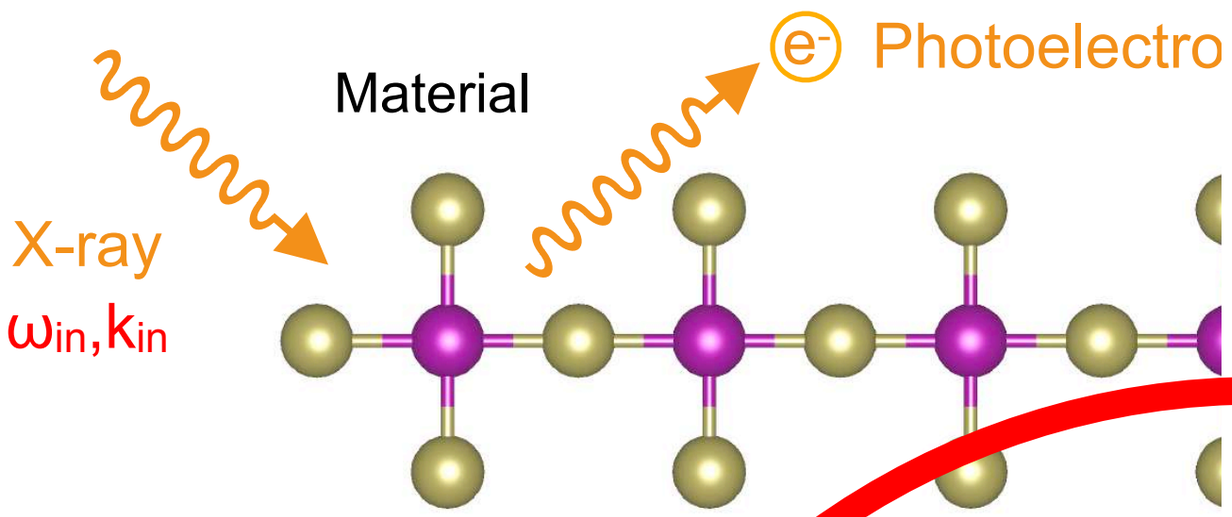

XPS spectrum in $LaNiO_3$ K. Yama ami et al., Appl. Phys. Lett. 118, 1

Core levels

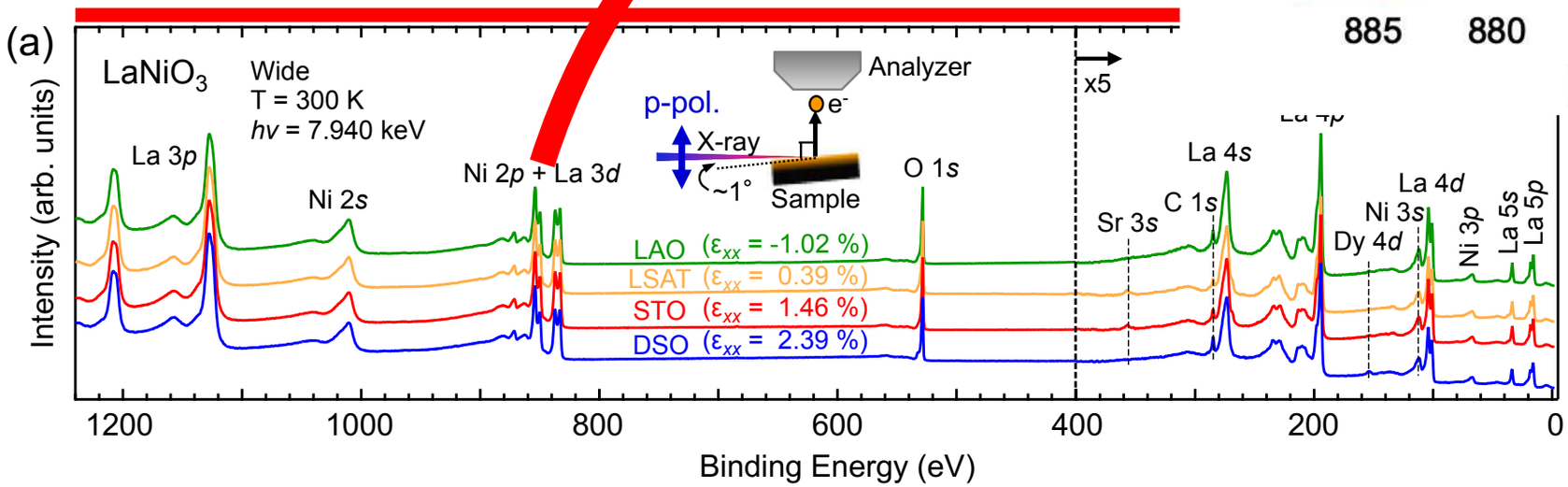

NiO

Many peaks ??

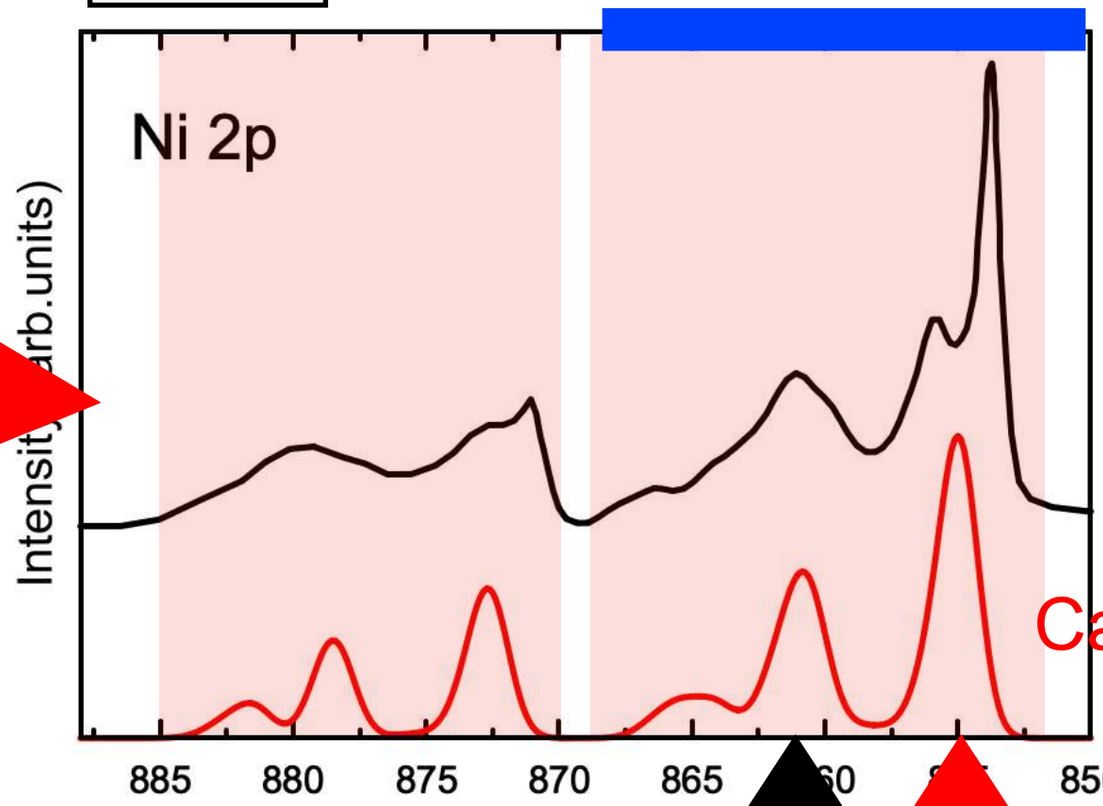

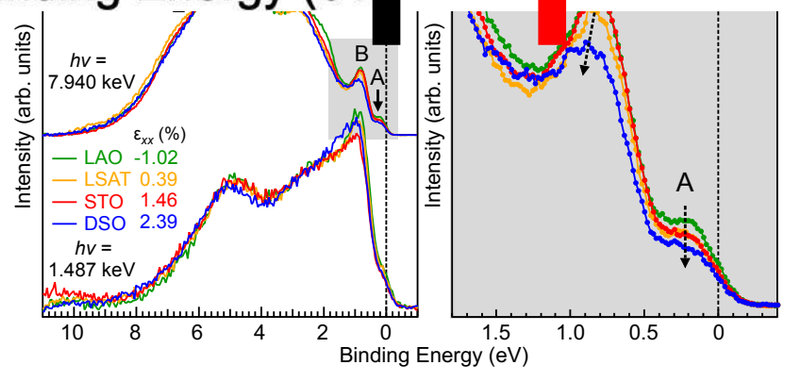

Core levels (no momentum dependence)

Core electrons (holes) completely localized at each ion

- Element specific information (valency)
- Local electronic structure
  (Hund's multiplet, crystal field, and more …)

1-particle Green's function

$$G_r(\varepsilon) = \langle \Phi_0^{(N)} | c_r^\dagger \frac{1}{\varepsilon - (E_0^{(N)} - \mathscr{H}) + i\delta} c_r | \Phi_0^{(N)} \rangle$$

photoemission

$$= \sum_n \left[\frac{| \langle \Phi_n^{(N-1)} | c_r | \Phi_0^{(N)} \rangle |^2}{\varepsilon - (E_0^{(N)} - E_n^{(N-1)}) + i\delta} \right]$$

Core-level x-ray spectroscopies

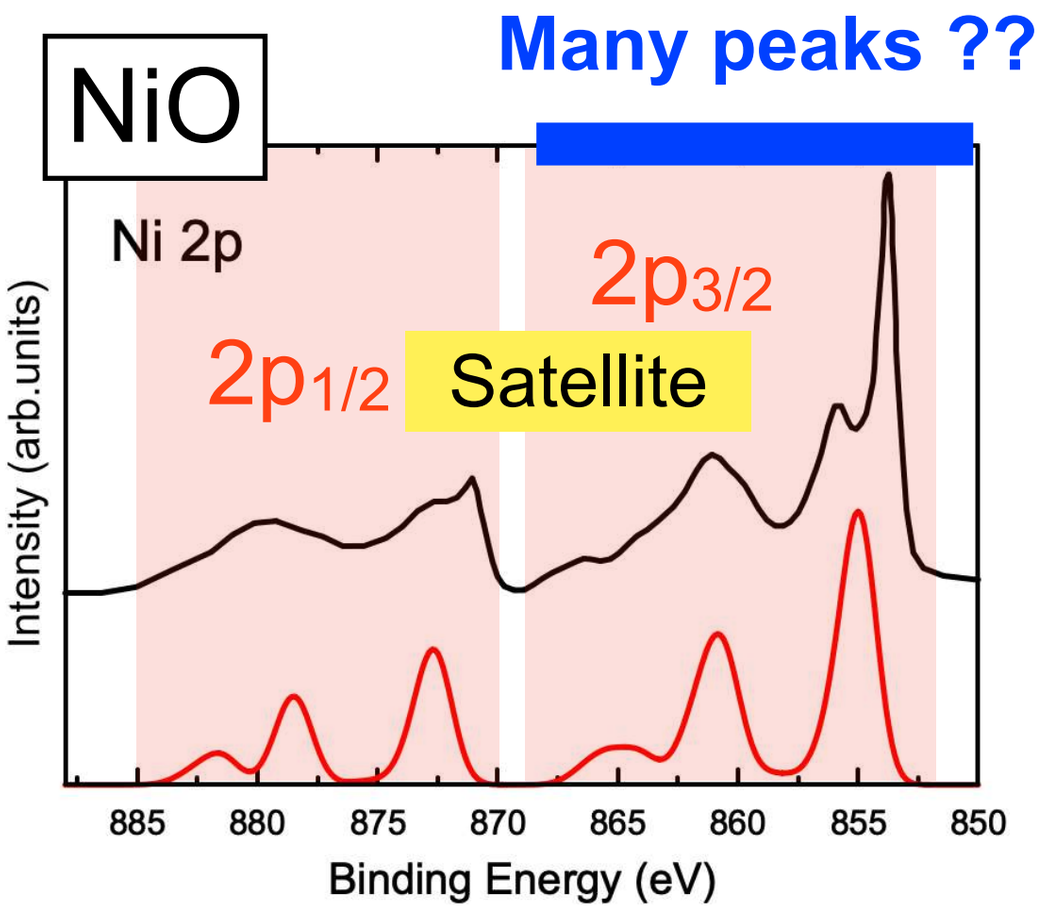

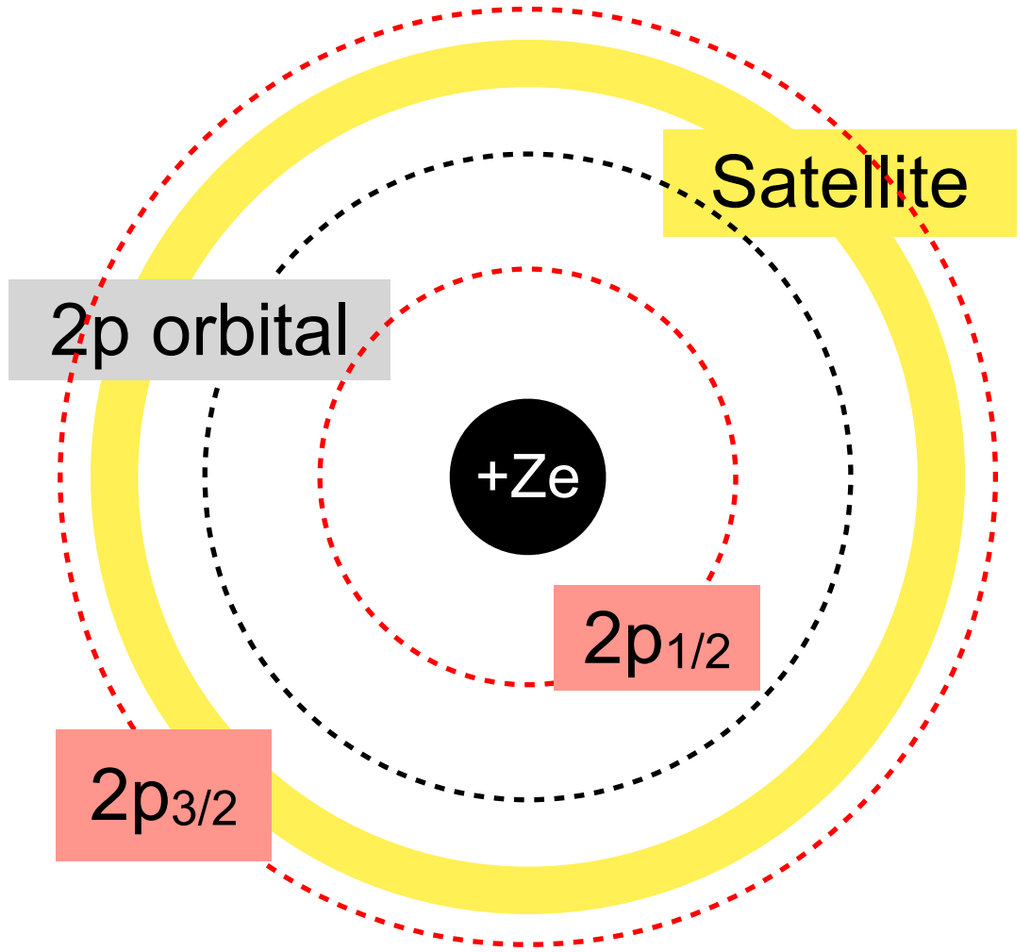

Atomic radial function
(from atomic Hartree-Fock calc.)

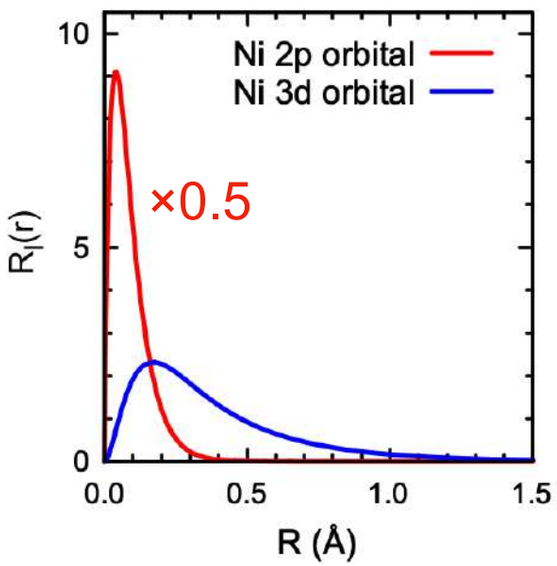

Spin orbit coupling

$$H_{\mathrm{soc}}^{\mathrm{atom}} = \xi \mathbf{L} \cdot \mathbf{S}$$

$$\xi_{\mathrm{Ni}\ 2p} = 11.5\ \mathrm{eV}$$
$$\xi_{\mathrm{Ni}\ 3d} = 0.08\ \mathrm{eV}$$

The origin of the satellite?

A. Many-body final-state effect due to interaction between core-hole and valence electrons

Core-level x-ray spectroscopies

Hubbard model with ligands included (dp model)

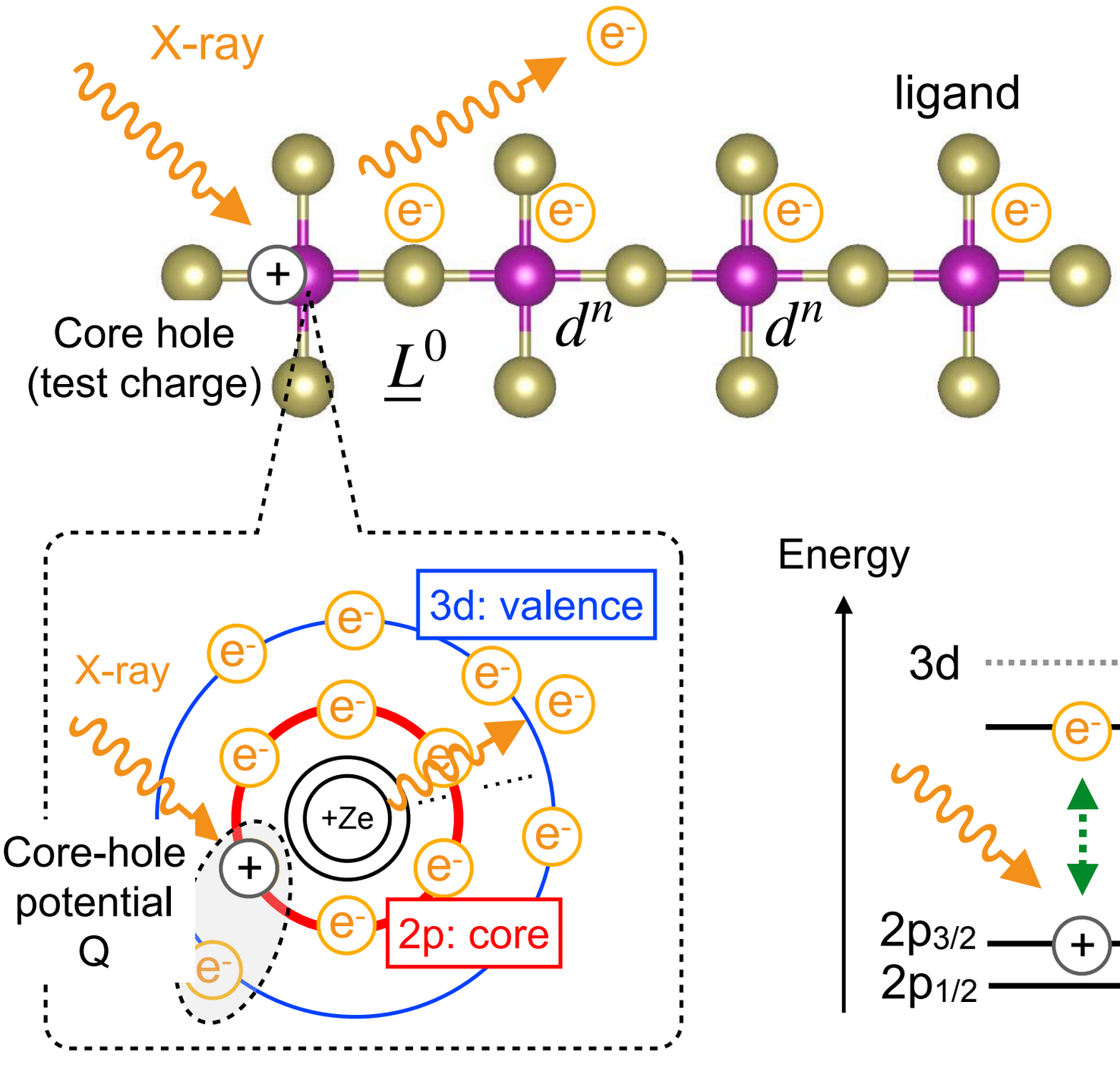

$$H_{\text{Hubbard}} = \sum_i U n_{i\uparrow} n_{i\downarrow}$$

: Core-hole potential

$$+Q \sum_i N_i (6 - N_c)$$

N_c : Number of electrons in 2p core levels

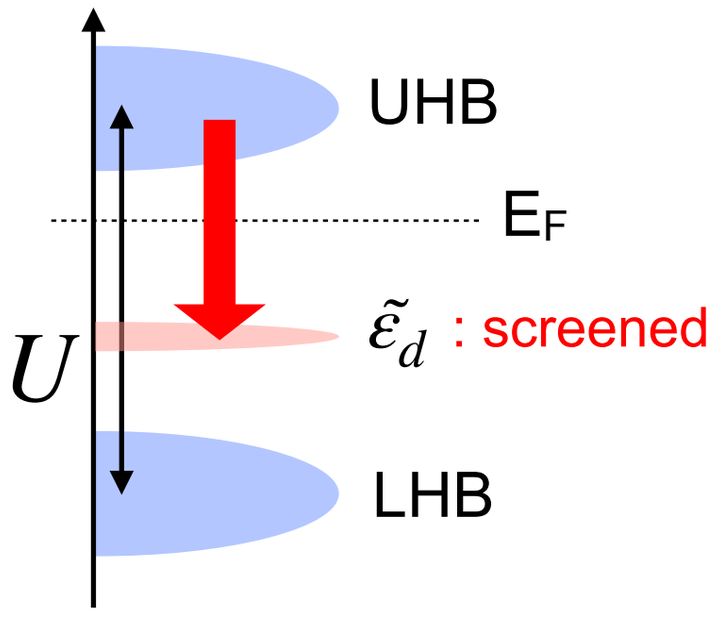

Core-level x-ray spectroscopies

Hubbard model with ligands included (dp model)

Metal - metal charge transfer : $d^n + d^n \rightarrow d^{n+1} + d^{n-1}$

: information on d bands (near Fermi energy)

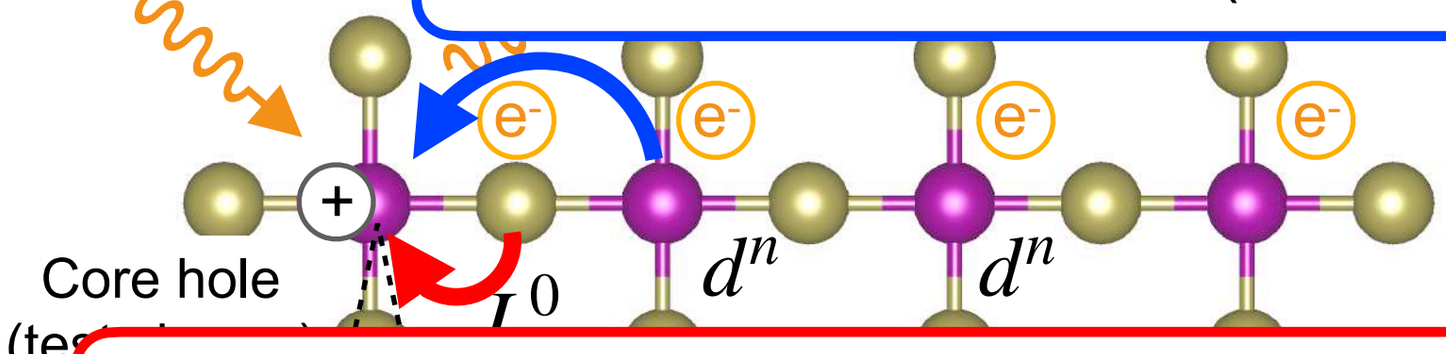

: Core-hole potential

$+Q\sum_i N_i(6-N_c)$

N_i : Number of electrons in 2p core levels

Metal - ligand charge transfer : $d^n + \underline{L}^0 \rightarrow d^{n+1} + \underline{L}^1$

: information on Δ_{CT}, hybridization with ligands

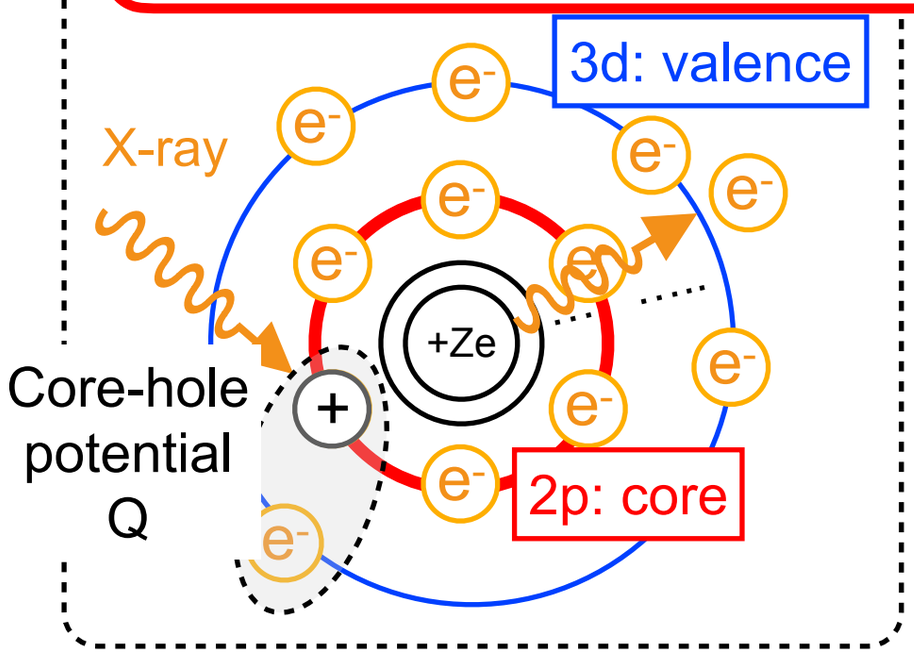

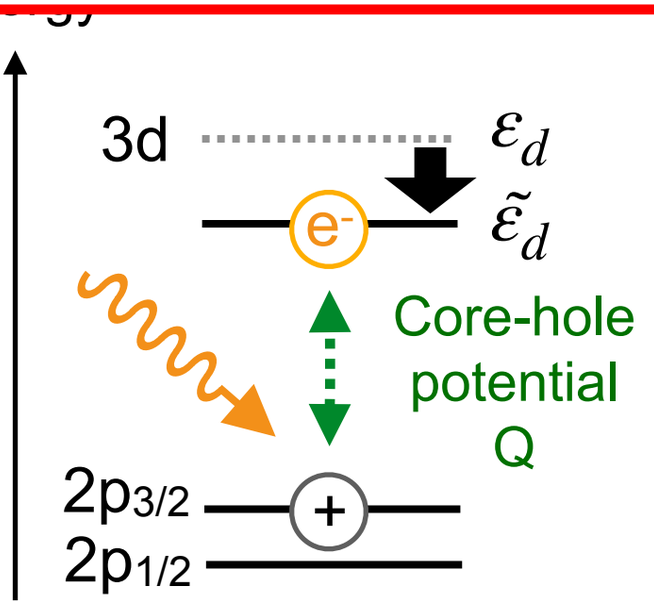

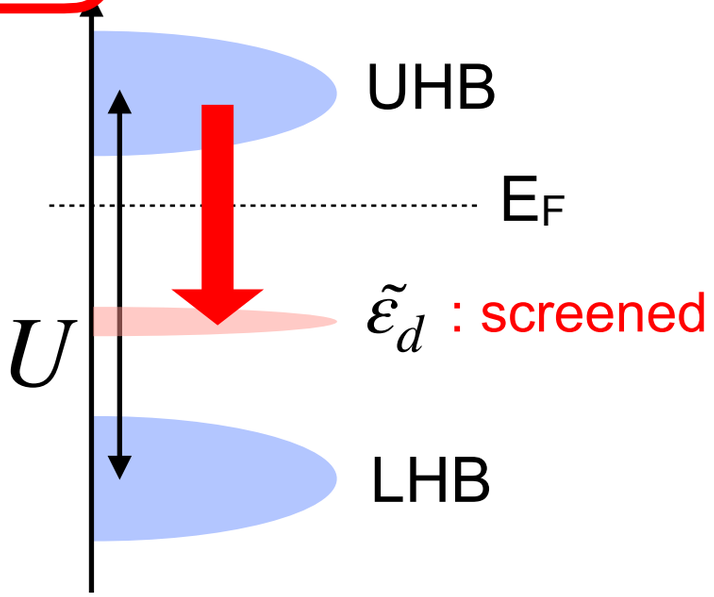

Core-level x-ray spectroscopies

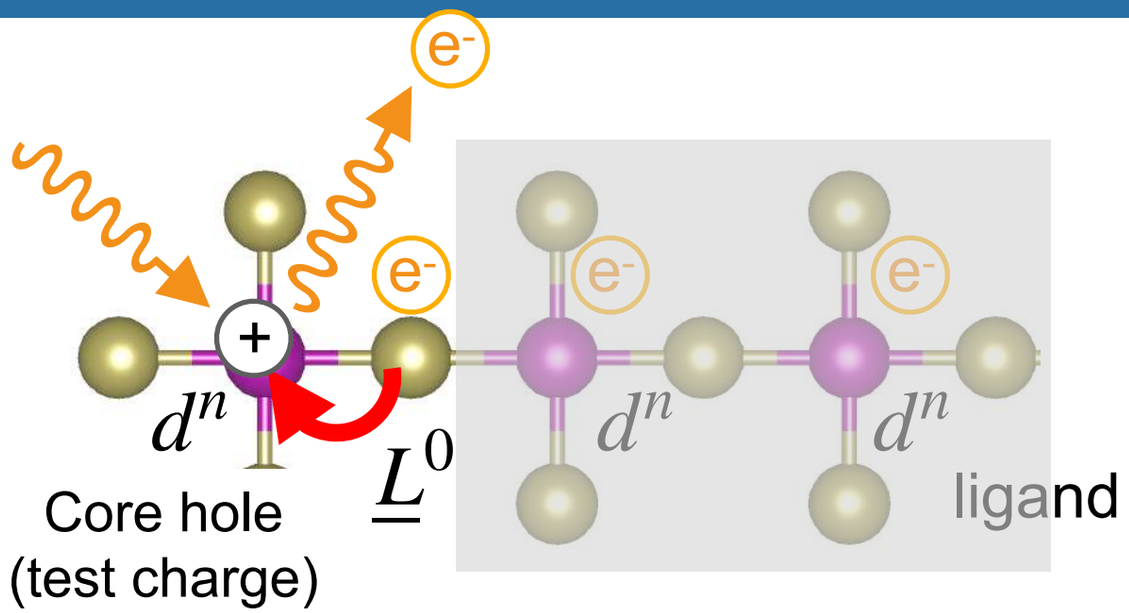

Fermi golden rule

X-ray transition (dipole)

$$F(E_B) = \sum_f |\langle f|\overline{T}|g\rangle|^2 \delta(E_B - E_f - E_g)$$

$$E_B = \omega - \varepsilon - \phi,$$

ε : Kinetic energy of PE

ω : Photon energy

Initial state:

$$|g\rangle = |d^n\rangle + |d^{n+1}\underline{L}\rangle + \cdots$$

Final state (with a core-hole):

$$|f\rangle = |\underline{c}d^n\rangle + |\underline{c}d^{n+1}\underline{L}\rangle + \cdots$$

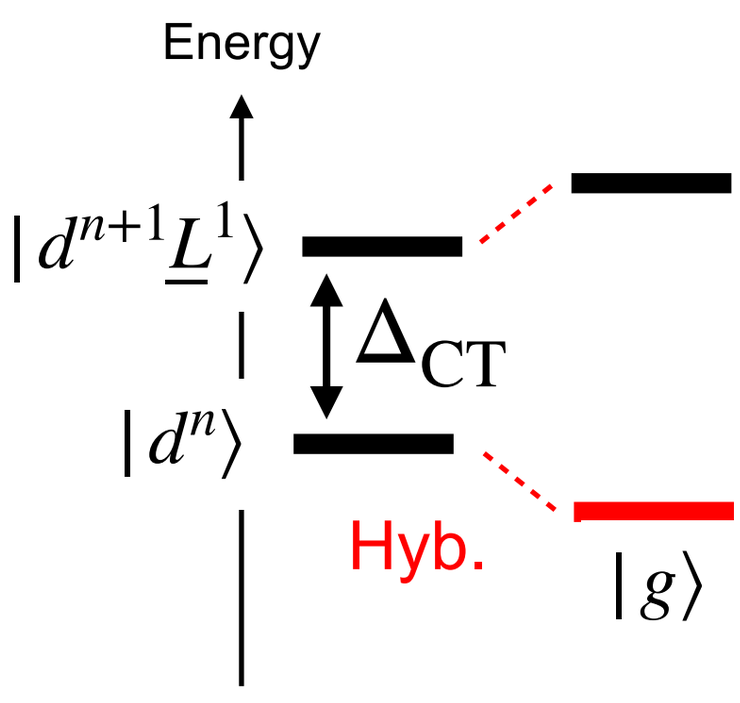

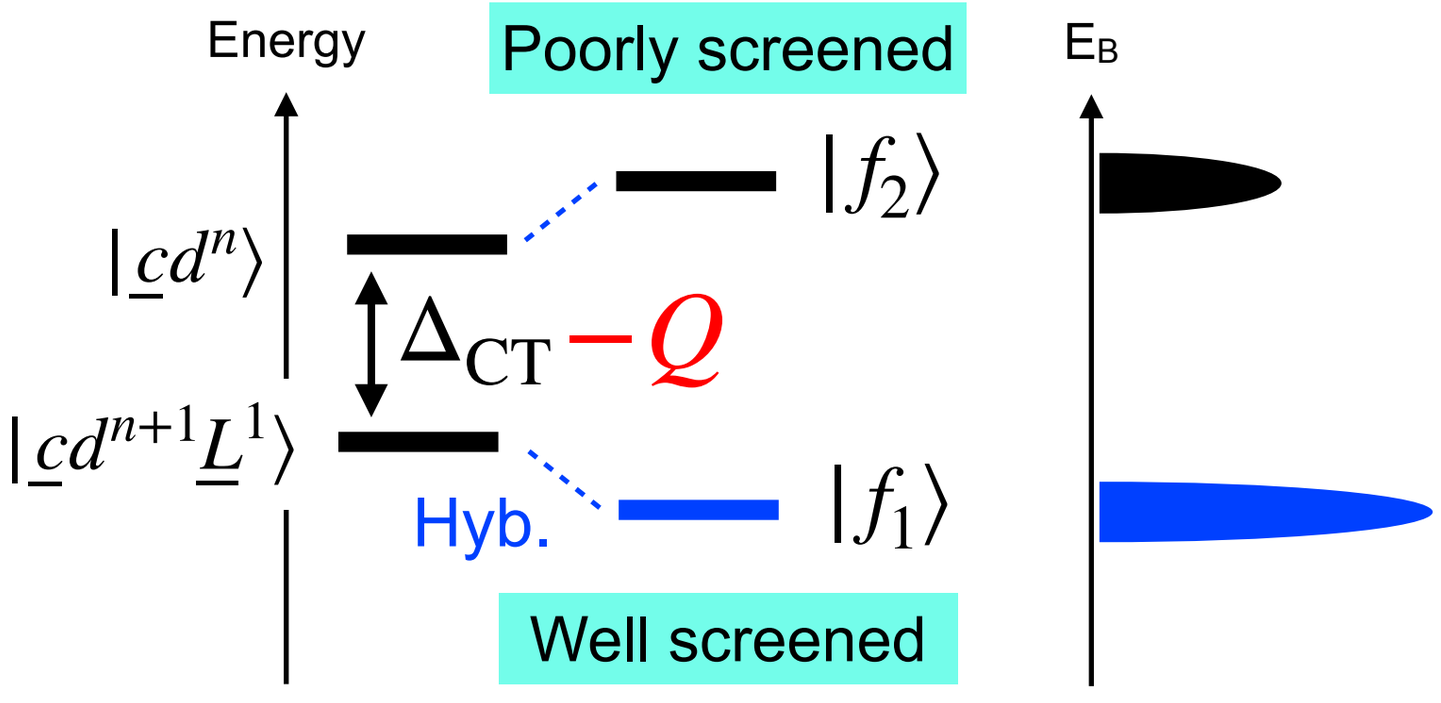

Core-level x-ray spectroscopies

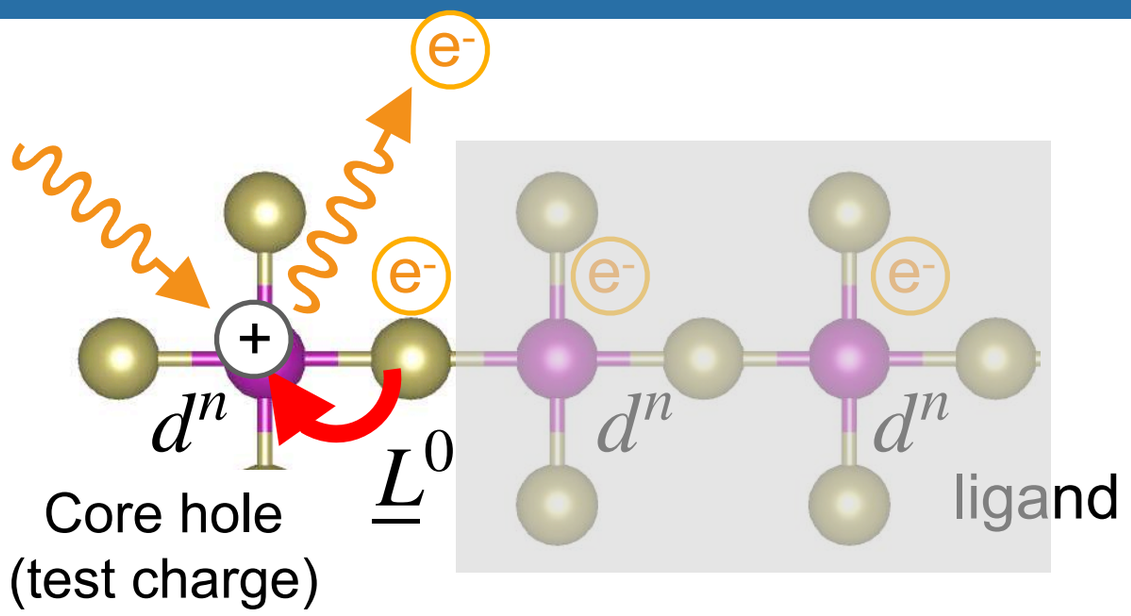

Final state (with a core-hole):

$$|f\rangle = |\underline{c}d^n\rangle + |\underline{c}d^{n+1}\underline{L}\rangle + \cdots$$

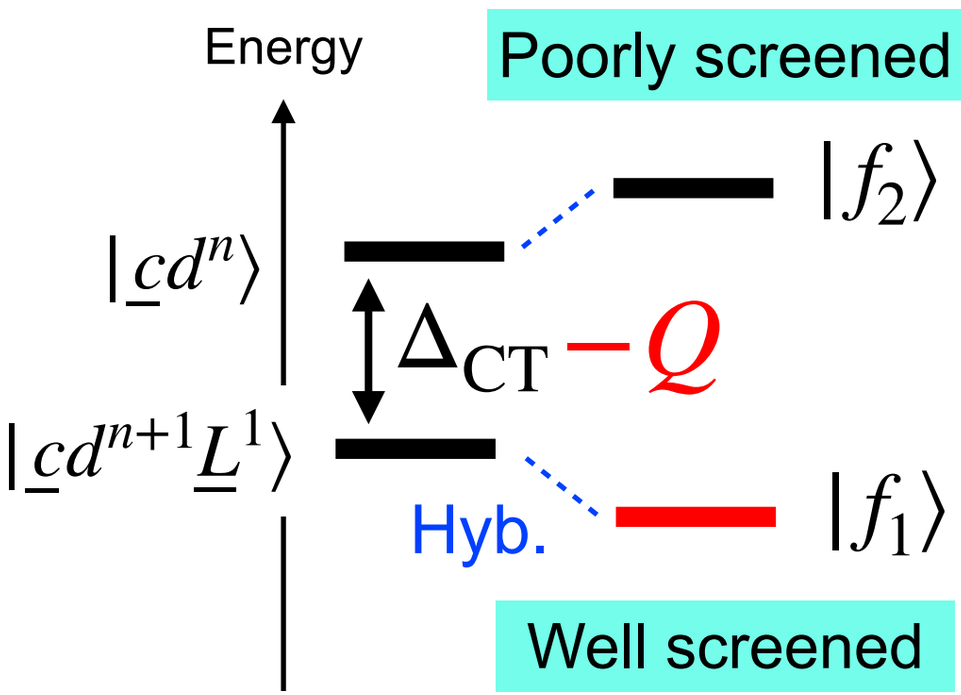

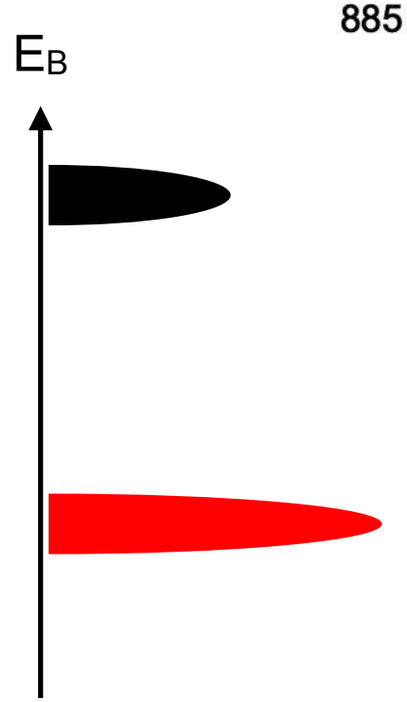

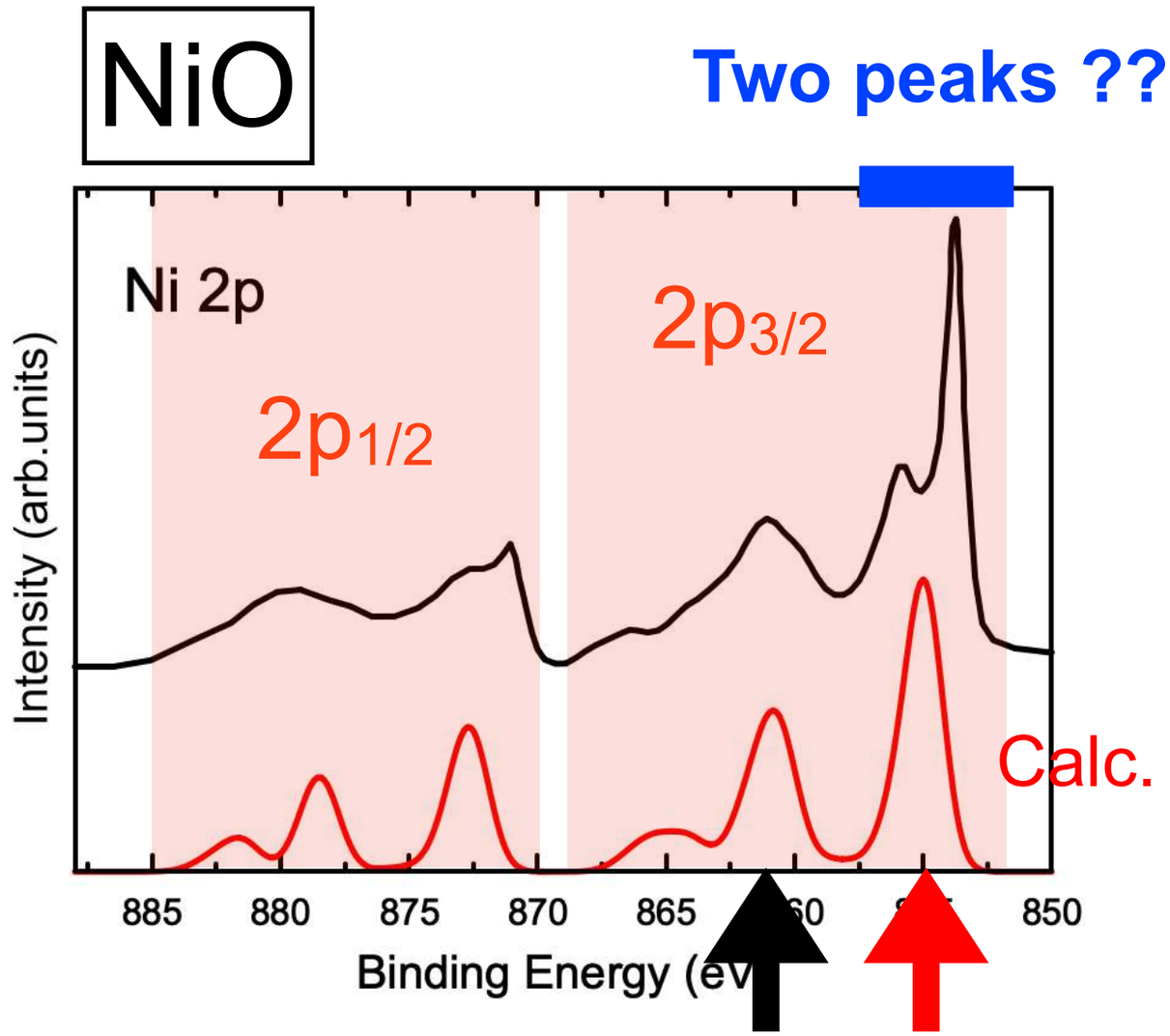

MO_6 cluster model (since 1980's)

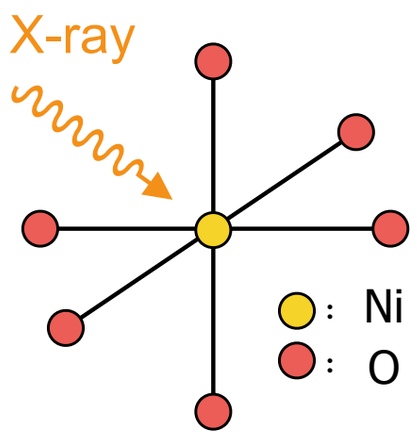

Multiplet ligand-field calculation (Cluster model)

MO_6 cluster model (since 1980's)

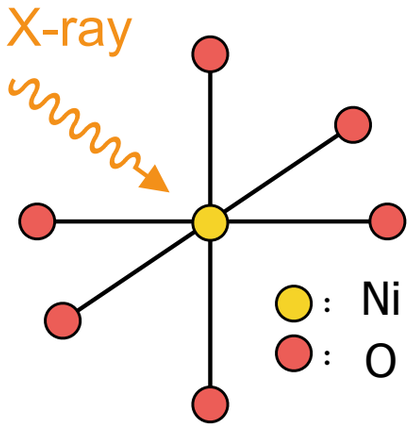

✔ All local interactions explicitly (incl. core orbitals at the excited site)

✖ Only nearest-neighboring ligands (no translational symmetry)

✖ Many adjustable parameters (fitted to reproduce the experimental data)

Cluster model from DFT

✔ Eliminate (most of) adjustable parameters

PHYSICAL REVIEW B **85**, 165113 (2012)

Multiplet ligand-field theory using Wannier orbitals

M. W. Haverkort,[1] M. Zwierzycki,[2] and O. K. Andersen[1]
[1]*Max Planck Institute for Solid State Research, Heisenbergstraße 1, 70569 Stuttgart, Germany*
[2]*Institute of Molecular Physics, Polish Academy of Sciences, M. Smoluchowskiego 17, 60-179 Poznań, Poland*
(Received 21 November 2011; revised manuscript received 7 March 2012; published 9 April 2012)

	V_{e_g}	$V_{t_{2g}}$	$10Dq$	T_{pp}	ζ_{3d}	$F^{(2)}_{dd}$	$F^{(4)}_{dd}$	ζ_{2p}	$F^{(2)}_{2p3d}$	$G^{(1)}_{2p3d}$	$G^{(3)}_{2p3d}$	ζ_{3p}	$F^{(2)}_{3p3d}$	$G^{(1)}_{3p3d}$	$G^{(3)}_{3p3d}$
NiO	2.06	1.21	0.56	0.72	0.08	11.14	6.87	11.51	6.67	4.92	2.80	1.40	12.87	15.89	9.58
MnO	1.92	1.15	0.67	0.53	0.04	9.35	5.78	6.85	5.29	3.77	2.14	0.77	10.93	13.56	8.15
$SrTiO_3$	4.03	2.35	1.79	0.99	0.02	8.38	5.25	3.78	4.23	2.81	1.59	0.43	9.85	12.08	7.35

Coulomb integrals (valence-valence, core-valence)

	$[00\frac{1}{2}]$ $d_{z^2}p_z$	$d_{xz}p_x$	$d_{z^2}p_z$
NiO	**1.19**	**−0.60**	0.00
MnO	**1.11**	**−0.57**	0.02
$SrTiO_3$	**2.33**	**−1.18**	—

	p_zp_z	p_xp_x	p_zp_z	p_xp_x	p_yp_y	$d_{z^2}d_{z^2}$	$d_{xz}d_{xz}$	$d_{xy}p_x$	$d_{yz}p_z$	$d_{z^2}p_y$	$d_{z^2}p_z$	$d_{xz}p_x$	$d_{xz}p_y$	$d_{xy}p_x$	[000] ϵ_p	ϵ_d
NiO	0.02	−0.04	—	—	—	−0.01	−0.03	0.00	0.02	−0.03	0.00	0.00	0.00	0.00	−4.75	−1.35
MnO	0.05	−0.03	—	—	—	−0.06	−0.05	0.00	0.02	−0.03	−0.01	0.00	0.00	0.00	−5.22	−0.39
$SrTiO_3$	−0.01	−0.11	0.06	−0.02	−0.02	0.05	−0.13	−0.02	0.05	−0.03	0.00	−0.02	−0.01	−0.02	−1.53	3.31

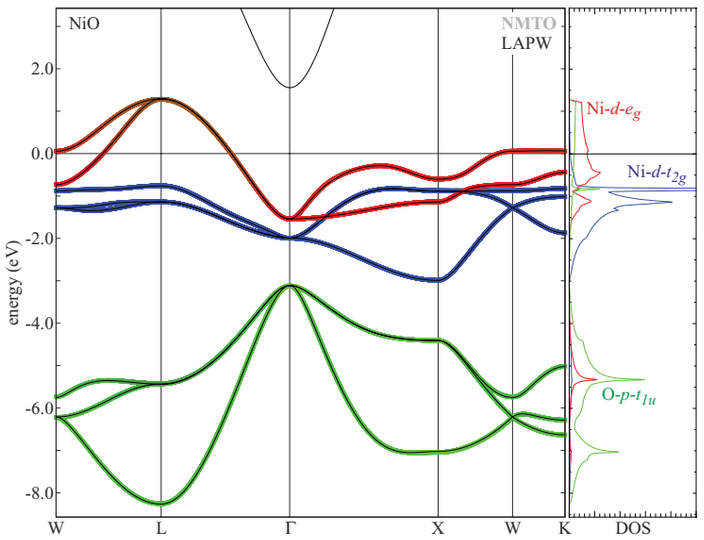

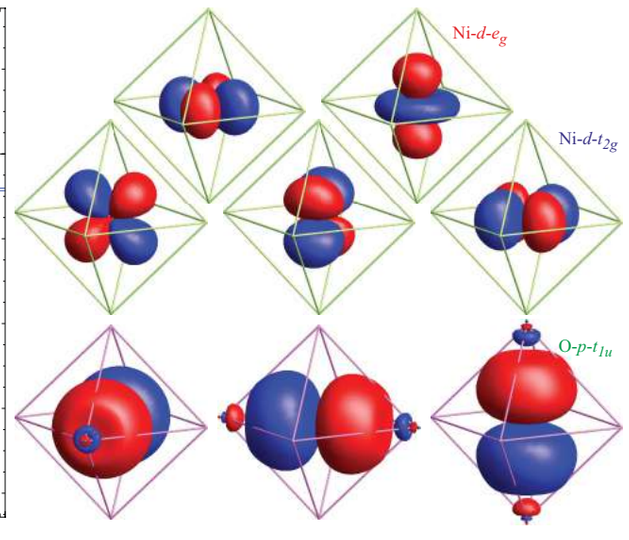

Localized wannier orbitals as basis functions

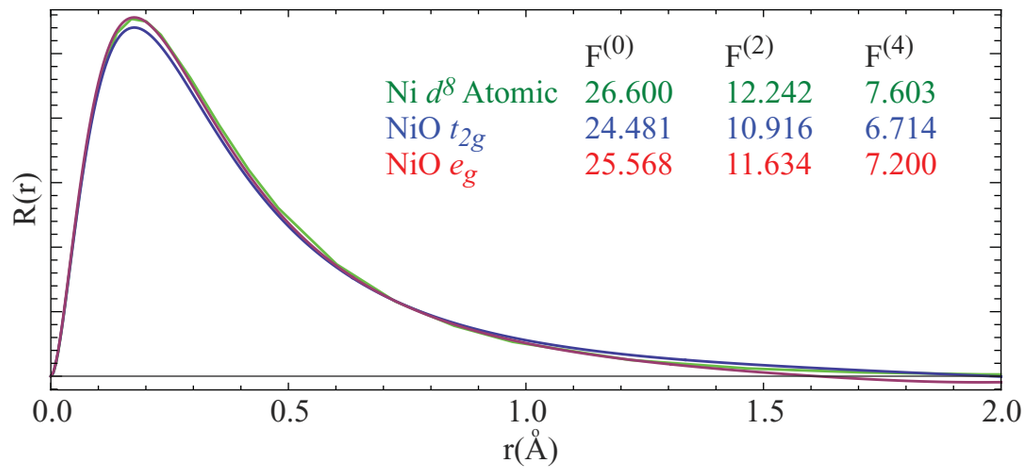

Local interaction: Coulomb interaction (valence-valence)

Coulomb interaction between 3*d* electrons

$$H_{3d-3d} = \sum_{k=2,4} F^k(3d,3d) \sum_{\omega_1<\omega_2,\omega_3<\omega_4} \left[f^k(d\omega_1 d\omega_2, d\omega_3 d\omega_4) - f^k(d\omega_1 d\omega_2, d\omega_4 d\omega_3) \right] (d\omega_1)^\dagger (d\omega_2)^\dagger (d\omega_4)(d\omega_3)$$

direct exchange

F⁰ omitted
(monopole part)

here, $\omega = (m_l, m_s)$

(orbital, and spin magnetic quantum number)

F^k is Slater integral : $F^k(3d,3d) = e^2 \int_0^{+\infty} r_1^2 r_2^2 dr_1 dr_2 R_{3d}^2(r_1) R_{3d}^2(r_2) \frac{r_<^k}{r_>^{k+1}}$

: F^0, F^2, F^4 allowed for 3*d*-3*d* interactions

$U = F_0$: **Hubbard parameter**

$J = \frac{F_2 + F_4}{14}$: **Hund's parameter**

Calculated from atomic Hartree Fock method,
constrained random phase approximation etc
: in reality, screening must be taken into account

Angular part of the integral:

$$f^k(\omega_1\omega_2, \omega_3\omega_4) = \delta_{m_{s1},m_{s3}} \delta_{m_{s2},m_{s4}} \sum_q (-)^q \langle l_1 m_{l1} | C_q^k | l_3 m_{l3} \rangle \langle l_2 m_{l2} | C_{-q}^k | l_4 m_{l4} \rangle$$

Calculated by CG coefficients (3j symbols) : $\langle lm | C_q^k | l'm' \rangle = (-)^m \sqrt{(2l+1)(2l'+1)} \begin{pmatrix} l & k & l' \\ 0 & 0 & 0 \end{pmatrix} \begin{pmatrix} l & k & l' \\ -m & q & m' \end{pmatrix}$

Local interaction: Coulomb interaction (core-valence)

Coulomb interaction between 2*p* (core) and 3*d* (valence) electrons

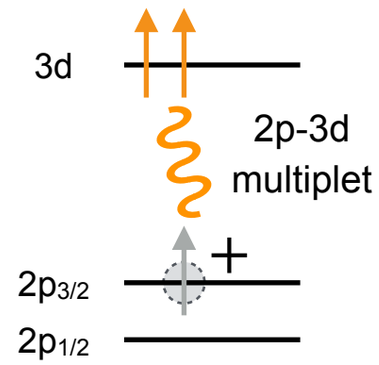

$$H_{2p-3d} = \sum_{\omega_1,\omega_2,\omega_3,\omega_4} \left[\underbrace{\left(p\omega_1 d\omega_2 \left| \frac{1}{r_{12}} \right| p\omega_3 d\omega_4 \right)}_{\text{direct}} - \underbrace{\left(p\omega_1 d\omega_2 \left| \frac{1}{r_{12}} \right| d\omega_4 p\omega_3 \right)}_{\text{exchange}} \right] (p\omega_1)^\dagger (p\omega_3)(d\omega_2)^\dagger (d\omega_4)$$

$$= F^2(2p,3d) \sum_{\omega_1,\omega_2,\omega_3,\omega_4} f^2(p\omega_1 d\omega_2, p\omega_3 d\omega_4)(p\omega_1)^\dagger (p\omega_3)(d\omega_2)^\dagger (d\omega_4)$$

F⁰ omitted
(monopole part)

: direct term

$$- \sum_{k=1,3} G^k(2p,3d) \sum_{\omega_1,\omega_2,\omega_3,\omega_4} f^k(p\omega_1 d\omega_2, d\omega_4 p\omega_3)(p\omega_1)^\dagger (p\omega_3)(d\omega_2)^\dagger (d\omega_4)$$

: exchange term

Atomic radial function
(from atomic Hartree-Fock calc.)

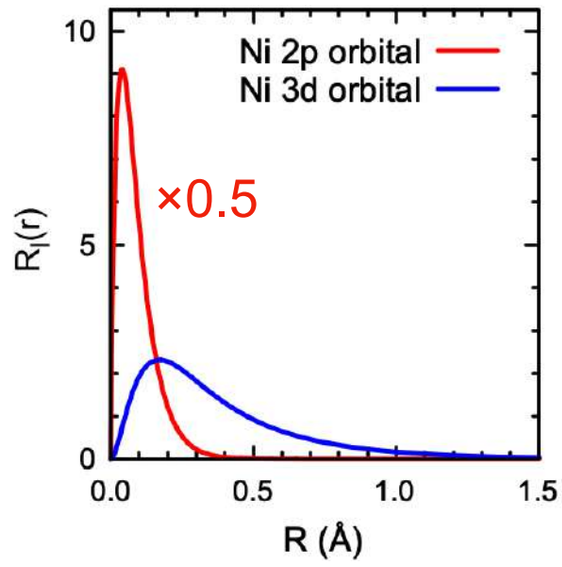

Slater integral

$$F^k(2p,3d) = \int_0^\infty \int_0^\infty R_{2p}^2(r_1) R_{3d}^2(r_2) \frac{r_<^k}{r_>^{k+1}} r_1^2 r_2^2 dr_1 dr_2$$

$$G^k(2p,3d) = \int_0^\infty \int_0^\infty R_{2p}(r_1) R_{3d}(r_1) R_{2p}(r_2) R_{3d}(r_2) \frac{r_<^k}{r_>^{k+1}} r_1^2 r_2^2 dr_1 dr_2$$

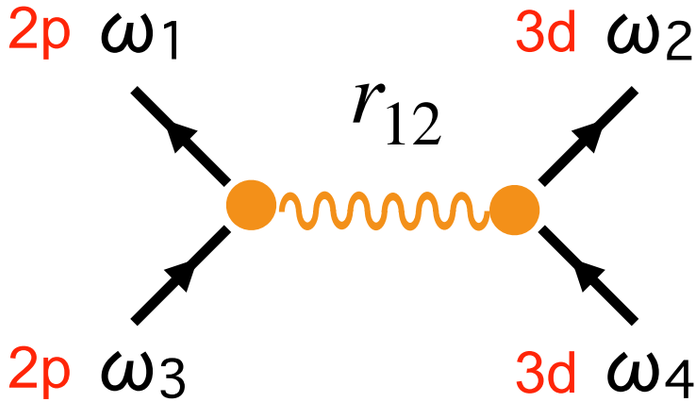

Core-level x-ray spectroscopies

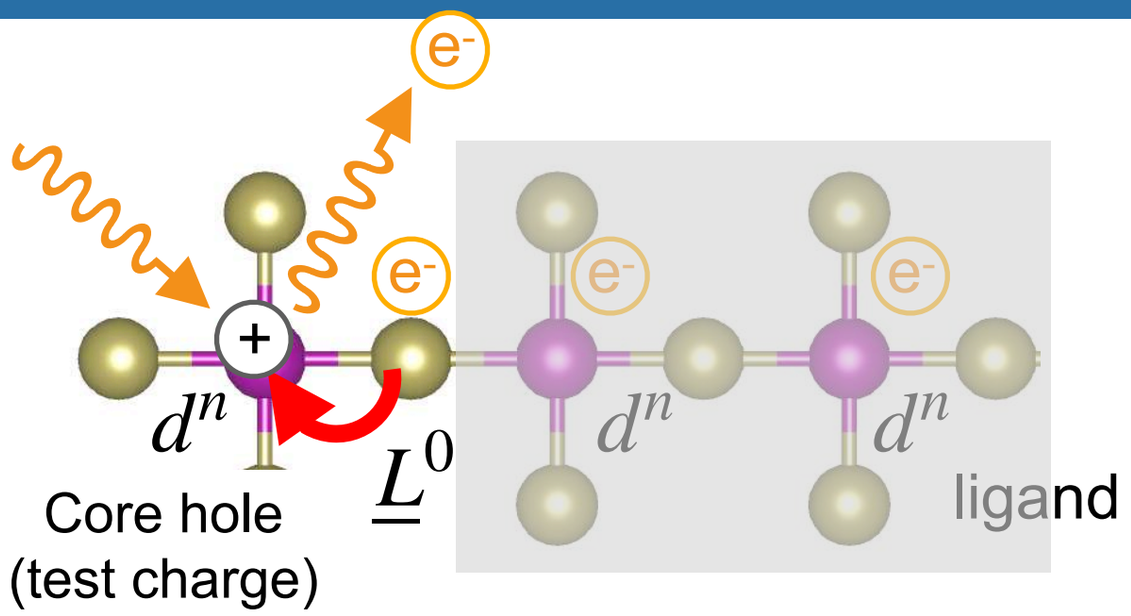

Final state (with a core-hole):

$$|f\rangle = |\underline{c}d^n\rangle + |\underline{c}d^{n+1}\underline{L}\rangle + \cdots$$

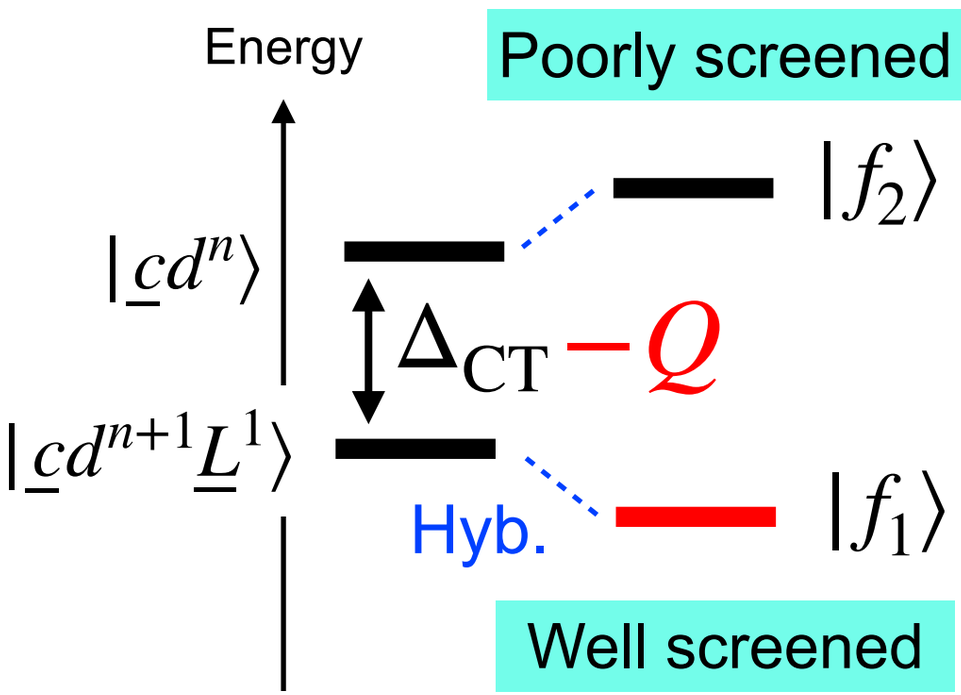

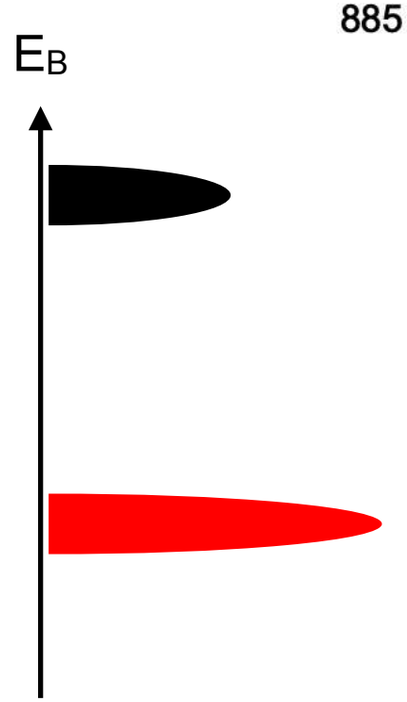

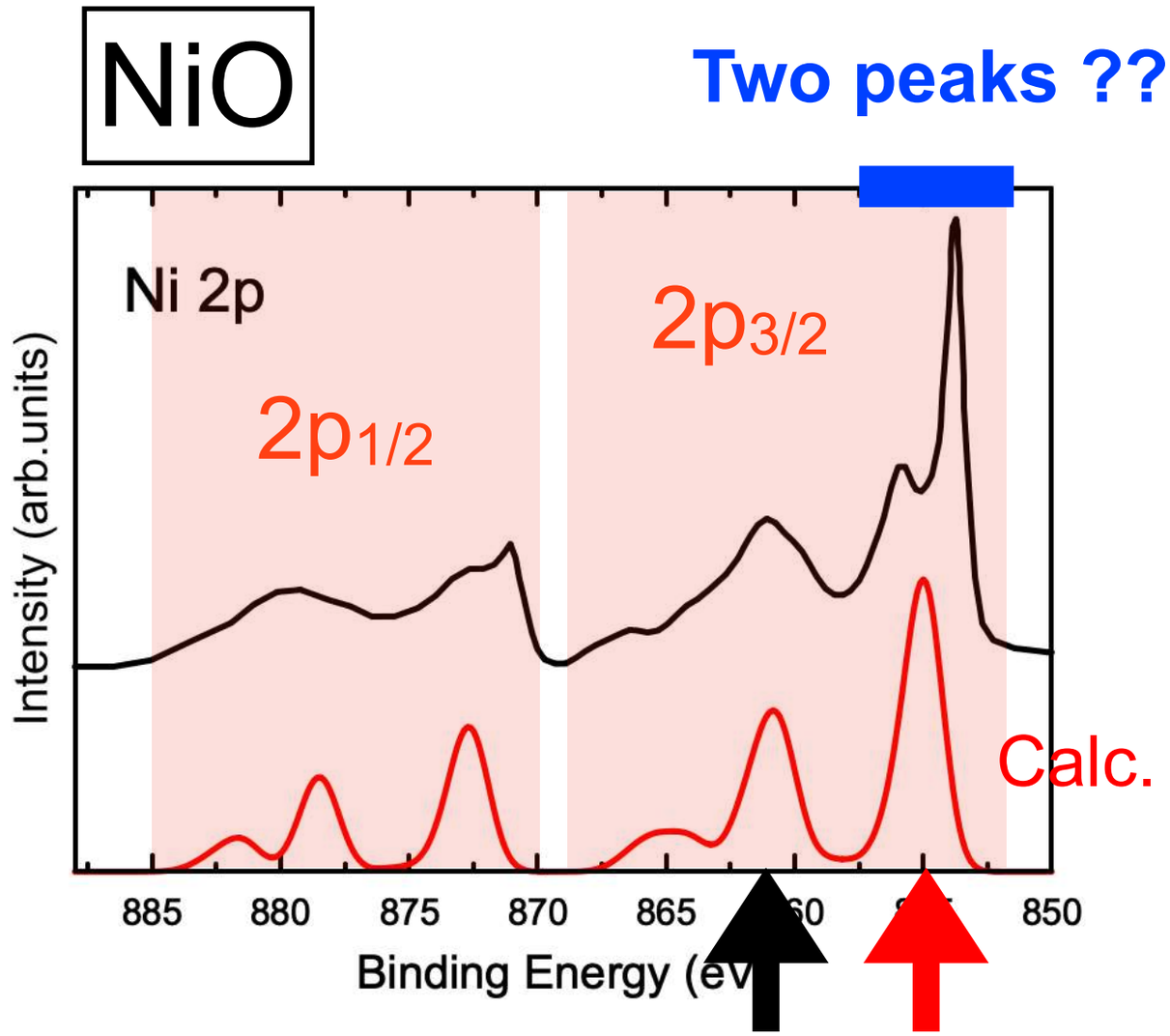

MO_6 cluster model (since 1980's)

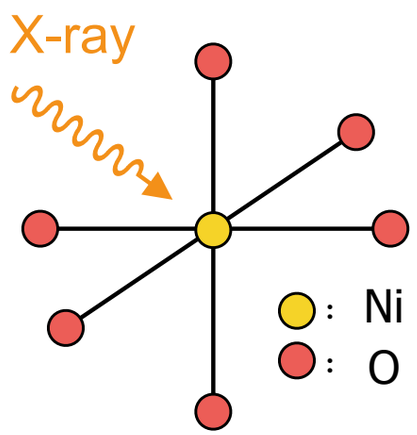

Metal - metal charge transfer : $d^n + d^n \rightarrow d^{n+1} + d^{n-1}$

: information on d bands (near Fermi energy)

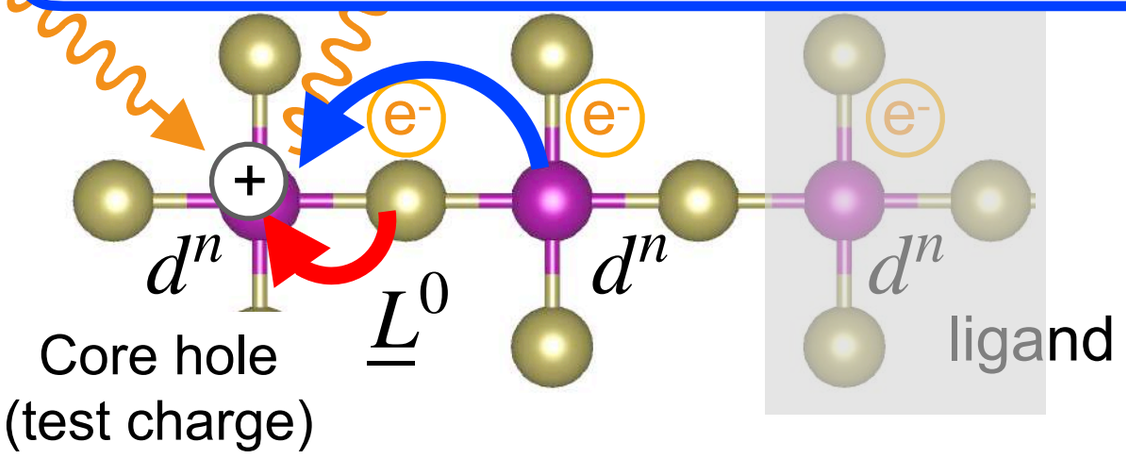

Final state (with a core-hole):

$$|f\rangle = |\underline{c}d^n\rangle + |\underline{c}d^{n+1}\underline{L}\rangle + \cdots$$

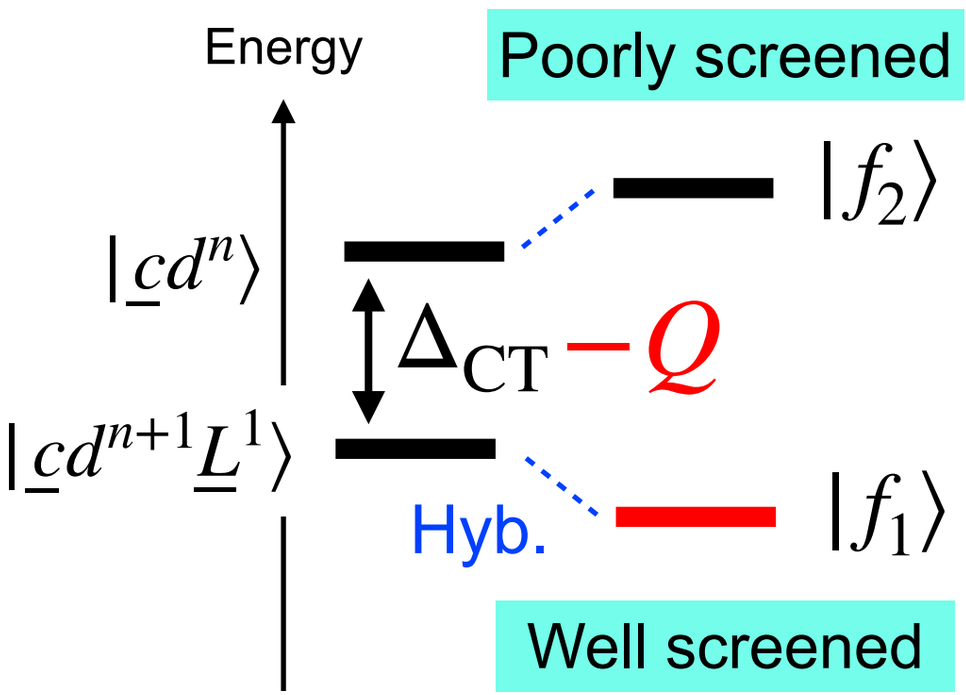

Two peaks ??

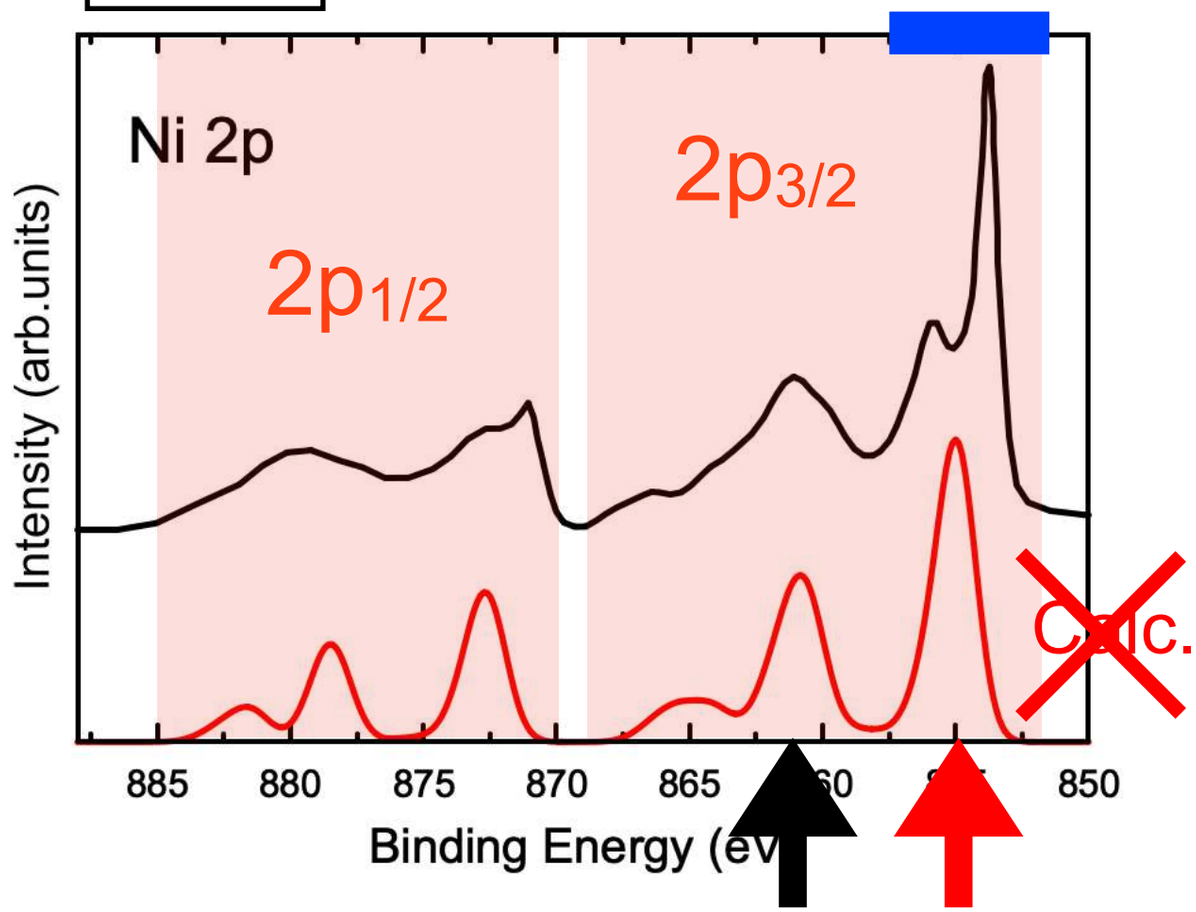

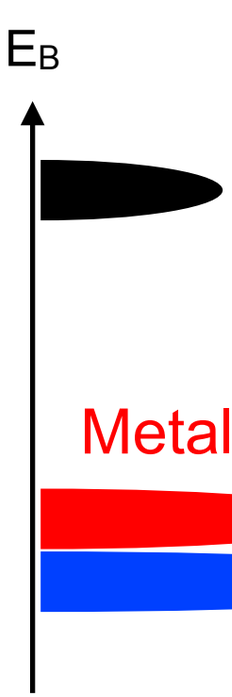

Metal-ligand charge transfer

Metal-metal charge transfer

: info. low-energy electronic structure

Quantum embedding approach to core-level spectroscopies

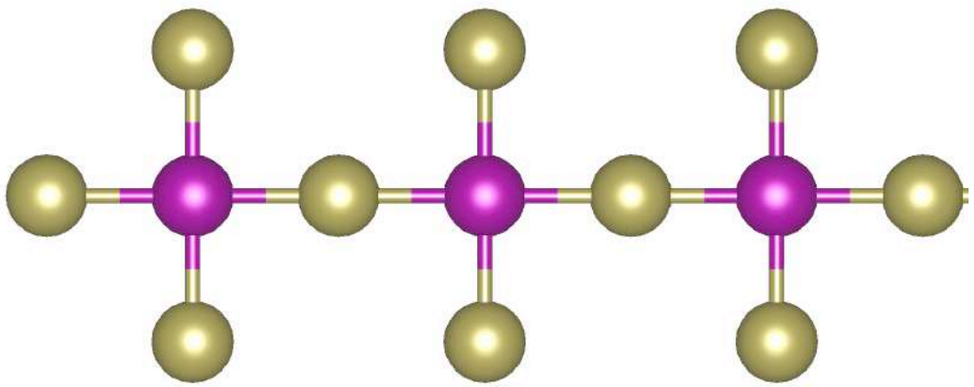

Quantum embedding

: DFT + DMFT

Anderson model

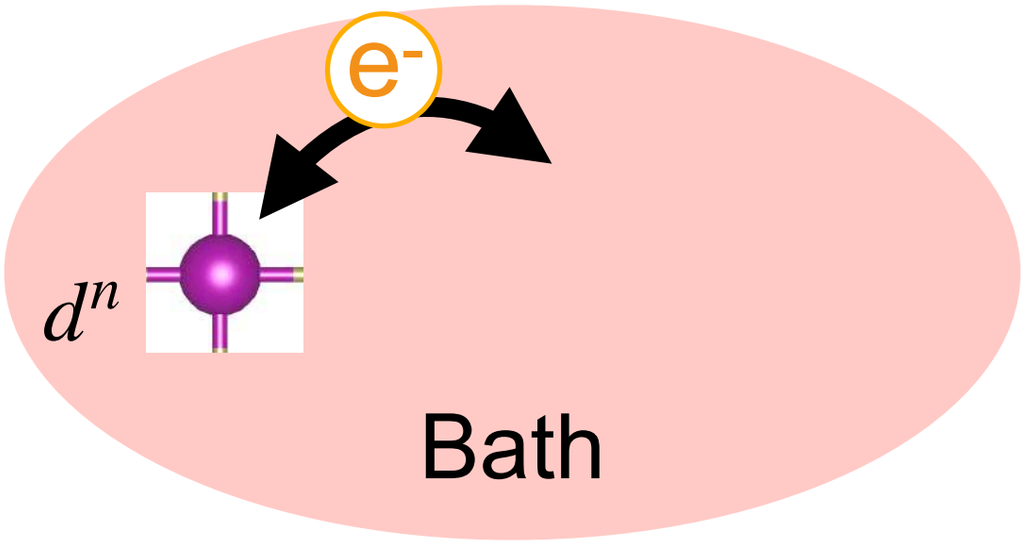

Incl. both ligand and

metal 3d bands

Fermi golden rule

X-ray transition (dipole)

$$F(E_B) = \sum_f |\langle f|\overline{T}|g\rangle|^2 \delta(E_B - E_f - E_g)$$

$$E_B = \omega - \varepsilon - \phi,$$

ε : Kinetic energy of PE

ω : Photon energy

Core orbitals and their interaction included

$$H_{\mathrm{DMFT-AIM}} + H_{\mathrm{core}} + H_{\mathrm{core-valence}}$$

: spin-orbit coupling

: core-valence Coulomb multiplet

(Monopole part is adjusted to fit the experimental spectrum)

Quantum embedding approach to core-level spectroscopies

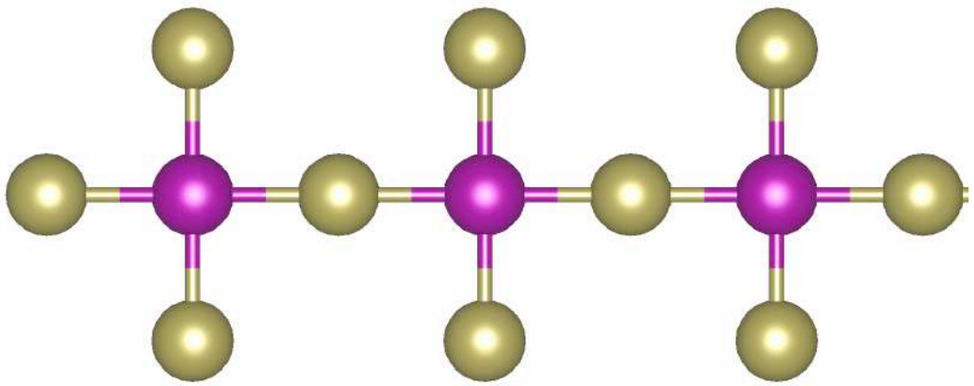

Quantum embedding

: **DFT + DMFT**
Anderson model

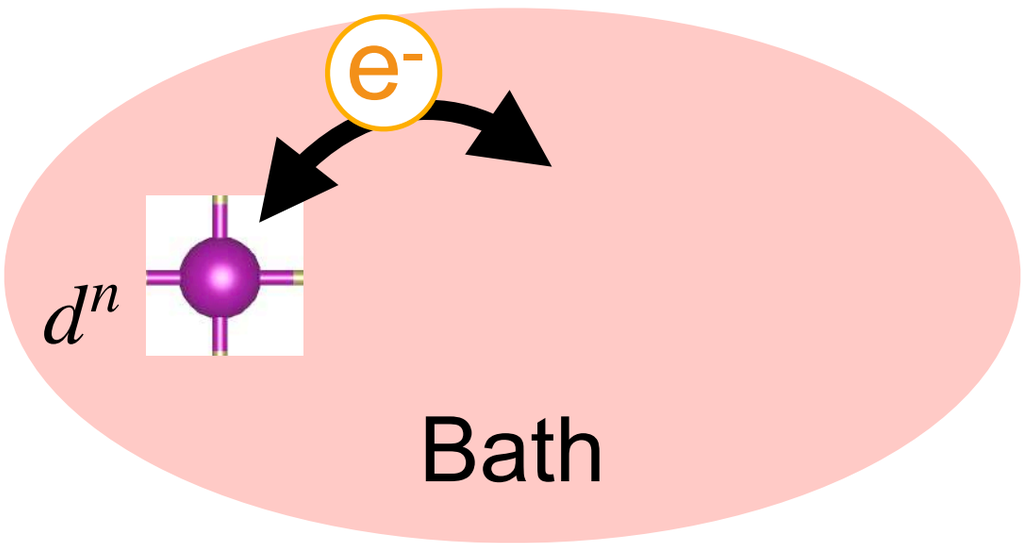

Incl. both ligand and
metal 3d bands

NiO

A. Hariki et al., PRB **96**, 045111 (2017)

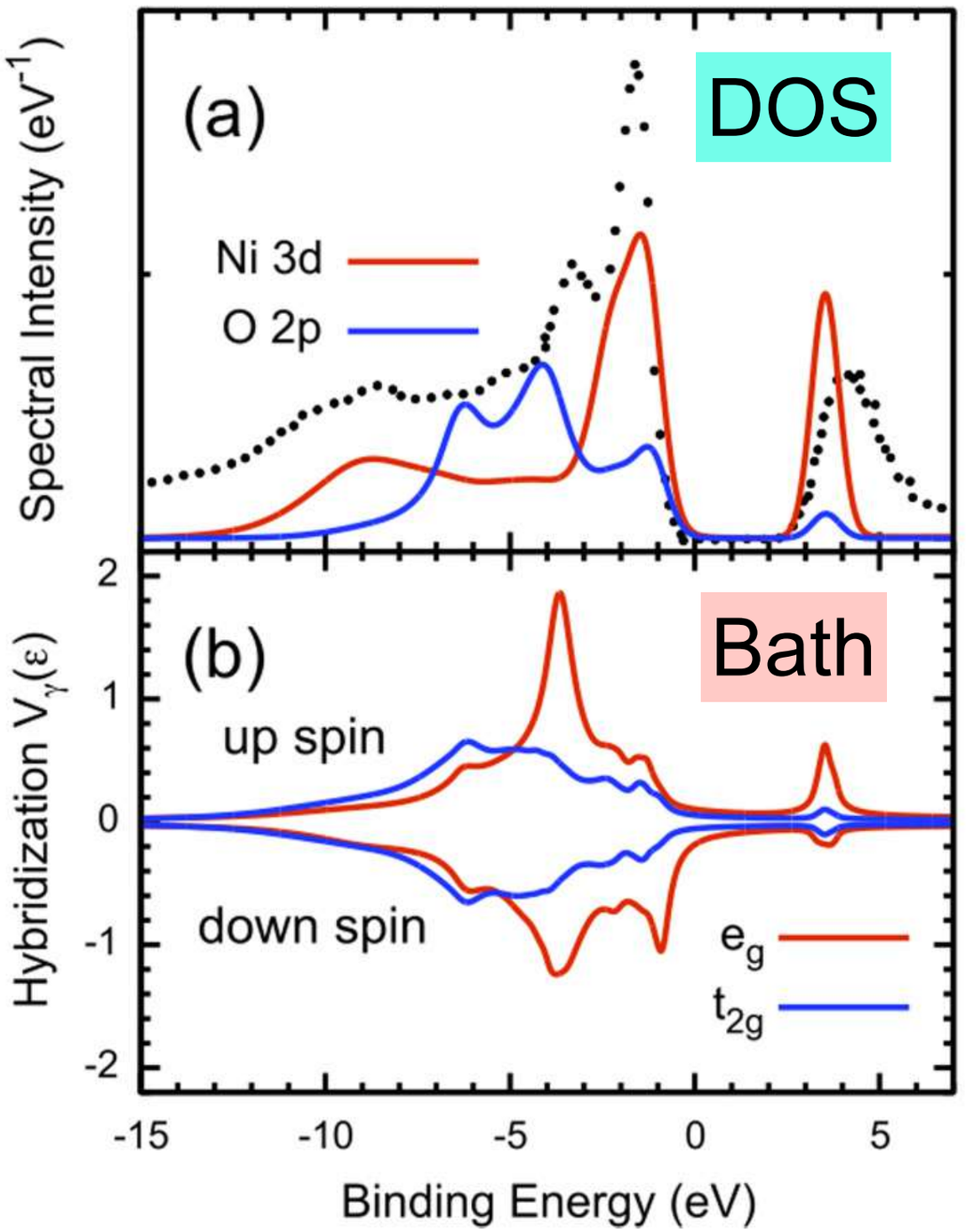

Quantum embedding approach to core-level spectroscopies

Hybridization density $V^2(\varepsilon)$: Key quantity in embedding approach

: hybridization property of 3d orbitals
in the metal site (impurity) with the crystal

Local Hamiltonian (at embedded site) — Local GF

$$\Delta(\varepsilon) = \varepsilon - H_{\mathrm{imp}} - \Sigma(\varepsilon) - G^{-1}(\varepsilon)$$

DMFT self-energy

$$V_\gamma^2(\varepsilon) = \sum_i |\langle \psi_{\gamma,i}|\hat{V}_{\mathrm{imp-host}}|d_\gamma\rangle|^2 \delta(\varepsilon - \varepsilon_{\gamma,i})$$

$$= -\frac{1}{\pi}\,\mathrm{Im}\,\langle d_\gamma|\hat{V}_{\mathrm{imp-host}}\frac{1}{\varepsilon - H_{\mathrm{host}}(\varepsilon)}\hat{V}_{\mathrm{host-imp}}|d_\gamma\rangle$$

$\Delta(\varepsilon)$

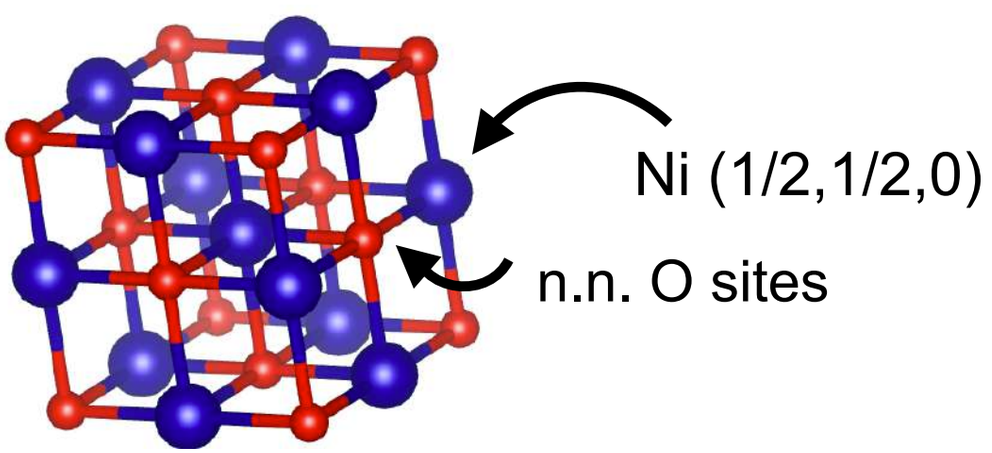

Hybridization density of Ni e_g orbital

M. Ghiasi, **AH** et al., Phys. Rev. B **100**, 075146 (2019)

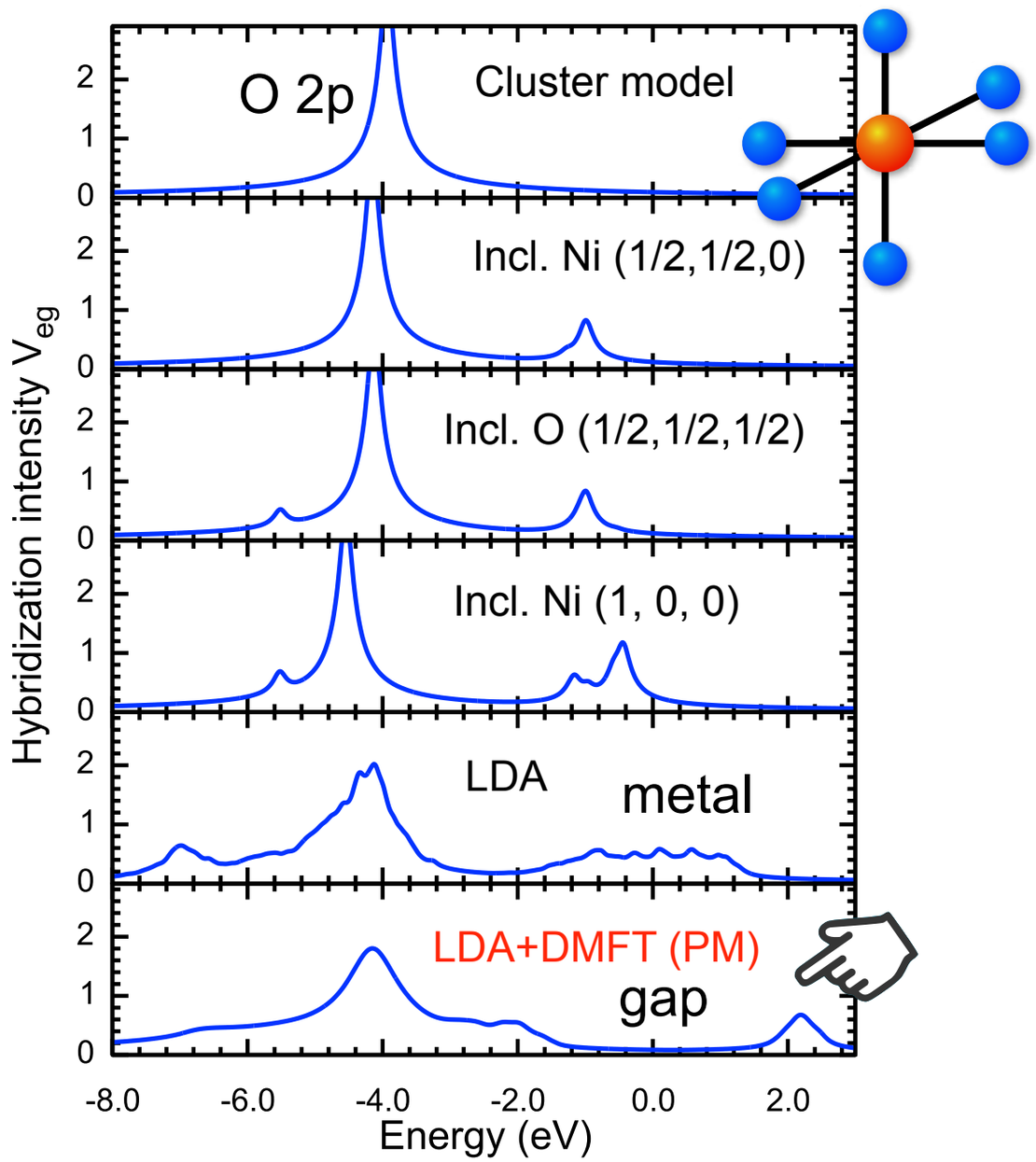

Note : Coulomb interaction is not included
in V(ε) of the finite-size clusters in figures

Quantum embedding approach to core-level spectroscopies

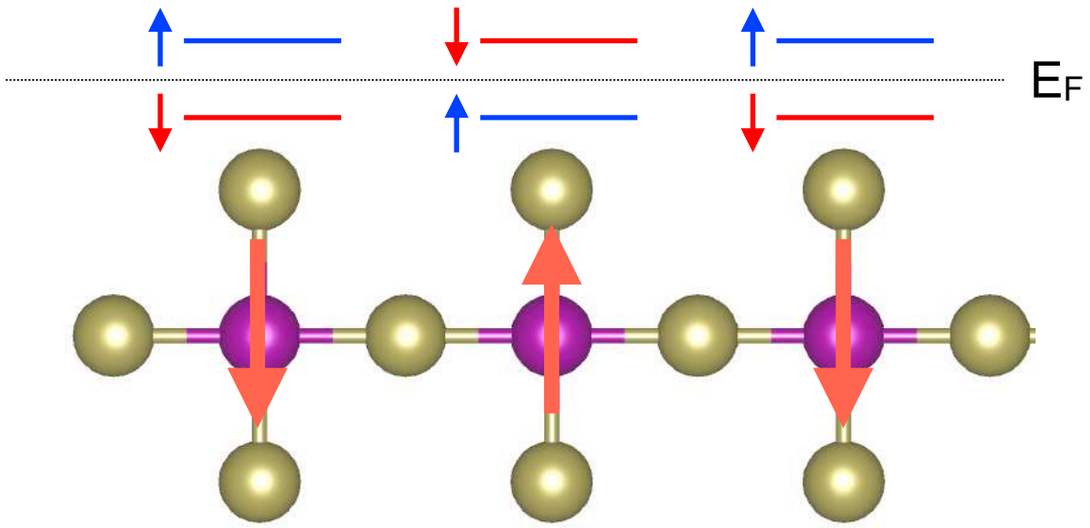

Quantum embedding

: **DFT + DMFT**

Anderson model

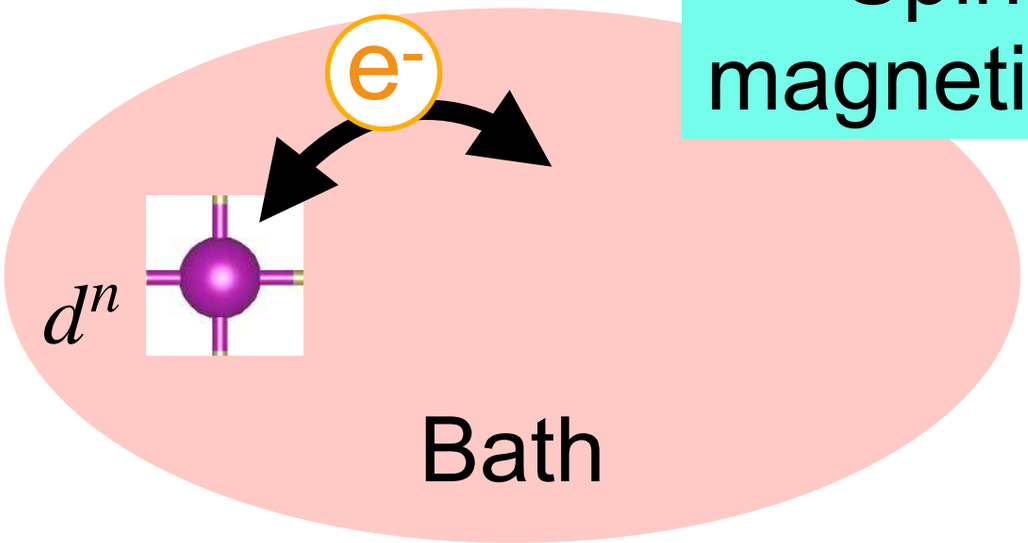

Incl. both ligand and metal 3d bands

NiO

A. Hariki et al., PRB **96**, 045111 (2017)

Spin dependent in magnetic ordered phase!

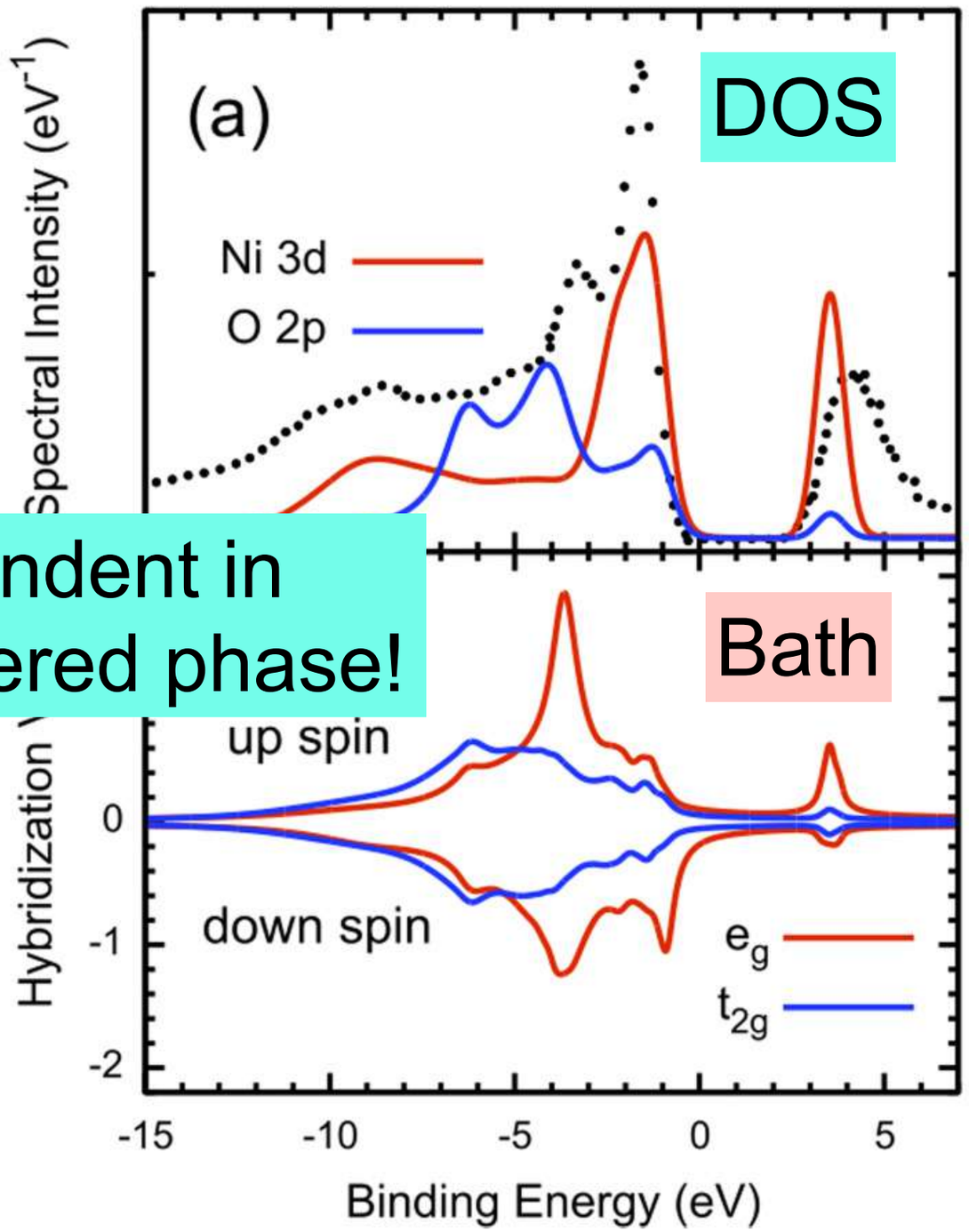

Quantum embedding spectroscopies

Metal - metal charge transfer : $d^n + d^n \rightarrow d^{n+1} + d^{n-1}$

: information on d bands (near Fermi energy)

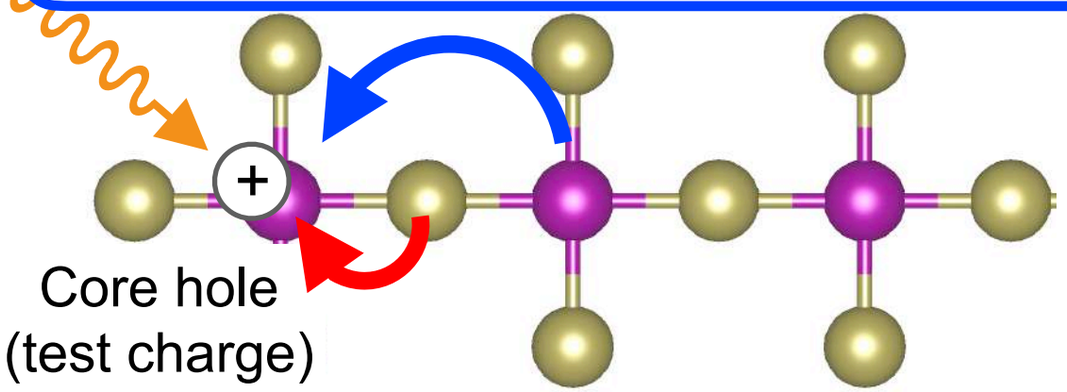

Quantum embedding

: DFT + DMFT

Anderson model

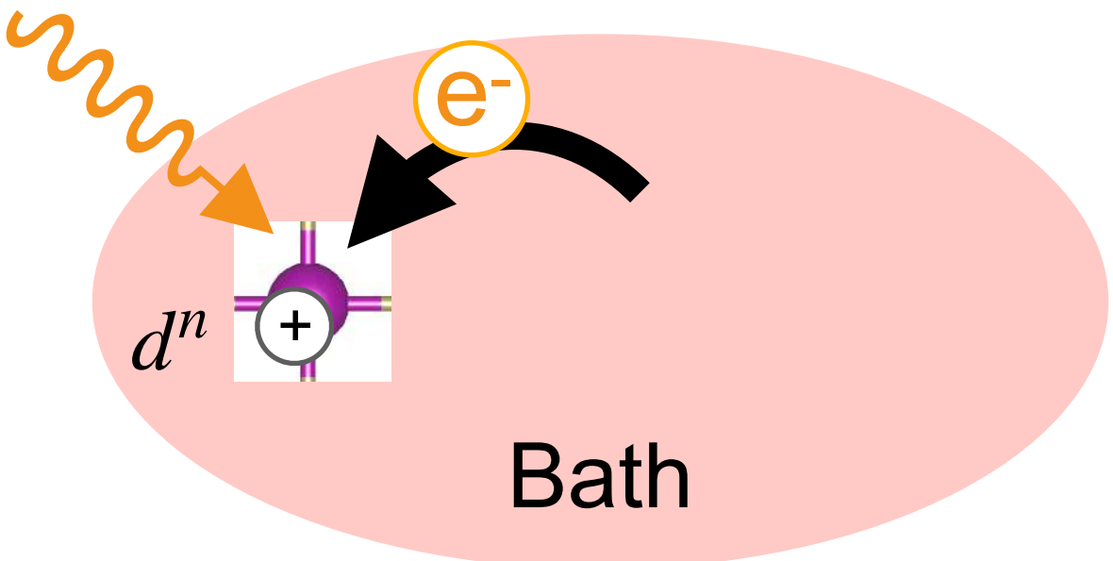

Incl. both ligand and

metal 3d bands

Calc. LDA+DMFT Anderson model

A. Hariki et al., PRB **96**, 045111 (2017)

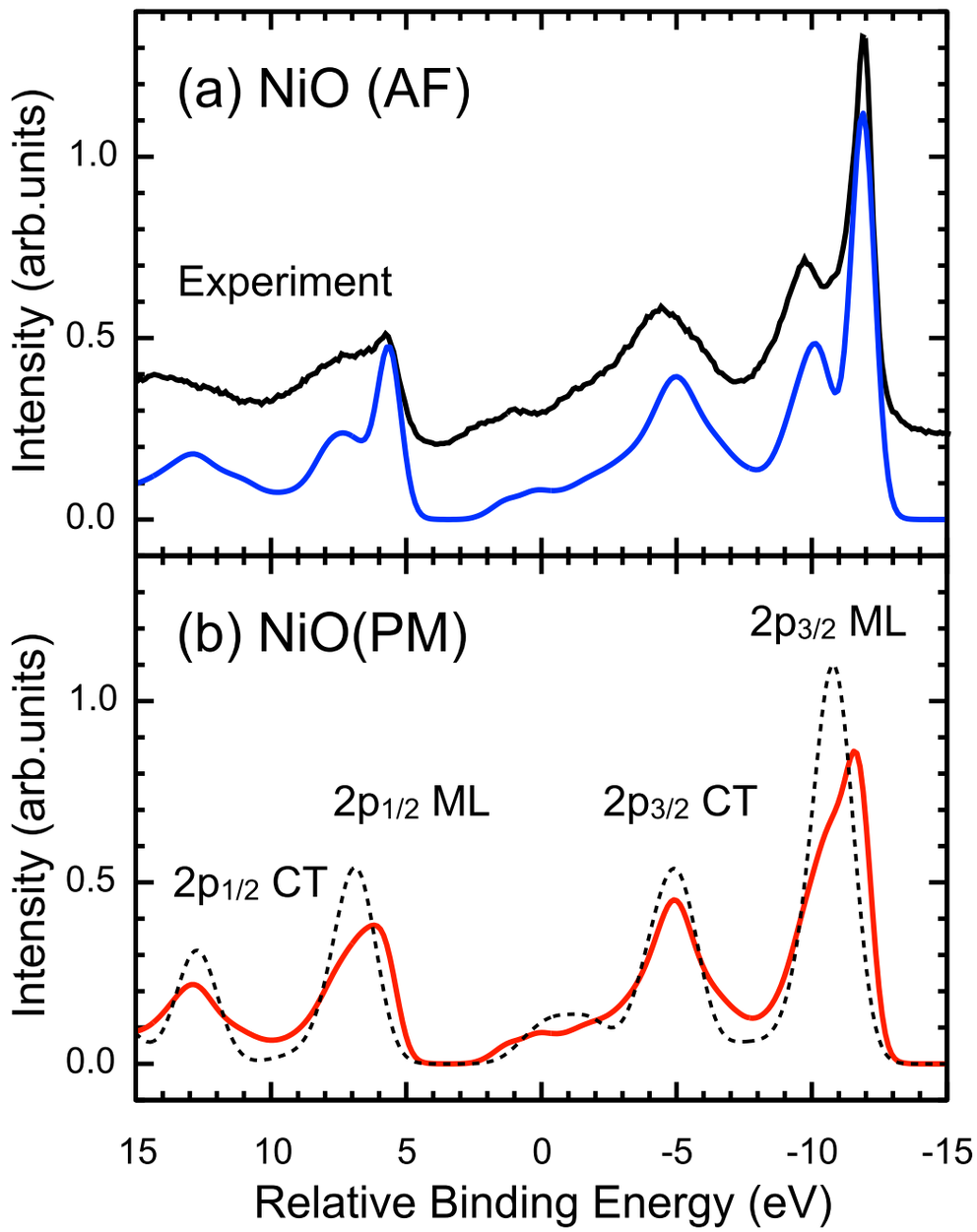

Spectroscopies

Metal - metal charge transfer : $d^n + d^n \rightarrow d^{n+1} + d^{n-1}$

: information on d bands (near Fermi energy)

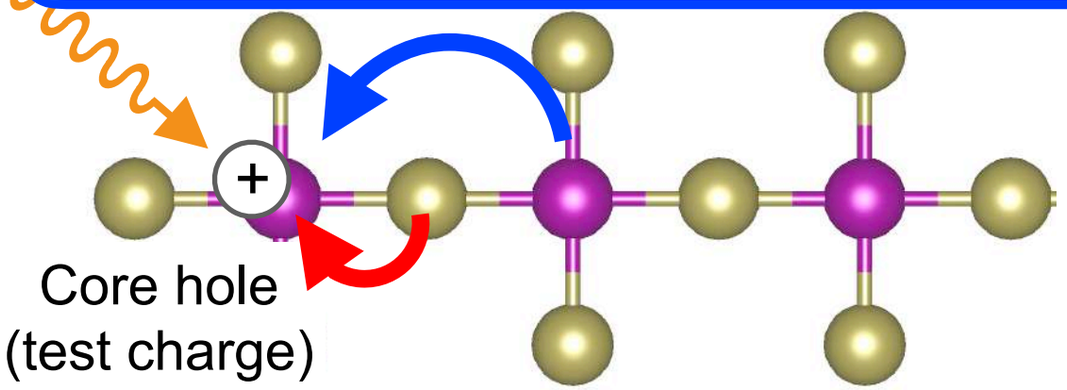

Antiferromagnetic phase:

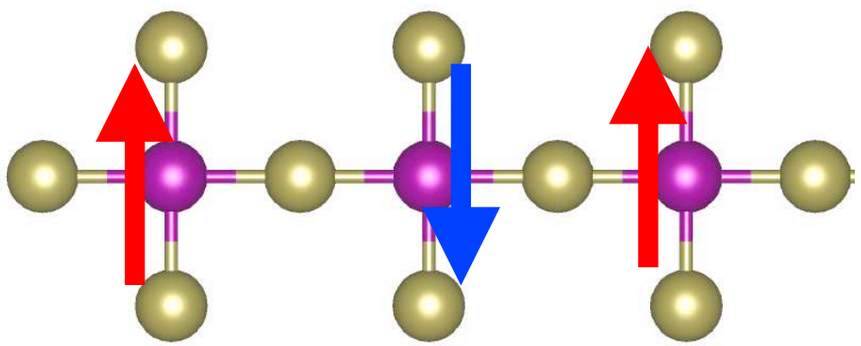

Paramagnetic phase (moment fluctuating):

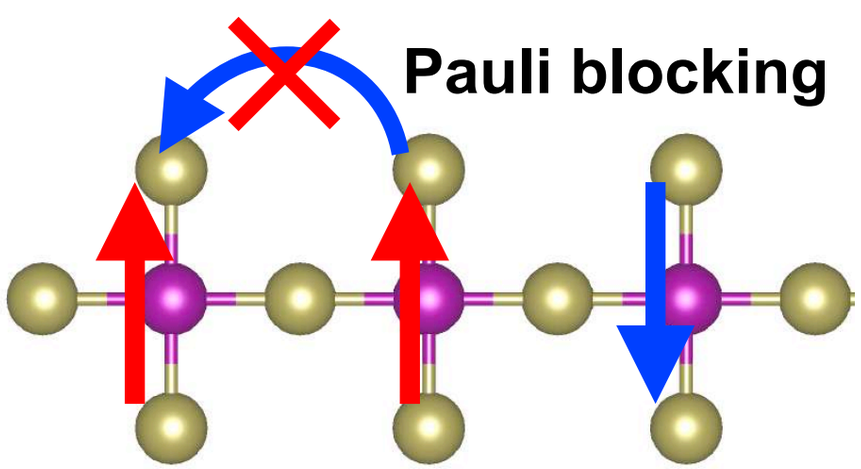

Calc. LDA+DMFT Anderson model

A. Hariki et al., PRB **96**, 045111 (2017)

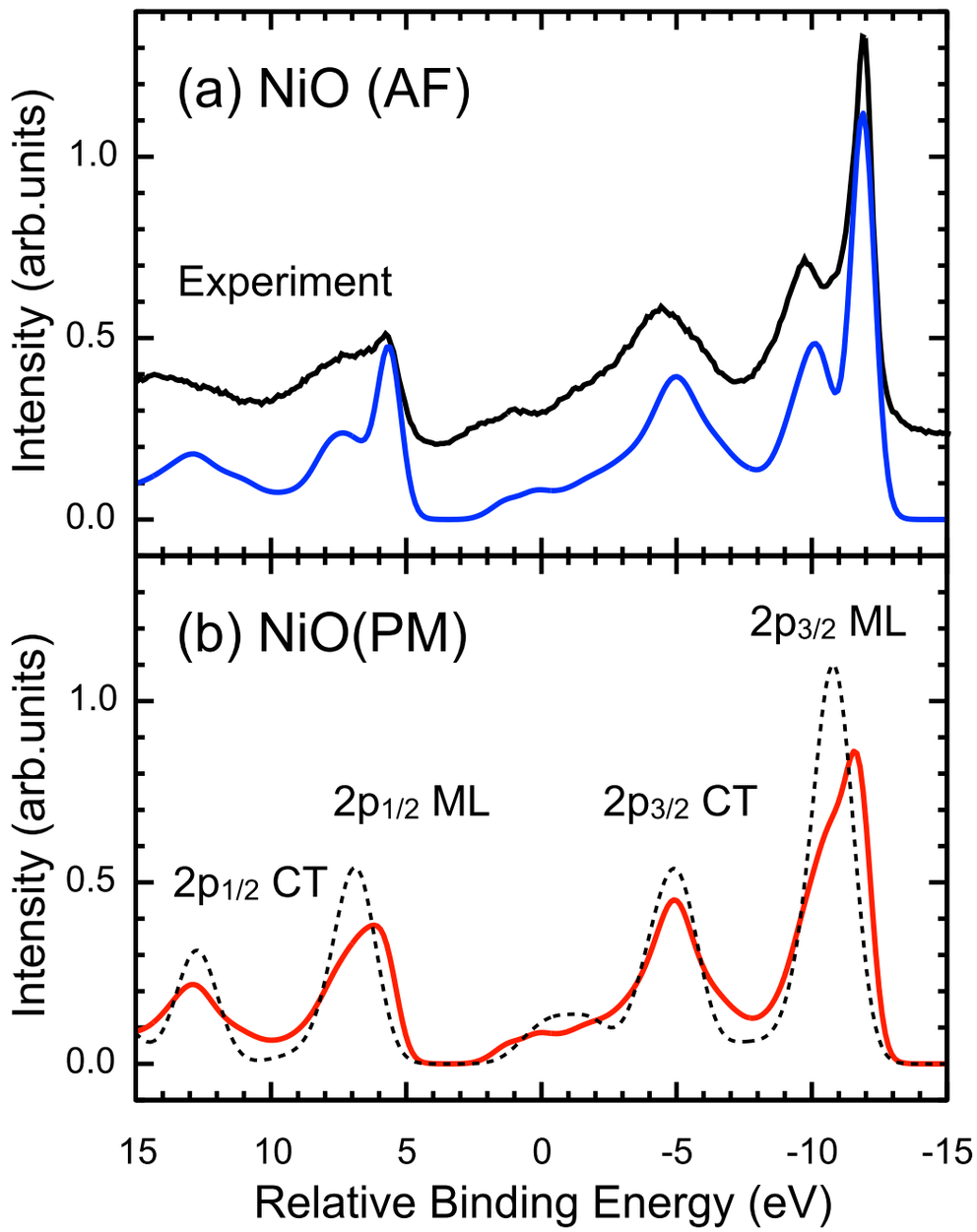

Spectroscopies

Metal - metal charge transfer : $d^n + d^n \rightarrow d^{n+1} + d^{n-1}$

: information on d bands (near Fermi energy)

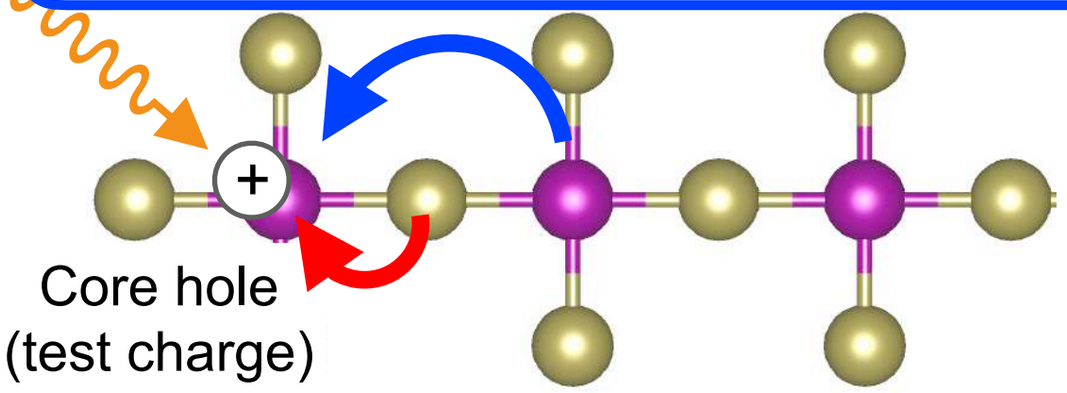

GO MOBILE » | ACCESS BY OSAKA METROPOLITAN UNIVERSITY

Spin-selective evolution of the Zhang-Rice state in binary transition metal oxide MnO(001) film

Asish K. Kundu[1,2,3,4,*], Polina M. Sheverdyaeva[2], Paolo Moras[2], Krishnakumar S. R. Menon[5], Subhasish Mandal[6,†], and Carlo Carbone[2]

Show more

Phys. Rev. B **109**, 195111 – **Published 3 May, 2024**

DOI: https://doi.org/10.1103/PhysRevB.109.195111

MnO, T_N~120K

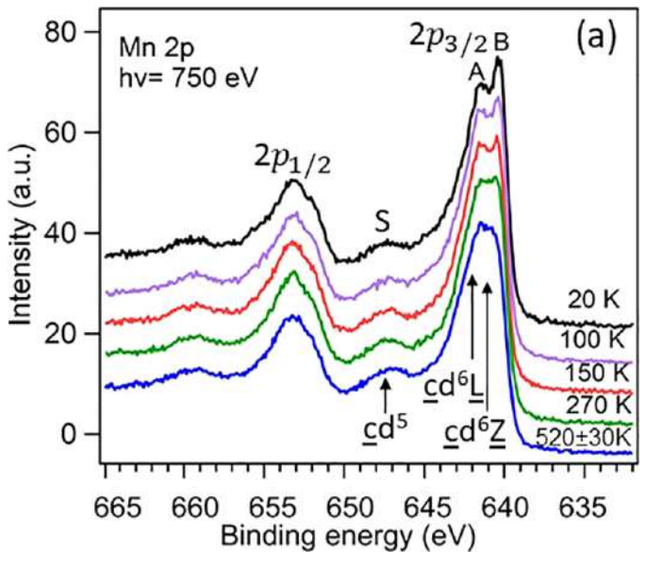

Calc. LDA+DMFT Anderson model

A. Hariki et al., PRB **96**, 045111 (2017)

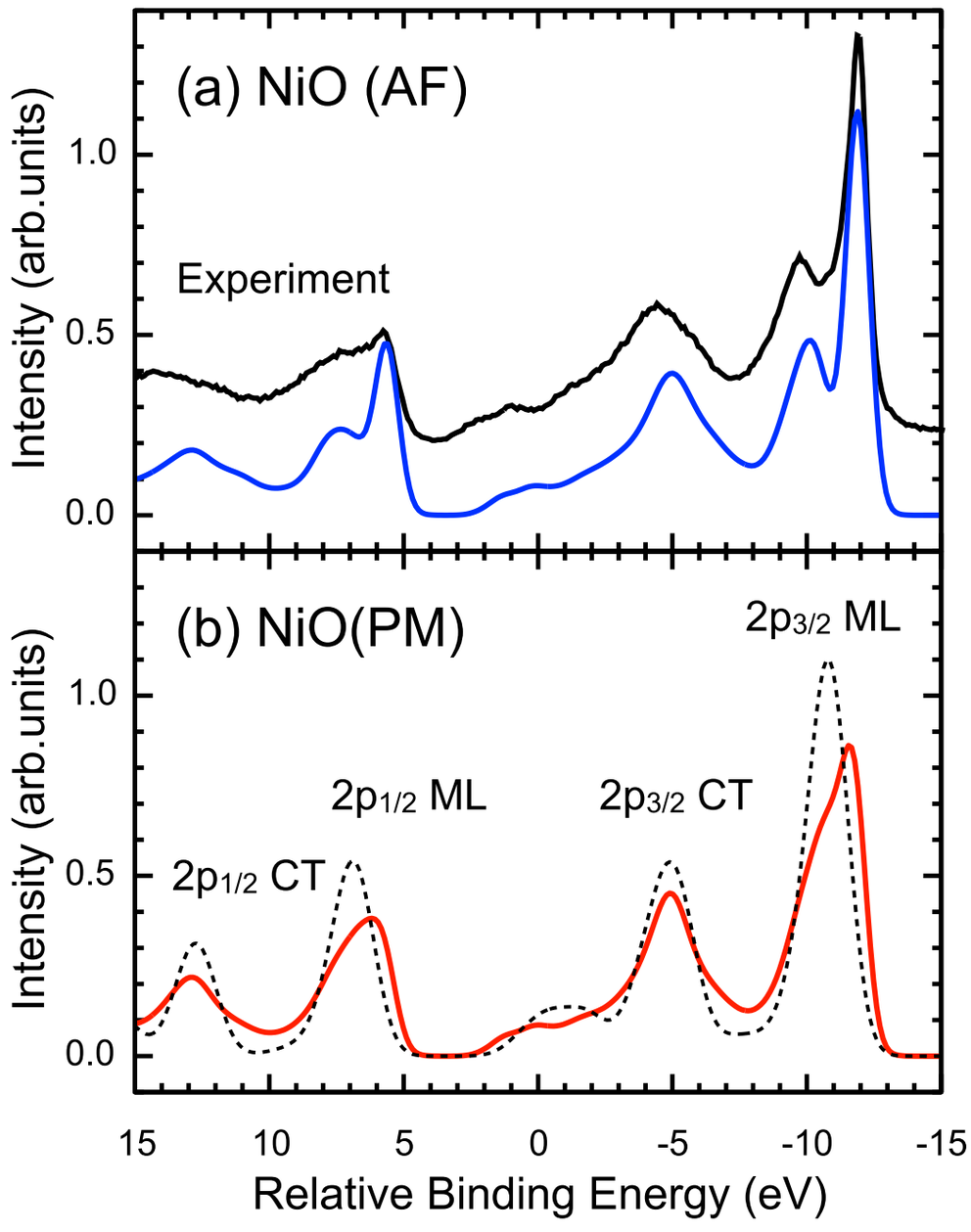

PHYSICAL REVIEW X **11,** 041009 (2021)

Core-Level X-Ray Spectroscopy of Infinite-Layer Nickelate: LDA + DMFT Study

Keisuke Higashi,[1] Mathias Winder,[2] Jan Kuneš,[2] and Atsushi Hariki[1,*]
[1]*Department of Physics and Electronics, Osaka Prefecture University 1-1 Gakuen-cho, Nakaku, Sakai, Osaka 599-8531, Japan*
[2]*Institute of Solid State Physics, TU Wien, 1040 Vienna, Austria*

(Received 11 May 2021; revised 4 August 2021; accepted 7 September 2021; published 13 October 2021; corrected 11 November 2021 and 23 November 2021)

Motivated by recent core-level x-ray photoemission spectroscopy, x-ray absorption spectroscopy (XAS), and resonant inelastic x-ray scattering (RIXS) experiments for the newly discovered superconducting infinite-layer nickelate, we investigate the core-level spectra of the parent compounds $NdNiO_2$ and $LaNiO_2$ using the combination of local density approximation and dynamical mean-field theory (LDA + DMFT). Adjusting a charge-transfer energy to match the experimental spectra, we determine the optimal model parameters and discuss the nature of the $NdNiO_2$ ground state. We find that self-doping from the Nd 5*d* states in the vicinity of the Fermi energy prohibits opening of a Mott-Hubbard gap in $NdNiO_2$. The present Ni L_3 XAS and RIXS calculation for $LaNiO_2$ cannot explain the difference from $NdNiO_2$ spectra.

nature

Explore content · About the journal · Publish with us

nature › letters › article

Letter | Published: 28 August 2019

Superconductivity in an infinite-layer nickelate

Danfeng Li, Kyuho Lee, Bai Yang Wang, Motoki Osada, Samuel Crossley, Hye Ryoung Lee, Yi Cui, Yasuyuki Hikita & Harold Y. Hwang

Nature **572**, 624–627 (2019) | Cite this article

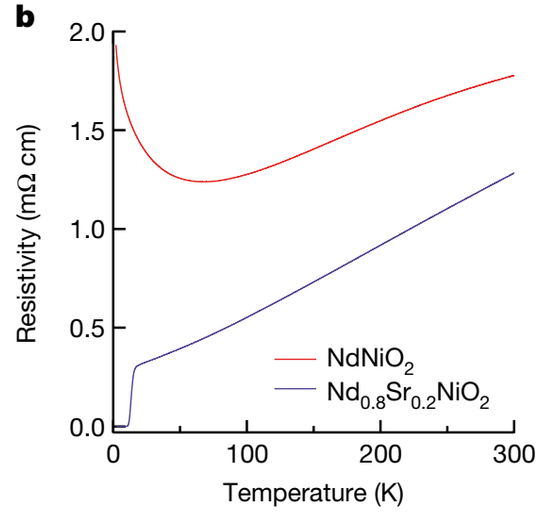

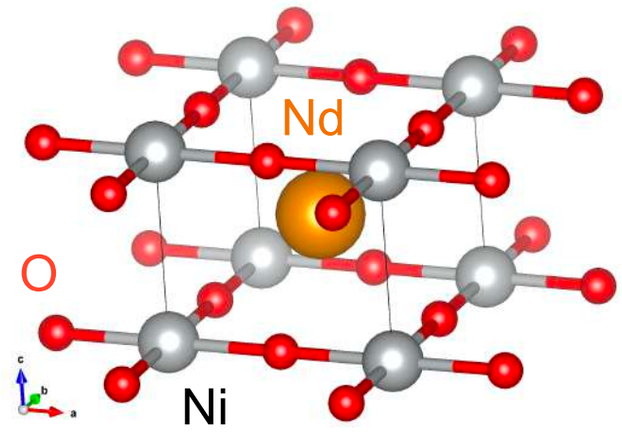

- ✔ Two dimensional structure
- ✔ Formally Ni is monovalent (d^9)

Ni 2*p* Core-level XPS

$$\Delta_{dp} = (\varepsilon_d^{\mathrm{LDA}} - \mu_{\mathrm{dc}}) + 9U_{dd} - \varepsilon_p^{\mathrm{LDA}}$$

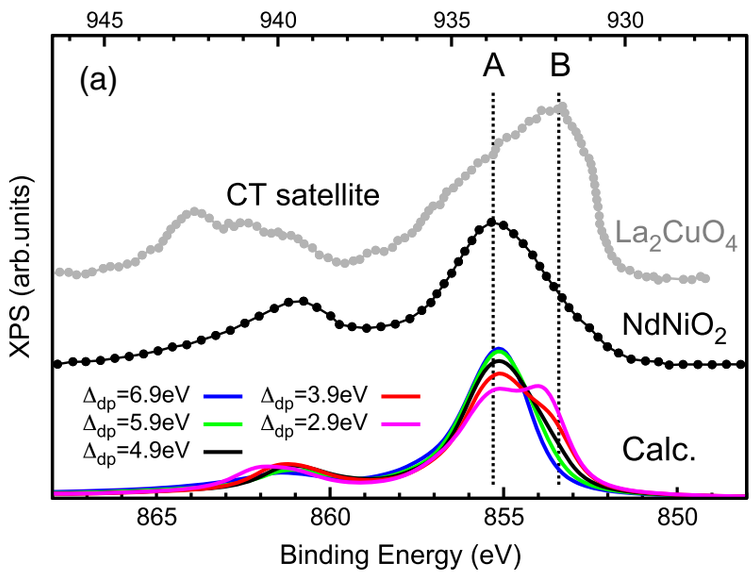

Ni valency and orbital occupation

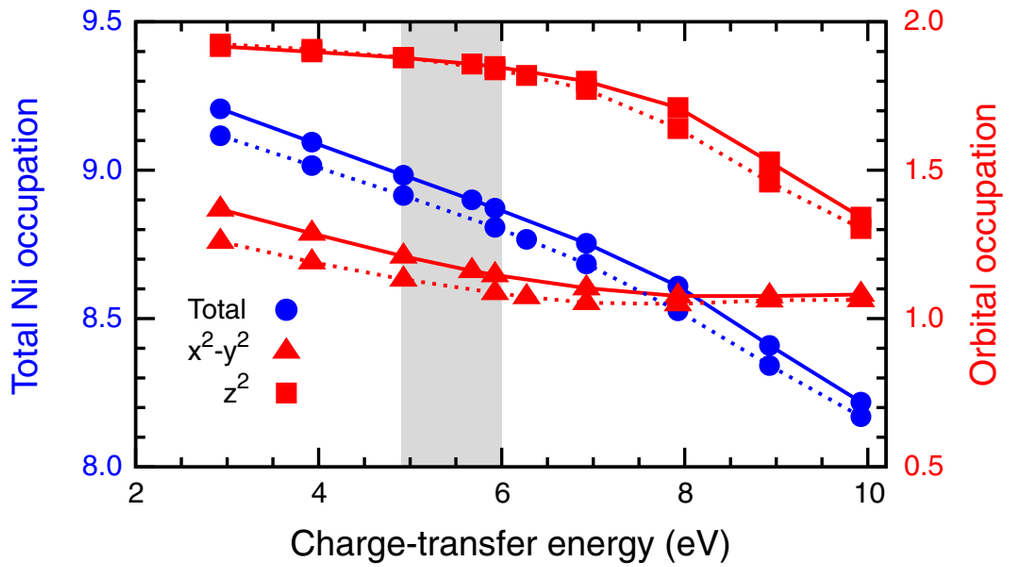

Valence spectra

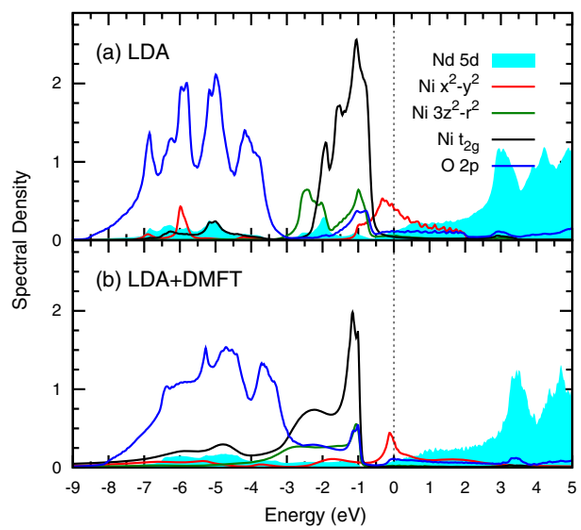

- ✔ Intermediate regime between the Mott-Hubbard and charge-transfer system
- ✔ Single band (Ni x^2-y^2) model with a small self-doping from Nd 5d states

Physical Review B

Highlights Recent Accepted Collections Authors Referees Press About Editorial Team RSS

ACCEPTED PAPER

Valence, charge transfer, and orbital-dependent correlation in bilayer nickelates $Nd_3Ni_2O_7$

Daisuke Takegami, Takaki Okauchi, Edgar Abarca Morales, Kouto Fujinuma, Mizuki Furo, Masato Yoshimura, Ku-Ding Tsuei, Grace A. Pan, Dan Ferenc Segedin, Qi Song, Hanjong Paik, Charles M. Brooks, Julia A. Mundy, Takashi Mizokawa, Liu Hao Tjeng, Berit H. Goodge, and Atsushi Hariki

Phys. Rev. B - **Accepted** 17 March, 2025

Accepted in PRB

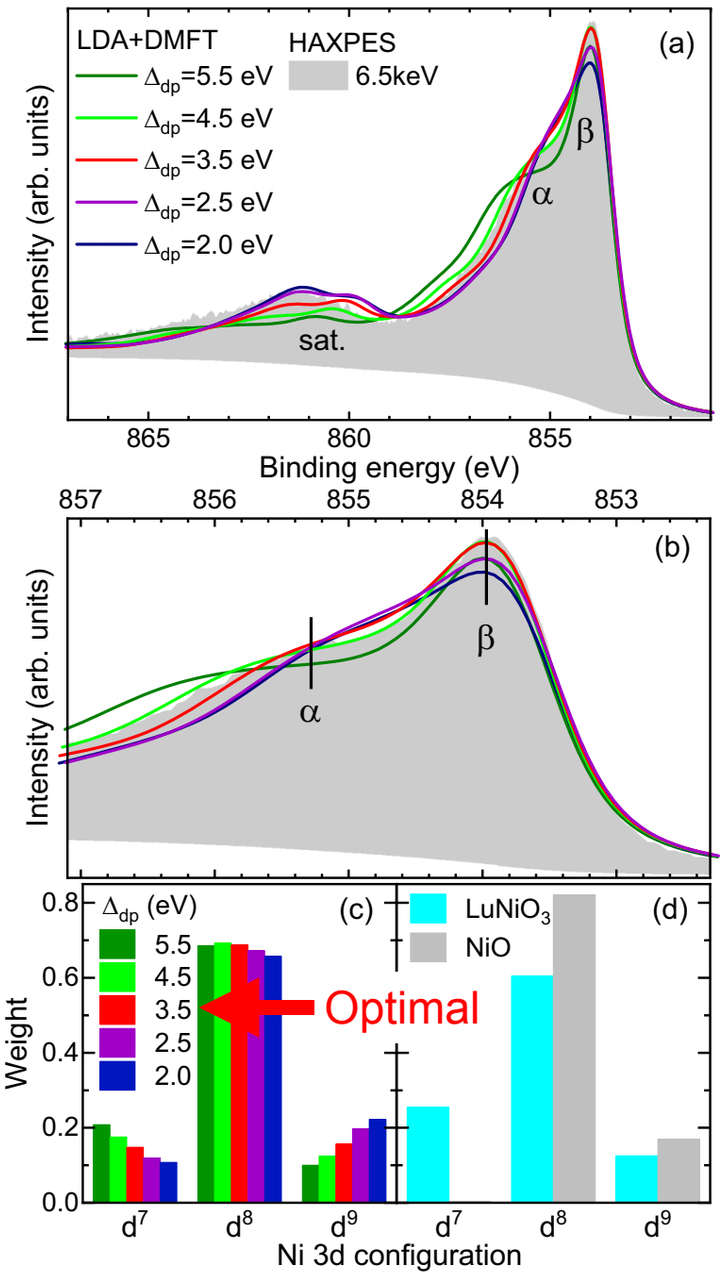

$R^{3+}{}_3Ni^{2.5+}{}_2O^{2-}{}_7$

Ni^{2+} + Ni^{3+} ?

Different multiplet, hybridization ?

nature

Explore content About the journal Publish with us

nature > articles > article

Article | Published: 12 July 2023

Signatures of superconductivity near 80 K in a nickelate under high pressure

Hualei Sun, Mengwu Huo, Xunwu Hu, Jingyuan Li, Zengjia Liu, Yifeng Han, Lingyun Tang, Zhongquan Mao, Pengtao Yang, Bosen Wang, Jinguang Cheng, Dao-Xin Yao, Guang-Ming Zhang ✉ & Meng Wang ✉

Nature **621**, 493–498 (2023) | Cite this article

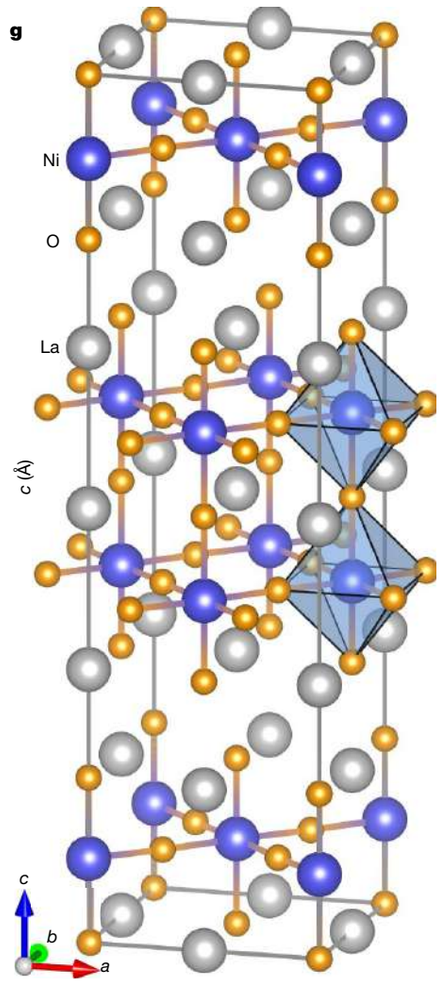

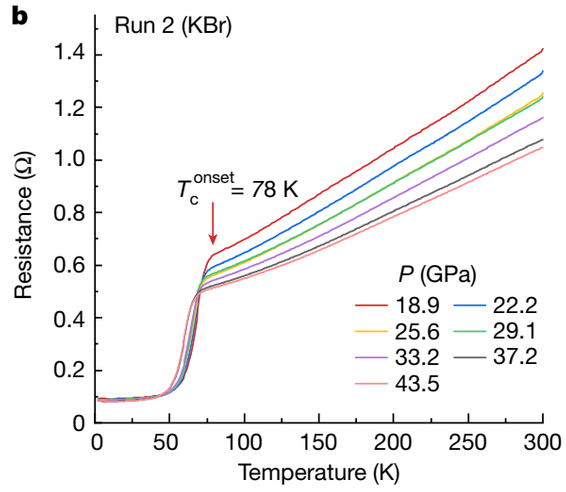

nature

Explore content About the journal Publish with us

nature > articles > article

Article | Published: 19 December 2024

Signatures of ambient pressure superconductivity in thin film $La_3Ni_2O_7$

Eun Kyo Ko ✉, Yijun Yu ✉, Yidi Liu, Lopa Bhatt, Jiarui Li, Vivek Thampy, Cheng-Tai Kuo, Bai Yang Wang, Yonghun Lee, Kyuho Lee, Jun-Sik Lee, Berit H. Goodge, David A. Muller & Harold Y. Hwang ✉

Nature **638**, 935–940 (2025) | Cite this article

Differences in different core levels?

AH et al., Phys. Rev. B. **106**, 205138 (2022)

$SrTiO_3$, TiO_2; band insulator ($3d^0$)

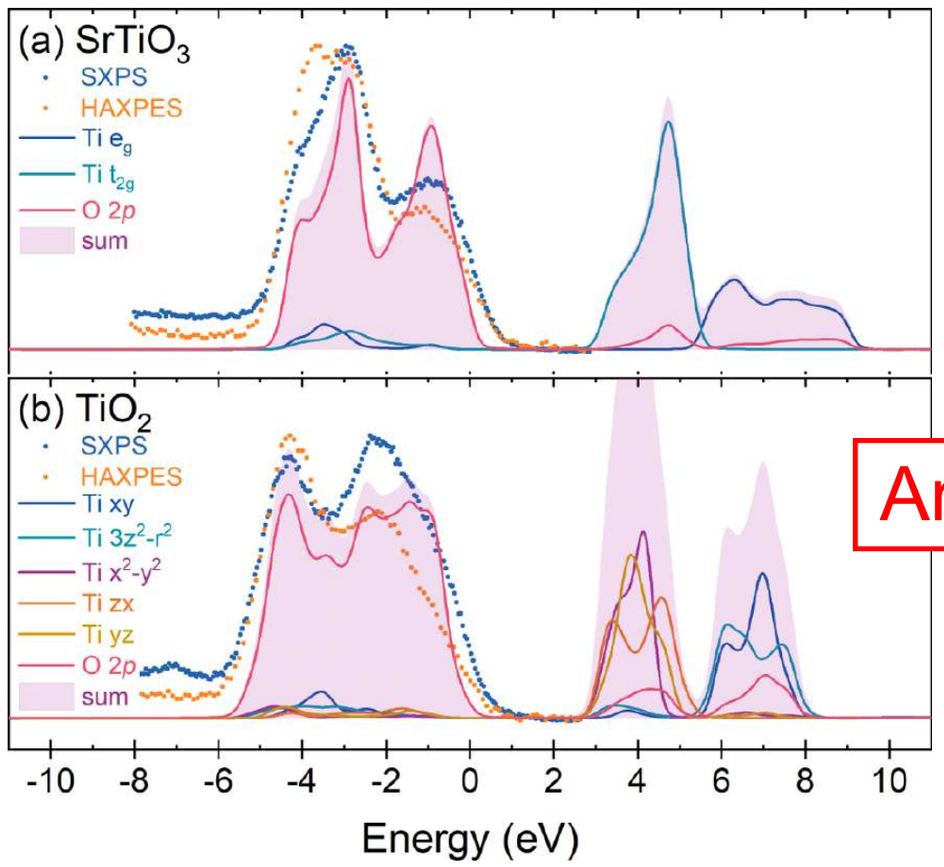

Hard x-ray (~10keV) survey of core-levels

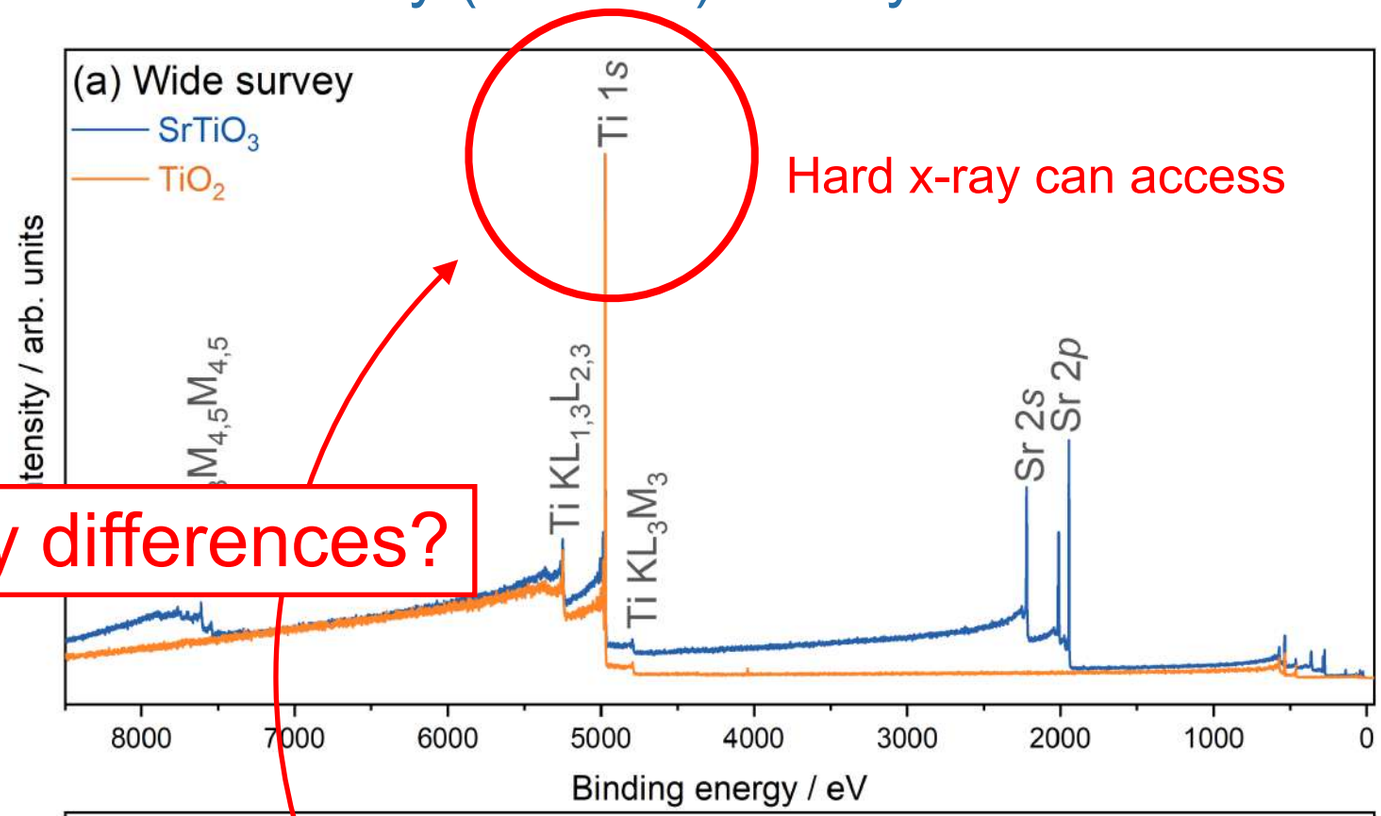

Hard x-ray can access

Any differences?

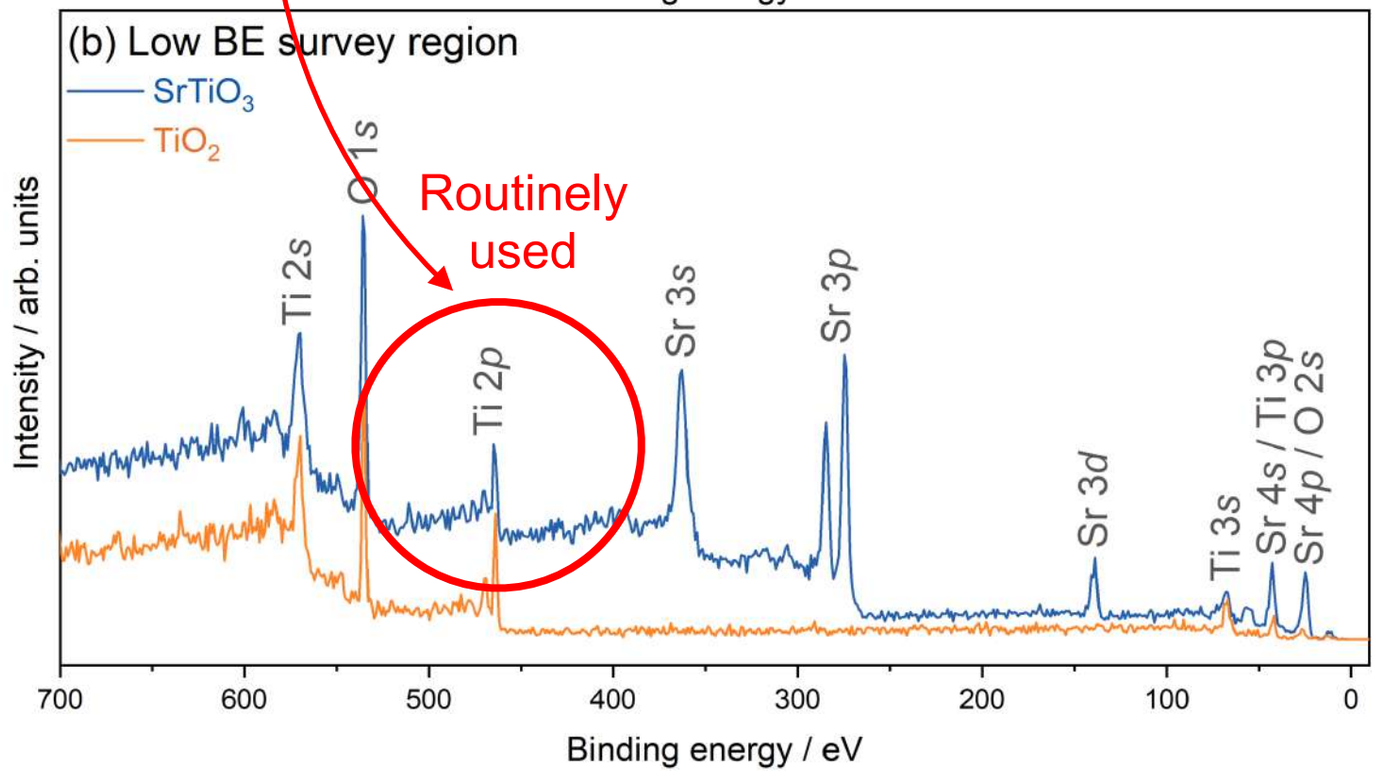

Routinely used

$SrTiO_3$ (Perovskite structure)

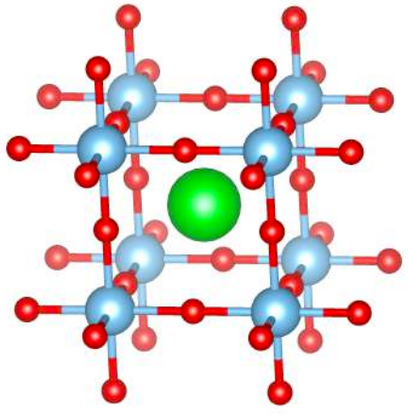

TiO_2 (Rutile structure)

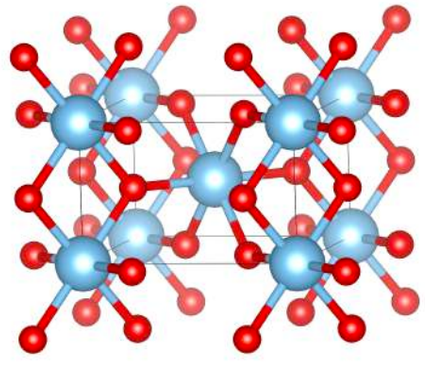

1) Absence of ***Spin-Orbit Coupling***

AH et al., Phys. Rev. B **106**, 205138 (2022)

Exp. Ti 1s and 2p HAXPES

First report : J. C. Woicik et al., Phys. Rev. B **101**, 245119 (2020)

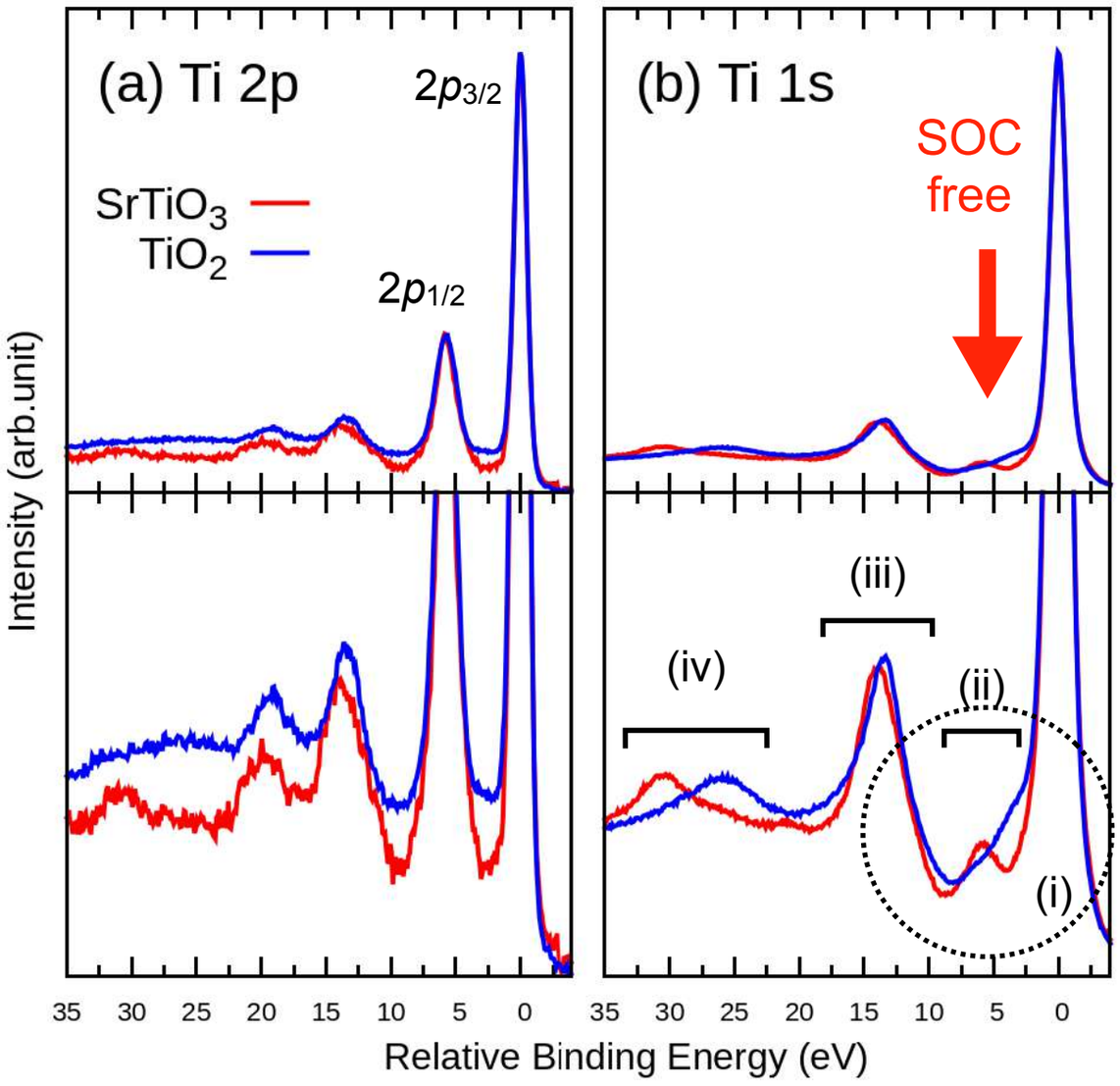

LDA+DMFT & cluster-model calc.

incl. O bands **incl. only nearest O sites**

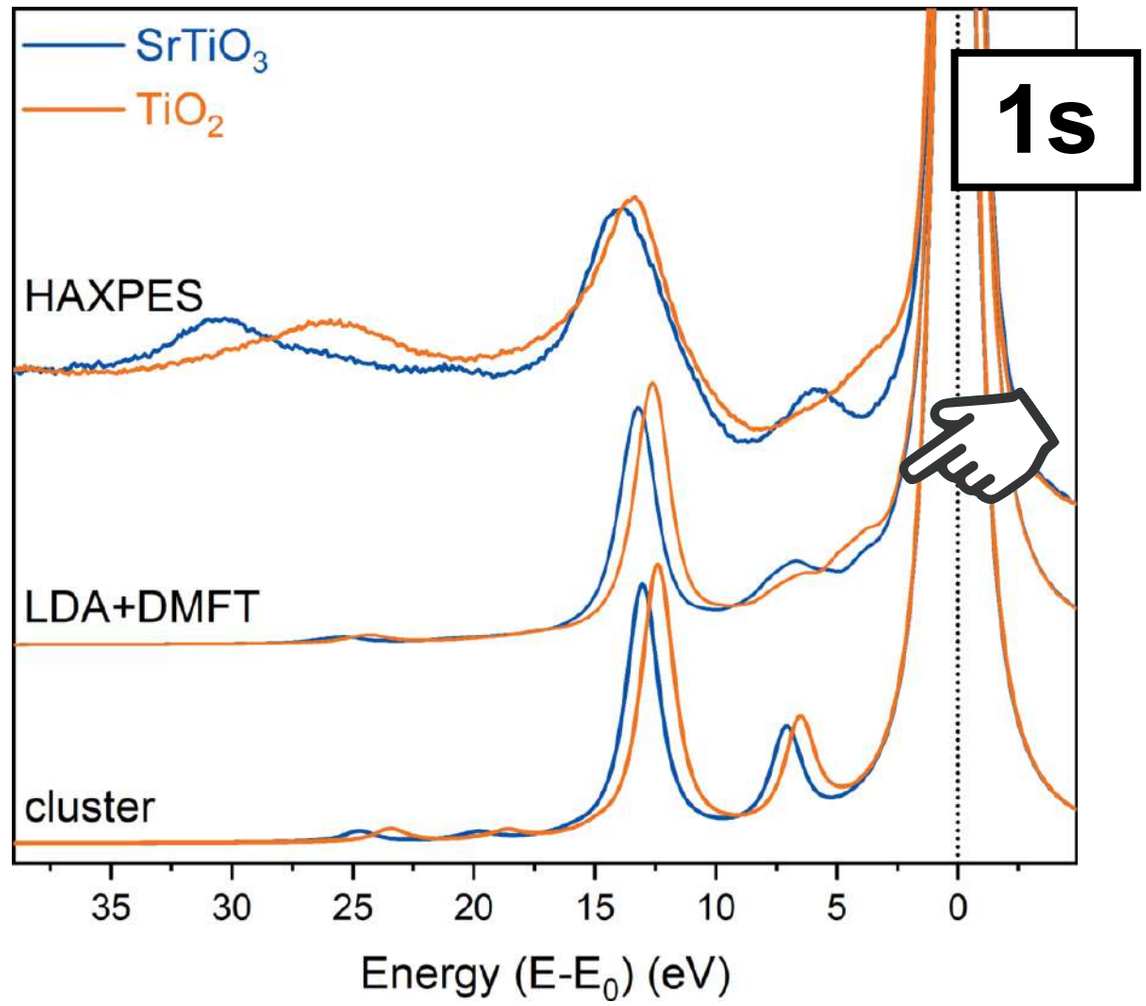

Material-dependent satellite in SOC-free 1s HAXPES

The hidden satellites reflect hybridization of Ti and O 2p bands

2) Absence of ***Core-Valence Multiplet***

T. Yamaguchi, **AH**, et al.,
Phys. Rev. B **109**, 205143 (2024)

VO_2 and CrO_2, correlated metals

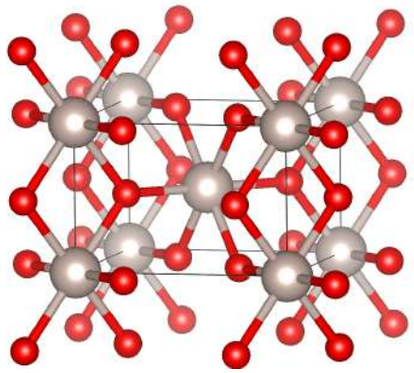

Rutile structure

LDA+DMFT valence band

Exp. R. Eguchi et al., Phys. Rev. B **78**, 075115 (2008)

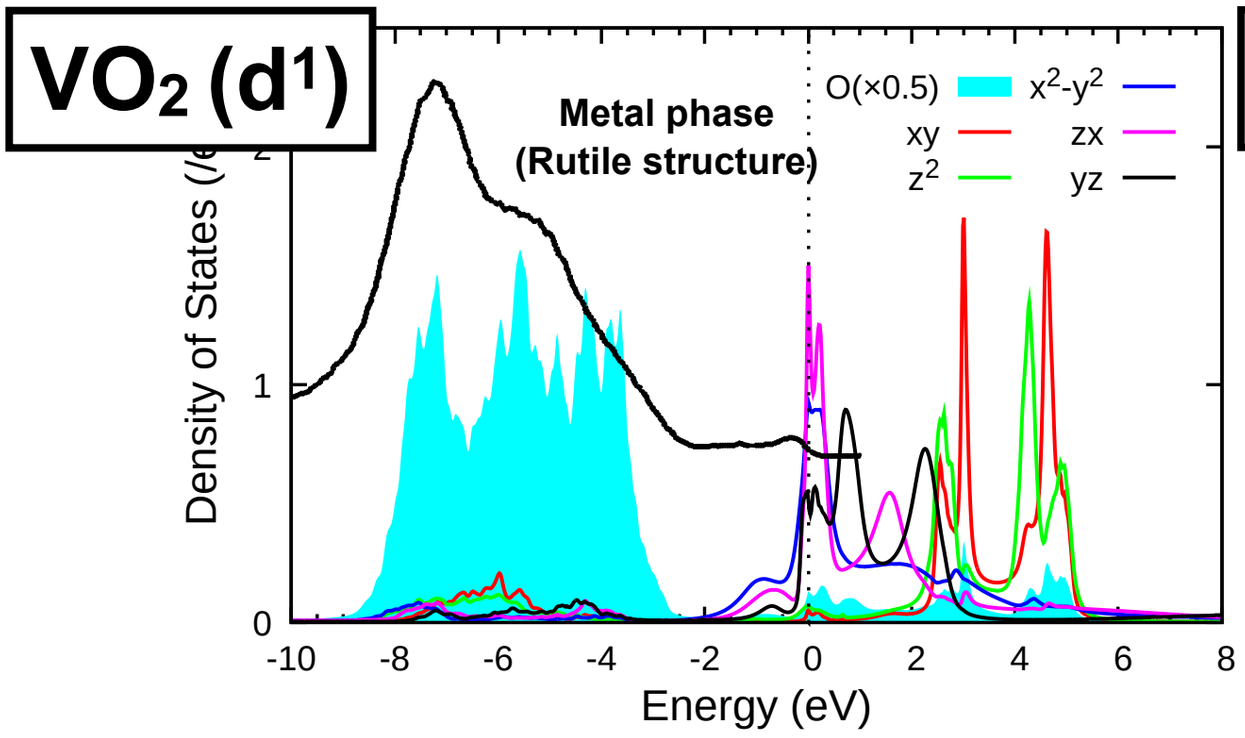

Exp. M. Sperlich et al., Phys. Rev. B **87**, 235138 (2013)

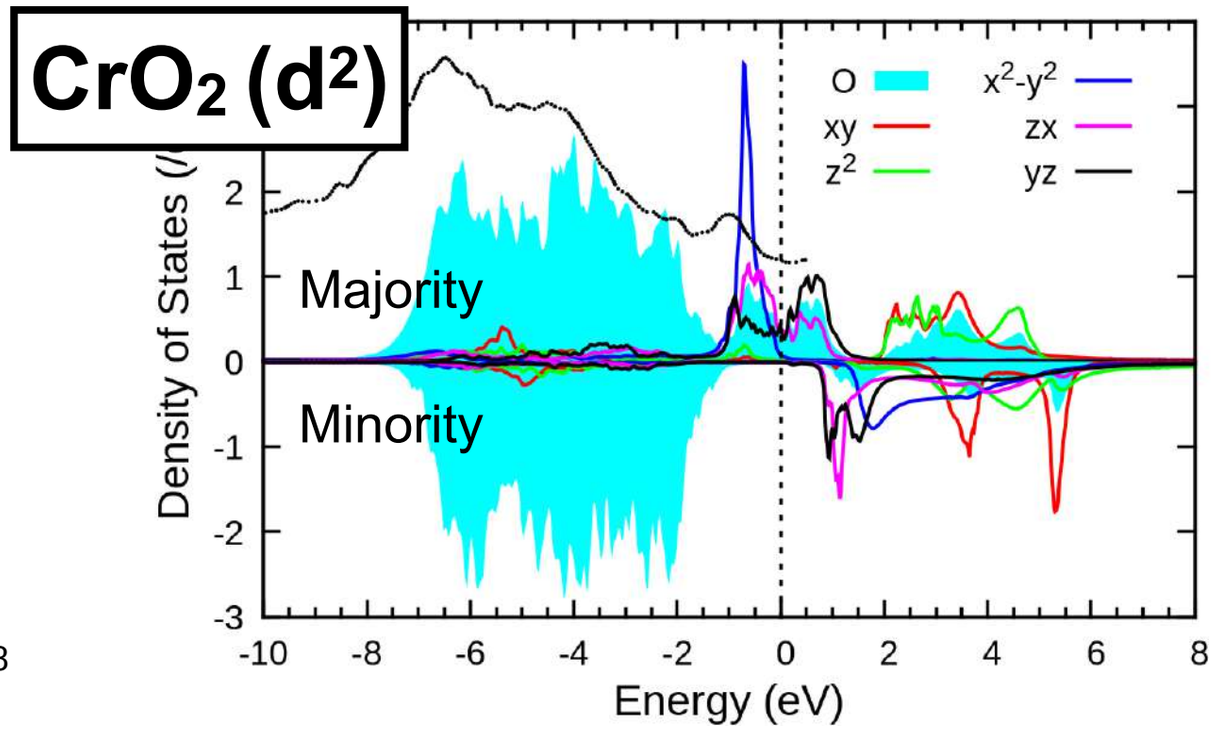

VO_2 : Quasiparticle peak & Hubbard bands

CrO_2 : Half-metallic electronic structure

S. Biermann et al., Phys. Rev. Lett. **94**, 026404 (2005)

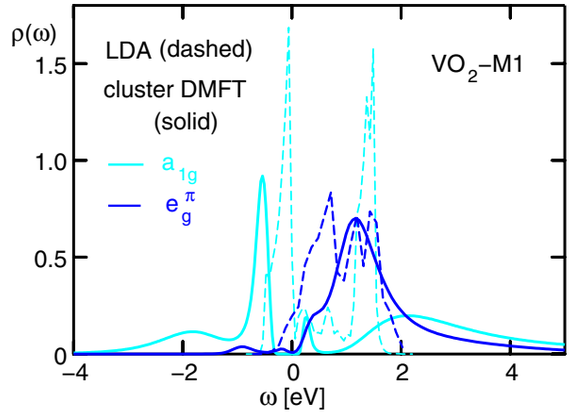

2) Absence of ***Core-Valence Multiplet***

T. Yamaguchi, **AH**, et al.,
Phys. Rev. B **109**, 205143 (2024)

V 1s and 2p HAXPES in VO_2

Exp. R. Eguchi et al., Phys. Rev. B **78**, 075115 (2008)

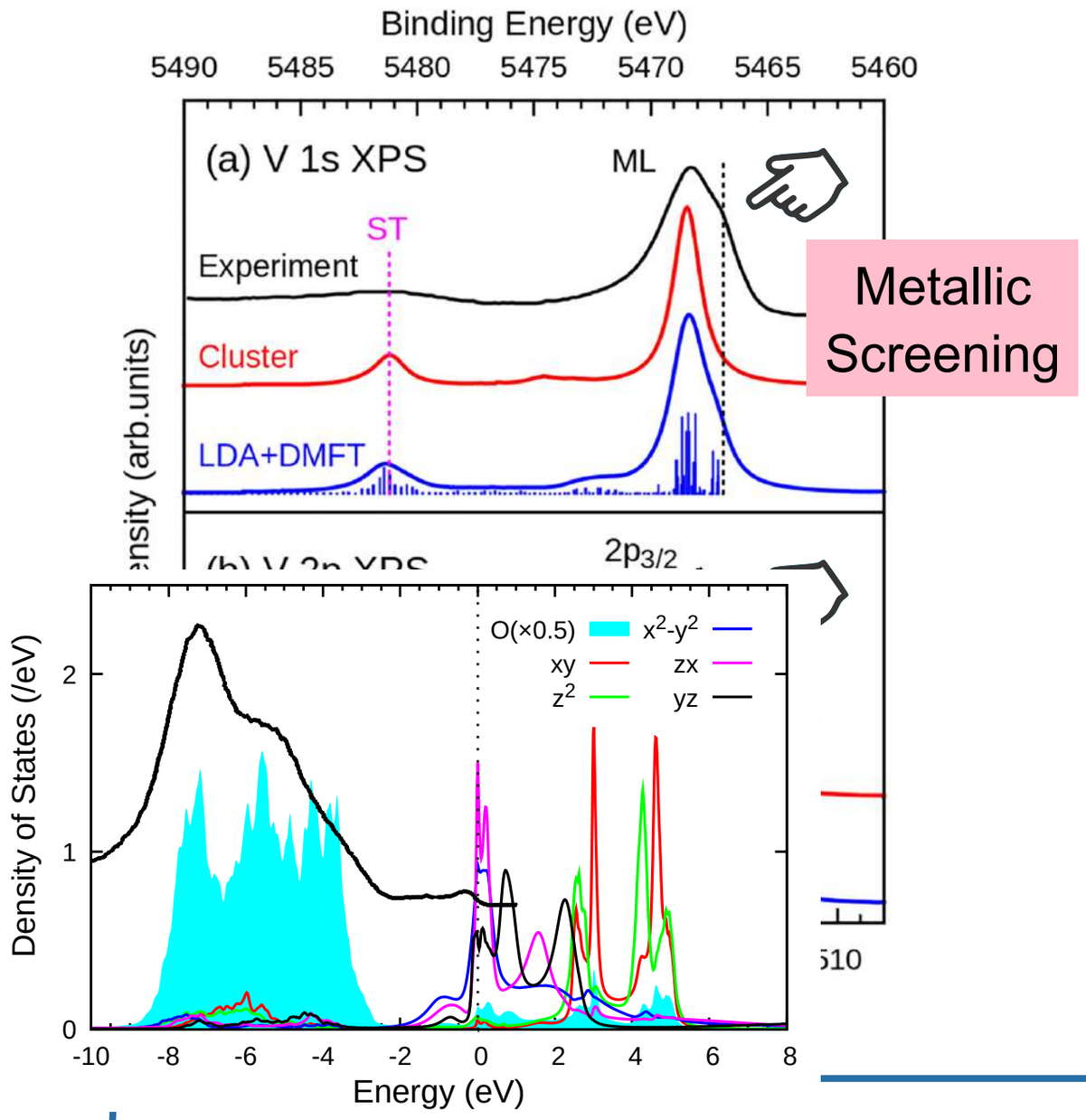

Metallic Screening

Cr 1s and 2p HAXPES in CrO_2

Cr 2p data: M. Sperlich et al., Phys. Rev. B 87, 235138 (2013)

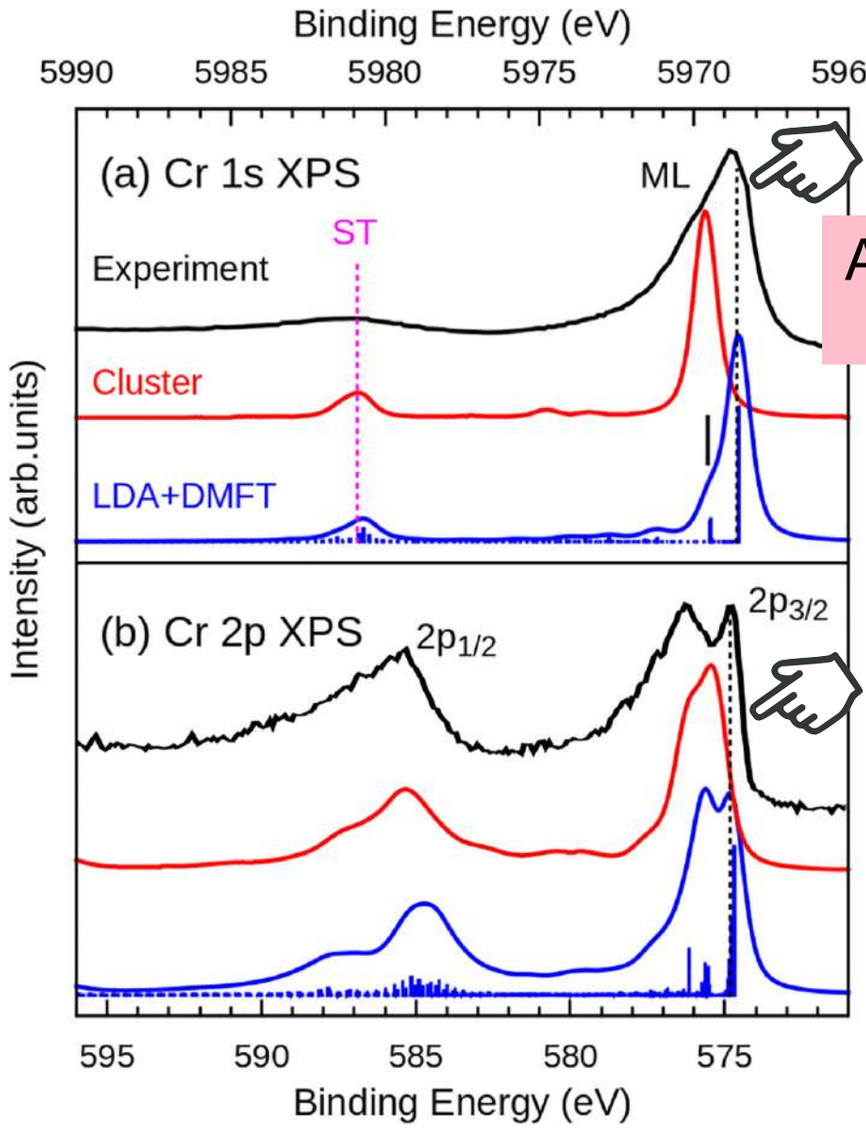

Asymmetric feature

Double peak

VO_2 : **1s is replica of 2p**, with nonlocal metallic screening feature

CrO_2 : Very different 1s and 2p line shape → **Why not replica ??**

2) Absence of ***Core-Valence Multiplet***

T. Yamaguchi, **AH**, et al.,
Phys. Rev. B **109**, 205143 (2024)

Calc. 2p-3d multiplet dependence

(Modify LDA+DMFT AIM Hamiltonian)

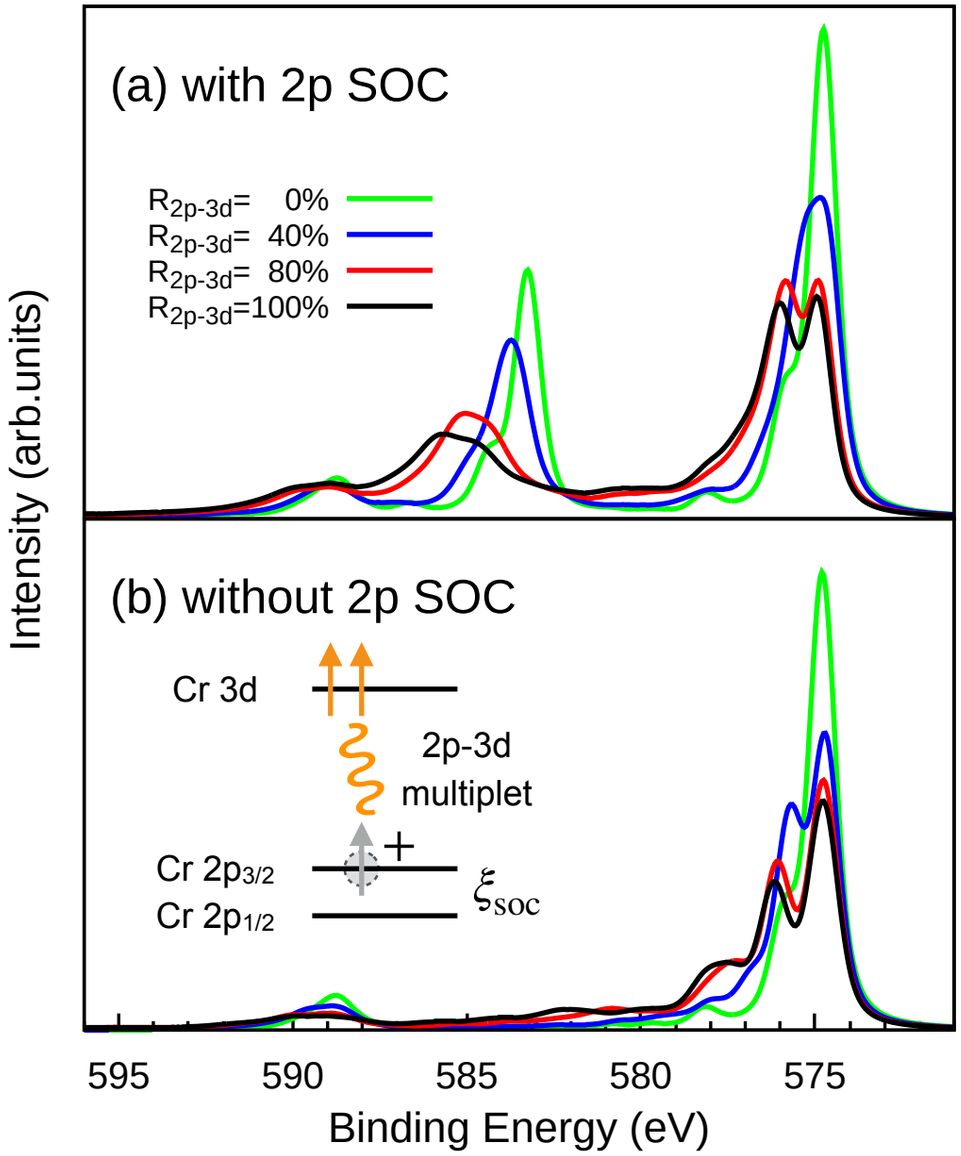

Cr 1s and 2p HAXPES in CrO_2

Cr 2p data: M. Sperlich et al., Phys. Rev. B 87, 235138 (2013)

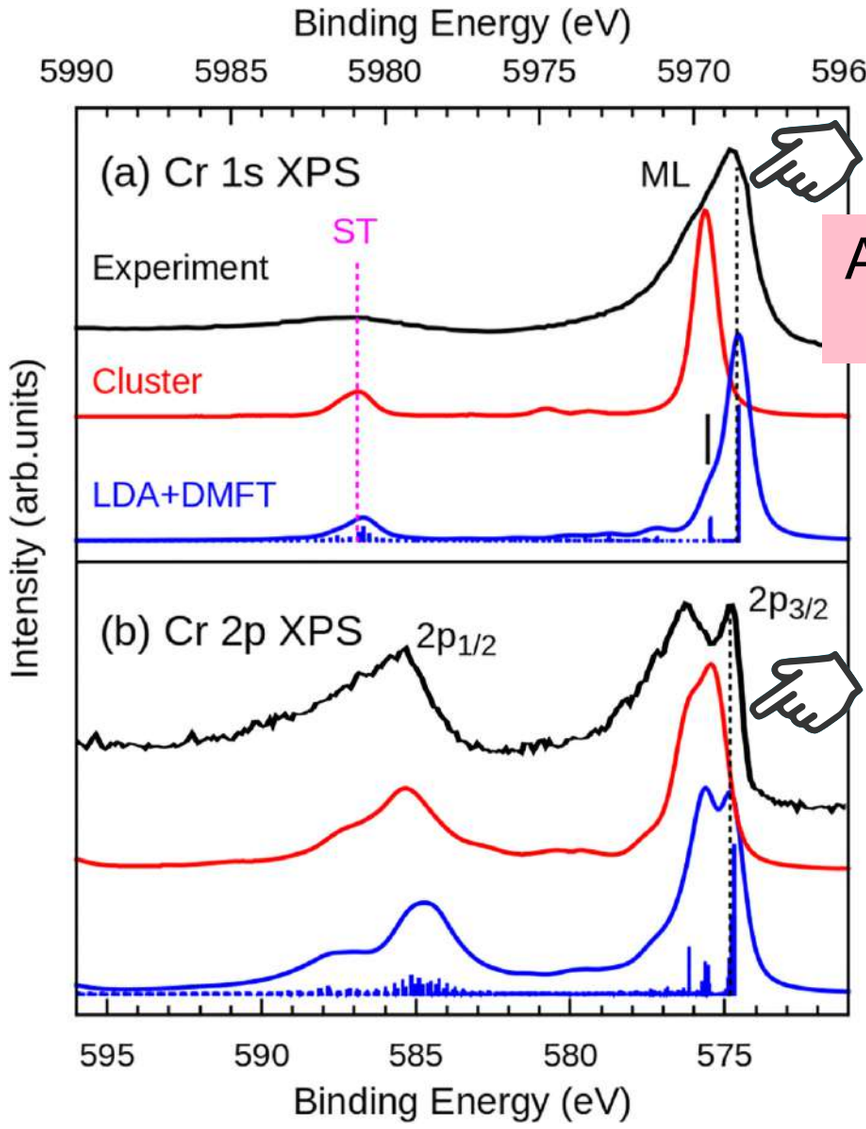

Asymmetric feature

Double peak

1s HAXPES is suited for studying charge transfer excitations,
when the core-valence multiplet is substantial (Cr, Fe, Mn …)

2) Absence of ***Core-Valence Multiplet***

T. Yamaguchi, **AH**, et al.,
Phys. Rev. B **109**, 205143 (2024)

Exp. M. Sperlich et al., Phys. Rev. B **87**, 235138 (2013)

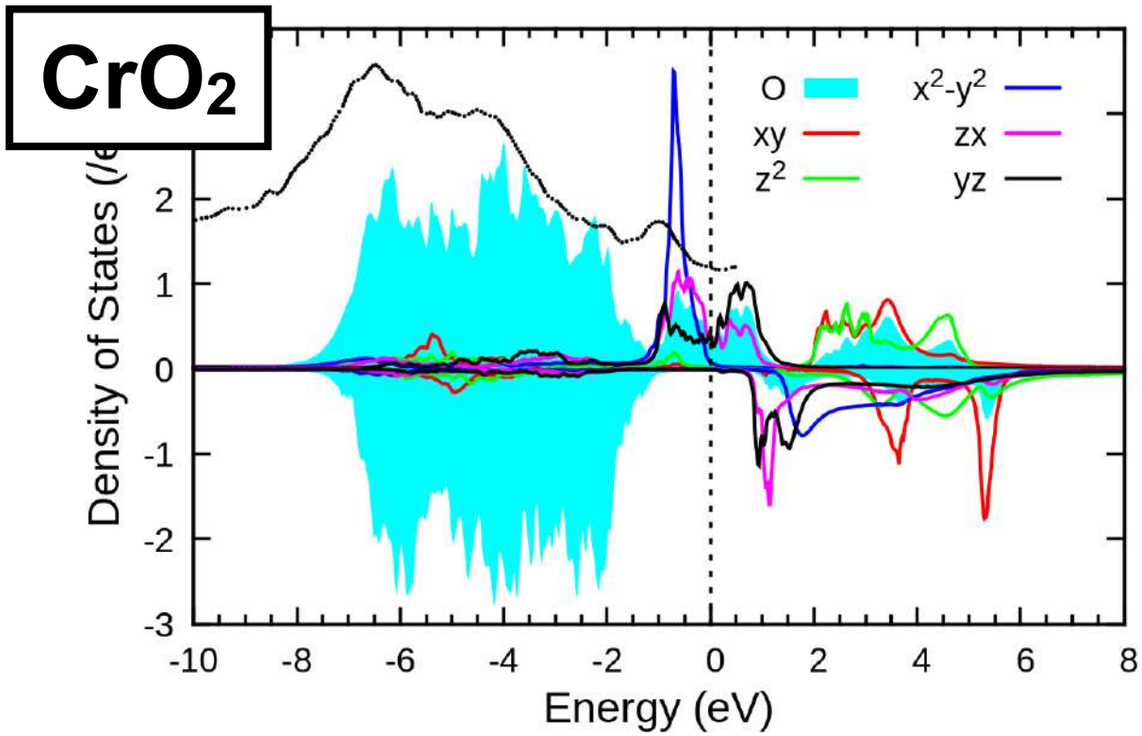

Main peak: Metallic screening

V

Tail : Local ligand screening

Cr 1s and 2p HAXPES in CrO_2

Cr 2p data: M. Sperlich et al., Phys. Rev. B 87, 235138 (2013)

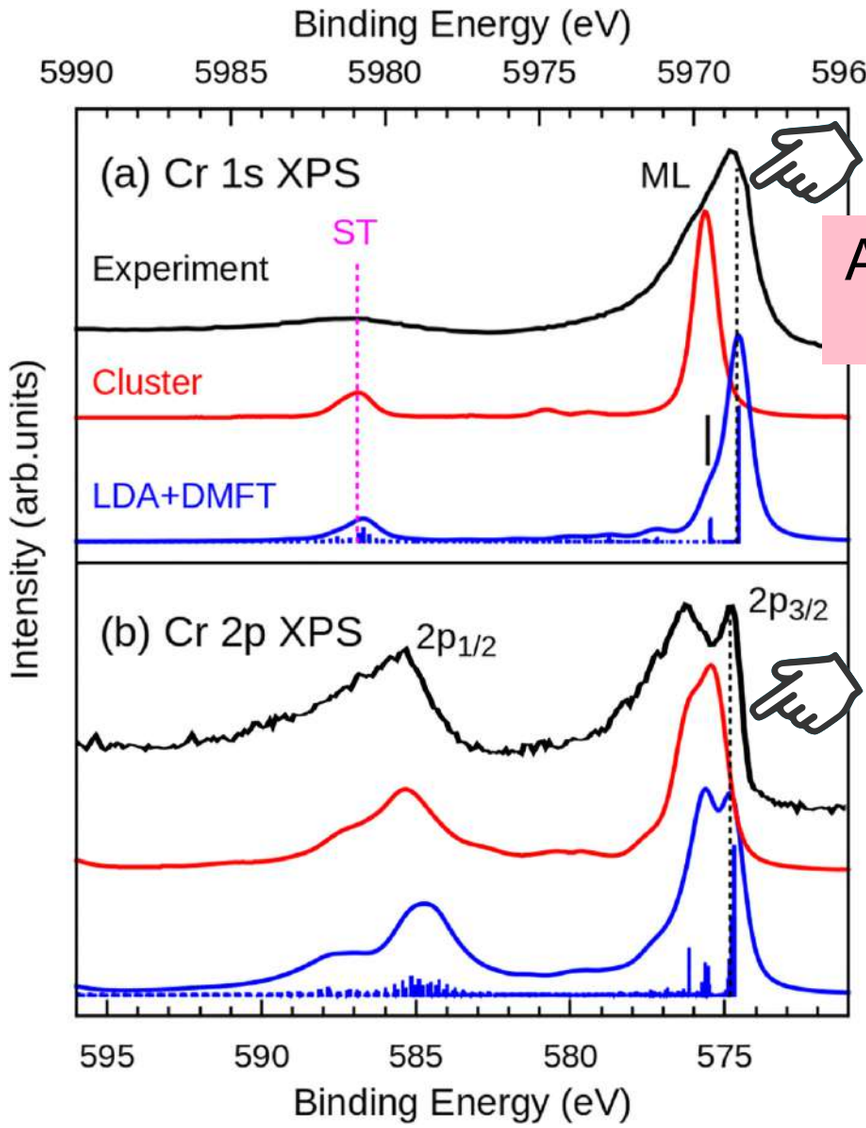

Asymmetric feature

Double peak

1s HAXPES is suited for studying charge transfer excitations,
when the 2p core-valence multiplet is effective (Cr, Fe, Mn …)

Table of contents

1. Core-level X-ray spectroscopy and DFT-based embedding approach

★ **Method**. DFT+ dynamical mean-field theory (DMFT)

A. Hariki, T. Uozumi, and J. Kuneš, Phys. Rev. B **96**. 045111 (2017)

A. Hariki, M. Winder, and J. Kuneš, Phys. Rev. Lett. **121**, 126403 (2018)

A. Hariki, M. Winder, T. Uozumi, and J. Kuneš, Phys. Rev. B **101**, 115130 (2020)

2. Application to various optical processes and compounds

★ **Excitations**. XPS, XAS, RIXS ★ **Materials**. *d*, *f* electron systems

★ **Physics**. Magnetism, valence structure, elementary excitations

K. Higashi, M. Winder, J. Kuneš, and A. Hariki, Phys. Rev. X **11**, 041009 (2021)

D. Takegami, A. Hariki et al., Phys. Rev. X **12**, 011017 (2022)

M. C. Rahn, K. Kummer, A. Hariki, et al., Nat. Commun. **13**, 6129 (2022)

J. Li, A. Hariki et al., Phys. Rev. X **13**, 011012 (2023)

A. Hariki et al., Phys. Rev. Let. **132**, 176701 (2024)

Core-level x-ray absorption spectroscopy

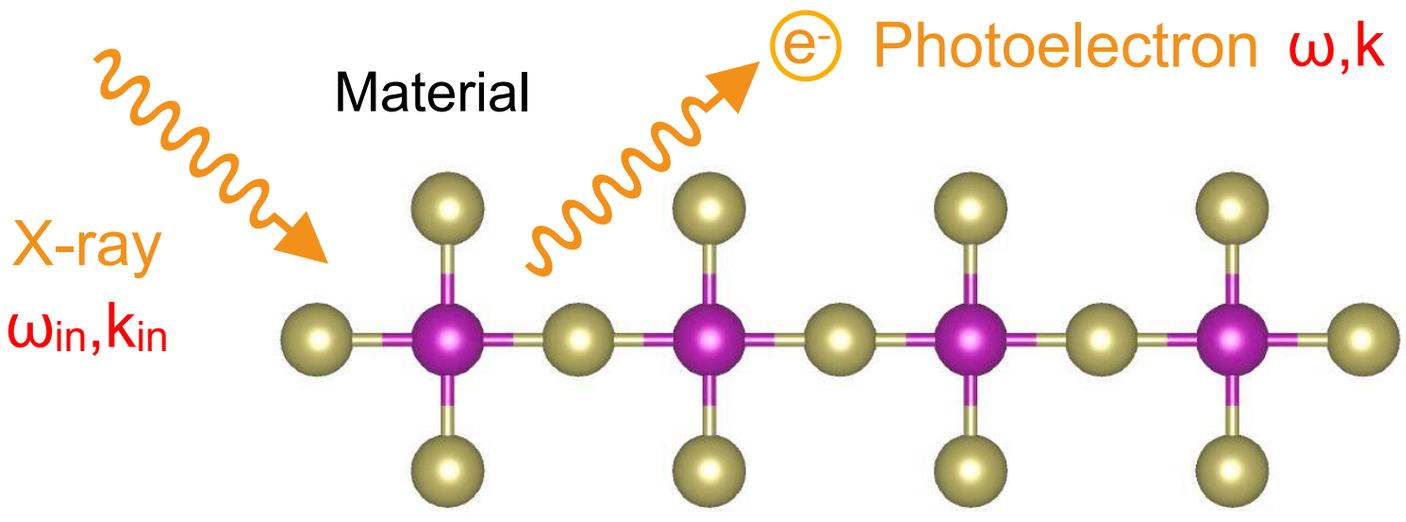

X-ray photoemission spectroscopy:

- Valence-band XPS (ARPES)
  directly measure the low-energy states
- Core-level XPS
  Site/element specific excitation

XPS spectrum in $LaNiO_3$ K. Yamagami et al., Appl. Phys. Lett. 118, 161601 (2021)

Core levels Valence bands Near Fermi (QP)

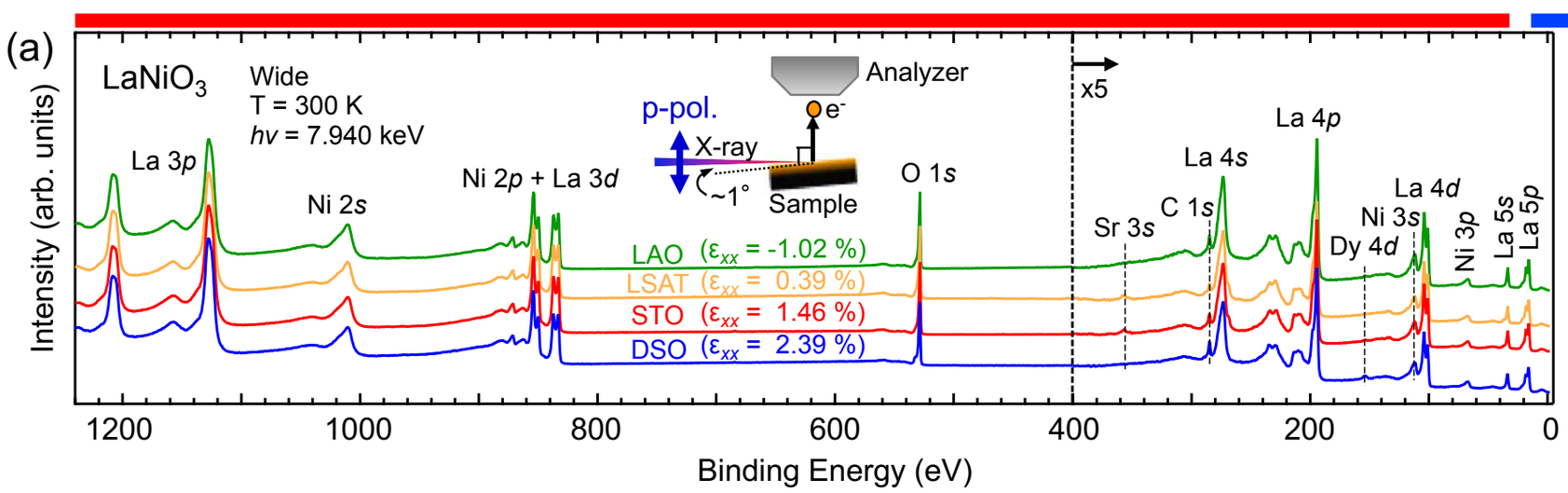

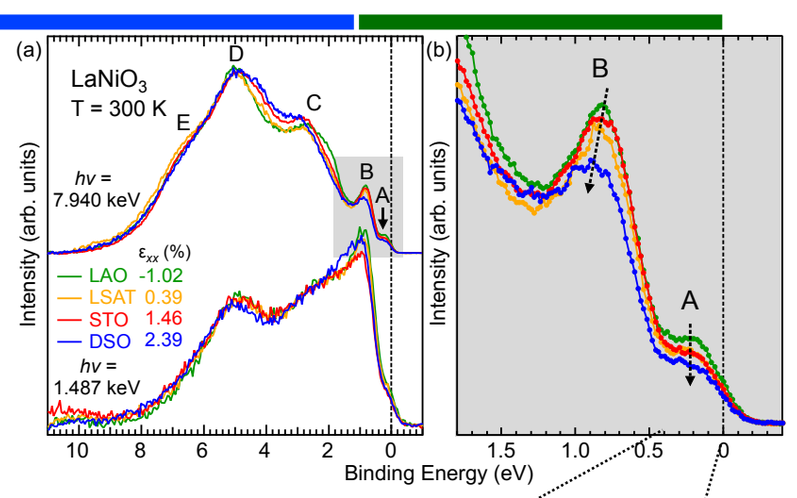

Core levels (no momentum dependence)

Core electrons (holes) completely localized at each ion

- Element specific information (valency)
- Local electronic structure
  (Hund's multiplet, crystal field, and more …)

ARPES:
resolve the momentum

E. A. Nowadnick et al.,
Phys. Rev. B **92**, 245109 (2015)

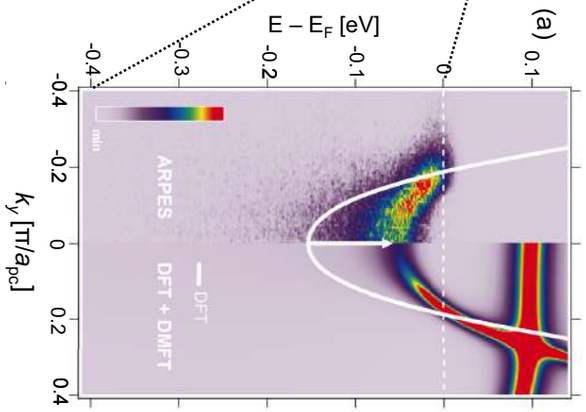

Core-level x-ray absorption spectroscopy

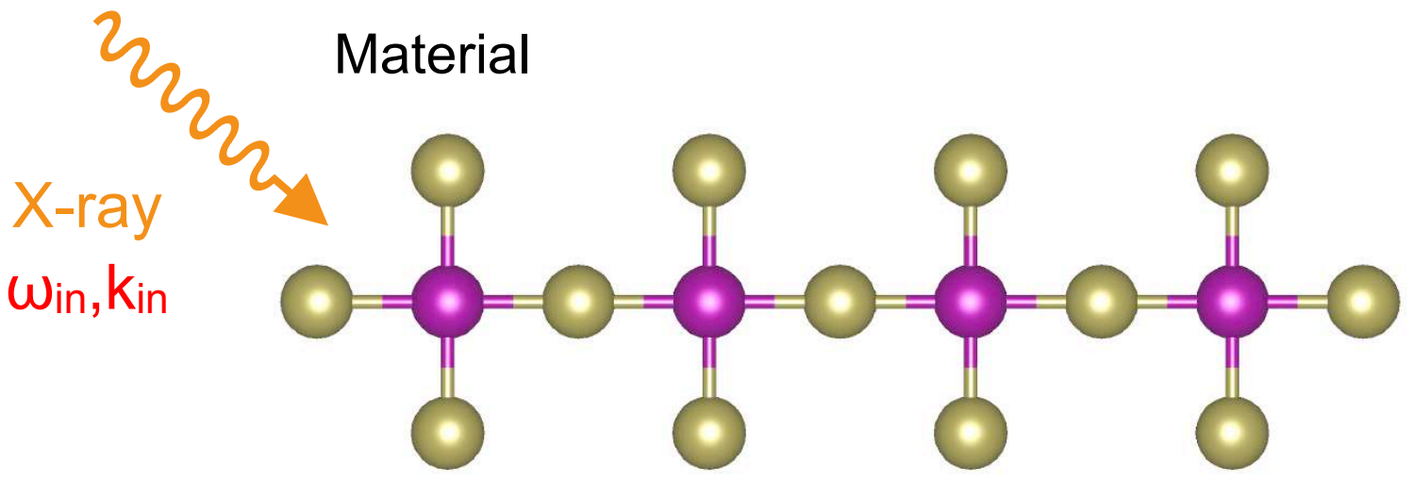

X-ray photoemission spectroscopy:

- Valence-band XPS (ARPES)
  directly measure the low-energy states
- Core-level XPS
  Site/element specific excitation

XPS spectrum in $LaNiO_3$ K. Yamagami et al., Appl. Phys. Lett. 118, 161601 (2021)

Core lev … Absorption into unoccupied Ni 3d states … e bands

Ni 2p core → Ni 3d states: **L-edge**

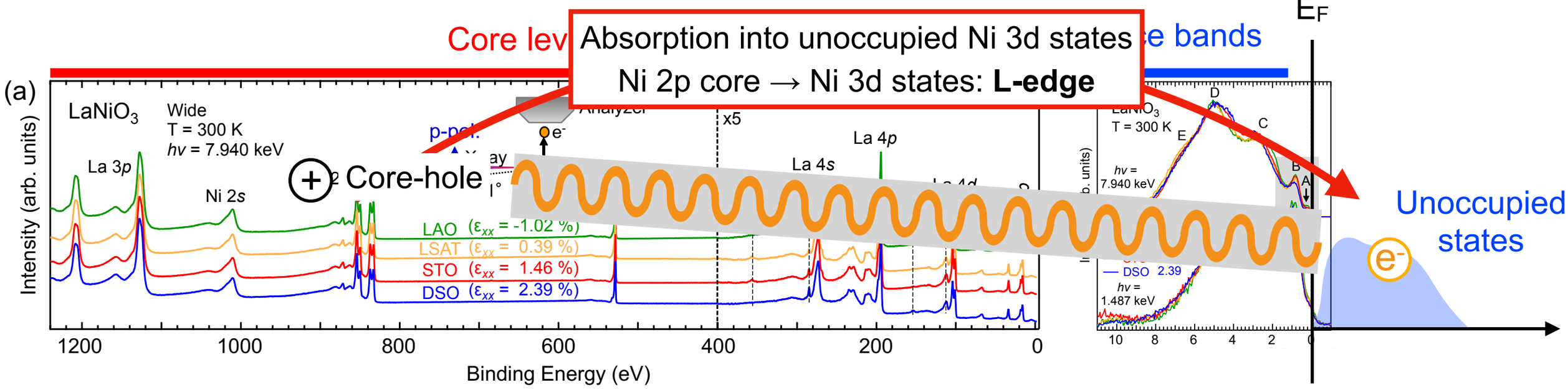

1-particle Green's function

$$G_r(\varepsilon) = \langle \Phi_0^{(N)} | c_r \frac{1}{\varepsilon - (E_0^{(N)} - \mathscr{H}) + i\delta} c_r^\dagger | \Phi_0^{(N)} \rangle + \langle \Phi_0^{(N)} | c_r \frac{1}{\varepsilon - (\mathscr{H} - E_0^{(N)}) + i\delta} c_r^\dagger | \Phi_0^{(N)} \rangle$$

Eigen state with a "core-hole"

photoemission

Inverse photoemission

$$= \sum_n \left[\frac{|\langle \Phi_n^{(N-1)} | c_r | \Phi_0^{(N)} \rangle|^2}{\varepsilon - (E_0^{(N)} - E_n^{(N-1)}) + i\delta} + \frac{|\langle \Phi_n^{(N+1)} | c_r^\dagger | \Phi_0^{(N)} \rangle|^2}{\varepsilon - (E_n^{(N+1)} - E_0^{(N)}) + i\delta} \right]$$

Core-level x-ray absorption spectroscopy

XPS spectrum in $LaNiO_3$ K. Yamagami et al., Appl. Phys. Lett. 118, 161601 (2021)

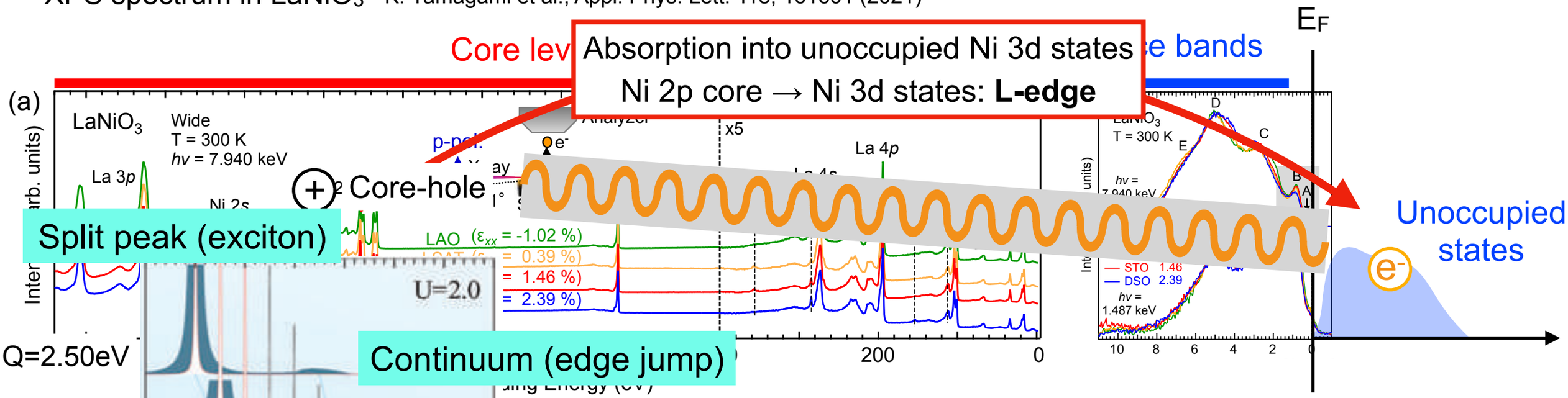

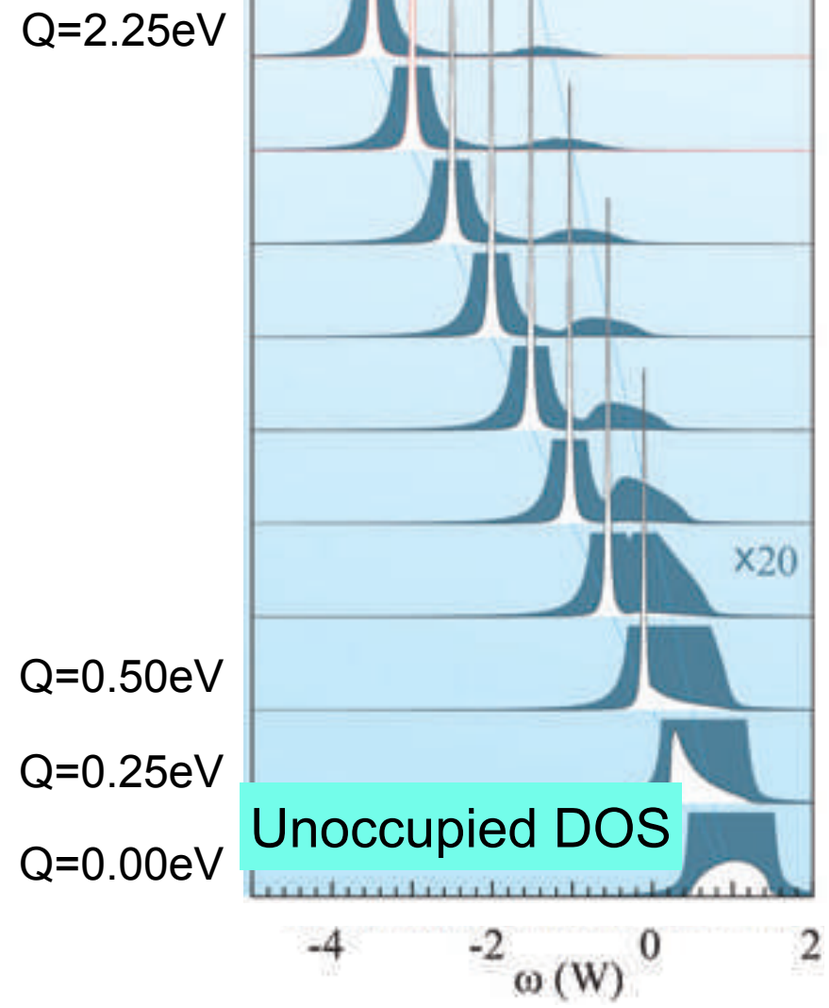

Core-level XAS spectrum in single-band Hubbard model

- Hubbard model solved with DMFT
- Core-valence interaction (core-hole potential) Q introduced

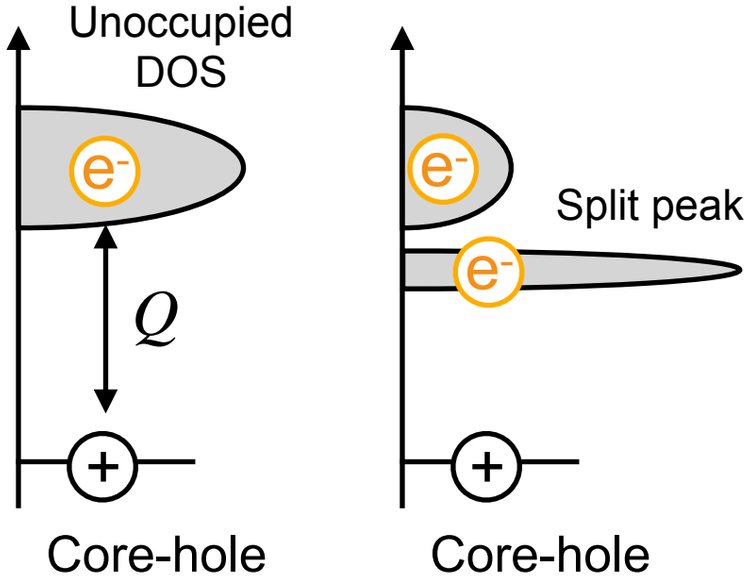

epl A Letters Journal Exploring the Frontiers of Physics
December 2014
EPL, **108** (2014) 57004 www.epljournal.org
doi: 10.1209/0295-5075/108/57004

Bands, resonances, edge singularities and excitons in core level spectroscopy investigated within the dynamical mean-field theory

M. W. Haverkort[1,2,3], G. Sangiovanni[4], P. Hansmann[5], A. Toschi[6], Y. Lu[1,2,3] and S. Macke[1,2]

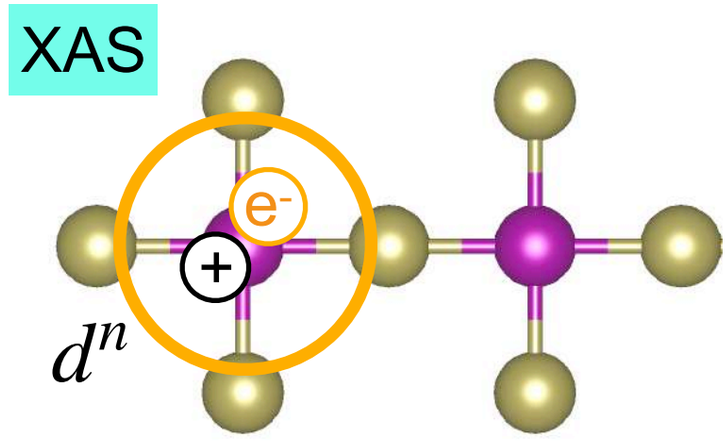

Core-level x-ray absorption spectroscopy

Single-band Hubbard model

M. W. Haverkort et al., EPL **108**, 57004 (2014)

Split peak (exciton)

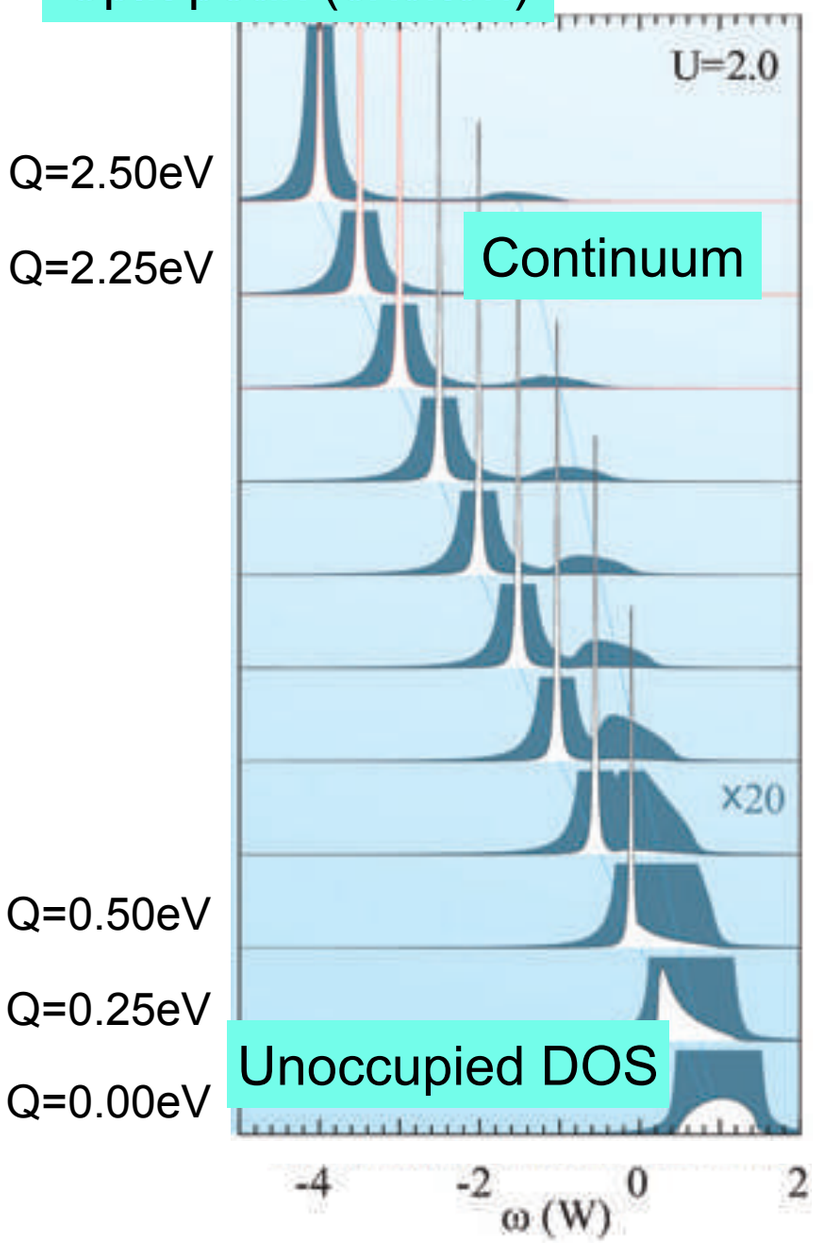

Correlated materials (Mott insulators)

D. Alders et al., PRB **57**, 11623 (1998)

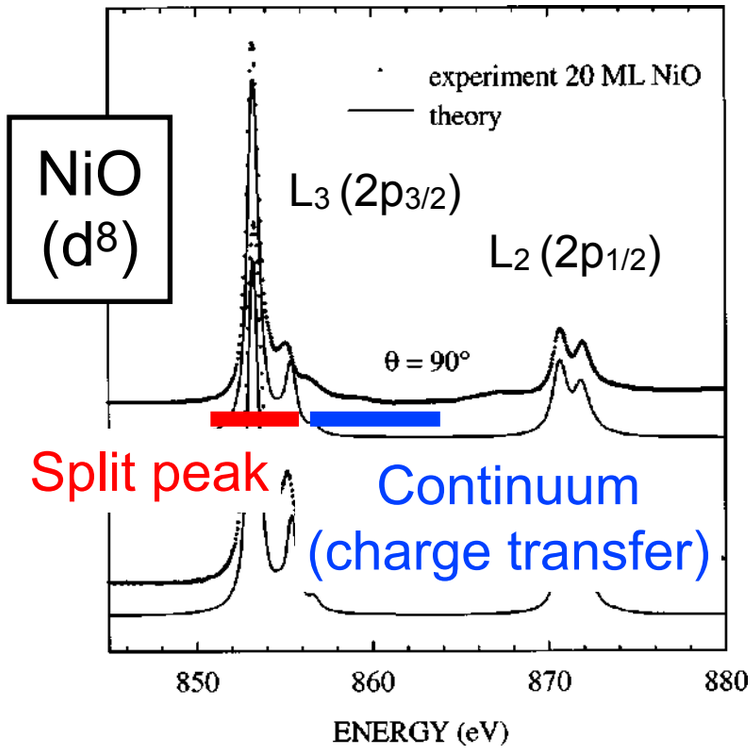

A. N. Vasiliev et al., PRB 7**7**, 10442 (2008)

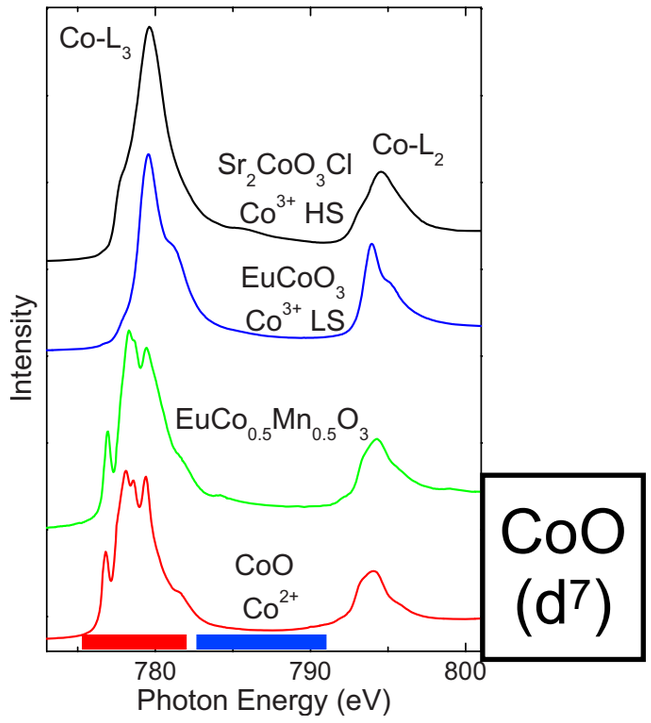

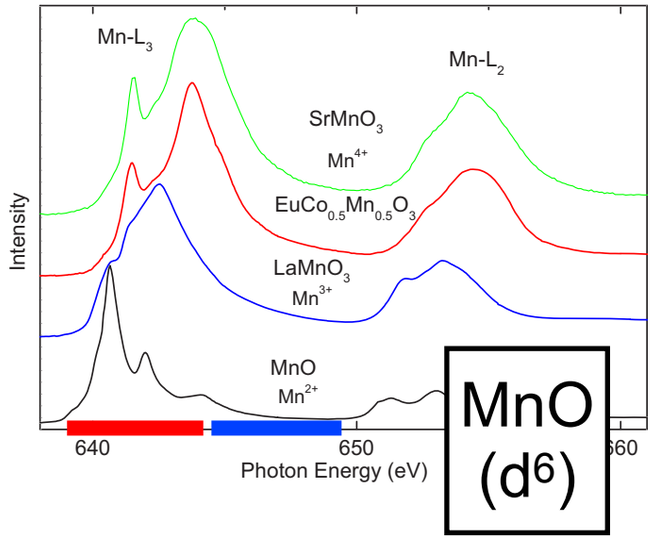

Rich inner features in the split peak, sensitive to valency, local crystal structure, spin (magnetic) states etc..

Core-level x-ray absorption spectroscopy

The main peak/part (split, excitonic) in localized electron systems can be well captured by ionic (atomic) model with a core-hole

PHYSICAL REVIEW B VOLUME 42, NUMBER 9 15 SEPTEMBER 1990-II

2p x-ray absorption of 3d transition-metal compounds: An atomic multiplet description including the crystal field

F. M. F. de Groot and J. C. Fuggle
Research Institute for Materials, University of Nijmegen, Toernooiveld, 6525 ED Nijmegen, The Netherlands

B. T. Thole and G. A. Sawatzky
Materials Science Centre, University of Groningen, Nijenborgh 18, Paddepoel, 9747 AG Groningen, The Netherlands
(Received 30 January 1990; revised manuscript received 4 June 1990)

D. Alders et al., PRB **57**, 11623 (1998)

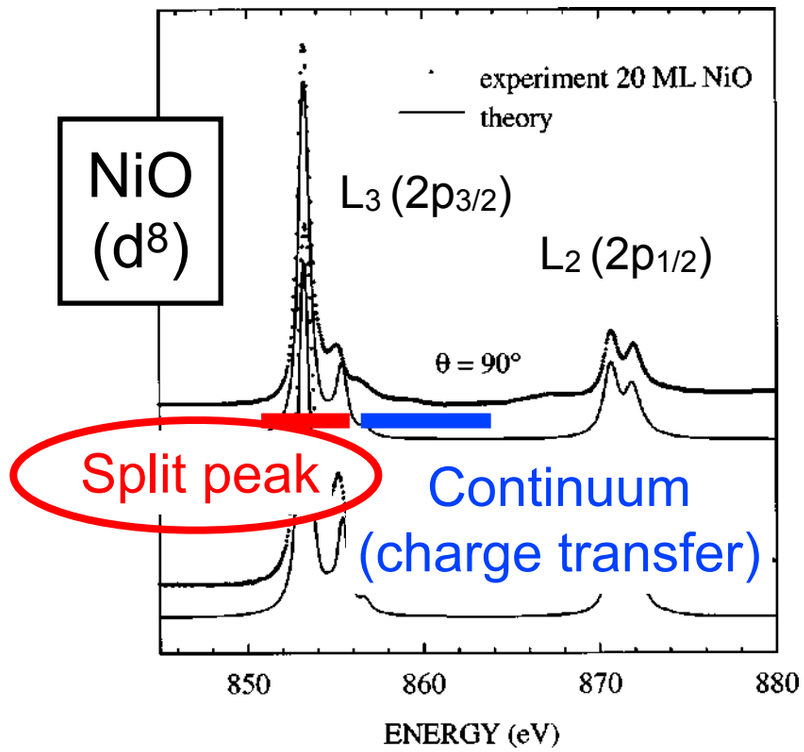

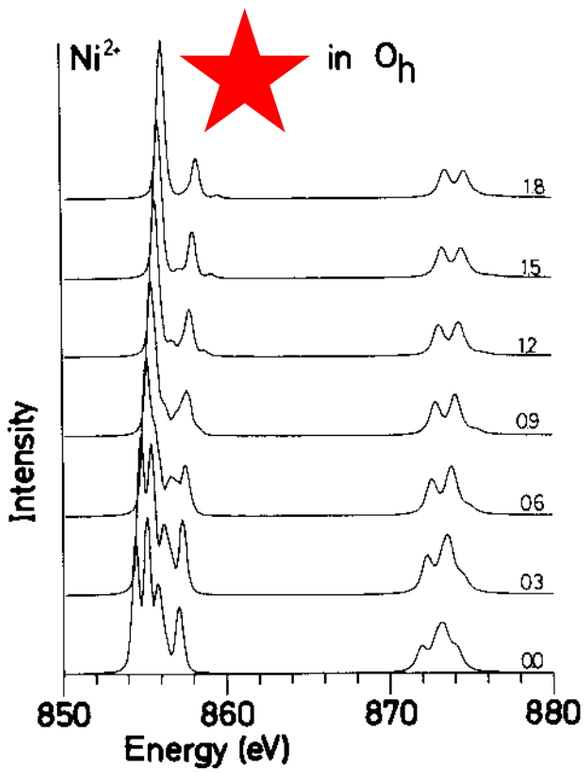

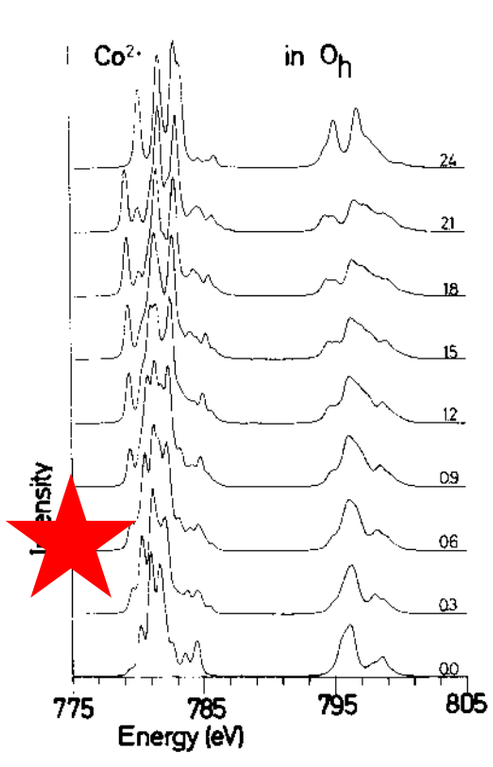

XAS

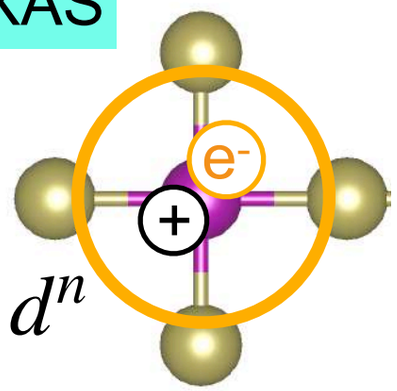

Multiplet fine features of excitons (core hole + d^{n+1})

A. N. Vasiliev et al., PRB **77**, 10442 (2008)

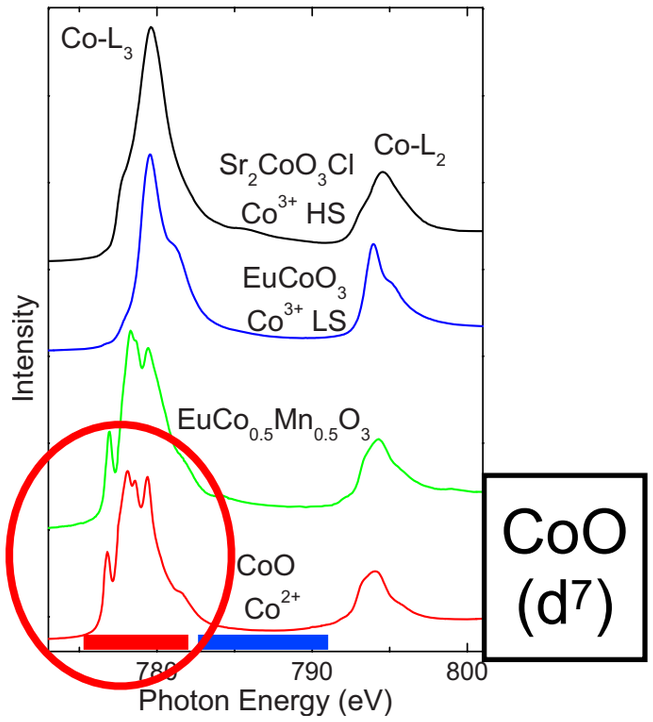

Core-level x-ray absorption spectroscopy

The main peak/part (split, excitonic) in localized electron systems can be well captured by ionic (atomic) model with a core-hole

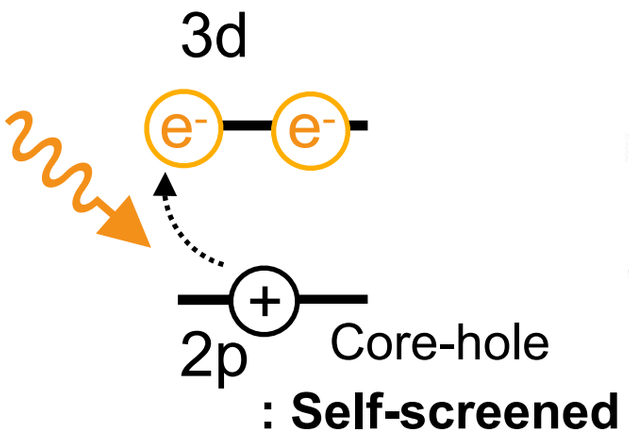

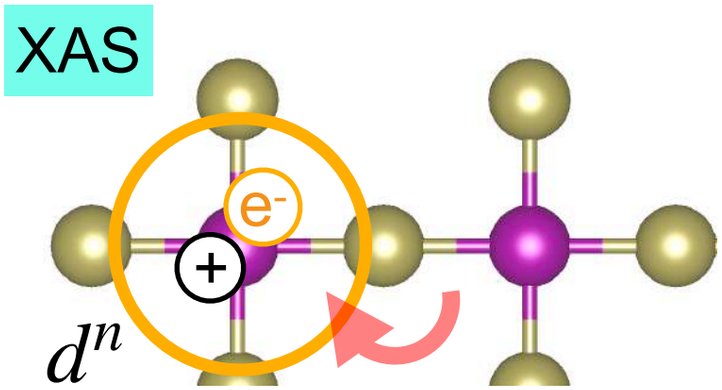

Charge transfer effect is weak

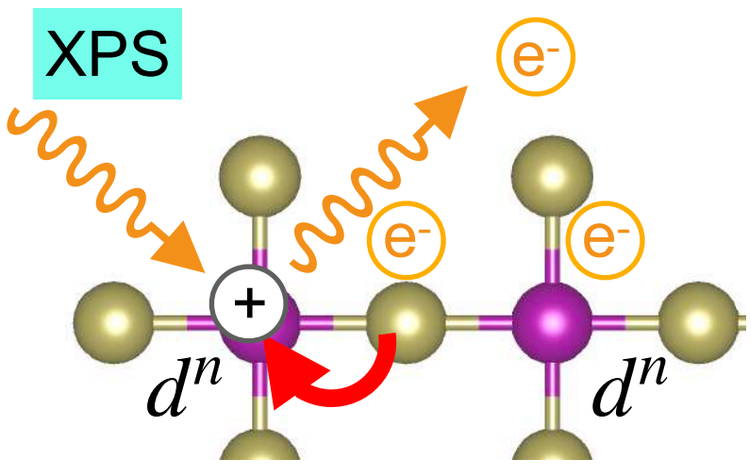

Charge transfer effect is strong

D. Alders et al., PRB **57**, 11623 (1998)

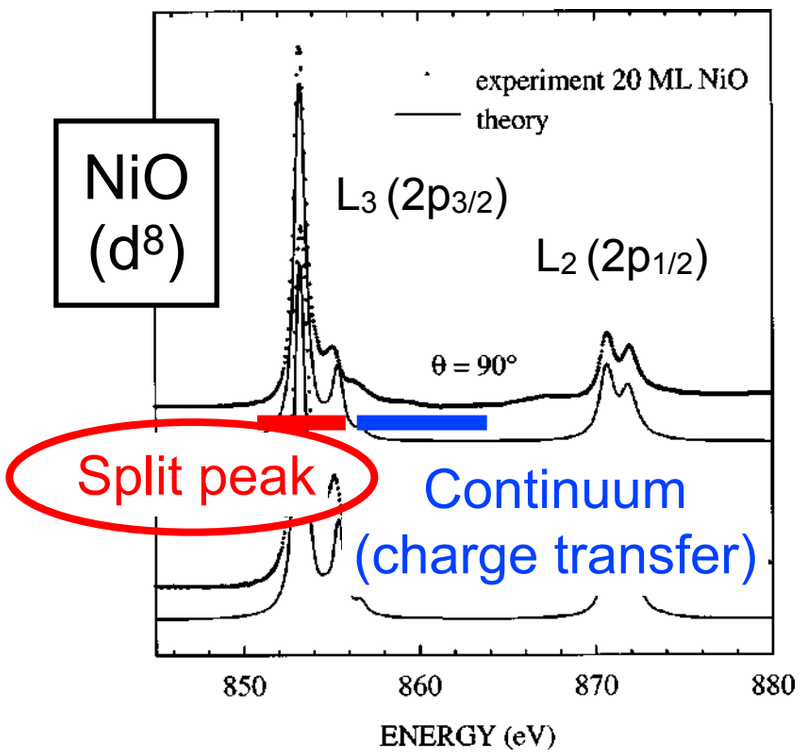

A. N. Vasiliev et al., PRB **77**, 10442 (2008)

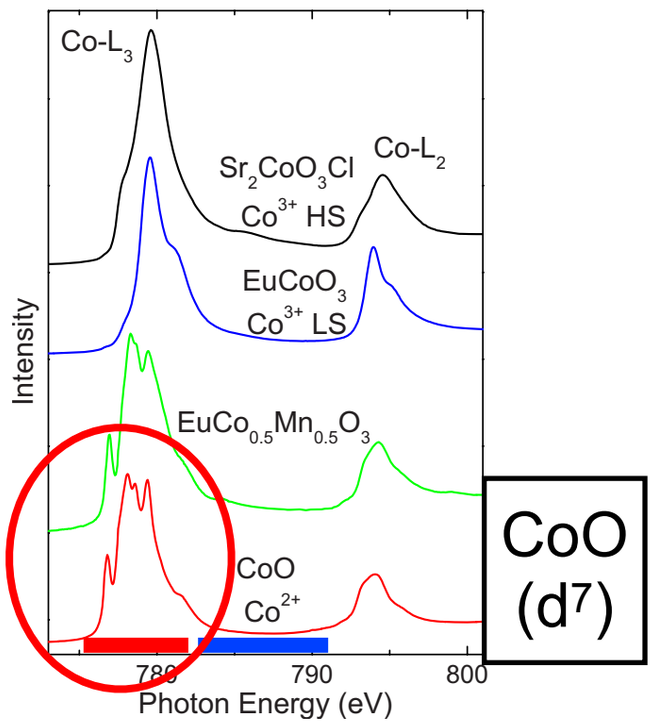

Core-level x-ray spectroscopies in solid

XAS

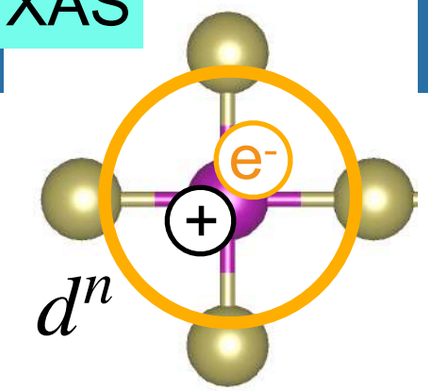

✔ Simpler DFT approach (DFT DOS + core-level) works for noninteracting (weakly correlated) systems

In intermediate or strong coupling regime

In addition to the unoccupied bands above E_F

1. Local core-hole potential needs to be included
2. Fine multiplet interaction needs to be described

➡ **DFT+DMFT embedding approaches covers the two limits!**

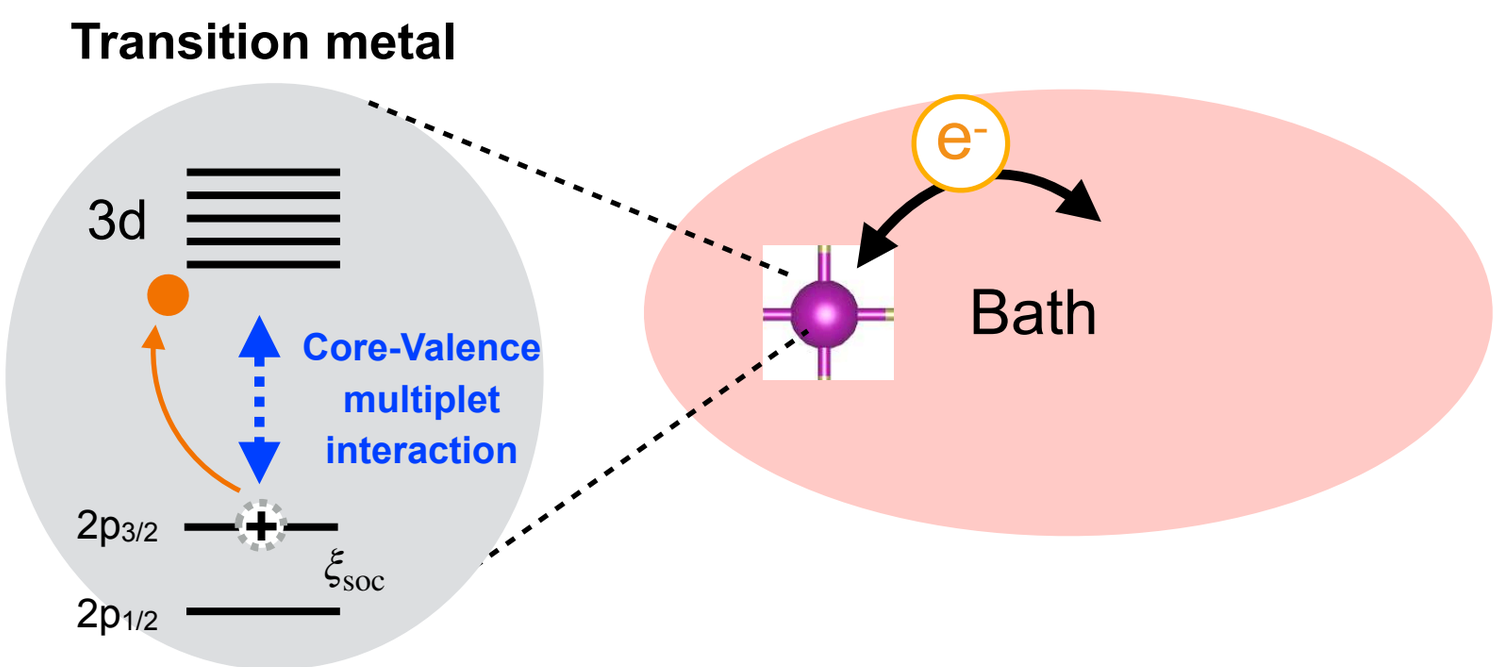

Split peak (exciton)

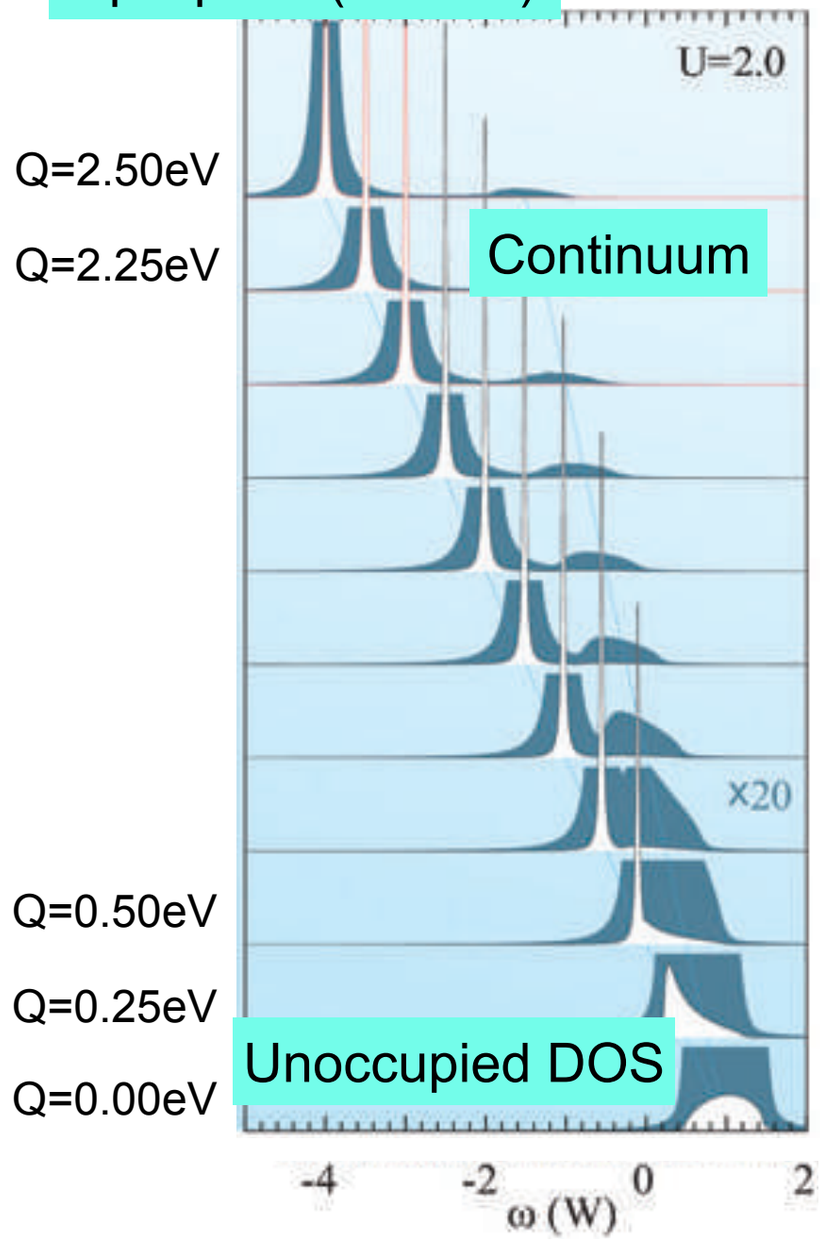

PHYSICAL REVIEW B **101**, 115130 (2020)

Editors' Suggestion

LDA + DMFT approach to resonant inelastic x-ray scattering in correlated materials

Atsushi Hariki,[1,*] Mathias Winder,[1,*] Takayuki Uozumi,[2] and Jan Kuneš[1,3]

[1]*Institute of Solid State Physics, TU Wien, 1040 Vienna, Austria*

[2]*Department of Physics and Electronics, Graduate School of Engineering, Osaka Prefecture University 1-1 Gakuen-cho, Nakaku, Sakai, Osaka 599-8531, Japan*

[3]*Institute of Physics, Czech Academy of Sciences, Na Slovance 2, 182 21 Praha 8, Czechia*

(Received 30 November 2019; accepted 21 February 2020; published 18 March 2020)

固体物理 2月号
（アグネ技術センター）

解説

共鳴非弾性 X 線散乱で見る 強相関電子系の励起スペクトル

大阪公立大学大学院工学研究科　播木　敦

NiO

L-edge XAS

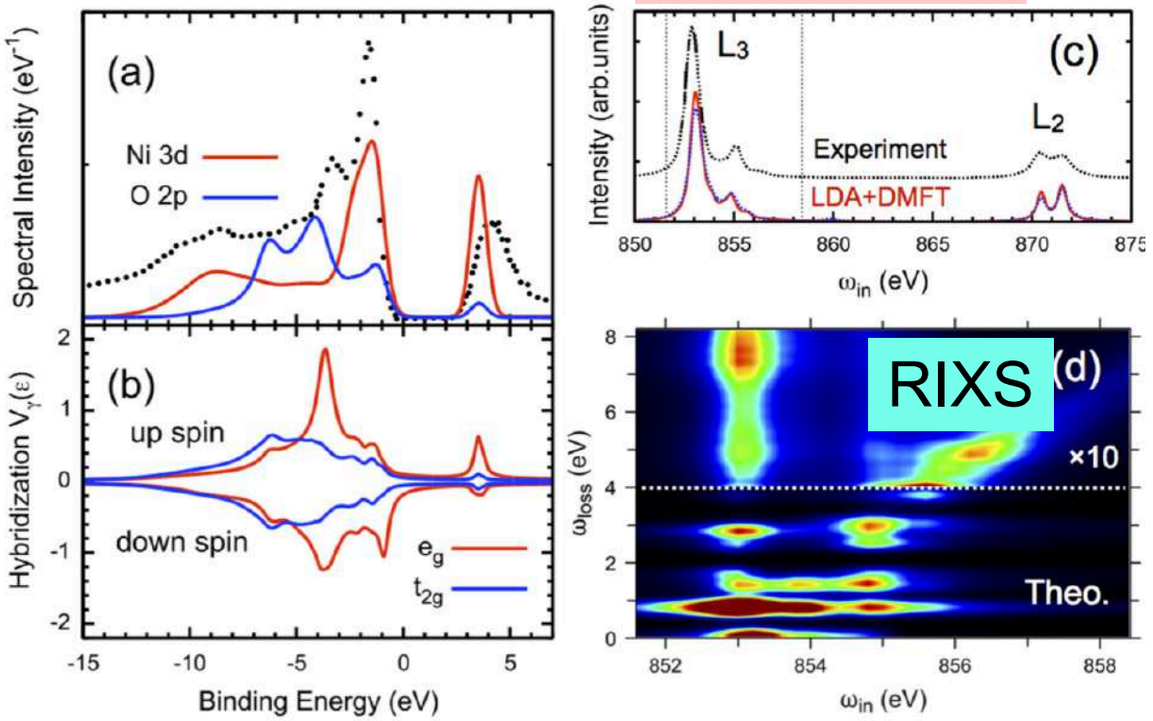

Fe_2O_3

L-edge XAS

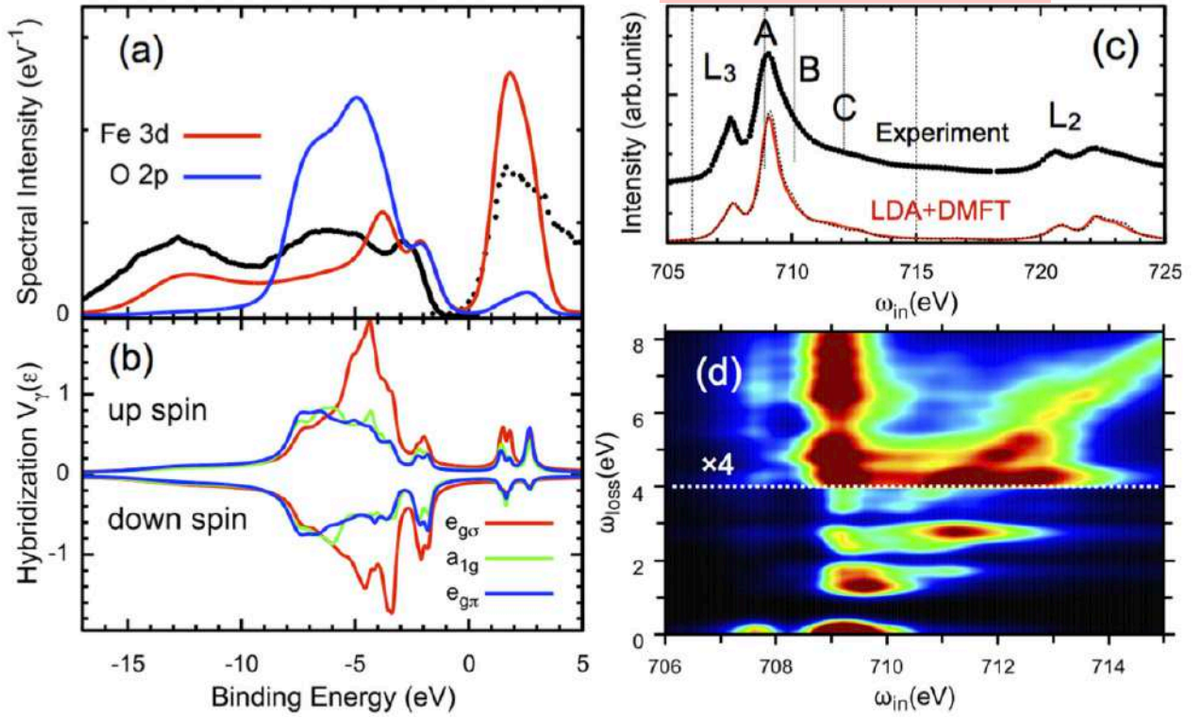

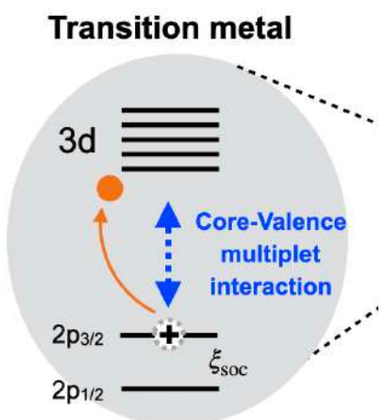

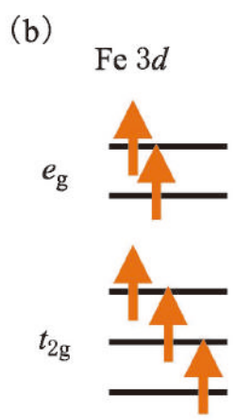

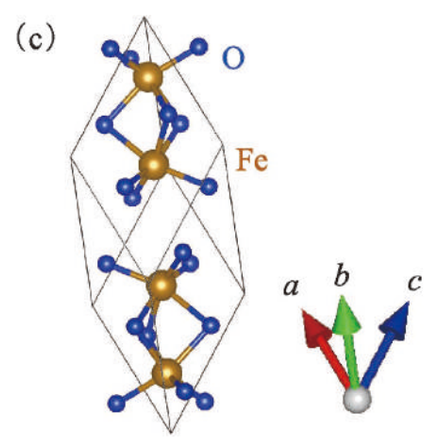

What is Altermagnet?

L. Šmejkal et al., Phys. Rev. X 12, 040501 (2022)

Altermagnet: a new class in collinear magnets (w/o spin-orbit coupling)

Ferromagnet

$M \neq 0$

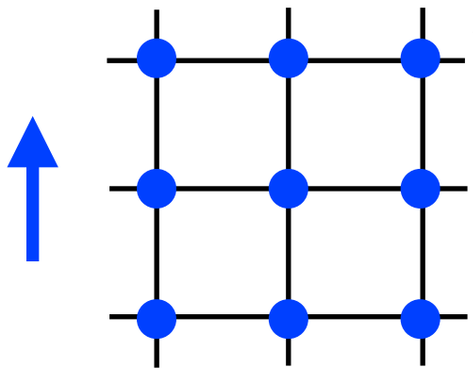

Time reversal $\mathcal{T}$

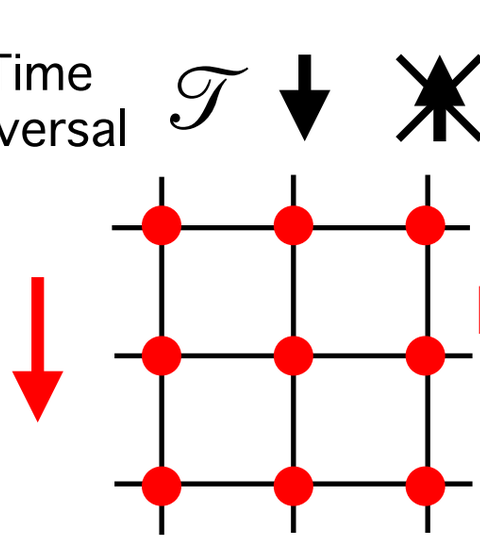

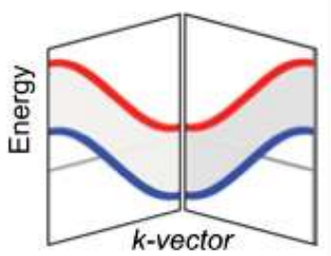

(Uniform) Zeeman splitting in band structure ($\mathcal{T}$-broken)

Antiferromagnet

$M = 0$

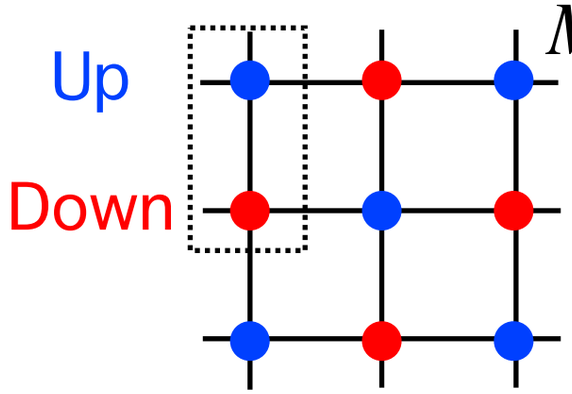

$\mathcal{T}$ T_R, P

T_R

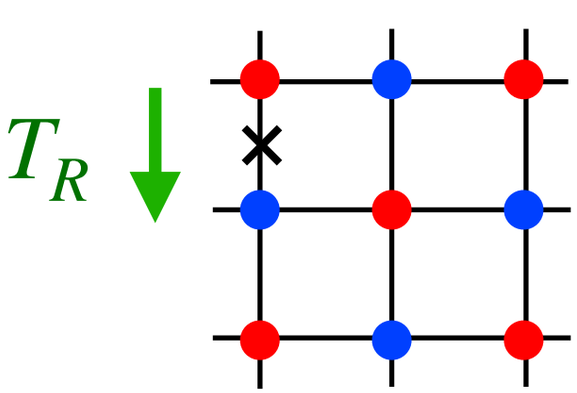

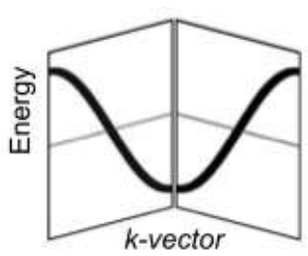

Spin degenerated bands (with $\mathcal{T}$ symmetry)

Altermagnet

$M = 0$

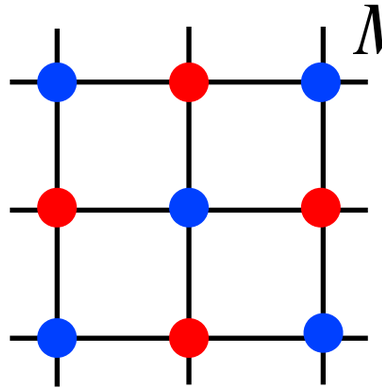

$\mathcal{T}$

T_R

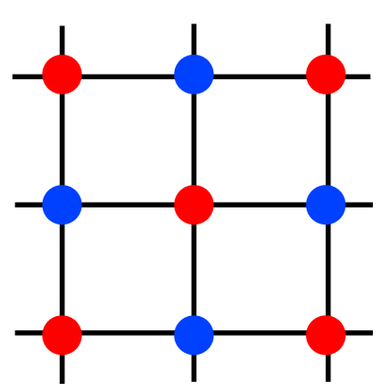

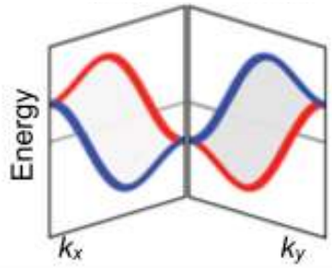

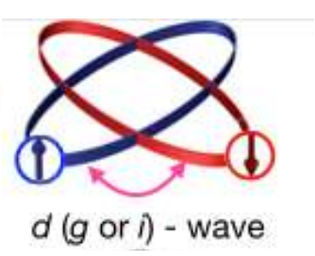

$\mathcal{T}$-broken bands with d/g/I-wave spin texture

What is Altermagnet?

L. Šmejkal et al., Phys. Rev. X 12, 040501 (2022)

Altermagnet: a new class in collinear magnets, split from antiferromagnets

Ferromagnet

$M \neq 0$

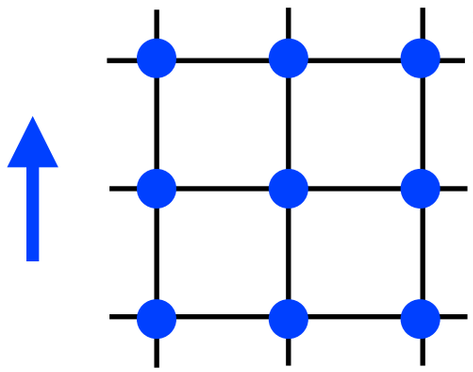

Time reversal $\mathcal{T}$

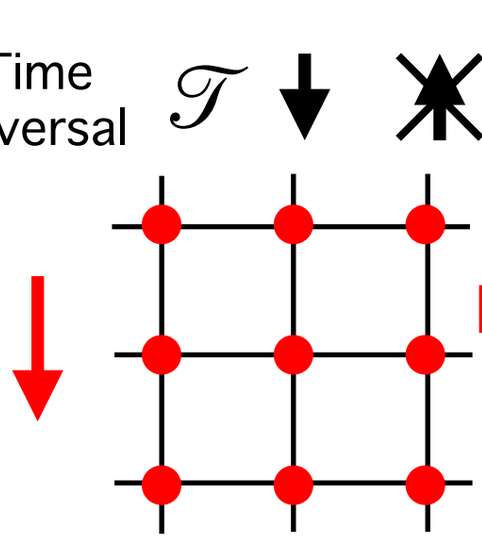

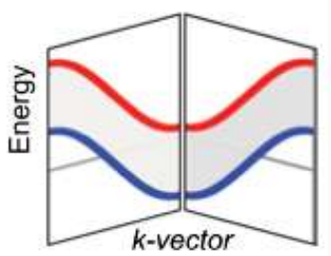

(Uniform) Zeeman splitting in band structure ($\mathcal{T}$-broken)

Antiferromagnet

$M = 0$

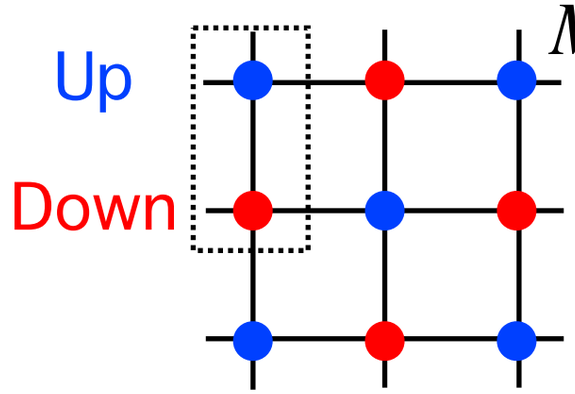

$\mathcal{T}$ T_R, P

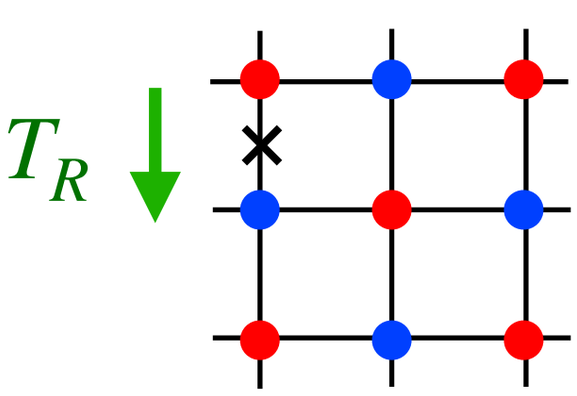

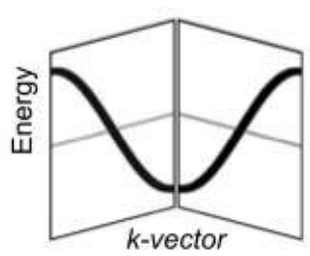

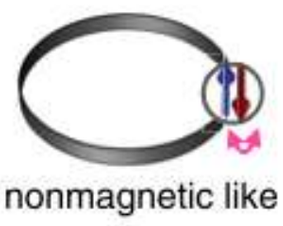

Spin degenerated bands (with $\mathcal{T}$ symmetry)

Altermagnet

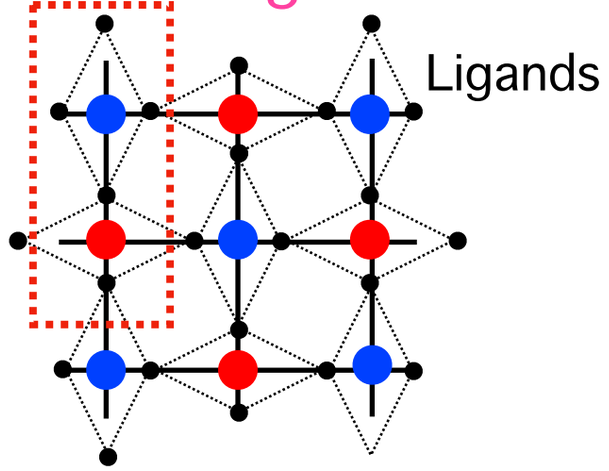

$\mathcal{T}$

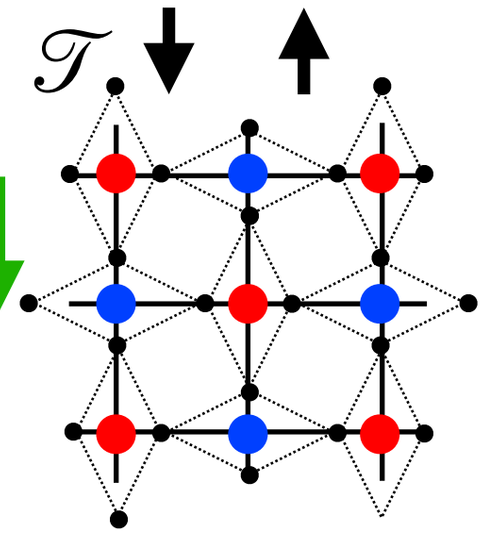

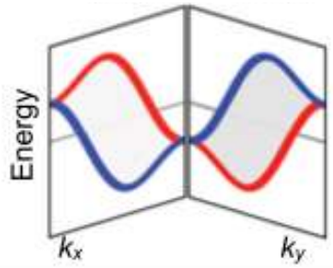

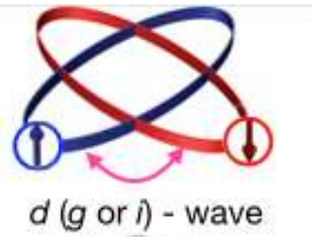

$\mathcal{T}$-broken bands with d/g/I-wave spin texture

What is Altermagnet?

L. Šmejkal et al., Phys. Rev. X 12, 040501 (2022)

Altermagnet: a new class in collinear magnets, split from antiferromagnets

Ferromagnet

$M \neq 0$

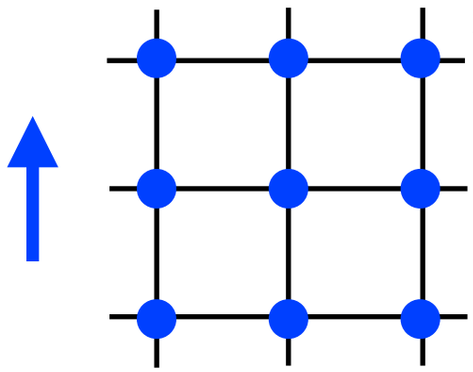

Time reversal $\mathcal{T}$

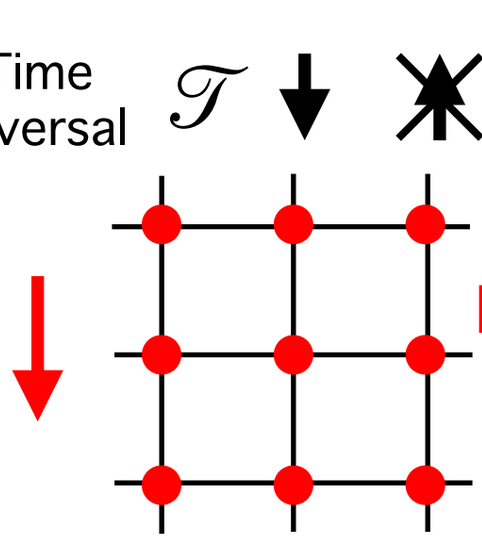

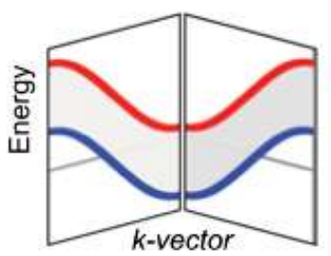

(Uniform) Zeeman splitting in band structure ($\mathcal{T}$-broken)

Antiferromagnet

$M = 0$

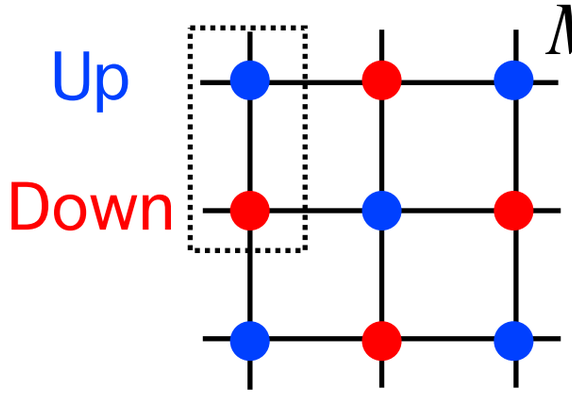

$\mathcal{T}$ T_R, P

T_R

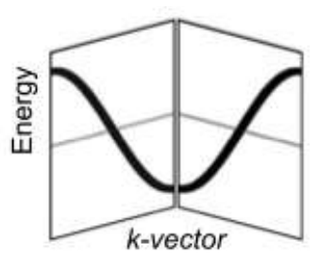

Spin degenerated bands (with $\mathcal{T}$ symmetry)

Altermagnet

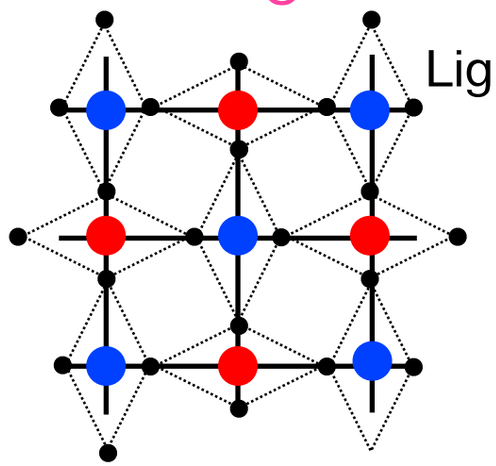

$\mathcal{T}$ R

R

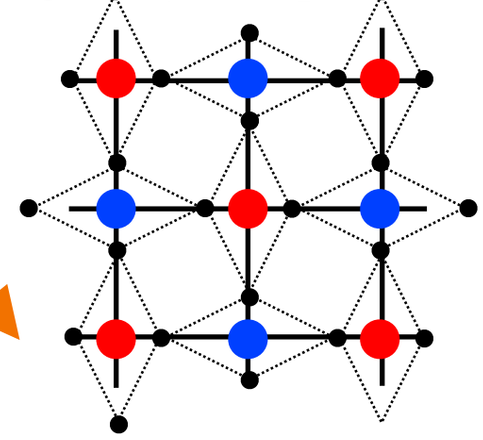

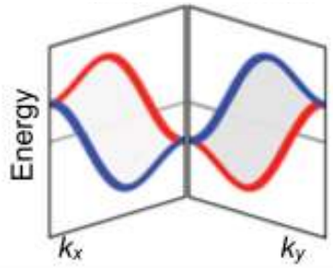

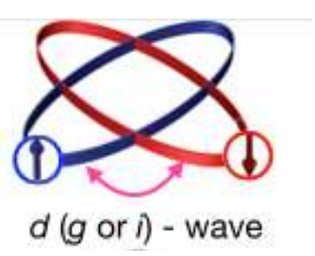

$\mathcal{T}$-broken bands with d/g/I-wave spin texture

What is Altermagnet?

PHYSICAL REVIEW B **99**, 184432 (2019)

Antiferromagnetism in RuO_2 as d-wave Pomeranchuk instability

Kyo-Hoon Ahn,[1] Atsushi Hariki,[2] Kwan-Woo Lee,[1,3] and Jan Kuneš[2,4]
[1]*Division of Display and Semiconductor Physics, Korea University, Sejong 30019, Korea*
[2]*Institute of Solid State Physics, TU Wien, 1040 Vienna, Austria*
[3]*Department of Applied Physics, Graduate School, Korea University, Sejong 30019, Korea*
[4]*Institute of Physics, Czech Academy of Sciences, Na Slovance 2, 182 21 Praha 8, Czechia*

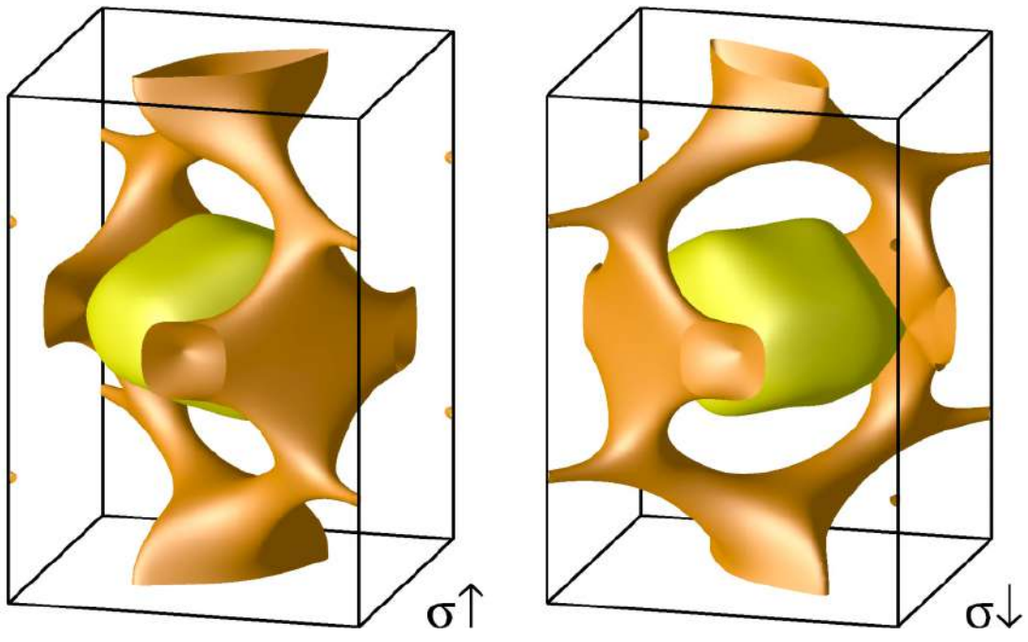

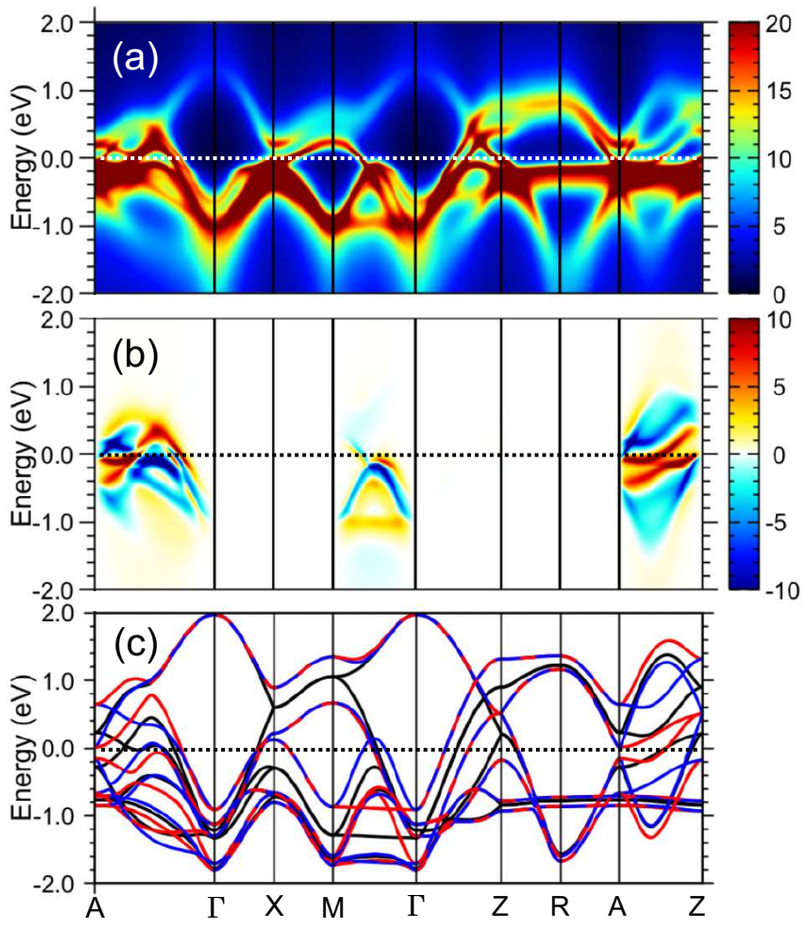

FIG. 1. (a) DFT+DMFT band structure, the spectral function $A_{\uparrow\uparrow}(\omega) + A_{\downarrow\downarrow}(\omega)$, along the high-symmetry lines in BZ. (b) The spin polarization of the band structure is calculated as $A_{\uparrow\uparrow}(\omega) - A_{\downarrow\downarrow}(\omega)$. (c) HF band structure: paramagnetic (black) and AFM (↑ red; ↓ blue). The energy is measured from the Fermi level.

nature communications

Explore content ∨ About the journal ∨ Publish with us ∨

nature > nature communications > articles > article

Article | Open access | Published: 20 September 2019

Spin current generation in organic antiferromagnets

Makoto Naka, Satoru Hayami, Hiroaki Kusunose, Yuki Yanagi, Yukitoshi Motome & Hitoshi Seo

Nature Communications **10**, Article number: 4305 (2019) | Cite this article

RESEARCH ARTICLE | MATERIALS SCIENCE

Crystal time-reversal symmetry breaking and spontaneous Hall effect in collinear antiferromagnets

LIBOR ŠMEJKAL, RAFAEL GONZÁLEZ-HERNÁNDEZ, T. JUNGWIRTH, AND J. SINOVA Authors Info & Affiliations

SCIENCE ADVANCES · 5 Jun 2020 · Vol 6, Issue 23 · DOI: 10.1126/sciadv.aaz8809

α-MnTe as altermagnet

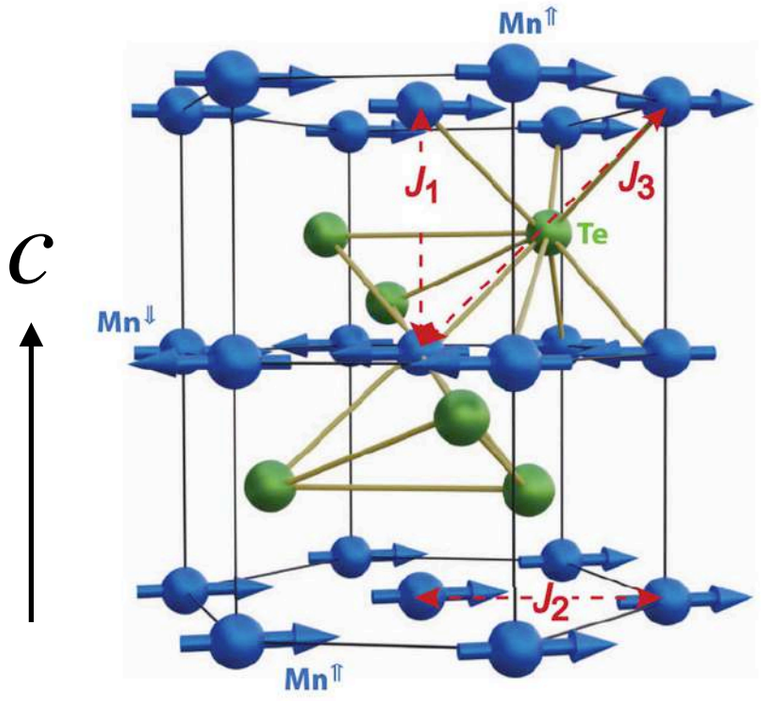

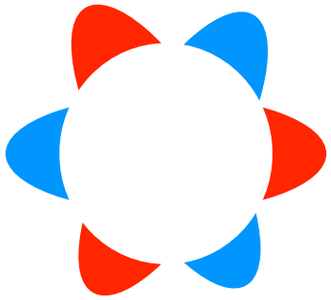

: g-wave spin splitting in band structure

- Mn atoms on hexagonal planes
- Te atoms at non-centrosymmetric positions
- Inversion at Mn (does not connect the magnetic sublattices)

Mn^{2+} : d^5 S=5/2

[from c-axis]

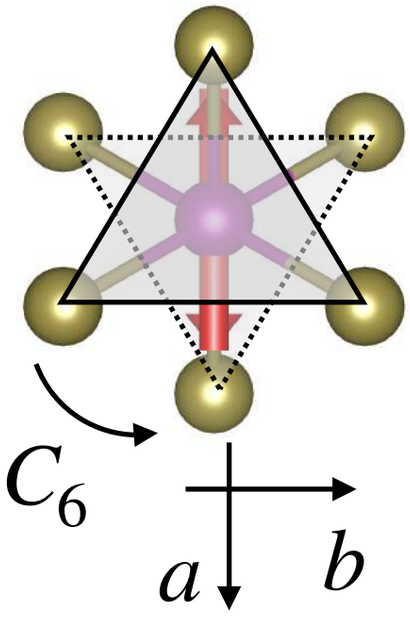

NiAs structure

$(P6_3/mmc)$

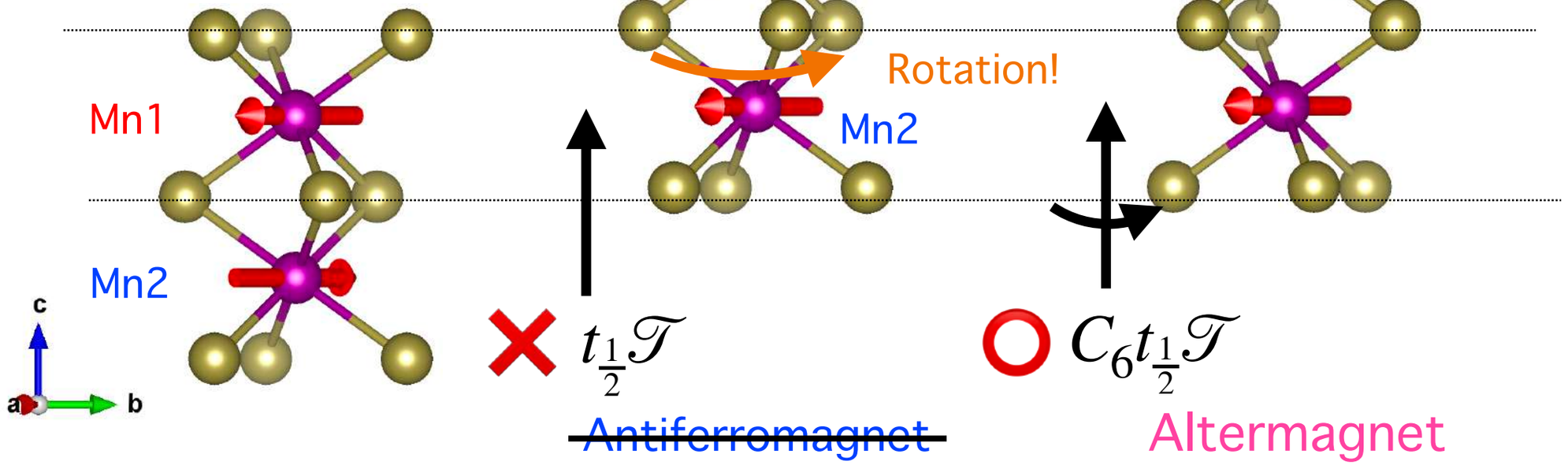

X-ray magnetic circular dichroism in altermagnet

X-ray magnetic circular dichroism (XMCD)

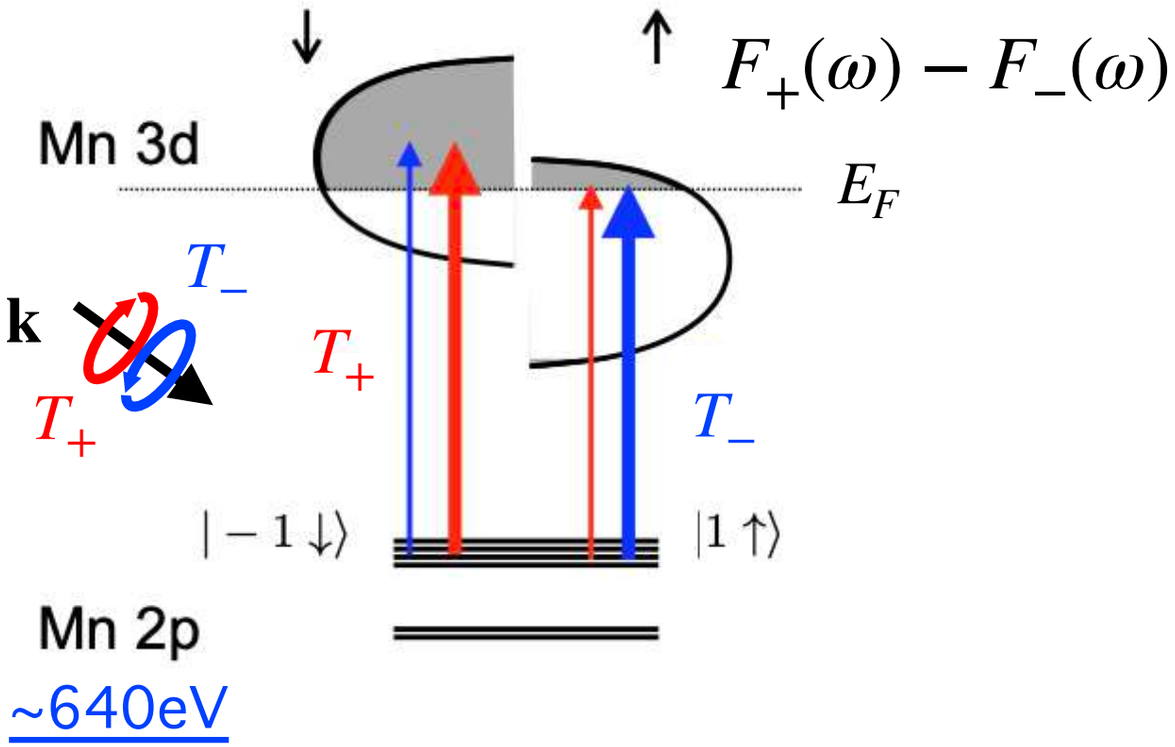

$F_+(\omega) - F_-(\omega)$

$$F_{\mathrm{XMCD}}(\omega) \sim 2\ \mathrm{Im}\ \mathbf{h}(\omega) \cdot \hat{\mathbf{k}}$$

Wave vector

$$\mathbf{h}(\omega) = \left(\sigma^a_{zy}(\omega), \sigma^a_{xz}(\omega), \sigma^a_{yx}(\omega)\right)$$

at Mn 2p core energy ~ 640eV

antisymmetric components of (dipole) optical tensor

(thus, the same symmetry with AHE)

Optical (electric dipole)

transition : $j = x, y, z$

$$F_{i,j}(\omega) \sim \langle g | T_i^\dagger \frac{1}{\omega - H} \overline{T_j} | g \rangle$$

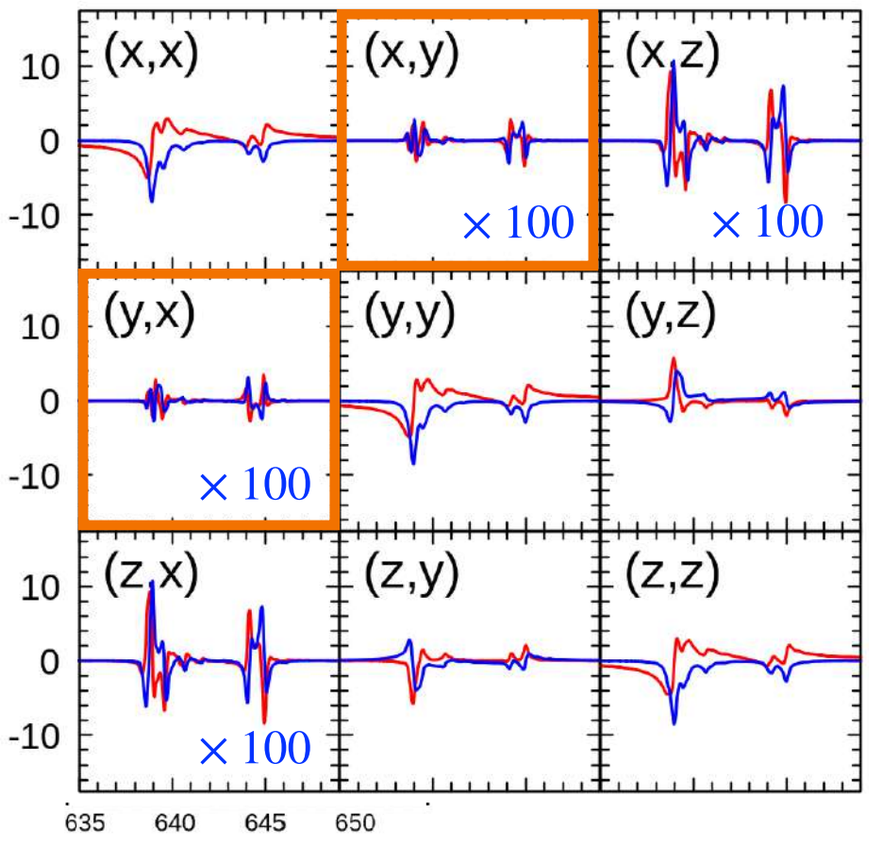

Anti symmetric part : XMCD

$$\sigma^a_{yx}(\omega) = F_{y,x}(\omega) - F_{x,y}(\omega)$$

Theory vs Experiment: Mn $L_{2,3}$-edge XMCD in α-MnTe

Experiment and Theory

(@ Diamond Light Source)

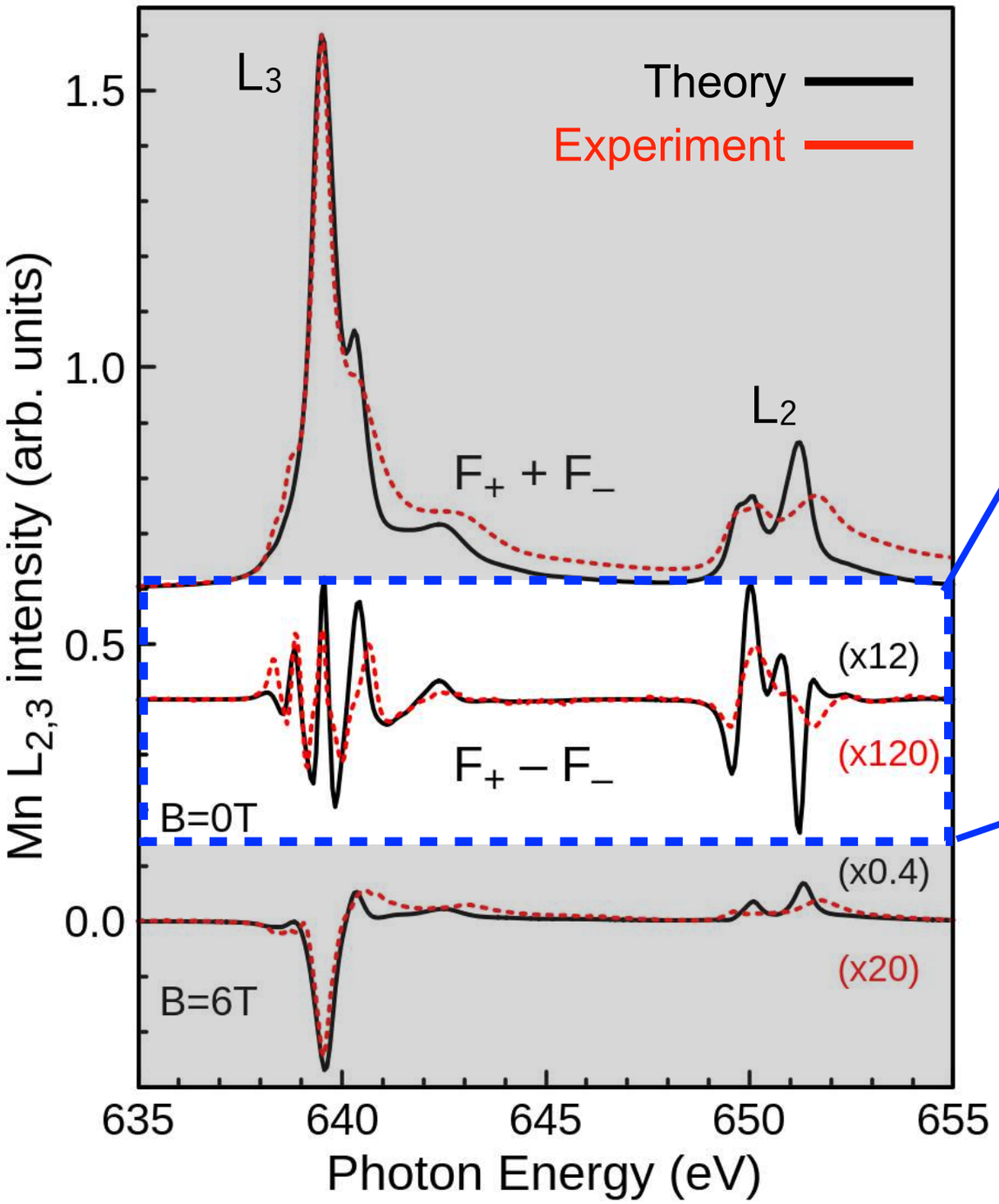

A. Hariki et al., Phys. Rev. Let. **132**, 176701 (2024)

Experiment $\mathbf{k}||\mathbf{c}$

- Cooled below T_c in field B(6T) || C
- Measured in B=0

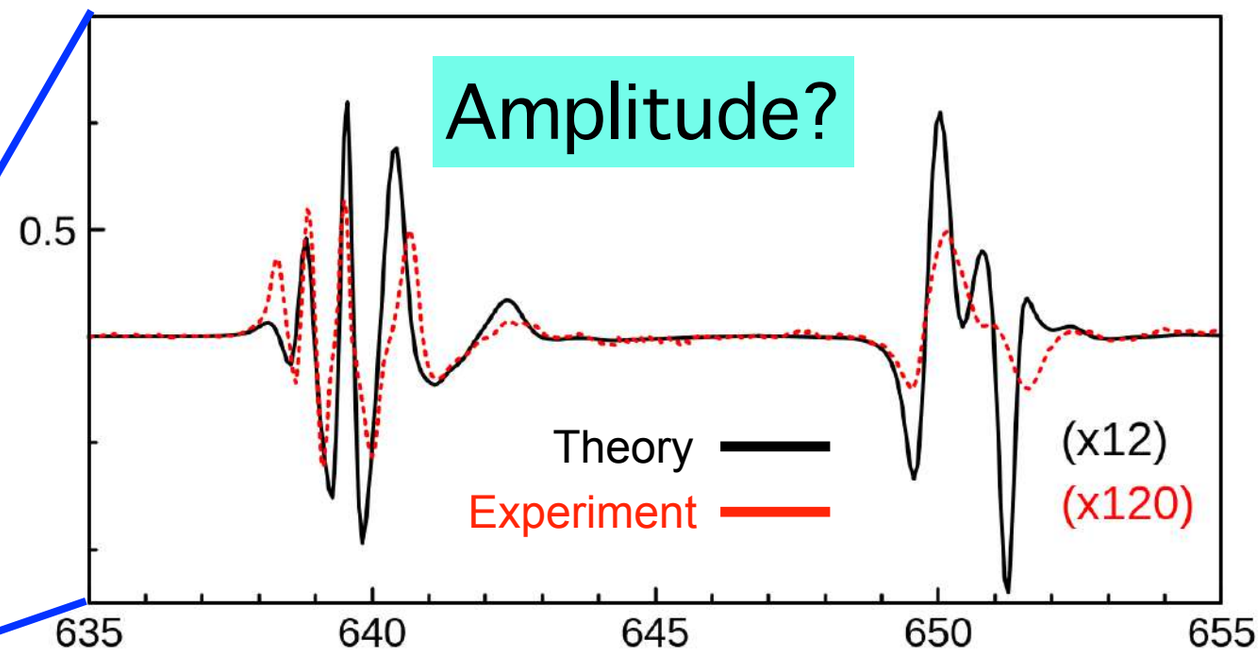

Wiggly XMCD shape
= fingerprint of altermagnetic MnTe
is confirmed experimentally

Theory vs Experiment: Mn $L_{2,3}$-edge XMCD in α-MnTe

Experiment $\Delta F_{\mathrm{avg}}(\omega) = \left(\sum_{p=0}^{5} (-)^p \times w_p \right) \Delta F(\omega)$ Theory

Domain weights

: minus for time-reversal Néel state

+L domains

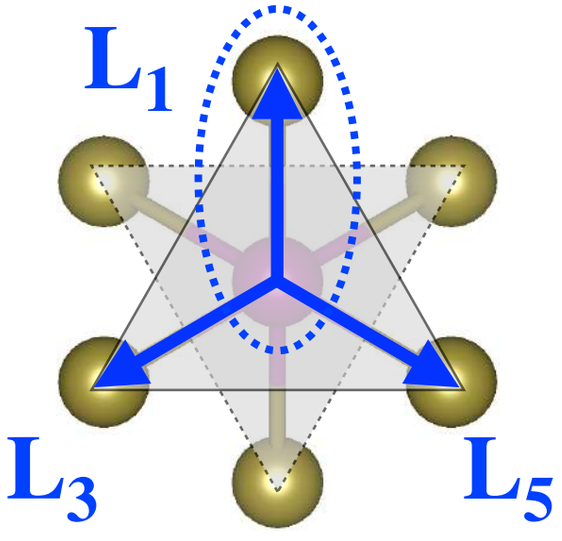

-L domains

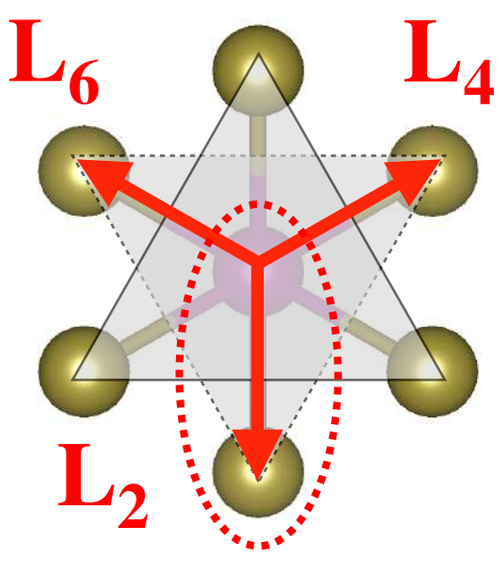

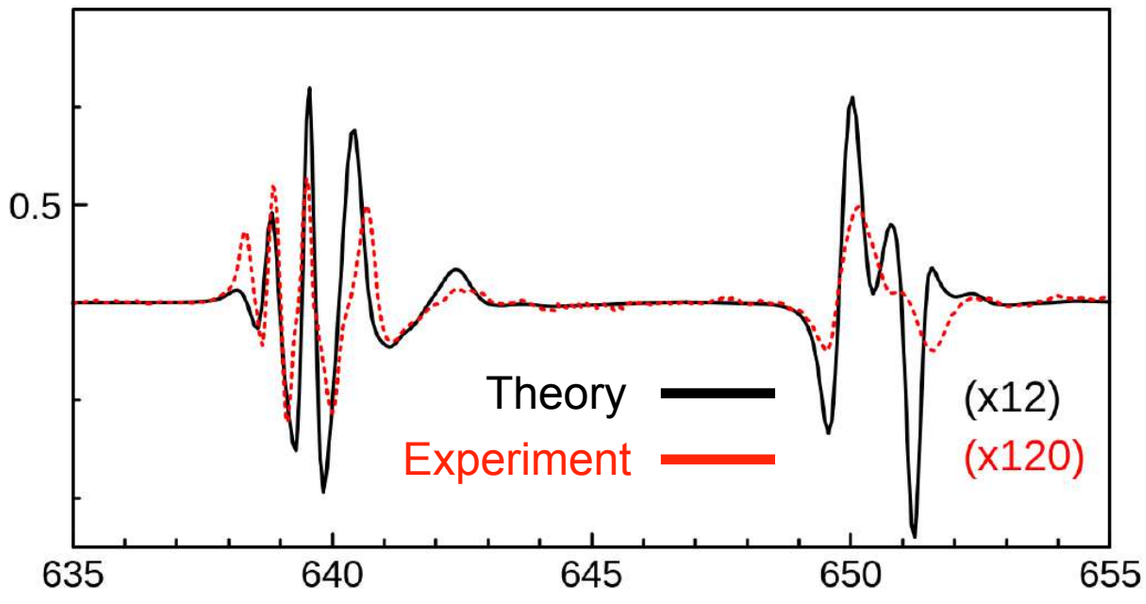

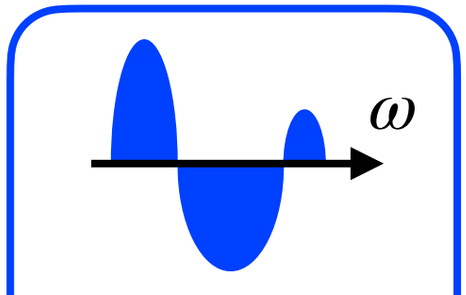

+

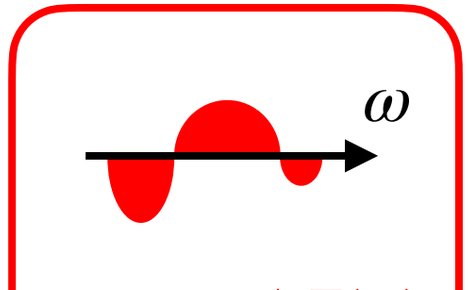

=

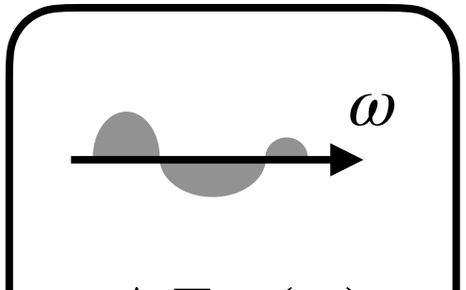

Imbalance

$w_L - w_{-L}$

Theory vs Experiment: Mn $L_{2,3}$-edge XMCD in α-MnTe

Supplemental Experiment

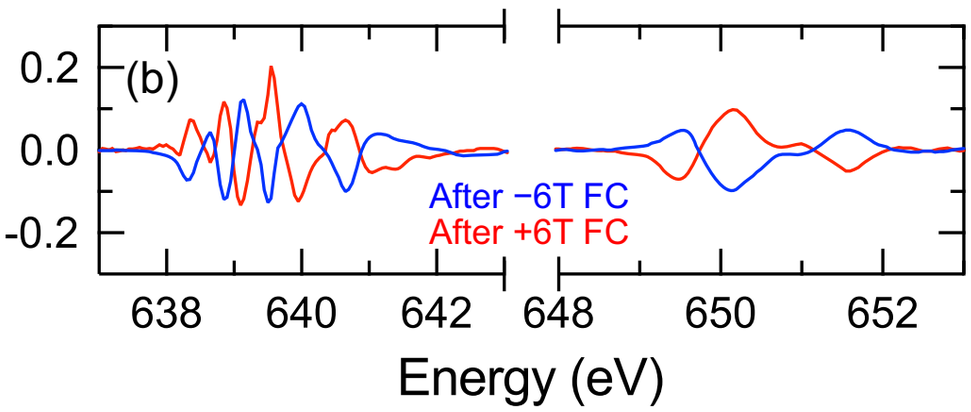

- Cooled below T_c in field B(=+6T,-6T) ll C
- Measured in B=0

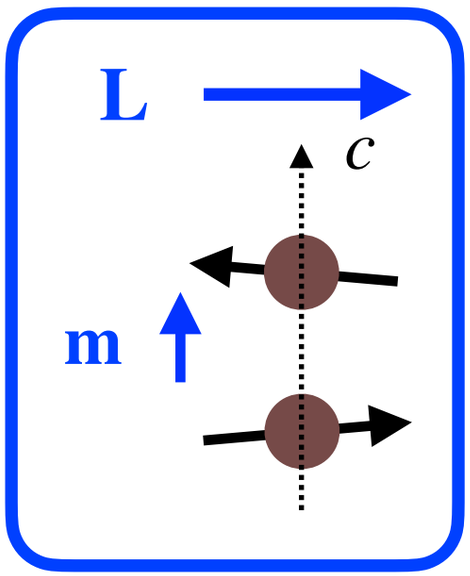

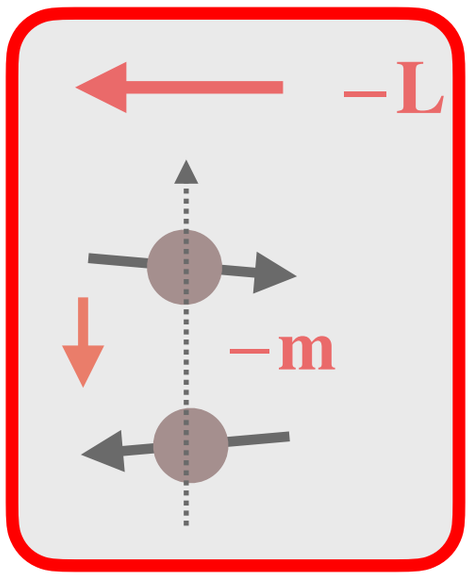

field (6T)

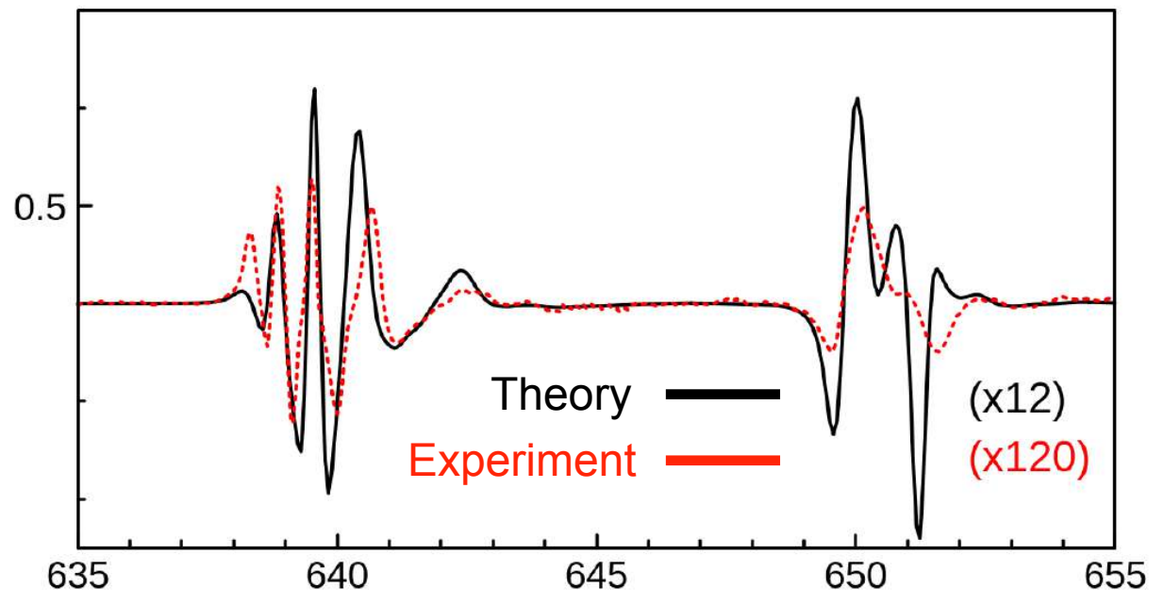

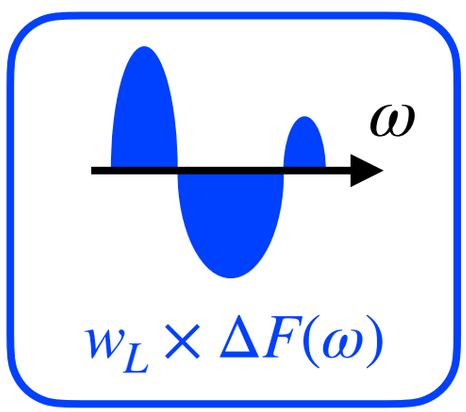

+

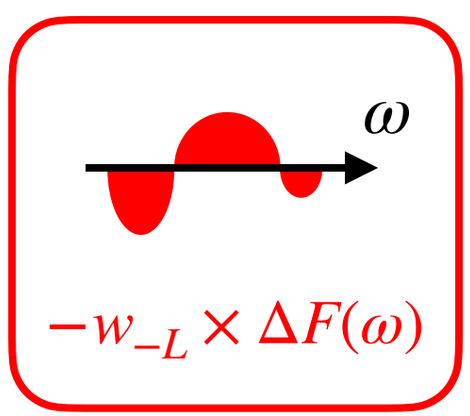

=

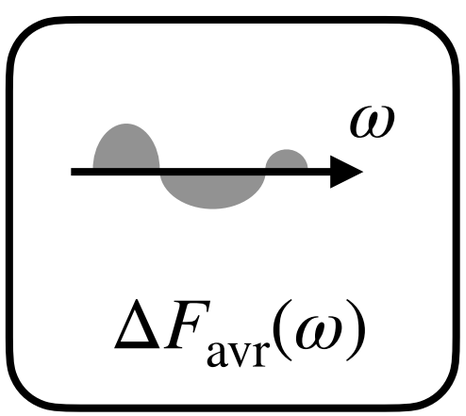

Imbalance

$w_L - w_{-L}$

Theory vs Experiment: Mn $L_{2,3}$-edge XMCD in α-MnTe

Experiment and Theory

(@ Diamond Light Source)

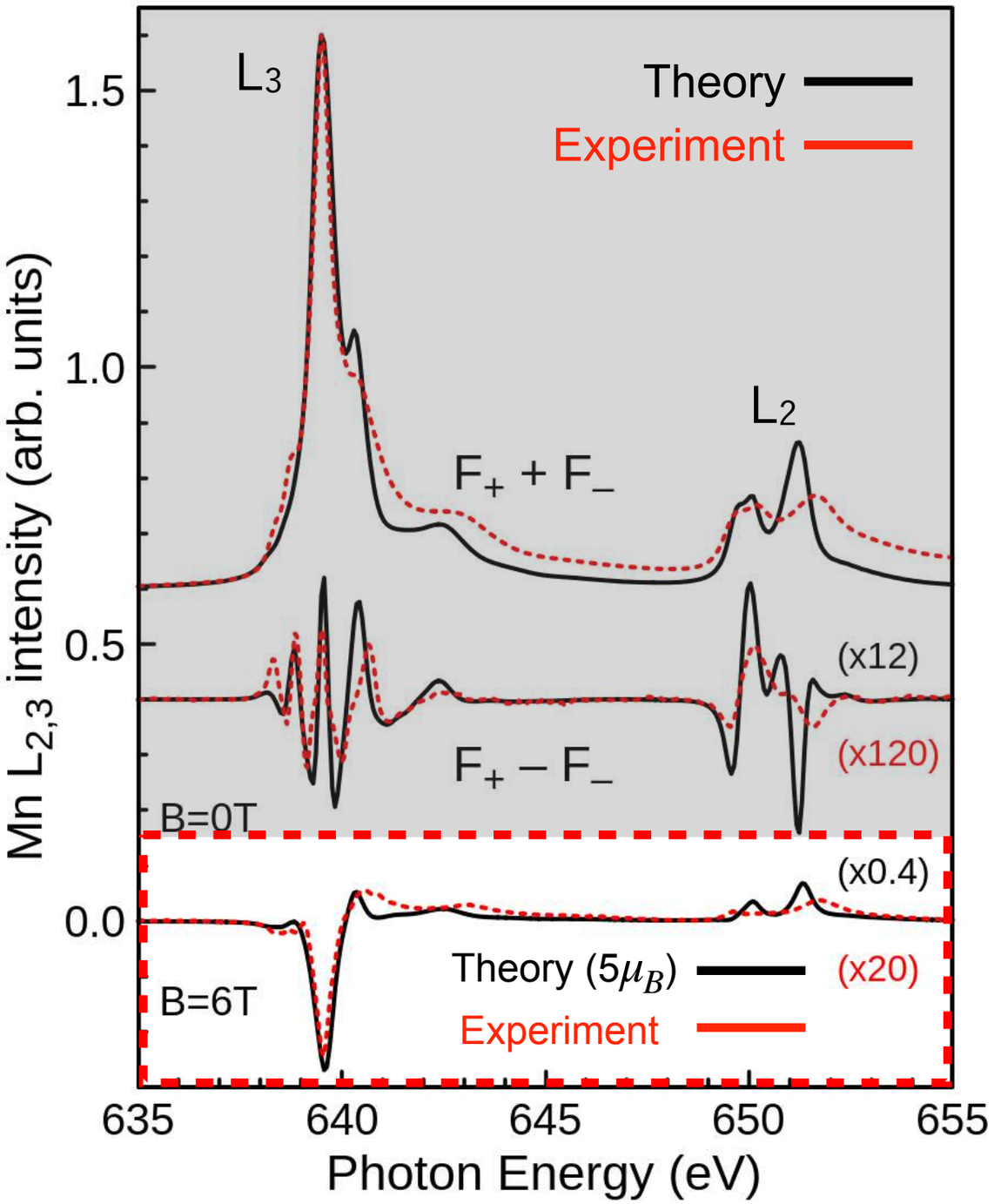

A. Hariki et al., Phys. Rev. Let. **132**, 176701 (2024)

Experiment $\mathbf{k}||\mathbf{c}$

- Cooled below T_c in field B(6T) ll C
- Measured in the field B

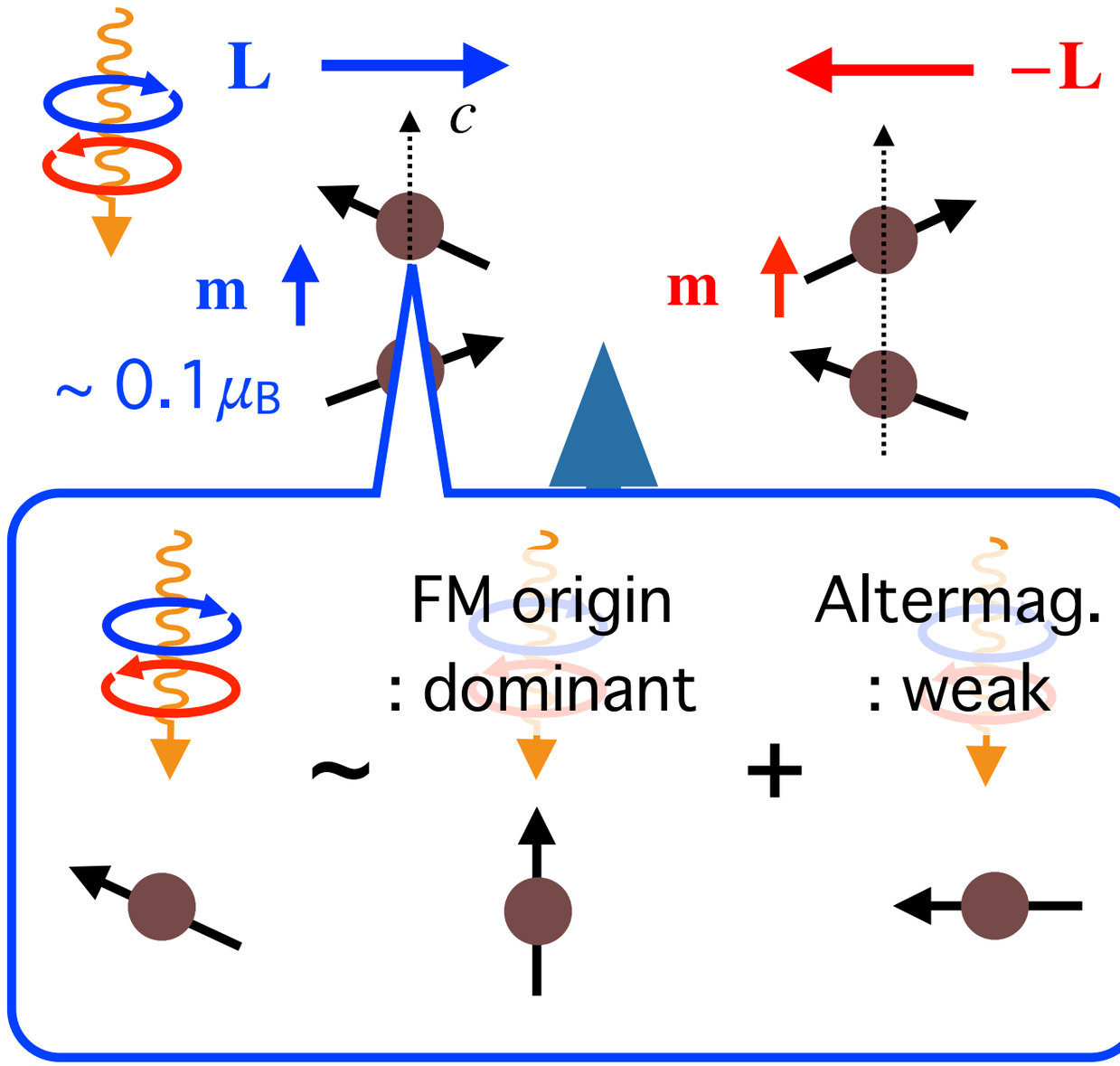

Theory vs Experiment: Mn $L_{2,3}$-edge XMCD in α-MnTe

Experiment and Theory

(@ Diamond Light Source)

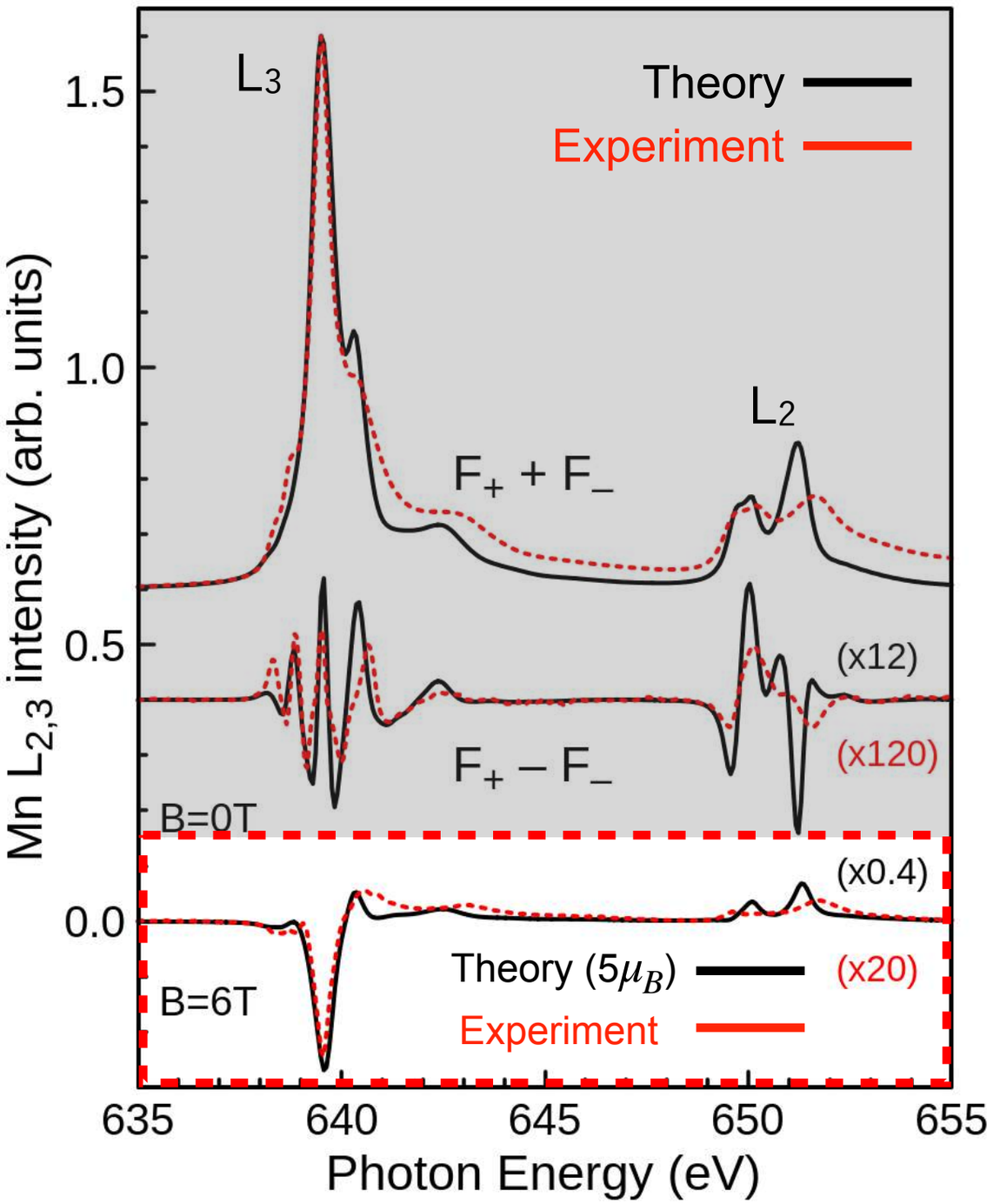

Experiment $\mathbf{k}||\mathbf{c}$

- Cooled below T_c in field B(6T) ll C
- Measured in the field B

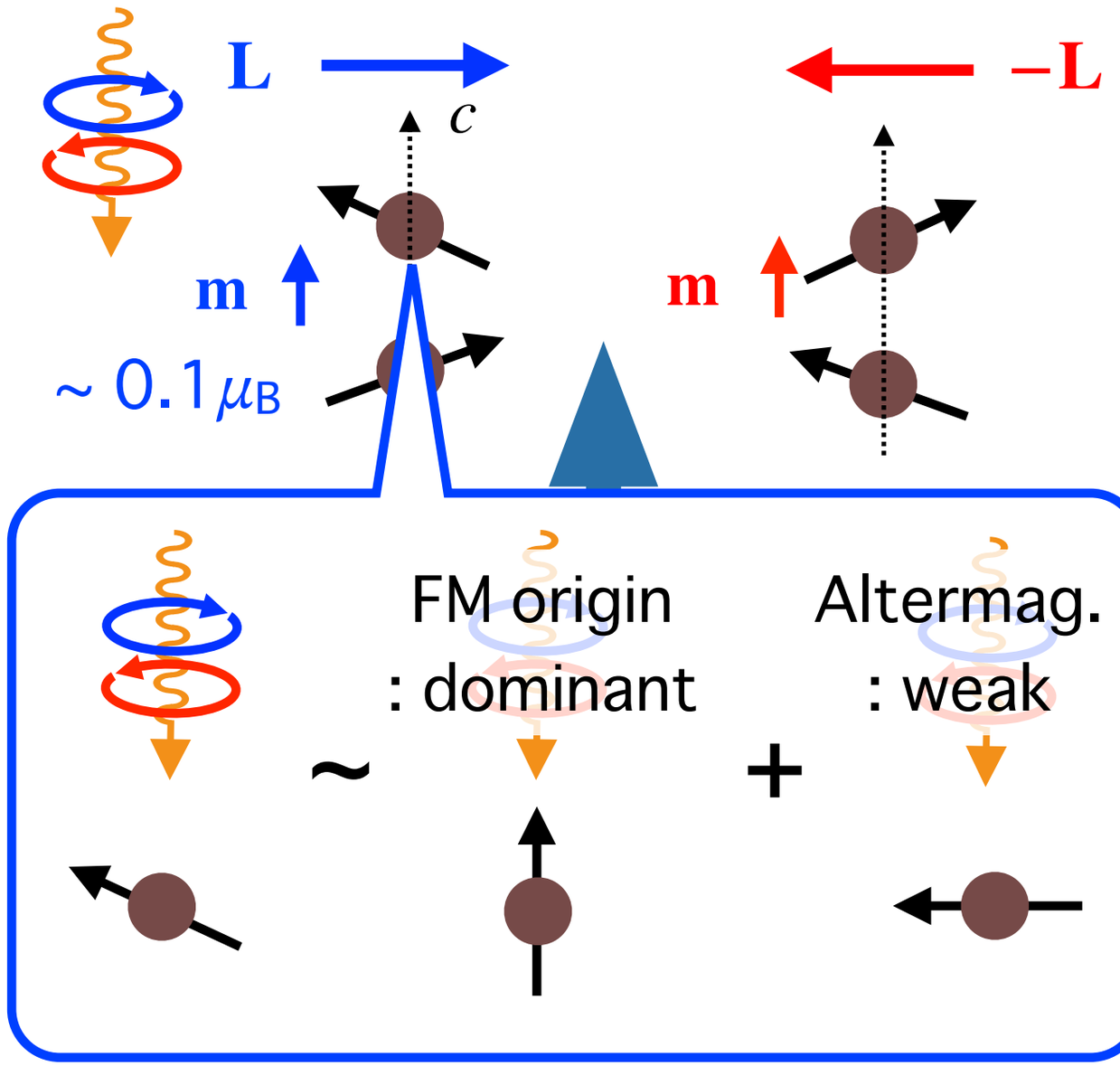

Theory vs Experiment: Mn $L_{2,3}$-edge XMCD in α-MnTe

Experiment and Theory

(@ Diamond Light Source)

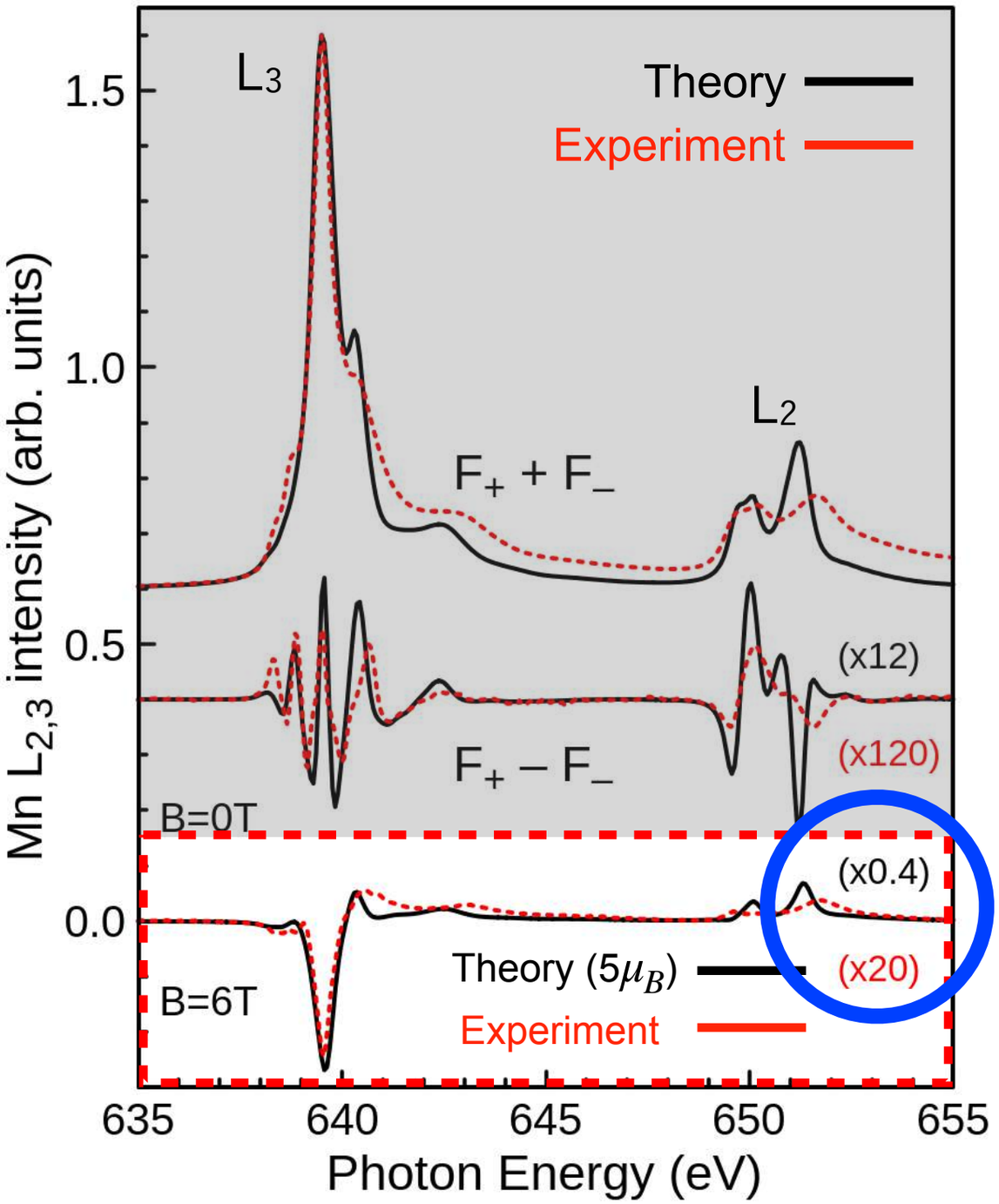

Experiment $\mathbf{k}||\mathbf{c}$

- Cooled below T_c in field B(6T) ll C
- Measured in the field B

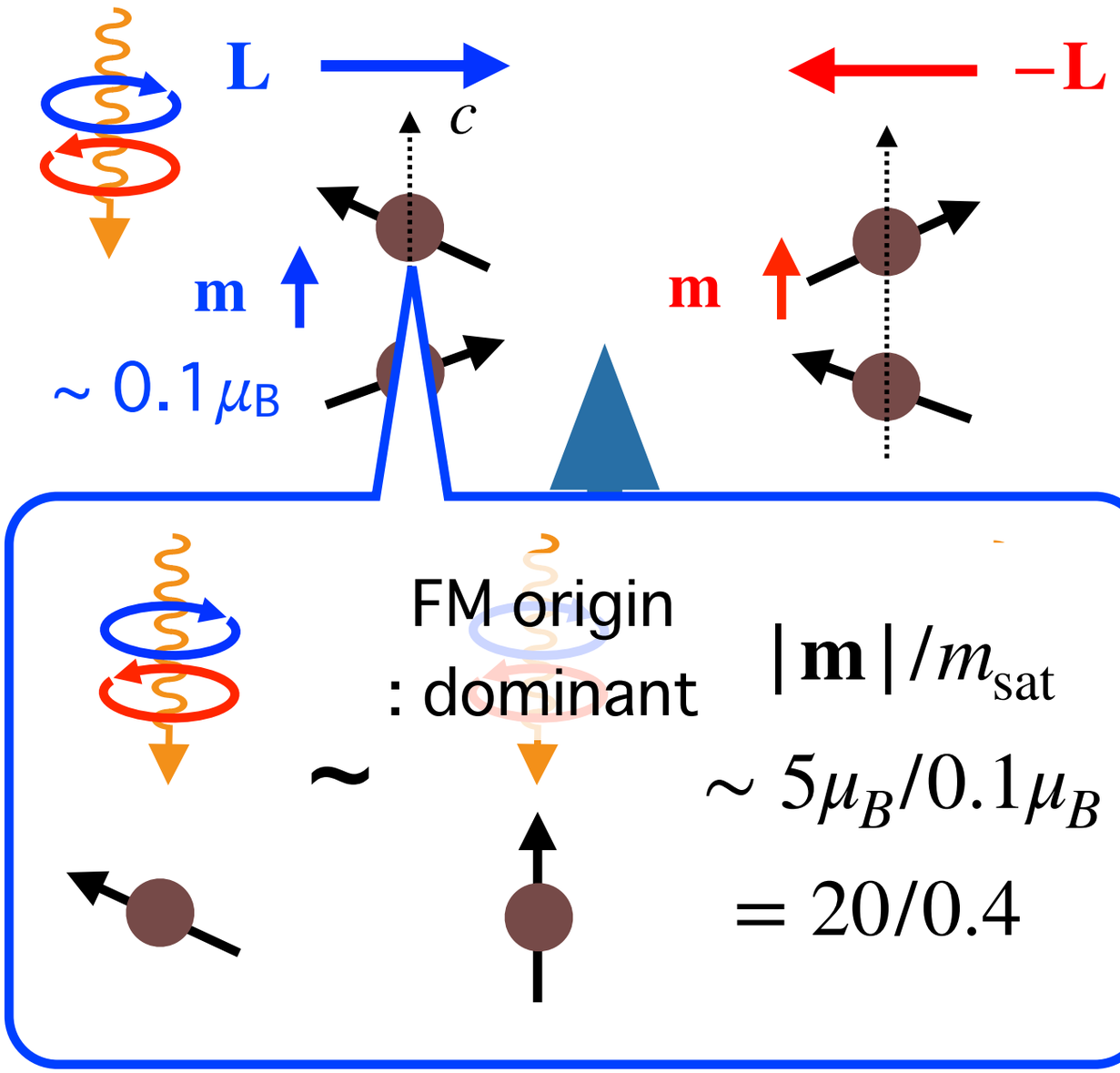

Recent XMCD experiment

arXiv > cond-mat > arXiv:2502.18597

Search... Help | Adva

Condensed Matter > Materials Science

[Submitted on 25 Feb 2025]

Altermagnetic nanotextures revealed in bulk MnTe

Rikako Yamamoto, Luke Alexander Turnbull, Marcus Schmidt, José Claudio Corsaletti Filho, Hayden Jeffrey Binger, Marisel Di Pietro Martínez, Markus Weigand, Simone Finizio, Yurii Prots, George Matthew Ferguson, Uri Vool, Sebastian Wintz, Claire Donnelly

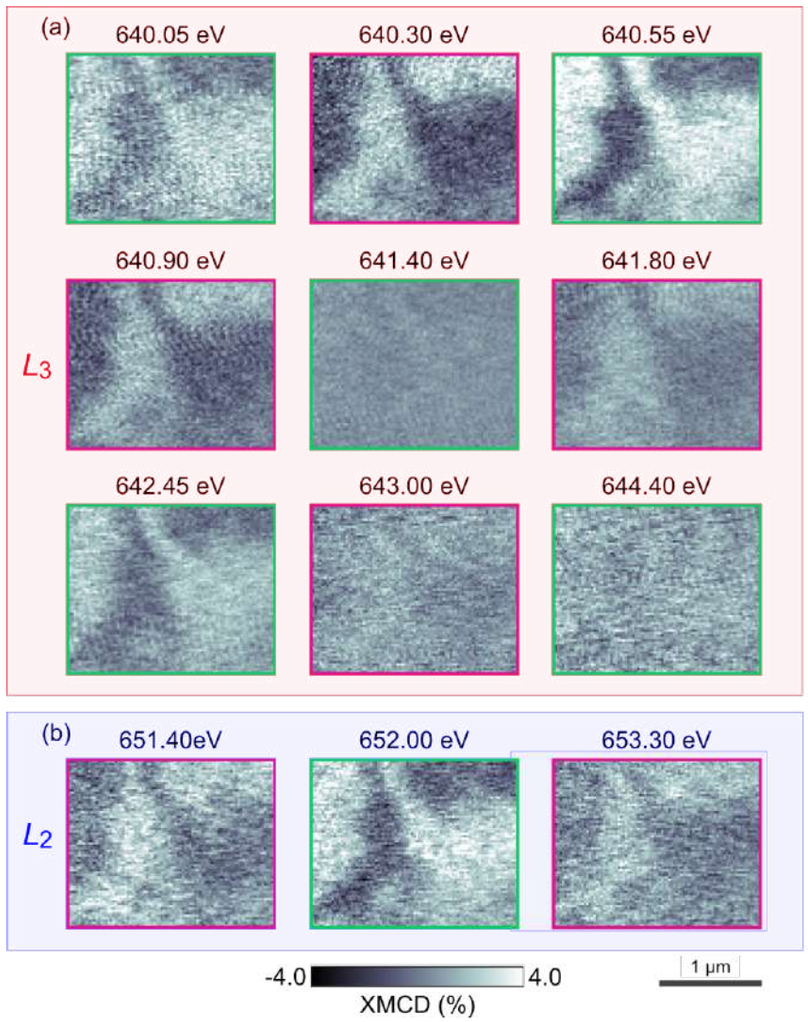

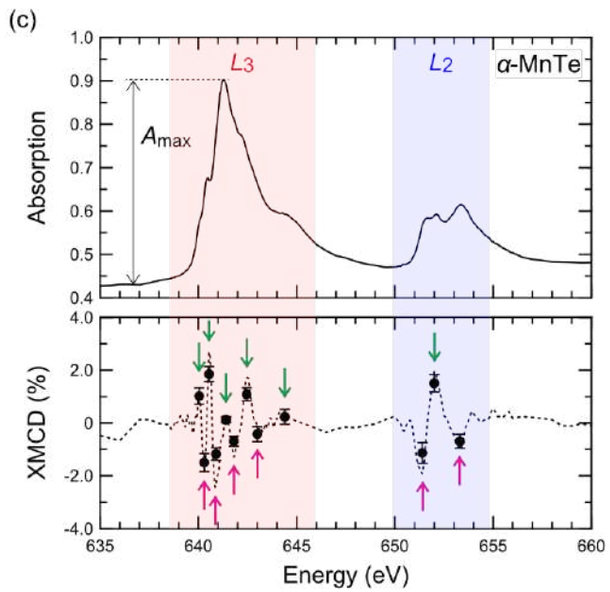

signal as well. Indeed, previous spectroscopic measurements reported an order of magnitude difference between the magnitude of the predicted, and measured altermagnetic XMCD signal [27]. Here, we observe a maximum XMCD contrast of $1.8 \pm 0.3\%$ of $A_{\max}$, the maximum absorption, which agrees well with the predicted XMCD contrast of 1.8% of $A_{\max}$ [27].

Our DFT+DMFT calculation

Origin of XMCD in altermagnetic MnTe

Calc. Mn single-site XMCD

$$\mathbf{k} \perp \mathbf{L} \; (\sim \sigma_{xy})$$

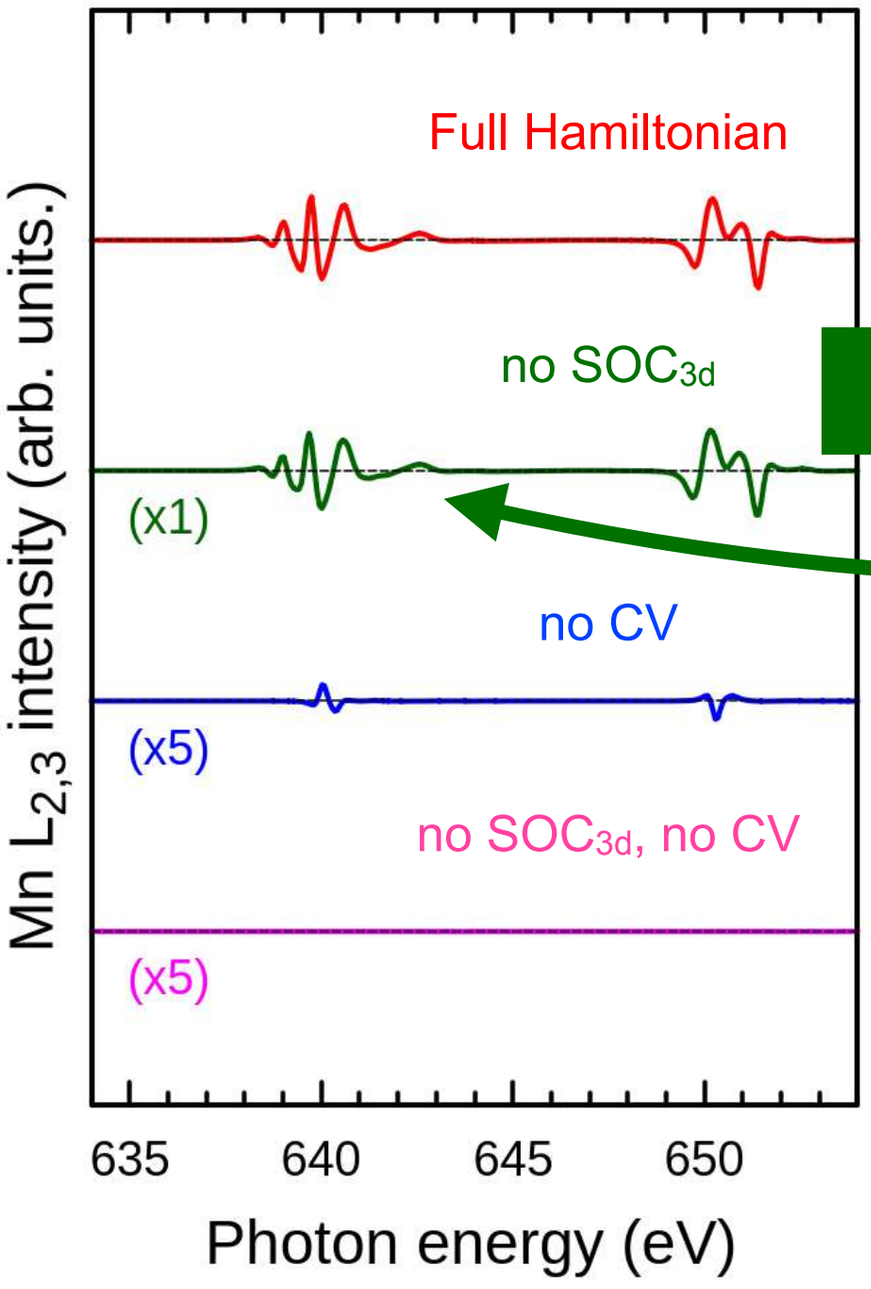

$$\hat{H}^0_{\rm at} = \epsilon_c \sum_{m,\sigma} \hat{p}^\dagger_{m\sigma}\hat{p}_{m\sigma} + \sum_{m,m,\sigma,\sigma'} h^{(2p)}_{m\sigma,m'\sigma'}\hat{p}^\dagger_{m\sigma}\hat{p}_{m'\sigma'}$$
$$+ \sum_{m,m',\sigma} h^{(CF)}_{mm'}\hat{d}^\dagger_{m\sigma}\hat{d}_{m'\sigma} + b\sum_{m,\sigma}\hat{d}^\dagger_{m\sigma}\hat{d}_{m-\sigma}$$
$$+ U_{pd}\hat{n}_p\hat{n}_d + \sum_{\substack{i,j,k,l \\ \sigma,\sigma'}} u^{\sigma\sigma'}_{ijkl}\hat{d}^\dagger_{i\sigma}\hat{d}_{j\sigma'}\hat{d}^\dagger_{k\sigma'}\hat{d}_{l\sigma}.$$

CV

$$\sum_{\substack{m,m' \\ \sigma,\sigma'}} h^{(3d)}_{m\sigma,m'\sigma'}\hat{d}^\dagger_{m\sigma}\hat{d}_{m'\sigma'}$$

3d SOC

3d SOC : negligible role

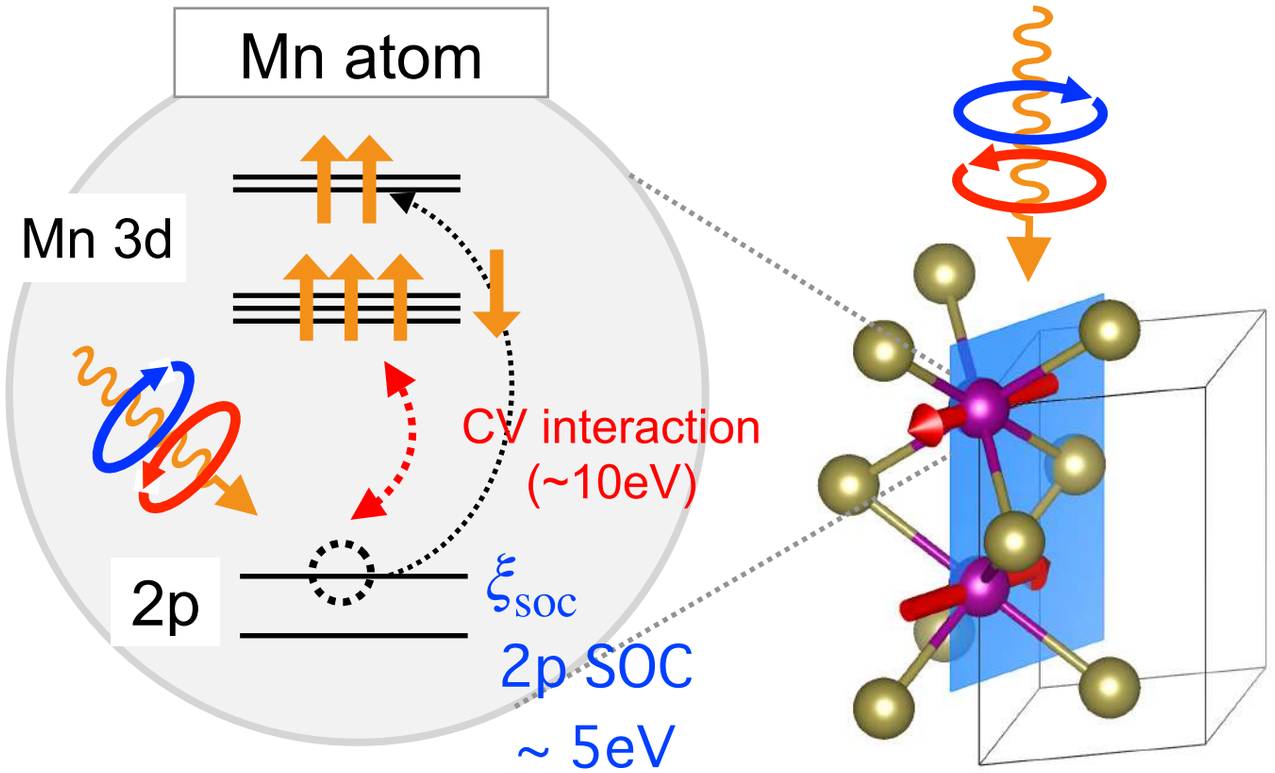

Origin of XMCD in altermagnetic MnTe

Calc. Mn single-site XMCD

$$\mathbf{k} \perp \mathbf{L} \; (\sim \sigma_{xy})$$

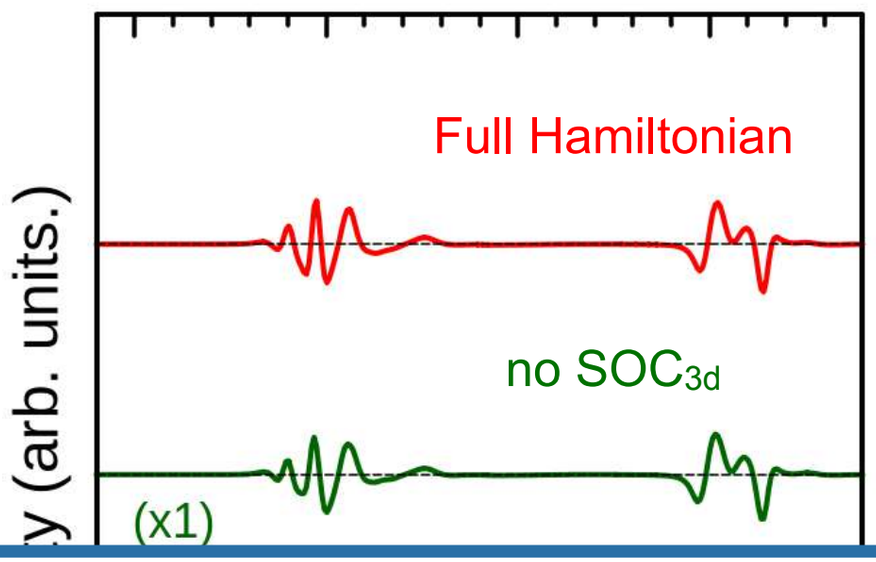

$$\hat{H}^0_{\rm at} = \epsilon_c \sum_{m,\sigma} \hat{p}^\dagger_{m\sigma}\hat{p}_{m\sigma} + \sum_{m,m,\sigma,\sigma'} h^{(2p)}_{m\sigma,m'\sigma'}\hat{p}^\dagger_{m\sigma}\hat{p}_{m'\sigma'}$$
$$+ \sum_{m,m',\sigma} h^{(CF)}_{mm'}\hat{d}^\dagger_{m\sigma}\hat{d}_{m'\sigma} + b\sum_{m,\sigma}\hat{d}^\dagger_{m\sigma}\hat{d}_{m-\sigma}$$
$$+ U_{pd}\hat{n}_p\hat{n}_d + \sum_{\substack{i,j,k,l\\ \sigma,\sigma'}} u^{\sigma\sigma'}_{ijkl}\hat{d}^\dagger_{i\sigma}\hat{d}_{j\sigma'}\hat{d}^\dagger_{k\sigma'}\hat{d}_{l\sigma}.$$

$$\hat{H}^1_{\rm at} = \sum_{\substack{i,j,k,l\\ \sigma,\sigma'}} w^{\sigma\sigma'}_{ijkl}\hat{d}^\dagger_{i\sigma}\hat{d}_{j\sigma'}\hat{p}^\dagger_{k\sigma'}\hat{p}_{l\sigma} + \sum_{\substack{m,m'\\ \sigma,\sigma'}} h^{(3d)}_{m\sigma,m'\sigma'}\hat{d}^\dagger_{m\sigma}\hat{d}_{m'\sigma'}$$

CV

3d SOC

Altermagnetism is a non-relativistic concept

dual role of SOC in altermagnetism :

- Necessary to observe AHE and magneto-optical effects (XMCD) etc ..
- May cause weak ferromagnetic, non-collinear magnetism

→ How to distinguish altermagnetic signal from ferromagnetic one?

Core-level XMCD :

Mn 2p SOC : necessary to observe XMCD

Mn 3d SOC : negligible effect on the spectra

XMCD + XMLD = domain imaging

Article | Open access | Published: 11 December 2024

Nanoscale imaging and control of altermagnetism in MnTe

O. J. Amin ✉, A. Dal Din ✉, E. Golias, Y. Niu, A. Zakharov, S. C. Fromage, C. J. B. Fields, S. L. Heywood, R. B. Cousins, F. Maccherozzi, J. Krempaský, J. H. Dil, D. Kriegner, B. Kiraly, R. P. Campion, A. W. Rushforth, K. W. Edmonds, S. S. Dhesi, L. Šmejkal, T. Jungwirth & P. Wadley ✉

Nature **636**, 348–353 (2024) | Cite this article

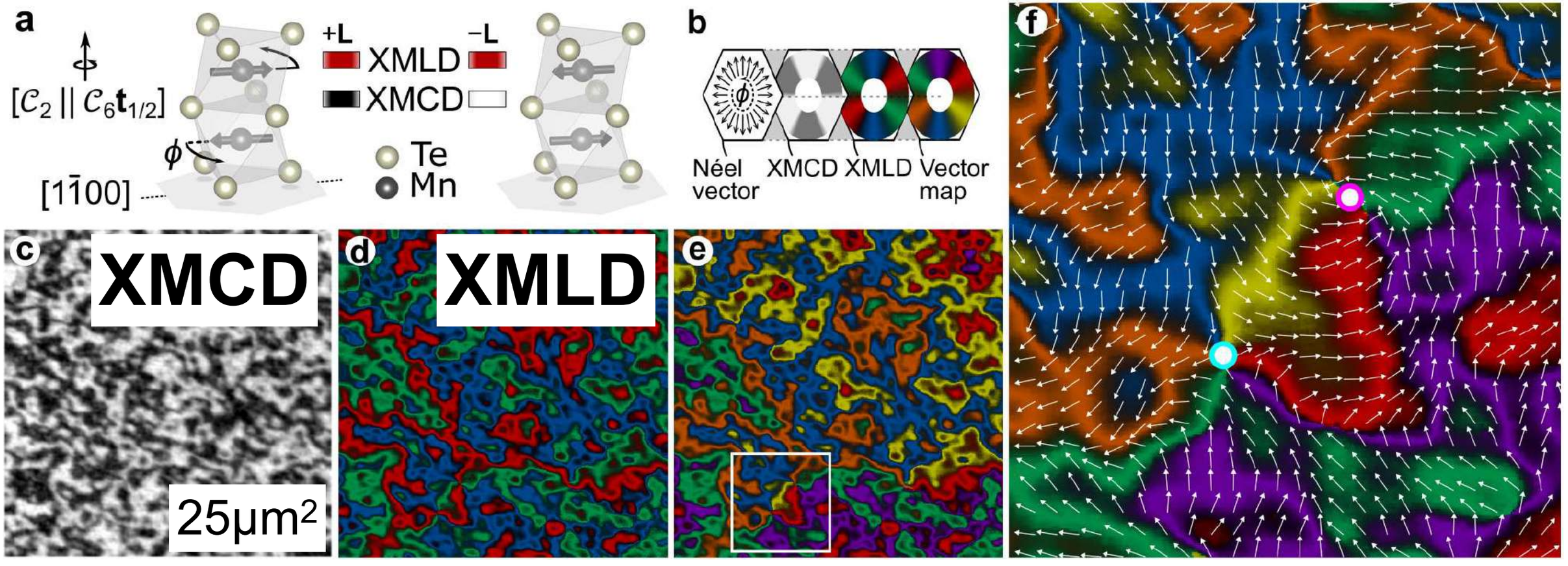

Table of contents

1. Core-level X-ray spectroscopy and DFT-based embedding approach

★ **Method**. DFT+ dynamical mean-field theory (DMFT)

A. Hariki, T. Uozumi, and J. Kuneš, Phys. Rev. B **96**. 045111 (2017)

A. Hariki, M. Winder, and J. Kuneš, Phys. Rev. Lett. **121**, 126403 (2018)

A. Hariki, M. Winder, T. Uozumi, and J. Kuneš, Phys. Rev. B **101**, 115130 (2020)

2. Application to various optical processes and compounds

★ **Excitations**. XPS, XAS, RIXS ★ **Materials**. *d*, *f* electron systems

★ **Physics**. Magnetism, valence structure, elementary excitations

K. Higashi, M. Winder, J. Kuneš, and A. Hariki, Phys. Rev. X **11**, 041009 (2021)

D. Takegami, A. Hariki et al., Phys. Rev. X **12**, 011017 (2022)

M. C. Rahn, K. Kummer, A. Hariki, et al., Nat. Commun. **13**, 6129 (2022)

J. Li, A. Hariki et al., Phys. Rev. X **13**, 011012 (2023)

A. Hariki et al., Phys. Rev. Let. **132**, 176701 (2024)

Thank you for your attention

Collaborators and acknowledgement

主な共同研究者

Jan Kunes
（マサリク大学）

東啓介、山口達也（大阪公立大学）

QCHybrid
Computational materials science based on quantum-classical hybrid algorithms
JSPS Transformative Area (B) 2023-2025
量子古典融合

科研費
KAKENHI

若手研究 2020-2023年度
「動的平均場理論を用いた共鳴非弾性X線散乱の
マルチスケール解析手法の開発と応用」

Thank you for your attention